LoC-SERS Technique Toward Drug Quantification in Complex Matrices

Kumulative Dissertation

Zur Erlangung des akademischen Grades

doctor rerum naturalium (Dr. rer. nat.)

vorgelegt dem Rat der Chemisch-Geowissenschaftlichen Fakultät

der Friedrich-Schiller-Universität Jena

M. Sc. Izabella Jolán Hidi

geboren am 27. Februar 1987 in Deva, Rumänien

Gutachter:

1. Prof. Dr. Jürgen Popp

2. Prof. Dr. med. Mathias Pletz

Tag der öffentlichen Verteidigung: 10. August 2016.

Index of Abbreviation

7-OH-MTX	7-hydroxy methotrexate
CE	chemical enhancement
CEDIA	cloned enzyme donor immunoassay
DAMPA	4-amino-4-deoxy-N10-methylpteroic acid
ELISA	enzyme-linked immunosorbent assay
EM	electromagnetic enhancement
EMIT	enzyme multiplied immunoassay technique
ESI	electron spray ionization
FLD	fluorescence detection
FPIA	fluorescence polarization immunoassay
GC	gas chromatography
HILIC	hydrophilic interaction liquid chromatography
HD	high-dose
HPLC	high-performance liquid chromatography
IPHT	Institute of Photonic Technology
IR	infrared
LC	liquid chromatography
LLE	liquid-liquid extraction
LoC-SERS	lab-on-a-chip surface enhanced Raman spectroscopy
LOD	limit of detection
LOQ	limit of quantification
LSPP	localized surface plasmon polariton
LD	low-dose
MCR-ALS	multivariate curve resolution alternating least square regression
MIC	minimum inhibitory concentration
MMIP	magnetic molecularly imprinted polymer
MS	mass spectrometry
MS/MS	tandem mass spectrometry
MTX	methotrexate
NTX	nitroxoline
OLSPE	on-line solid phase extraction

PLS	partial least square
PD	pharmacodynamic
PK	pharmacokinetic
PP	protein precipitation
PSPP	propagating surface plasmon polariton
RAM	restricted access material
SAM	standard addition method
SAS	standard addition steps
SERRS	surface enhanced resonance Raman spectroscopy
SERS	surface enhanced Raman spectroscopy
SFC	supercritical fluid chromatography
SPE	solid-phase extraction
SPME	solid phase microextraction
SRM	selected reaction monitor
SSPE	selective solid phase extraction
TDM	therapeutic drug monitoring
TFC	turbulent flow chromatography
UHPLC	ultra-high performance liquid chromatography
UV	ultraviolet

Table of Contents

“It’s far more important to know what person the disease has

than what disease the person has.”

Hippocrates

Chapter 1

Zusammenfassung

Eine der größten Herausforderungen, die an die Entwicklung und Implementierung analytischer Methoden gestellt wird, ist der sensitive und spezifische Nachweis der gesuchten Substanzen (z.B. Medikamenten) sowie deren Quantifizierung in hochkomplexen Probenmatrizes. Einerseits, werden klinische Proben, wie Blut oder Urin, routinemäßig analysiert, um Diagnosen stellen oder den Behandlungsfortschritt erfassen zu können. Andererseits, wächst das Interesse an der kontinuierlichen Überwachung pharmazeutisch aktiver Substanzen bei der Aufbereitung von Ab- und Oberflächenwässern, vor allem um der Problematik der antibakteriellen Resistenz in unserem Ökosystem entgegenzutreten. In der Routineanalytik stellen chromatographische Verfahren, gekoppelt mit unterschiedlichen Detektionstechniken, den derzeitigen Goldstandard dar. Insbesondere in Kombination mit der Massenspektrometrie als Nachweisverfahren, wird eine hohe Sensitivität und Spezifität erreicht. Vor der eigentlichen Analyse sind für gewöhnlich jedoch technisch anspruchsvolle und arbeitsintensive Probenaufbereitungsverfahren zur Reduzierung störender Matrixeffekte durchzuführen. Weiterhin, erlaubt die dafür benötigte technische Instrumentierung/Ausstattung keine einfache Analyse auf Knopfdruck, ist in ihrer Anschaffung sowie dem Betrieb mit hohen Kosten verbunden sowie aufgrund ihrer Größe nicht für Vor-Ort-Anwendungen geeignet. Weiterhin bestehen keine einheitlichen Standards für Analyseprotokolle, wodurch jeweils eine individuelle Kalibrierung in Abhängigkeit der gesuchten Substanz notwendig ist. Eine weitere Methode, die bereits fest in der klinischen Praxis verankert ist, stellen Immunoassays dar, von denen derzeitig mehr als 25 verschiedene „Kits“ kommerziell verfügbar sind. Ihr hoher Grad an Automatisierung ermöglicht eine einfache Implementierung dieser Technik in klinischen

Laboratorien und die Resultate verschiedener Zentren weisen eine hohe Vergleichbarkeit auf. Allerdings ist das Auftreten unerwünschter Kreuzreaktionen, auch 60 Jahre nach der ersten Demonstration, nach wie vor ein großes Problem. In diesem Zusammenhang erweist sich die Multiplexdetektion ebenfalls als große Herausforderung.

Zu den neu entwickelten analytischen Techniken gehörend, weist die oberflächenverstärkte Raman-Spektroskopie (SERS, engl. surface enhanced Raman spectroscopy) großes Potential als Alternativmethode für die Detektion klinisch- sowie umweltsrelevanter Moleküle in komplexen Probenmatrizes auf. Die Methode beruht auf den molekularen Informationen, erhalten durch inelastische Lichtstreuung an sich in der Probe befindlicher Moleküle, vereint mit der Signalverstärkung (bis zu 10^{11}) durch die plasmonischen Eigenschaften von Nanopartikeln aus Münzmetallen. Damit erfüllt SERS die wichtigen Voraussetzungen, Spezifität und Sensitivität, an analytische Techniken. Die größten Hindernisse, welche den Einsatz in der Standardanalytik bisher weitgehend verhindert haben, sind die geringe Reproduzierbarkeit der Resultate sowie die mangelnde Automatisierung der Methode. Eine oft vorgeschlagene Methode zur Erhöhung der Zuverlässigkeit besteht in der Verwendung hochgeordneter, planarer Strukturen als SERS-Substrat. Diese sind jedoch mit hohen Herstellungskosten verbunden. Des Weiteren stellt die Frage nach der optimalen Auftragung des Probenmaterials eine Herausforderung dar. Bisher konnte kein automatisiertes Messverfahren mit planaren Substraten realisiert werden. Ein alternativer Ansatz, welcher reproduzierbare und automatisierte Messbedingungen unter Einsatz kostengünstiger SERS-Substrate gewährleistet, ist die tropfenbasierte, mikrofluidische Lab-on-a-Chip SERS- (LoC-SERS) Technik. Diese Plattform ermöglicht eine direkte, chipbasierte Untersuchung der Proben gestützt auf die präzise Manipulation von Nanopartikel- und Probelösung über ein computergesteuertes Pumpensystem.

In letzter Zeit häufen sich Studien, die auf die Wichtigkeit und Notwendigkeit einer personalisierten Medizin hinweisen. Methotrexat gehört zu den wirksamsten Chemotherapeutika, verursacht jedoch häufig toxische Ereignisse aufgrund einer Überdosierung. Für Studien zur Auffindung optimal wirksamer Dosen für Antibiotika, wie Levofloxacin, wird oft auf gesunde Freiwillige zurückgegriffen. Die mittels dieser Studien gefundenen Werte können jedoch häufig nicht auf Patienten, die sich auf der Intensivstation befinden, übertragen werden. Darüber hinaus ist eine kontinuierliche Anpassung der Behandlungsvorschriften notwendig, um dem Auftreten multiresistenter Erreger sowie der Entwicklung neuer, wirksamerer antibakterieller Medikamente zu begegnen. Nitroxilin ist eines von mehreren Antibiotika, welche erst kürzlich in diesem Zusammenhang von dem Nationalen Antibiotika-

Sensitivitätstest-Komitee in Bonn (NAK) neu bewertet wurden. Ein weiterer wichtiger Aspekt ist die Tatsache, dass die Entwicklung multiresistenter Keime nicht nur räumlich beschränkt, beispielsweise in medizinischen Einrichtungen, sondern im gesamten Ökosystem abläuft. Der übermäßige Einsatz von Antibiotika in der Humanmedizin und der Massentierhaltung ist ein ernsthaftes Problem unserer Zeit. Dadurch gelangen aktive Metaboliten als auch unveränderte Substanzen im Fall solcher Medikamente, die nur geringfügig verstoffwechselt werden, ins Ökosystem. Letzteres ist beispielsweise bei dem Antibiotikum Ciprofloxacin der Fall.

Das Ziel der vorliegenden Dissertation ist die Beurteilung des Potentials sowie der Limitierungen der LoC-SERS-Technik für den Nachweis und die Quantifizierung unterschiedlicher Medikamente in komplexen Probenmatrizes. Als SERS-Substrate kommen dabei einfach herstellbare Silbernanopartikel in einer kolloidalen, wässrigen Lösung zum Einsatz. Die Probenaufreinigung beschränkt sich auf Filtration und Verdünnung mit Wasser. Die verwendeten Urinproben stammen von gesunden Freiwilligen sowie Patienten mit Harnwegserkrankungen. Weiterhin werden Flusswasserproben in der vorliegenden Arbeit untersucht. Die analytische Leistungsfähigkeit, gemessen an Parametern wie dem Detektionslimit (LOD, engl. limit of detection), dem linearen und dynamischen Bereich und der Wiederholbarkeit von Messungen, wird für die Medikamente Methotrexat, Levofloxacin, Nitroxolin und Ciprofloxacin getestet. Darüber hinaus, wird durch die Verwendbarkeit eines transportablen Messgerätes anstelle eines fest installierten Aufbaus das Potential der LoC-SERS-Plattform für Vor-Ort-Anwendungen demonstriert.

1.1 Summary

Detection and quantification of drugs in complex matrices challenged each analytical method at its moment of development and implementation. On one side, clinical samples, i.e. blood and urine, are routinely analyzed for diagnosis and treatment follow-up purposes. On the other side, monitoring the successful removal of pharmaceutically active compounds in waste and surface water is of high interest to overcome the occurrence of antibacterial resistance in the ecosystem. Before the actual analysis, sophisticated and labor-intensive sample clean-up procedures are commonly applied in the routine analysis to reduce matrix effects. Regardless of the application field, chromatography coupled with various detection methods is the gold standard. Sensitivity and specificity, two key requirements of analytical instrumentation, represent the strength of chromatography platforms, especially for the ones using mass spectrometry as a detection technique. However, they are not "turn-key" instruments, they are associated with high initial and maintenance costs, and thus, they are not accessible for small medical centers, they lack standardization and the big footprint inhibits their on-site application. In clinical chemistry practice, immunoassays are also well established. Currently, more than 25 commercial immunoassays are available on the market. Because of their automation, they are easily integrated into clinical laboratories and results obtained by different clinical centers are comparable. Nevertheless, after more than 60 years since their first use, cross-reactivity is still a drawback, while multiplex detection is a big challenge.

Among the newly developed analytical techniques, surface enhanced Raman spectroscopy (SERS) has high potential to be considered as an alternative analytical technique for the detection of clinically and environmentally relevant molecules in complex matrices. The method takes advantage of the molecular information offered by the inelastically scattered light by molecules in the sample and the signal enhancement (up to 10^{11}) caused by the plasmonic properties of coinage metallic nanoparticles. Consequently, SERS fulfills the key requirements, specificity and sensitivity, of analytical instrumentations. The biggest barrier for its application is the low reproducibility of measurements and automation. One of the suggested solutions to increase reliability is to use highly ordered planar structures as SERS active substrates. Nevertheless, these imply high production costs, challenges regarding the correct sample deposition appear and the automation is not achieved. An alternative solution that requires low-cost SERS substrates and offers reproducible and automated measurement conditions at the same time is represented by the droplet based lab-on-a-chip SERS (LoC-SERS) technique. This

platform offers the advantage of highly precise controlled manipulation of nanoparticle and sample solution via computer controlled systems and a direct, on chip detection.

Recently, many studies reported on the importance and necessity of personalized medicine. Methotrexate is one of the most potent anticancer drugs, but at the same time, it is also the one having the most reported toxic events. Dose finding studies for antibiotics, i.e. levofloxacin, often recruit healthy volunteers. Fixed dose regimens derived from these clinical trials fail in the critically ill intensive care unit patients. Moreover, a continuous change of treatment guidelines is needed because of the occurrence of antibacterial resistances or because of the discovery of new, more potent antibiotics. Nitroxoline is one of the antimicrobial agents recently reevaluated by the German Antimicrobial Susceptibility Testing Committee. One other site for the development of antibacterial resistances, beside medical centers, is the ecosystem. Overuse of antimicrobial agents weakly metabolized, i.e. ciprofloxacin, or with active metabolites, in live-stock raising and medical treatments present a major issue of the human society.

Consequently, the aim of the present thesis was to assess the potential and limitations of the LoC-SERS technique to detect and quantify drugs in various complex matrices. As SERS active substrates, easy-to-prepare silver nanoparticles in a colloidal solution were employed and as sample clean-up procedure filtration and dilution with water was carried out. Urine samples originating from healthy volunteers and patients with urinary tract infection, as well as river water sample were included in the present study. Analytical performances, such as lower limit of detection (LOD), linear and dynamic range and measurement reproducibility, were tested for methotrexate, levofloxacin, nitroxoline and ciprofloxacin. Furthermore, the potential of the LoC-SERS platform for on-site applications is also demonstrated by replacing the bench-top Raman microscope by a portable one.

1.2 Motivation

Health care and environment protection are two of the main concerns of nowadays society. Although the two aspects seem to have no interconnection, the emerging antibacterial resistances are the result of irresponsible use of antimicrobial agents in medical treatments followed by the unsuccessful removal of pharmaceutically active compounds from the ecosystem. The World Economic Forum Global Risks reports have classified antibacterial resistance as one of the greatest threats to human health and associated it with high financial costs [1, 2]. An additional factor that puts a high burden on health care costs is the ineffectiveness of fix dose medical treatments caused by the individuality of each patient, the patient compliance, bioavailability of the drug, rate of drug metabolism as well as the protein binding capability of the drug [3]. Therefore, in order to increase the efficiency of medical treatments and lower the associated financial costs personalized medicine is highly encouraged.

In pharmacotherapy, two different parameters are used to assess the required dose of a drug to achieve a given medical outcome. Pharmacokinetics (PK) describes the drug concentration in body fluids over time for a specific drug dose, while pharmacodynamics (PD) gives information about the effect of a certain drug concentration [4]. PK/PD modelling links the administered dose with the concentration in body fluids and the therapeutic response and predicts the effect over time of a certain drug dose. Nowadays, different physiological indices of pharmacological response are routinely measured (lipid concentrations, blood glucose, blood pressure) in order to determine the PK/PD characteristics of drugs. However, there are many drugs with insufficiently sensitive or no direct indicator of their therapeutic response. In these cases, therapeutic drug monitoring (TDM) is applied which was defined as "*the measurement made in the laboratory of a parameter that, with appropriate interpretation, will directly influence prescribing procedures. Commonly, the measurement is in a biological matrix of a prescribed xenobiotic, but it may also be of an endogenous compound prescribed as a replacement therapy in an individual who is physiologically or pathologically deficient in that compound*" [5].

The determination of drug levels in biological fluids is performed by methods based on chromatographic separation or immunological assays [6-23]. On one hand, the first approach offers great specificity and sensitivity for, theoretically, all existing drugs, but it is mainly available in reference clinical laboratories and academic centers because of the required high initial financial investment. On the other hand, immunological assays (or immunoassays) are

easy to integrate in a clinical setting, but they are available for only a limited number of drugs due to the need of specific antibodies.

Among the emerging techniques, methods based on vibrational spectroscopy yield the required specificity for drug detection and are considered as potential alternative analytical instrumentation to chromatography platforms [11, 24-32]. Especially Raman spectroscopy can be easily performed in biological fluids due to the low scattering cross section of the water molecules. Hence, no or very reduced sample clean-up procedure is needed prior to the measurements. The method is based on the inherently weak inelastic light scattering of photons by the sample and, thus, the detection of trace amount of molecules is inhibited. Various signal enhancement strategies have been applied throughout the years among which SERS was widely recognized for its exquisite sensitivity at single molecule level [33-35]. The technique gains its high sensitivity from the enhanced local electromagnetic field of plasmonic nanostructures excited with the appropriate electromagnetic radiation. The development of a high diversity of SERS active substrates [36-42] is driven by the need of a stable, easy-to-synthesize and cost-effective nanostructure which offers homogenous signal enhancements (for analytical applications) or strong local electromagnetic fields (for single molecule applications). Colloidal silver and gold solutions obtained by chemical reduction [40, 42-44] are the most commonly used plasmonic substrates, regardless of the aimed application. The drawbacks associated with these nanoparticles, i.e. low reproducibility of the measurements because of the aggregation time dependent SERS signal and low automation [45], can be easily overcome by applying them in microfluidic setups [46-55]. By employing the droplet based LoC-SERS technique the manipulation of the nanoparticles and sample solutions is controlled with high precision via computer controlled systems and the detection is carried out on-line [29, 50, 55-58]. Furthermore, LoC-SERS measurements can be easily carried out with portable Raman setups significantly reducing the overall costs and facilitating its on-site application.

The aim of the present study was to assess the potential and limitation of the LoC-SERS technology for the detection and quantification of drugs in both clinical and environmental samples. For this, the antifolate drug methotrexate (MTX) and three antibiotic agents, levofloxacin, nitroxoline (NTX) and ciprofloxacin were investigated.

Low-dose (LD) (5-25 mg/week) MTX is first-line therapy for the treatment of rheumatoid arthritis, while the drug is administered in high-dose (HD) (5000 mg/week) for cancer treatment [6, 59-61]. The exact mechanism of action of the drug in the LD schemes is not completely understood. Four different routes have been suggested in literature: MTX might inhibit (1) the proliferation of cells responsible for synovial inflammation or (2) the synthesis of

potentially toxic compounds that accumulate in chronically inflamed tissues; (3) it might reduce intracellular glutathione levels or (4) adenosine might mediate its anti-inflammatory effects. In HD treatments, the drugs block the action of folic acid, and thus it inhibits the dihydrofolate reductase process in cells [62]. However, this is not restricted only to cancerous cells and concomitant administration of leucovorin, a form of folic acid, is practiced [61]. To reduce the side effects of MTX TDM is performed during HD treatment schemes [12, 63]. In most medical guidelines a plasma MTX concentration ≤ 0.2 μM allows the clinician to stop leucovorin administration [63], at 42 h after the start of MTX infusion target concentrations are ≤ 1 μM, while high risk toxic effect are associated with concentrations ≥ 10 μM [64, 65].

Levofloxacin is a second generation fluoroquinolone antibiotic widely used against infections caused by both Gram-negative and Gram-positive bacteria [66, 67]. The fluorine atom attached to the quinolone backbone provides increased potency against organisms, while the piperazine moiety is responsible for pseudonomal activity [68]. Its PK/PD parameters, as in the case of most antimicrobial agents, was assessed during clinical trials carried out with healthy volunteers instead of patient volunteers [66, 69, 70]. However, multiple studies have been reported demonstrating that fixed dose regimens derived from such studies fail in critically ill intensive care unit patient [71]. Furthermore, even though levofloxacin is generally well tolerated, various studies report about its adverse effects, such as: tenosynovitis [72], crystal nephropathy [73], hepatotoxicity [74], PK interaction [75, 76], Achilles rupture and [77] metabolic coma [78]. Additionally, in the case of obese patients altered clearance rates of the antibiotic have been observed, as compared with the case of normal patients with normal weight [79]. Levofloxacin undergoes limited metabolism in the human body. More than 85 % of the administered dose is eliminated in urine unchanged [66]. Thus, its clearance rate can be easily monitored by determining its urinary concentration. Based on PK studies carried out with healthy volunteers, the expected drug concentration in urine after 4 h from the administration of a single oral dose of 500 mg are 1.38 mM ± 0.68 mM (498 ± 247 μg/ml) with the minimum measured concentration of 0.45 mM (162.6 μg/ml) [69, 70].

Fluoroquinolones have been widely used to treat urinary tract infections, especially cystitis and acute pyelonephritis [80]. However, medical guidelines indicate the co-administration of a second, long-acting antimicrobial agent if the regional resistance rate is higher than 10% [80]. Generally, the emerging antibacterial resistances require the change of treatment guidelines in order to provide an effective treatment. As the number of the newly developed antimicrobial agents is very limited, the attention of the medical community is often directed toward older antibiotics. NTX has been recently reevaluated by the by the German

Antimicrobial Susceptibility Testing Committee [81]. The drug acts by chelating the divalent cations required for bacterial RNA polymerase [82]. The minimum inhibitory concentration (MIC), defined as the lowest concentration of an antimicrobial that will inhibit the visible growth of a microorganism after overnight incubation, in the case of NTX is 2-4 mg/l (10.5-21.0 μM) for various *E. coli* strains, 4 mg/l (21.0 μM) for *K. pneumoniae* and 8 mg/l (42.1 μM) for *Proteus mirabilis* and *S. saprophyticus* [81, 83]. These values are in the susceptible range, while MICs≥16 mg/l (84.2 μM) are regarded as resistant. The information available in the literature concerning analytical methods for NTX detection is very scarce. Thus, there is a high need for the development of a new, easy to access instrumentation dedicated to determine NTX levels in order to avoid the occurrence of resistances.

Even though personalized medicine is highly desired and recommended, it encounters big obstacles due to the absence of accessible analytical instrumentation and due to the way medical practice is carried out. Generally, drug indigestion is followed by its absorption, distribution, metabolism and elimination. Therefore, pharmaceutically active compounds will be present in wastewaters. Monitoring the successful removal of antibiotics from the ecosystem is of high importance. Drinking water treatment plants play an important role in the removal of the unwanted compounds. Nevertheless, because of the strong fluctuations throughout the year, the effectiveness of the cleaning process has to be continuously monitored. Ciprofloxacin, also a fluoroquinolone antibiotic, is excreted in urine, with the parental drug representing more than 50 %. This and the fact that for some medical treatments the drug dose is 1000 mg [66], its concentration in environmental samples might exceed the MIC values (0.024 μM for *E. Coli* to 12 μM for *S. aureus*). Therefore, in order to avoid the creation of drug-resistant bacteria strains, beside responsible medical practice, also the prevention of the presence of antibiotics in the ecosystem is of high interest.

In the following section of the thesis, the current state of research will be summarized. Details concerning the basic principles of the reference analytical methods will be described together with their application in the detection of the four drugs presented above. This will be followed by the introduction of the LoC-SERS technique as an alternative detection method to the available reference methods. In the last section of the thesis, the results published in five different manuscripts will be summarized with highlighting the potential and limitations of the applied analytical method.

1.3 Analytical Methods for Drug Detection – current state of research

1.3.1 Reference analytical methods

Clinical samples

At the beginning of the 20th century neither the PK or PD concept existed. The first mathematical model describing drug elimination rates was published in 1924 by Widmark and Tandberg [84, 85]. 40 years later drug level determinations were established in the clinical environment. The biggest barrier against advancement was the absence of appropriate analytical methods. Although gas chromatography (GC) was already used to monitor antiepileptic drugs at the beginning of the 1950s, the antibody-based immunoassays won the competition twenty years later due to their accuracy and easy integration into clinical laboratory. Nowadays, both chromatography and immunoassay methods are in use due to the different needs and capabilities of individual laboratories [86]. In the following, a brief description of these techniques will be presented together with their pros and cons and their application for detecting MTX, levofloxacin and NTX in body fluids.

Immunoassays

The discovery of the immunization process by Berson and Yalow [87] led to the first insulin immunoassay. Currently, there are over 25 immunoassays commercially available and routinely used in drug monitoring [88]. Among the homogeneous platforms, fluorescence polarization immunoassay (FPIA), enzyme multiplied immunoassay technique (EMIT®) and the cloned enzyme donor immunoassay (CEDIA®) are leading the market. Heterogeneous assays are ADVIA Chemistry, Centaur®, ACCESS®, Elecsys® and AxSym®.

The working principle of the platforms is governed by the antigen-antibody binding reaction. The technique gains its high specificity and sensitivity from three important properties of the antibodies: (1) the ability to bind to both natural and synthetic molecules, (2) specific binding and (3) the binding strength [89].

Two different designs are available: immunometric and competition assays [88]. The first one is also referred to as “sandwich” assay because it uses two different specific antibodies that form a sandwich around the target of interest. These platforms (i.e. the enzyme-linked

immunosorbent assay (ELISA)) are mainly applied for the detection of molecules with large molecular weight, such as proteins or peptides. For the detection of small weight molecules, i.e. drugs, the competition design is preferred. Here, the target molecule competes with a fixed amount of tracer (labeled molecule) for a limited number of antibodies [9]. The affinity for the antibody of the molecule is higher as compared with the affinity of the tracer. Therefore, when the target molecule is present in the sample, fewer tracers will bind to the antibody as compared with the situation when the sample contains no such molecule. The activity (i.e. radiation, fluorescence or enzymatic activity) of the tracer is the one measured in order to determine the concentration of the molecule in the sample. If the signal comes from the bound tracers the concentration of the molecule will be indirectly proportional to the signal, whereas when the free fraction is measured, the concentration is directly proportional to the signal. There are two variations of the competitive assays: the heterogeneous and the homogeneous one. In the first case, the unbound tracers are separated by physical or chemical techniques from the antibody-antigen complex prior to measurements. In the second case, the tracer generates a signal only when it is bound to the antibody, therefore, no separation is needed.

MTX is one of the most potent anticancer drug, but at the same time, it is also the one having the most reported toxic events. Thus, the number of developed immunoassays for its detection is very high. Siemens commercializes the ARK™ Methotrexate Assay [90, 91], while Abbott Diagnostics offers the TDx/TDxFLx Methotrexate II assay [92] and the Architect Methotrexate chemiluminescent assay [93]. A forth assay is available at a Japanese company, the Nanopia eTDM Methotrexate from SEKISUI MEDICAL CO. [12]. Generally, the analytical range of these platforms is between 0.01 μM and 1.2 μM. For samples having MTX concentration higher than the upper limit of quantification (LOQ) dilution must be carried out. This presents two main disadvantages: (1) longer analysis time due to repetition and (2) errors induced by a subsequent step. Furthermore, each assay has its own specific reagents. Once the company is withdrawing the reagents from the market, the detection platforms have to be also changed [63] if no new generation reagents are provided. This will lead to unexpected costs for the clinical laboratories. Additionally, it was reported, the change of the reagents, can lead to overestimation of the MTX concentrations [63]. No commercial immunoassay is available for levofloxacin or NTX detection in biological fluids. However, recently a study has been published by Shanin *et al.* [94] concerning the detection of levofloxacin by FPIA in human urine. Garenoxacin tagged by 4'-aminomethylfluorescein was used as tracer yielding a detection limit of 1 ng/ml and a linear dynamic range between 2.5 to 50 ng/ml. Because levofloxacin concentrations in human urine are high (~498 ± 247 μg/ml), the urine samples were diluted 40

times prior to the measurements. Furthermore, cross-reactivity was observed for multiple drugs closely related to levofloxacin.

Overall, immunoassays offer numerous advantages and thus, they are often encountered in the clinical chemistry laboratories [86]. They are easily integrated due to their simplicity. The excellent automation removes the potential source of human errors. Immunoassays purchased from the same manufacturer share the same method leading to comparable results in between laboratories. But, after more than 60 years of history, immunoassays are still presenting cross-reactions with metabolites and other substances, while multiplexing is still a big challenge. The development of new assays is time-consuming (up to one year) and most often the consumer has to rely on immunoassays developed by companies. Furthermore, in many cases, a dilution of the samples is needed in order to decrease the concentration of the target molecule in the sample. This can lead to errors as well as to increased reagent volumes needed for analysis.

Chromatography methods

Although immunoassays are leading the market in the field of clinical chemistry, chromatography techniques are still considered to be the reference methods for drug detection and monitoring. Their main advantages over immunoassays are the exquisite selectivity, the ability to develop new assays in a more rapid time frame, as well as the possibility to detect several compounds in a single run [86].

Chromatography methods can be divided into three main classes: GC, liquid chromatography (LC) and supercritical fluid chromatography (SFC). For drug detection both GC and LC techniques are commonly applied, whereas SCF is mainly used in industry for the separation of chiral molecules [95]. Regardless of the chosen chromatography method, the sample analysis process has three steps. The first one consists in a sample pre-treatment procedure. This is followed by the separation of individual compounds in distinct elution bands. Finally, the identification is carried out with various detectors.

The sample preparation plays a major role in the analytical procedure as it has a great influence on all subsequent analytical steps. The aim of all sample clean-up procedures is to extract the target analyte from the biological samples with high recovery rates and to minimize the matrix effects [96]. The most commonly encountered sample treatment procedures include liquid-liquid extraction (LLE), protein precipitation (PP) and solid-phase extraction (SPE). Decades ago these protocols were developed in-house, making it impossible to compare results in between laboratories. Additionally, it was the most labor-intensive and error-prone process in

the overall bioanalytical methodology [96]. Currently, for many of these procedures, commercial kits are available. For example, the development of membrane-based PP filter plates [97, 98] allowed the automation of the PP step and the reduction of the sample preparation time from 4-5 h to 1-1.5 h. Furthermore, a major advancement was brought by the introduction of the on-line solid phase extraction (OLSPE) platforms. Two types of OLSPEs are commercialized: the restricted access material (RAM) column [99, 100] and the turbulent flow chromatography (TFC) column [101]. Both columns separate small molecules, such as drugs, from large molecular species (proteins) in a biological matrix. They function as pre-column units and are combined with the analytical column via a column switching procedure.

After an effective sample clean-up procedure, the chromatographic separation is carried out. The working principle of all systems relies on a mobile phase having the role to transport the analytes through a column that contains the stationary phase [95]. The molecules in the sample interact with the stationary phase. Depending on the chemical structure of each analyte, the interaction strength is varying. Thus, the separation is achieved based on the retention time in the separation column.

Although GC has a great analytical performance, it is limited to the detection of volatile non-polar compounds [88, 95]. LC, on the other hand, has no such limitations, both polar and non-polar molecules can be successfully separated. After more than one century from its discovery by Michael Tswett, there have been numberless variations of LC techniques reported and summarized in review articles [14, 22, 102-106]. Column based LC method is the most commonly used one. Separation can be performed in the “normal” configuration, where the stationary phase is polar and the mobile phase is nonpolar; or in the “reverse phase” configuration, where the stationary phase is nonpolar and the mobile phase is polar. The last developments in the field aimed toward fast LC [106]. For this, new column sorbents were prepared [107, 108], separation was performed at high temperatures [109] or ultra-high performance liquid chromatography (UHPLC) [18, 19] was introduced. Another popular analytical method for drug analysis application is the hydrophilic interaction liquid chromatography (HILIC) [23, 110, 111].

Chromatographic separation only does not provide information about the identity of the eluted molecules. For identification, different detectors can be used, such as UV-Vis absorption, fluorescence detection (FLD), Fourier transformed infrared spectroscopy or mass spectrometry (MS) [95]. UV-Vis detectors are commonly available on the high-performance liquid chromatography (HPLC) platforms since most of the organic molecules have a chromophore capable of absorbing either UV or visible light. Fluorescence detectors can be used for

molecules capable of fluorescing, whereas MS is a universal detector. Initially, HPLC-MS techniques were mainly used only in research facilities due to their high costs. However, because of their exceptional sensitivity and selectivity originating from the detection of charged particles based on their mass, the accessibility was increased thanks to the undertaken technological advances.

Contrary to the case of immunoassays, chromatography methods are not "turnkey" analyzers. Protocols are in-house developed and adapted for specific requirements. This leads to an impressive number of publications. Molecules which cannot be detected by immunoassays because of the absence of an appropriate antibody can be easily quantified with LC methods.

More than 300 publications related to the LC determination of MTX in biological fluids have been reported, with more than 40 studies published in the last five years. **Table 1** summarizes the analytical performances achieved in selected publications. Most of these studies used MS for detection. Furthermore, most often beside MTX also its metabolites were quantified. As biological matrix either human plasma or serum was considered. Prior to measurements, manual PP was carried out and only in one case SPE was applied. Information regarding the run-time of the chromatographic separation was not provided by all authors. The linear response and the LOQ values varied strongly between methods. This is one of the factors which inhibits result comparison in between laboratories.

Table 1. Recently published studies on MTX detection.

Method	Detected molecules	Sample	Sample treatment	Run-time	Linear range	LOQ	Ref.
HPLC-UV	MTX	serum	SPE	12 min	0.025-5 µM	0.01 µM	[62]
LC-MS/MS	MTX 7-OH-MTX	plasma	on-line PP	-	0.025-50 µM	0.025 µM	[7]
HPLC-UV	MTX	serum	centrifugation	-	0.058-1.39 µM	0.019 µM	[112]
HPLC-UV	MTX	serum	PP	10 min	0.11 –22 µM	0.044 µM	[113]
TFC–LC–MS/MS	MTX, 7-OH-MTX, DAMPA	serum	PP		0.01-1 µM	0.01 µM	[114]
LC-MS/MS	MTX	plasma	PP	5 min	110 pM–55 nM	110 pM	[115]
LC-MS/MS	MTX	serum	PP	5 min	0.01–1 µM	0.01 µM	[116]
LC-MS/MS	MTX	plasma	dilution, PP	3 min	0.005-50 µM	0.005 µM	[10]
HPLC-FLD	MTX, 7-OH-MTX, DAMPA	plasma	PP	-	0.010-20 µM	0.005 µM	[117]

Abbreviations: 7-OH-MTX: 7-hydroxy methotrexate, SRM: selected reaction monitor, DAMPA: 4-amino-4-deoxy-N10-methylpteroic acid.

In the case of levofloxacin, nine publications are summarized in **Table 2**. In comparison with the LC assays for MTX detection, the number of concomitantly determined drugs is higher. Additionally, beside human plasma, other biological samples were also analyzed. As in the case of MTX, the most commonly encountered sample clean-up procedure was done by PP. The run-times are considerably longer when compared with the run-times in **Table 1**. But this is due to the simultaneous detection of multiple antibiotics in the same run. Linear ranges and LOQs are once again method dependent. By taking into account that no commercial immunoassay is available for levofloxacin detection in biological fluids, LC methods found a niche and present a great advantage due to their multiplexing capabilities.

As already mentioned before, in the case of NTX the number of reported studies concerning its detection is very limited. In 1981 Sorel *et al.* [118] published the first and only

Table 2. Recently published studies on levofloxacin detection.

Method	Detected molecules	Sample	Sample treatment	Run-time	Linear range	LOQ	Ref.
HPLC-UV	linezolid rifampicin levofloxacin moxifloxacin	plasma	PP	28 min	-	0.63 µM	[119]
HPLC-UV and FLD	levofloxacin + 5 quinolones	plasma	ultrafiltration	-	0.13-27 µM[i] 0.055-13 µM[ii]	-	[120]
SPE-HPLC-UV	levofloxacin	plasma, bone tissues	SPE	12 min	-	0.2 µg/g	[121]
HPLC-UV	levofloxacin gatifloxacin moxifloxaci	plasma	on-line extraction	-	0.34-11 µM	0.34 µM	[122]
HPLC-FLD	levofloxacin	plasma		-	0.14–14.4 µM	0.14 µM	[123]
HPLC-UV	linezolid tinidazole levofloxacin + 5 quinolones	plasma	PP	-	0.27–27 µM	0.27 µM	[124]
HPLC-UV	levofloxacin + 4 quinolones	plasma	PP	-	0.055–13 µM	0.055 µM	[125]
UHPLC–MS/MS	beta-lactams aminoglycosides penicillins cephalosporins carbapenems quinolones	urine, serum	dilution, PP	<6 min	-	1.38 µM[iii] 0.27 µM[iv]	[126]
HPLC-UV	levofloxacin	plasma	PP	4.5 min	0.276–33 µM	-	[127]

[i]UV, [ii] FLD, [iii] urine, [iv] serum

Abbreviations: MS/MS: tandem mass spectrometry

HPLC analysis of NTX in human urine and plasma. The determined limit of detection was 0.42 μM and a linear range between 0.415 and 208 μM was obtained for the plasma samples. However, the method presented tailing effects due to co-elution of NTX with structurally related compounds present as impurities. More than twenty years later, Kang *et al*. [128] reported the detection of NTX by HPLC-UV method. Nevertheless, the molecule was detected in its pure form for the purpose of quality control rather than for clinical purposes.

Environmental samples

Chromatographic separation combined with MS is also the reference analytical method for the detection of pharmaceutically active chemicals in environmental samples. Before detection, the molecules have to be pre-concentrated via either off-line or on-line SPE procedures. The sampled volumes range between 500-1000 ml for the off-line SPE method, whereas for on-line pre-concentrations this can be reduced to 50-100 ml [129]. When tandem MS is employed as detection, the sample volume is reduced below 5 ml, but the equipment cost is considerably increased.

Depending on the objectives pursued, the screening methods for environmental samples were divided in three different categories [129]. Qualitative and semi-quantitative techniques aim to quickly detect the presence of one or more compounds in the sample. Quantitative methods provide the exact concentration of the chemical compound in the sample, whereas confirmatory methods certify the identity of the compound with or without quantitative determinations. Another classification is based on whether the detection is focused on one specific molecule or not [130]. In the case of the pre-target screening, the molecule is *a priori* selected and no other compounds are detected. For the post-target screening all molecules are detected followed by the confirmation of the identity of a post-selected molecule. Finally, the non-target screening, referred to as general unknown screening, detects all chemicals accessible to the particular analysis and focuses on unexpected or unknown substances. The pre-targeted screening method is currently the most commonly used technique facilitating the detection of multiple molecules [131-134].

FLD and MS/MS techniques are commonly used for ciprofloxacin detection after the chromatographic extraction with LC or HPLC. Table **3** summarizes eight selected publications. All techniques perform multiplex analysis. Besides ciprofloxacin two to nine other fluoroquinolones were simultaneously detected in various environmental samples. After SPE or filtration procedures the LOQ values range between 1.44 pM to 2.33 nM.

Table 3. Recently published studies on ciprofloxacin detection.

Method	Detected molecules	Sample	Sample treatment	Linear range	LOQ	Ref.
LC-FLD LC-MS/MS	Ciprofloxacin 9 other FQ	sewage	SPE	0.27-59 nM	100 pg*	[135]
LC-MC/MS	Ciprofloxacin 4 other FQ	surface water sewage	SPME	0.3-300 nM	51 pM	[136]
LC-FLD LC-MS/MS	Ciprofloxacin 3 other FQ	sewage	SSPE	-	30 pM	[137]
LC-fluorescence	norfloxacin ciprofloxacin enrofloxacin	surface water	filtration	150-3000 nM	75 pM	[138]
HPLC-FLD	Ciprofloxacin 4 other FQ	surface water groundwater sewage	SPME	2.3–150 nM	2.33 nM	[139]
LC-MS/MS	Ciprofloxacin 5 other FQ	surface water	MMIP	60 pM-6 nM	16 pM	[140]
LC-FLD	Ciprofloxacin 3 other FQ	surface water	SPE	-	1.44 pM	[141]
coupled-column LC-FLD	Ciprofloxacin 8 other FQ	surface water	Online SPE	60–950 pM	60 pM	[142]

* instrumental quantification limit calculated as absolute amount injected in pg (injection volume 200 µl)
Abbreviations: SPME – solid phase microextraction; SSPE – selective solid phase extraction; MMIP - magnetic molecularly imprinted polymer.

In conclusion, chromatographic methods have a high analytical power in the detection of low weight molecular species for clinical and environmental applications. However, one should not forget that the analytical methods based on the chromatographic separation require a large initial capital investment and, later, high service costs. There is a lack of standardization, therefore results from different laboratories are not comparable. Furthermore, they are sophisticated methods requiring qualified staff and are not suitable for on-site detection.

1.3.2 Surface Enhanced Raman spectroscopy as alternative detection method

For the identification of drugs in complex matrices, the analytical method has to yield great specificity. Vibrational spectroscopies are well known for giving molecular specific information. Both vibrational infrared (IR) and Raman spectroscopy take advantage of the vibrational modes of molecules, which result from the interaction of the sample with electromagnetic radiation. IR spectroscopy is based on the absorption of the near and mid-IR electromagnetic radiation by molecules undergoing a change in the dipole moment during vibration. In the case of Raman spectroscopy, molecules, which present a change in polarization during vibration, inelastically scatter the electromagnetic radiation. Water, one of the main constituents of the biological and environmental samples, has high absorption in the IR range, whereas its scattering cross section is very low. Thus, for analysis of aqueous samples Raman spectroscopy is preferred instead of IR absorption spectroscopy.

The first experimental evidence for the inelastic light scattering was given by C. V. Raman and K. S. Krishnan [143] in 1928. Since its discovery, Raman spectroscopy found a large variety of applications in material and life sciences. The effect is based on the inelastic scattering of light by molecules. When an electromagnetic radiation (ω_0)[1], i.e. photons of a laser beam, interacts with the molecules of a sample, besides the elastically scattered photons (referred to as Rayleigh scattering) also photons with a modified frequency ($\omega_s=\omega_0-\omega_{vib}$ Stokes scattering and $\omega_s=\omega_0+\omega_{vib}$ anti-Stokes scattering) are scattered [144]. The Raman effect is a two photon process [145], where a photon with energy $\hbar\omega_0$ is annihilated and a new photon with energy $\hbar\omega_s$ (or $\hbar\omega_{AS}$) is created as a consequence of the radiation-material interaction. If the molecule is in the electronic ground state, the inelastic scattering process via a virtual state[2] results in the energy loss of the incident photon and the scattering is referred to as Stokes Raman scattering [145]. On the other hand, if the electrons of the molecule are in a vibrational energy level of the ground electronic state, the inelastic scattering process via the virtual state leads to energy gain of the incident photons and the scattering is referred to as anti-Stokes scattering.

[1] ω_0 is the angular frequency of the incident electromagnetic radiation. $\omega_0=2\pi\nu_0=2\pi c_0\tilde{\nu}_0=2\pi c/\lambda_0$, where ν_0 is the frequency, $\tilde{\nu}_0$ is the absolute wavenumber and λ_0 is the wavelength of the incident radiation, whereas c_0 is the speed of light in vacuum.
[2] the virtual state is a mathematical construction of the quantum mechanical perturbation theory.

Enhanced Raman Spectroscopies

The inelastic light scattering is a very weak process, thus only a very small amount of the incident photons will be inelastically scattered [145]. Consequently, the detection of analyte molecules present at very low concentration is limited. To overcome this drawback, different signal enhancement strategies can be applied. The two most commonly encountered techniques are resonance Raman spectroscopy and SERS. The resonance Raman effect appears when the incident electromagnetic wave has energy close to the energy needed for an electronic dipole transition within the molecule [145, 146]. The positions of the Raman bands are at electronic ground state vibrational frequencies, whereas the intensities are considerably enhanced (up to six orders of magnitude [146]) due to the electronic dipole transition [147]. However, the Stokes shift between the absorption and fluorescence of the molecule has to be big enough in order to avoid the overlapping of Raman bands with the fluorescence background.

The SERS effect was first observed in 1974 by Fleischmann while recording the Raman spectrum of pyridine adsorbed on a roughened silver electrode [148]. Forty years later, 15% of the overall Raman publications are related with this topic (according to the numbers provided by the ISI Web of Science). The SERS technique gained popularity due to its high sensitivity. SERS combines the Raman technique with the plasmonic properties of nanostructured coinage metals. Its high signal enhancement originates from two mechanisms: the electromagnetic enhancement (EM) and the chemical enhancement (CE) [34-36, 149, 150].

The main driving force of surface enhanced spectroscopies is the plasmon, "*a quantum quasi-particle representing the elementary excitations, or modes, of the charge density oscillations in a plasma"* [151]. When, i.e., a spherical metallic particle interacts with an electromagnetic radiation with ($\lambda >> d$)[3], polarization within the nanoparticle is induced. If the frequency of the incident wave (ω_0) matches the oscillation frequency of the charge density, the particle acts as a dipole antenna and emits light. The plasmon resonance condition for a spherical nanoparticle is fulfilled when ($\epsilon(\lambda) = -2\epsilon_m$)[4]. This condition is only partially met because of the presence of the imaginary part, Im($\epsilon(\lambda)$), of the dielectric function. The resonant excitation is associated with a local field enhancement referred to as the dipolar localized surface plasmon polariton (LSPP) [151]. Furthermore, under appropriate experimental conditions (Kretschmann

[3] λ is the wavelength of the incident electromagnetic radiation, whereas d is the diameter of the spherical nanoparticle.
[4] $\epsilon(\lambda)$ represents the dielectric function of the nanoparticle, whereas ϵ_m is the dielectric constant of the surrounding medium.

or Otto configuration) propagating surface plasmon polaritons (PSPP) can be also induced at the interface between a dielectric and a metallic layer [151]. The increased local electric field ($E_{loc}(\omega_0)$) caused by the dipolar LSPP or PSPP is the source of the signal enhancement and the basis of the EM mechanism. If a molecule is in the vicinity of the metallic particle supporting LSPP, first an increased scattering intensity will arise because of the induced dipole moment given by $\mu_{ind}=\alpha_{molecule}E_{loc}(\omega_0)$ instead of $\mu_{ind}=\alpha_{molecule}E_0(\omega_0)$. Furthermore, the inelastically scattered light (ω_s) will also be enhanced if the frequency of the scattered electromagnetic wave is in resonance with the plasmon of the metallic particle. Therefore, the overall SERS intensity will be given by following mathematical relation: $I_{SERS}=I_{loc}(\omega_0)I_{loc}(\omega_s)=|E_{loc}(\omega_0)|^2|E_{loc}(\omega_s)|^2$ [40]. For incident electromagnetic waves having wavelengths in the blue and green region $\omega_s= \omega_0-\omega_{vib}\approx \omega_0$ and the approximation $I_{SERS}\approx|E_{loc}(\omega_0)|^4$ is valid [150, 152].

The EM mechanism was proved to account for signal enhancements up to 10^{11} [153]. However, factors of 10^{14}-10^{15} [33, 154, 155] have been reported in literature. The additional signal gain was attributed to the CE mechanism. Three different processes have been suggested to contribute to this: (1) chemical interaction of the nanoparticle and molecule in the electronic ground state; (2) resonant excitation of the charge-transfer process between the molecule and the nanoparticle; and (3) the resonance Raman enhancement [156, 157]. In the first case, the molecule is not covalently bound to the surface of the nanoparticle. However, the presence of the metal perturbs the electronic structure of the analyte inducing a slight change in its electronic distribution. In the second case, it was shown, depending on the relative energies of the Fermi level of the nanoparticle, the highest occupied molecular orbital and the lowest unoccupied molecular orbital of the molecule, charge transfer from molecule to metal or from metal to molecule can occur. Lastly, the resonance Raman enhancement coupled with the presence of nanoparticles, also referred to as surface enhanced resonance Raman spectroscopy (SERRS), it is based on matching the energy of the incident radiation with the energy needed for an electronic dipole transition within the molecule.

As mentioned above, Raman bands are observed for those vibrational modes of the molecules that present a change in their dipole electric polarizability during vibration. However, under SERS conditions, vibrational modes forbidden by this selection rule have been reported [158, 159]. The unusual phenomenon was associated with the strong evanescent character of the local electromagnetic field at the surface of the metallic nanoparticles. When the size of the molecule to be detected is comparable with the local electric field gradient, the excitation of

multi-pole transitions becomes significant. The effect is referred to as the gradient-field effect or "quadrupole-SERS" [35, 160].

A second effect influencing the SERS spectrum is the orientation of the molecules on the metallic surface; effect known as surface selection rules [161]. According to these rules, when the polarizability of the local electric field is perpendicular to the surface, Raman modes of the adsorbed molecule with strong polarizability tensor component normal to the surface are selectively enhanced as compared with the Raman modes with strong parallel polarizability tensor components [161, 162]. Therefore, the overall SERS spectrum will be influenced by the orientation of the molecule and will differ from the reference Raman spectrum.

SERS active substrates

Silver and gold are the most commonly used metals for fabricating SERS active substrates. Silver is preferred when the aim is focused on high signal enhancement, whereas gold is chosen mainly because of its higher stability under atmospheric conditions. The difference between the strength of the LSPP of the two metals can be explained by comparing their dielectric functions. The real part of the dielectric function ($\mathrm{Re}(\epsilon(\lambda))$) is comparable because of the similar electronic densities of the two metals [151]. However, gold has a considerably higher absorption at $\lambda<600$ nm associated with a higher magnitude of the $\mathrm{Im}(\epsilon(\lambda))$ because of the inter-band electronic transitions [163]. Therefore, for this spectral region, the strong LSP resonances of small gold nanoparticles are significantly damped. Gold particles with diameter > 50 nm present resonances in the $\lambda>600$ nm spectral region. However, at this dimensions also radiation damping starts to become important and it limits the strength of the LSP resonance [164].

SERS active nanostructures can be synthesized in numerous ways, such as bottom-up methods for obtaining metal colloids or core-shell nanoparticles, self-organization or template-assisted methods and top-down processes [42]. Despite of the great technological advances, metallic colloids represent the most simple and accessible route to SERS. The Ag nanoparticles prepared by the Lee-Meisel protocol [165] are the most widely used ones. Here, silver nitrate is reduced by sodium citrate at water boiling temperature. An alternative to this, is to synthesize nanoparticles via the Leopold-Lendl protocol [81]. The reaction takes place at room temperature by reducing silver nitrate with hydroxylamine hydrochloride in the presence of sodium hydroxide. Both protocols yield silver nanoparticles with diameters between 30-40 nm and a plasmonic resonance maximum around 410 nm. The direct optical extinction measurements

(UV-Vis spectroscopy) are one of the simplest methods to characterize metallic colloidal solutions [43]. The UV-Vis spectra exhibit one, or sometimes more, bands associated with the resonant wavelength of the LSP resonances of the substrate. However, the connection between the extinction spectrum and the magnitude of the electromagnetic SERS enhancements is in general indirect. For example, the single particle LSP resonances present a strong extinction band despite their no or very low SERS signal enhancement [44], whereas coupled-LSP resonances originating from two or more closely located nanoparticles ("hot-spots") have a weak extinction spectrum despite of their large local field enhancement.

SERS applications

Throughout the last years, SERS advanced from being a technique mainly used to characterize molecule-metal interactions [166, 167] and detection of dye molecules in pure water [168, 169] to quantification of biomolecules in clinical and environmental samples [170-173] as well as the detection of biomarkers of various diseases [174, 175]. The clinical and environmental matrices have a rich chemical composition. Therefore, the target molecule to be detected will compete with the molecules of the complex matrices for binding sites on the metallic surface. Whole blood, plasma and serum represent the biggest challenge [25, 176], whereas urine samples and environmental samples are easier to handle.

SERS measurements in blood samples were carried out mainly to discriminate between blood samples of patients having cancer and blood samples of healthy individuals [174, 175, 177-180]. The number of reports focused on the SERS detection of drugs in blood is very low. Folic acid was detected in spiked blood serum diluted to 1% with water with a limit of detection of 9 nM [181] or in serum diluted to 80% followed by protein precipitation at 1 μM [182]. Paclitaxel, an anti-cancer drug, was quantified in spiked human plasma down to 10^{-8} M [183]. A recent publication [184] reported on the successful determination of MTX spiked in human serum. The employed SERS active substrates were prepared by depositing gold nanoparticles on paper by a dip-coating procedure for one week. Calibration standards were prepared by spiking a drug-free serum with MTX dissolved in phosphate buffered saline solution at a ratio of 1:4. The samples were deposited on the SERS active substrate by drop coating. The linear dynamic range was assessed to be between 0.1-150 μM. As mentioned in the previous sections, the number of developed assays for MTX quantification is very high. Thus, for a new method to be taken under consideration as an alternative detection technique, it has to provide good analytical

performances, lower costs, and easy access. The preparation of SERS active substrates by long dip-coating procedures presents a great handicap. In one other report, levofloxacin lactate was detected in mouse blood via SERS and an optical fiber nanoprobe coated with gold nanoparticles [185]. The authors compared the detection of the molecule in a conventional setup by employing the gold nanoparticles in colloidal solution as SERS substrate with the detection capabilities of the fiber nanoprobe. However, the publication does not assess the analytical performances of the method and no details regarding the detected concentrations in blood are provided. Concerning, nitroxoline detection in biological fluids, no literature is available on this topic up to date.

The complexity of urine samples as compared to the blood ones is considerably reduced. Water is the main component, followed by urea and creatinine. The protein content is very low in the case of healthy individuals, therefore the number of interferences is considerably reduced as compared to blood. Endogenous molecules, such as creatinine [30, 31, 186, 187] and uric acid [28, 32, 188], drugs, i.e. opioid tramadol [172], benzodiazepines [11], 3, 4-methylenedioxy methamphetamine [173, 189, 190], and tobacco-related biomarkers [26, 171] were successfully detected by SERS in urine samples. MTX is strongly metabolized. Thus, its detection in urine samples is not feasible. On the other hand, antibiotics used for treating urinary tract infections are most often present in high concentrations in urine. Despite this fact, studies related with neither levofloxacin or nitroxoline detection have not been reported. Instead, moxifloxacin, another fluoroquinolone, was quantified by SERS and multivariate curve resolution on nanostructured gold surface [170]. However, the matrix was strongly diluted (to 1%) in order to obtain good results.

Environmental samples, especially surface water samples, present the lowest matrix complexity. However, the molecules to be detected are very different. Pesticides, polycyclic aromatic hydrocarbons, polychlorinated biphenyl, explosives, heavy metal ions, antibiotics, hormones, pathogens and many other compounds are considered as water pollutants [191]. Multiple SERS reviews summarize the successful detection of these molecules [37, 191-193]. Ciprofloxacin detection was reported by using various SERS substrates [39, 194-196]. The detection limits ranged from 1 nM in distilled water in the case of the core–shell structured magnetic molecularly imprinted polymers to 0.2 μM in the case of dendritic silver nanostructures. However, none of the publications proved the feasibility of SERS for detecting the molecule in environmental samples.

Quantitative SERS measurements

The above reviewed studies were based on using dry, planar SERS substrates or metallic nanoparticles in colloidal solutions. In the first case, challenges appear because of the correct sample deposition on the substrate. Commonly, drop coating is practiced. This creates a heterogeneous layer of analyte molecules on the surface due to the coffee-ring effect yielding SERS signals with low reproducibility. When the substrates are incubated into the sample, the incubation time will strongly influence the final SERS results. On the other hand, metallic colloids need to be aggregated to create hot-spots. This can be achieved via: (1) the effect of the analyte itself acting as an aggregating agent by changing the surface charge of the nanoparticles, (2) the addition of a passive electrolyte such as KNO_3, (3) the addition of an active electrolyte such as KCl or by (4) the addition of polymers or long-chain ions [43]. The aggregated metallic nanoparticles yield great signal enhancements, but the SERS spectrum of the molecule to be detected becomes dependent on the time elapsed between the induction of the aggregation and the measurement [45]. Furthermore, the mixing order, ratio and time lapse between mixing of the nanoparticles, the analyte solution, and the aggregation agent have a crucial influence on the SERS signal [56, 197]. All these parameters will yield a very poor reproducibility of the SERS signals of the molecules to be detected and will result in the impossibility to perform quantitative measurements.

Various strategies have been developed to overcome these limitations. One of the approaches consists in the implementation of internal standards [24, 27, 52, 55, 198-202]. In order to have reliable results, the signal of the internal standard has to be influenced by the presence of the plasmonic nanostructures, yielding a SERS signal rather than just a Raman spectrum.

A second approach to achieve reproducible measurement conditions combines SERS with microfluidic platforms. Microfluidics offers the great advantage of highly precise controlled manipulation of nanoparticle and sample solution and high sample throughput. Two different designs are available: the continues-flow and the segmented-flow approach [29, 50, 57]. In the first case, the SERS active nanostructures are generally immobilized on the surface of the microchannel, the sample is continuously pumped into the channel, while the detection is carried out on the surface of the channel wall. An alternative to this is the simultaneous flow of the nanoparticle solution and sample. Nevertheless, because of the continuous flow, analyte molecules can stick to the channel walls and the reliable detection is inhibited by the “memory

effects". Additionally, the immobilization of SERS active substrates in the channel walls is not trivial.

In the second approach, also referred to as droplet based microfluidics, the solutions are dispensed into individual droplets surrounded by an immiscible liquid phase. Therefore, the liquid of interest does not wet the channel walls and cross contamination can be prevented as long as the molecules do not diffuse to the carrier fluid [58]. The flow of the liquids is controlled either by volume, i.e. using syringe pump systems, or by pressure, i.e. hydrostatic reservoirs. The droplets can be trapped, sorted, mixed, or split, based on the specific experimental requirements [58, 203]. Commonly, the employed nanoparticles are previously synthesized and then injected into the chip, but also the *in-situ* nanoparticle synthesis has been reported [38, 41, 204, 205]. This offers a great advantage because the challenges represented by batch-to-batch reproducibility and colloidal solution aging effect can be avoided. Furthermore, each droplet can be considered as a micro-cuvette or a micro-reactor. The colloids are mixed with the analyte in a reproducible way and by mounting the chip on the microscope stage and fixing the focus point the aggregation time can be easily controlled.

Traditional quantitative measurements are carried out by first establishing a calibration curve. Generally, each analyte will give different signals; therefore, the analytical response has to be measured for each analyte at known concentrations using standard solutions. Based on these measurements, calibration curves are constructed using the method of least squares and the concentration of the analyte in the unknown sample can be determined. However, this procedure will yield correct results only if the chemical composition of the standard solutions and the unknown sample is identical. If this is not the case, the so called matrix effects will inhibit the correct prediction of the unknown concentration. Furthermore, in the case of SERS, because of the batch-to-batch quality variations of the plasmonic substrates, this strategy is not feasible.

A solution to this problem is represented by the standard addition method (SAM). Here, all analytical measurements, including the calibration curve, are performed using the sample itself and the slight variation between colloid batches will have no impact on the final results.

The SAM experiments are carried out as follows: (1) equal amounts of the sample are pipetted into several volumetric flasks, (2) increasing volumes of standard are added to each flask, (3) the content of each flask is diluted to the same volume (Figure 1) [206]. Therefore, every flask contains the same concentration of the unknown and different concentrations of the standard. The standard solutions contain the same analyte as the one to be quantified. The number of flasks minus one represents the number of the standard addition steps (SAS). The

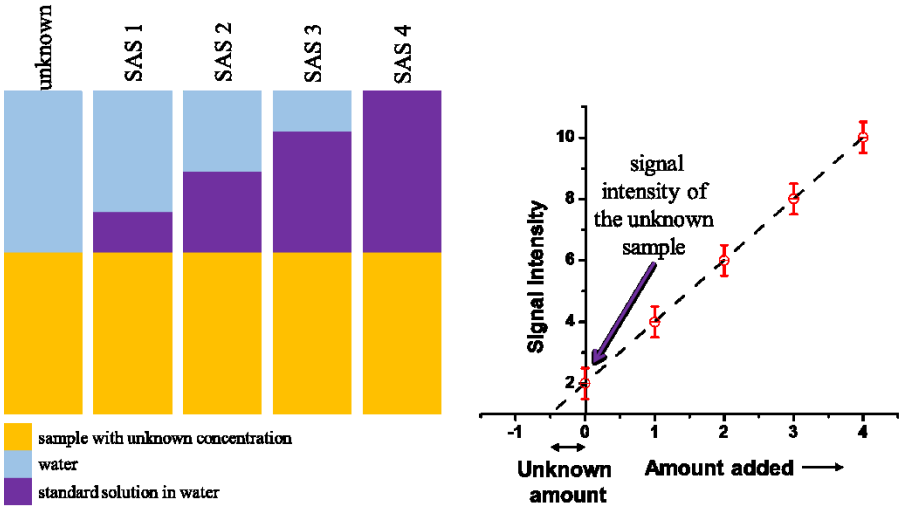

Figure **1**. The standard addition method.

signal intensity for all flasks is measured and plotted as shown in Figure 1. The intercept of the linear regression with the x axis will give the concentration of the analyte in the unknown sample and it is the ratio of the intercept at y=0 and the slope of the regression [207].

For the SAM to work, two conditions have to be fulfilled: (1) the signal of the molecule in the unknown sample has to be detectable by the instrument and (2) the signal intensity as function of the concentration has to be linear. In order for the analyte in the unknown sample to generate a signal, its concentration must be above the detection limit (referred to also as the lower LOD). According to the IUPAC definition, the LOD is equal to the signal of the blank plus three times its standard deviation. Another defined quantity is the lower LOQ, which is commonly defined as the blank plus ten times its standard deviation, and represents the smallest amount that can be measured with reasonable accuracy. The linear range of an analytical method is the analyte concentration range over which the measured signal is proportional to the concentration. The dynamic range, on the other hand, represents the concentration range over which there is a measurable response of the signal to the presence of the analyte, even if the response in not linear.

Multiple SERS studies combined with SAM have been published in the last five years. Buserilin was determined in human urine [208], 4-aminophenol in a pharmaceutical formulation [209], melamine in milk [210], nicotine in artificial urine [171], moxifloxacin in urine [170], congo red [211] and uric acid [28].

In conclusion, the combination of fingerprint specificity of Raman spectroscopy, high sensitivity of SERS, reproducible and automated measurement conditions offered by LoC platforms with the quantification provided by SAM yields a powerful analytical tool for the detection and quantification of both clinical and environmental relevant molecules. Furthermore, thanks to the development of portable Raman setups, the costs of LoC-SERS platforms is significantly lower as compared to chromatography setups. The LoC-SERS measurements can be easily carried out even in the absence of a microscope, just by using i.e. a fiber probes for focusing the laser beam in the microfluidic channels and collecting the inelastically scattered light. Furthermore, the footprint is small facilitating the on-site analysis.

1.4 Own Research Results

1.4.1 Influence of molecule-metal interactions on the SERS signal

It is a prerequisite to first understand the nature of the Raman and SERS spectra of molecules before detecting and quantifying them in complex matrices. During the thesis, the interaction of four different drugs with the surface of the silver colloids was addressed. Reference Raman spectra of the drugs in the powder form were compared with the recoded SERS spectra in cuvettes of the molecules solved in purified water. Based on previously published vibrational characterization performed with density functional theory calculations and by taking into account the surface selection rules described in the previous chapter, the orientation of the molecules on the metallic surface is proposed. However, in order to confirm the validity of the suggested orientations further calculations are required, which are beyond the purpose of the present thesis.

The conformation of the antifolate drug MTX consist of two planar groups: one is the 2,4-diaminoptreidine group and the second one is the (p-aminobenzoyl)-L-glutamat group. The molecule has both hydrophobic (the pteridine and the benzoyl group) and hydrophilic (carboxylate groups) structural groups. In purified water MTX is just sparingly soluble. Therefore, during the experiments presented in reference [IH1] the SERS spectra were recoded under basic pH conditions. The reference Raman spectrum presented in Figure **3** [IH1] has a rich fingerprint in the 200-2000 cm^{-1} spectral range. SERS spectra were obtained by using citrate reduced Lee-Meisel silver nanoparticles. After the nanoparticles were mixed with MTX solution, 1 M KCl was added to induced the creation of hot-spots. Compared with the Raman spectrum, the SERS spectrum of MTX at pH 12 presents slight differences. Three different factors can cause this difference: (1) the molecule-metal interaction, (2) orientation of the molecule on the metallic surface and (3) the deprotonation of the molecule at the carboxylic moiety. Generally, molecules can interact with the silver surface either via the lone pair electrons of the nitrogen or oxygen atoms or via the π orbitals of the aromatic rings. In the case of MTX, possible adsorption sites are via the amino groups. This hypothesis is confirmed by the shift of the Raman band located at 1327 cm^{-1} and ascribed to the NH_2 deformation by 19 cm^{-1} in the SERS spectrum as compared to the recorded Raman spectrum. Further observed differences were associated with the orientation of the molecule on the metallic surface. Namely, the disappearance in the SERS spectrum of the Raman band assigned to the C=N vibration of the pteridine ring suggest that this ring might be parallel with the metallic surface. Simultaneously, the ring breathing mode located

at 956 cm^{-1} of the aromatic ring presents a high SERS signal intensity. Based on the surface selection rules, when the in-plane ring vibrations are enhanced an upright orientation of the molecule is assumed, whereas in the case of the enhanced out-of-plane vibrations the molecule adopts a parallel orientation on the metallic surface. Therefore, the aromatic ring might be perpendicular on the surface. The suggested orientation is graphically illustrated in the inset of Figure **4** [IH1].

The MTX SERS study was carried out with Lee-Meisel nanoparticles [165]. The chemical reaction, during which silver nitrate is reduced by citrate, require water boiling temperature and it lasts for more than one hour. During my experiments, the synthesis was not always successful and the quality of the prepared colloids varied strongly among batches. Therefore, an alternative synthesis procedure was needed. The silver nanoparticles synthesis described in the Leopold-Lendl protocol [81] is carried out at room temperature by adding the silver nitrate solution to the hydroxylamine hydrochloride and sodium hydroxide solution under rigorous string. The reduction of the nanoparticles takes place instantaneously. The colloid batches prepared in this way were stable for more than half a year and the quality variation in between batches was not significant. Recorded UV-Vis spectra are shown in all subsequent publication [IH2-IH5]. Generally, the maximum of the extinction band was located ~408 nm and a full-width-at-half maximum of 80 nm indicates the creation of nanoparticles with a mean size of ~35 nm.

To the best of my knowledge, the first recoded SERS spectrum of levofloxacin was reported in the publication presented in the frame of the current Ph.D. thesis [IH2]. The backbone of the levofloxacin molecule is formed by the quinolone ring system having attached a fluorine atom and a piperazine moiety. The molecule has a zwitterion character at neutral pH due to the presence of both anionic and cationic groups. The reference Raman spectrum measured on powder and in a saturated aqueous solution (Figure **2** [IH2]) differ because, once the molecule is solved in water, the strong packing present in the crystalline form is destroyed, thus, also the polarizability of the molecule might change. As marker bands for the characterization of levofloxacin, the Raman signals at 1395 cm^{-1} (coupled vibration of the quinolone ring system + symmetric COO^- stretching) and 1614 cm^{-1} (C=C stretching) were chosen.

In the case of MTX the aggregation of the Ag nanoparticles was induced by the presence of KCl. Levofloxacin, however, presented a completely different behavior. When the molecule was added to the colloidal solution, the color of the nanoparticles changed. The intensity of the extinction band of the single LSP resonance diminished and a broad band at higher wavelengths appeared in the UV-Vis spectra (Figure **4** [IH2]) of the colloid-analyte

mixture. The most intense SERS signals were recorded when no additional aggregation agent was added to the mixture (Figure **3** [IH2]. In conclusion, levofloxacin itself is inducing the aggregation of the nanoparticles. Furthermore, the order of mixing of the nanoparticles with the analyte solution and KCl was shown to have a major significance. If KCl is added after mixing the nanoparticles with the levofloxacin solution, the SERS signal intensity is lower as compared with the case when no KCl is added. This might be because of an "over aggregation" of the nanoparticles. If the order is changed, and first the nanoparticles are aggregated and only afterwards levofloxacin is added, the two Raman marker bands are almost indistinguishable from the background at a concentration of 1 mM. This behavior might have two explanations. On one side, the chloride ions might block the free binding sites on the surface of the silver nanoparticles. On the other side, by pre-aggregating the nanoparticles, levofloxacin will adsorbed on the surface of the large aggregates instead of the gaps between the single nanoparticles. These features of levofloxacin will have a big influence on the detection of the molecule in the human urine samples. First, because the nanoparticles are aggregated by the antibiotic, the background signal originating from the molecules of the urine samples might be influenced by the aggregation degree of the plasmonic substrate. Second, the salt content will vary among the samples and thus, it can result in sample dependent, increased detection limits.

The interaction of levofloxacin with the metallic surface and its orientation was established based on the differences observed between the reference Raman and the SERS spectrum. First, the ratio of the two Raman marker bands is changing for the different measurements. An increase in relative intensity of the band located at 1395 cm^{-1} (due to the coupled vibration of the quinolone ring system and symmetric COO^- stretching) in the SERS spectra as compared to the Raman spectra might suggest an interaction via the oxygen atoms or the delocalized electrons of the COO^- group. Second, in the SERS spectrum of levofloxacin without KCl additions, a band appears at ~230 cm^{-1}. This was ascribed to the Ag-O stretching vibration. Third, the enhancement of the Raman band located at 1554 cm^{-1} and assigned to the in-plane vibration of the quinolone ring system and the absence of the bands due to the out-of-plane ring vibrational modes might suggest an upright orientation when no KCl is added. Upon KCl addition, this mode (at 1554 cm^{-1}) diminishes in intensity, which might suggest a change in the orientation into a tilted configuration. The suggested orientation of the molecule is illustrated in Scheme **2** [IH2].

NTX is a quinolone derivative with an OH group bound to the carbon atom at the 8^{th} position and a nitro ($-NO_2$) group at the 5^{th} position (chemical structure in Figure **1** [IH4]). Generally, molecules can either physisorb or chemisorb on the metallic surface. In the first case,

the SERS spectra are very similar with the Raman ones, whereas in the second case, relative band intensity ratios change and the position of the bands is shifted. The recorded SERS spectrum of NTX is considerably different as compared with the reference Raman spectrum (Figure **1** [IH4]) indicating that the molecule might be chemisorbed on the metallic surface. More exactly, in the SERS spectrum the intensity of the Raman modes located ~840 cm^{-1} and 998 cm^{-1} are significantly enhanced as compared with their intensity in the Raman spectrum. The two modes were assigned to the aromatic in- and out-of-plane C-H bending modes. Additionally, the intense C-O stretching band at 1313 cm^{-1} is downshifted by ~25 cm^{-1} and the C=N stretching mode at 1465 cm^{-1} is enhanced as compared to the Raman spectrum. A further prove for the chemisorption process is given by the following experiment. When the NTX solution is mixed with the mineral oil, later used as separation medium for LoC-SERS measurements, a certain amount of the molecule will diffuse from the aqueous solution to the oil phase because of the presence of hydrophobic groups in the chemical structure. This will lead to decreased SERS intensities in the subsequent measurements carried out with the LoC platform. However, if NTX is first mixed with the silver nanoparticles the addition of mineral oil does not lead to a SERS signal decrease. This happens due to the high chemical affinity of the molecules toward the metallic surface. This property of the molecule will have a major importance for its successful detection in complex matrixes.

Inconsistencies between available band assignments and the observed spectral changes make the determination of the molecule orientation hard to assess. Namely, both Raman modes at ~800 cm^{-1} and ~840 cm^{-1} were assigned to the C-H out-of-plane bending modes. In the SERS spectrum only the second band is selectively enhanced. The same was observed also for the bands ascribed to the C-H in-plane bending modes at 987 cm^{-1} and 1153 cm^{-1}. Generally, it is expected that bands associated with the same vibrational mode will be equally influenced by the local electromagnetic field of the plasmonic structures. Because this is not the case, the vibrational modes of the molecules have to be newly calculated before a correct description of the orientation of NTX molecule on the Ag surface can be given.

The last investigated molecule in the frame of the thesis was ciprofloxacin. The antibiotic is a fluoroquinolone derivative; therefore, its chemical structure is very similar with the one of levofloxacin (chemical structure in Figure **1** (A) [IH5]). However, its water solubility at neutral and close to neutral pH is limited to ~0.2 mM. In the first part of the published work [IH5] the influence of the pH of the ciprofloxacin solution on its Raman and SERS spectra is discussed. At low pH, the protonation takes place at the amino group of the piperazinyl ring, whereas at high pH the carboxylic acid moiety is deprotonated. In the case of the Raman spectra

of saturated aqueous solution at pH 1 the spectral feature at 1362 cm^{-1} ascribed to the ring stretching vibration of the piperazinyl ring is downshifted by 17 cm^{-1} as compared to the Raman spectrum of the powder and the intensity of the band at 1452 cm^{-1} associated with the CH_2 deformation of the same ring is increased. Upon deprotonation, the relative intensity of the 1382 cm^{-1} band assigned to the combined C=C and symmetric COO^- stretching is increased.

In the presence of the metallic surface the protonation/deprotonation state of the molecule plays a major influence on the molecule-metal interaction. The SERS spectra recorded at acidic pH are considerably weaker in intensity as compared with the SERS spectra of the basic solutions. For low pH values, the free electron pairs interact with the protons of HCl. Hence, they can no longer optimally bind to the Ag surface and the intensity is considerably lower than the one recorded at basic pH. Concerning the orientation of the molecule on the metallic surface, at acidic pH, the piperazinyl and cyclopropane ring might be in the close proximity of the metallic surface or their polarizability tensor has such an orientation that its *zz* components are perpendicular to the surface. This is suggested by the enhanced Raman modes in the high wavenumber region associated with the sp^3 hybridized carbon atoms localized at these rings. When the molecule is deprotonated, the Raman band that is ascribed to the C=C stretching of the quinolone ring system at 1616 cm^{-1} in the Raman spectrum is shifted by 8 cm^{-1} compared to the band position in the Raman spectra of the saturated aqueous solutions. The shift may be caused by the interaction of the aromatic ring system with the Ag surface. Therefore, the deprotonated ciprofloxacin molecule probably adopts a flat orientation with interactions via the nitrogen atoms of the piperazinyl ring. As in the case of levofloxacin, ciprofloxacin also induces the aggregation of the nanoparticles yielding higher SERS intensities as compared with the case when additional aggregation agents were added. Thus, when ciprofloxacin measurements were carried out with environmental samples, no additional activation agent was added.

1.4.2 Dynamic range and limits of detection of drugs in purified water

Reliable quantitative SERS measurements require reproducible and, ideally, automated measurement conditions. At the Leibniz Institute of Photonic Technology (IPHT), the Microfluidics Group developed a glass based microfluidic chip (chip design in Figure **2**). Glass has a low Raman scattering cross section, therefore is an ideal material for manufacturing microfluidic chips for SERS measurements. Prior to the measurements, a silanization procedure is carried out to obtain hydrophobic channel walls. This will facilitate the successful creation of aqueous droplets in the continues phase of oil. The microfluidic platform has the following

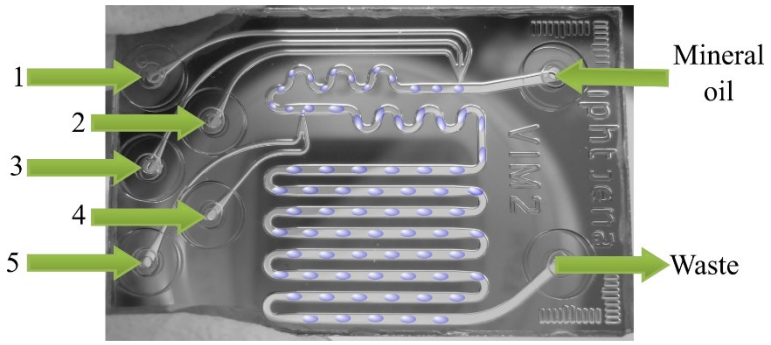

Figure 2. Droplet-based microfluidic chip used for quantitative and semi-quantitative SERS measurements.

operational units: a droplet generator where the aqueous solutions are dispensed into the flow of mineral oil via a T-junction, a dosing unit where further aqueous solutions are injected into the already existing droplet, two meander channels assuring an optimal mixing of the droplet content and a long measurement loop. Generally, through port 1-3 the analyte solutions and the solvent (purified water, simulated urine, urine or river water) are pumped, while the Ag nanoparticles and KCl, as aggregation agent, are injected via port 4 and 5. The flow rate of the continues phase was fixed at 9 nl/s, the sum of the flowrates at the droplet generator was 14 nl/s and at the dosing unit 11 nl/s. The various solutions are filled into glass syringes that are connected with the chip via Teflon capillaries. The software provided with the pump system (neMESYS Cetoni GmbH) controls the flow rates.

Throughout the studies included in the present thesis, different analyte concentrations have been defined. If not otherwise stated, the "*in-droplet*" concentration of the analyte is depicted in the graphs. This represents the concentration of the target molecule in the solution that will be mixed with the nanoparticles in the chip. The further dilution with the colloidal solution and KCl is not considered. A second concentration, referred to as the "*urinary*" concentration, is used to express the concentration of the drug in the clinical sample, before its dilution with water. Because, none of the urine samples originated from individuals under medical treatment with levofloxacin or NTX, the antibiotics were artificially added in form of aqueous solution to the urine samples.

During the thesis, the dynamic ranges and LODs of the LoC-SERS technique were assessed for MTX, levofloxacin and NTX solved in purified water. Stock aqueous solutions were prepared for each analyte. By varying the flowrates of the analyte containing solution and purified water different in-droplet concentrations were obtained.

In the case of MTX the measured concentrations ranged between 0.16 μM to 100 μM. In Figure **5** [IH1] the mean SERS spectra and their double standard deviation for selected concentrations are illustrated. For data visualization, the Lorentz fitted peak area of the Raman band at 965 cm^{-1} assigned to the ring breathing mode of the aromatic ring perpendicularly orientated on the metallic surface was plotted as function of the in-droplet concentration. Based on Figure **6** [IH1] and the definitions given in the previous section, the achieved LOD is 0.17 μM, the linear range spans from 0.2 μM to 2 μM and the dynamic range is between 0.2 μM to 10 μM. When the in-droplet MTX concentration exceeds 10 μM, the peak area of the Raman marker band does not increase with the increment of the concentration. This phenomenon is referred to as "the poisoning effect". The number of free binding sites on the surface of the metallic nanoparticles is limited. When the concentration of the molecules exceeds a given, analyte dependent, threshold the further addition of molecules will not yield a signal increment. A second parameter playing an important role is the evanescent character of the local electromagnetic field. The SERS intensity scales with $\sim r^{-12}$, where r is the distance from the surface. Therefore, SERS is a truly surface sensitive technique and only the molecules in the first layers contribute to the measured signal. The analytical performances offered by LoC-SERS are theoretically sufficient for monitoring the MTX levels for patients undergoing high-dosage MTX treatments. More exactly, the MTX concentration at 42 h from the start of the treatment should be at most 1 μM. High risk toxic effects can occur at concentrations higher than 10 μM. Therefore, the clinically relevant concentration ranges from 1 to 10 μM. However, MTX concentrations have to be determined in human plasma or serum and this will bring further challenges due to the increased complexity of the matrix. The aim of the present thesis was directed toward the quantification of antibiotics in human urine and in river water sample. Thus, no further analysis was carried out for MTX.

In-droplet levofloxacin concentrations in purified water were measured in the 1-100 μM concentration range. In Figure **5** [IH2] the recorded mean SERS spectra of 15 differently concentrated solutions are depicted, while Figure **6** [IH2] shows the integrated peak area of two Raman bands. The Raman band at 1395 cm^{-1} was ascribed to the coupled quinolone ring system and symmetric COO^- stretching vibrations, while the one at 230 cm^{-1} to the vibration of Ag-O. For low levofloxacin concentrations, the peak areas of both signals exponentially increase, whereas at 20 μM the saturation regime appears. Based on the spectroscopic characterization of the levofloxacin molecule described in the previous section, the molecule interacts with the metallic surface via the carboxylate group and the band at 230 cm^{-1} appears because of the binding process. Therefore, the Raman mode at 230 cm^{-1} band is due to the levofloxacin

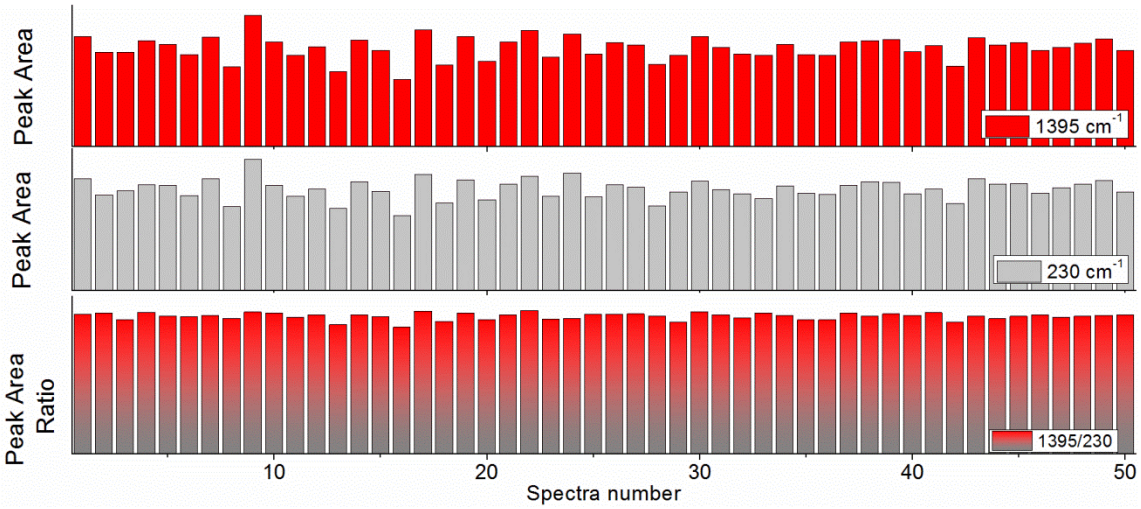

Figure **3**. Peak area of the Raman modes of levofloxacin and their ratio.

molecules in the first layer on the surface of the metallic nanoparticles, whereas the intensity of the 1395 cm^{-1} is increasing also due to the molecules present in the upper layers, but still located in the hot-spots. Because of these two different underlying mechanisms, the Raman band ascribed to the Ag-O vibration was implemented as internal standard. After the normalization procedure, the linear analytical response was significantly improved and it ranged between 0.8 µM to 15 µM with a detection limit of 0.8 µM. The normalization also improved the relative standard deviation from ~10 % to ~2 %. This proves that the signal of the chosen internal standard is influenced by the LSP field and can compensate for variations induced by the heterogeneity of the field magnitude at different hot-spots (Figure **3** compares the variation of the peak area of the two selected bands and of their ratio). Urinary levofloxacin concentrations range between 1.38 ± 0.68 mM (after 4h from treatment administration) to 7 ± 5 µM (after 72 h). Thus, LoC-SERS has high potential for monitoring the clearance of levofloxacin.

The MIC values of NTX against uropathogens are between 10 to 40 µM. To assess the LOD of NTX solved in purified water concentrations between 1 µM to 100 µM were measured by the LoC-SERS setup [IH4]. The characteristic Raman bands of NTX can be clearly identified at 2.5 µM concentration in the mean SERS spectrum showed in Figure **2** [IH4]. The Raman band associated with the C-H out-of-plane bending mode at 840 cm^{-1} was integrated with the Simpson rule and the peak areas are plotted in the same figure. The achieved detection limit is 2.5 µM, which is five times lower than the required sensitivity. The signal showed a linear dependency as function of the concentration for the 2.5-10 µM range, while the dynamic range extends up to 85 µM. At this concentration the previously mentioned poisoning effect appears.

In conclusion, the three drugs, MTX, levofloxacin and NTX, were successfully detected in purified water, with good sensitivity and sufficient dynamic range for clinical applications. In the next sections the challenges brought by the complexity of biological and environmental samples will be addressed.

1.4.3 Complex matrix and its challenges for drug detection

The detection and quantification of one single molecule out of a complex matrix can be similar with finding a needle in a haystack. Especially, when the SERS active substrates are not beforehand functionalized to capture one specific molecule. One of the objectives of the thesis was directed toward assessing the capabilities and limitations of the LoC-SERS technique using conventional, easy to prepare colloidal nanoparticles, to detected and quantify antibiotics used against uropathogens in human urine and environmental samples. But before this, an artificial matrix mimicking human urine samples was investigated to get insights into the parameters influencing the overall SERS signal. For this, levofloxacin was chosen as test molecule and the Raman band at 1395 cm^{-1} was used as marker band for discussing the effect of various parameters.

The artificial urine was prepared according to an already published protocol [81] and contained the following chemical compounds: 13.72 mM calcium chloride, 34.21 mM sodium sulfate, 5.92 mM magnesium sulfate, 85.99 mM ammonium chloride, 5.46 mM sodium citrate, 17.05 mM sodium dihydrogen phosphate, 162.71 mM potassium chloride, 23.69 mM sodium chloride, 832.5 mM urea and 19.44 mM creatinine [IH3]. The SERS spectrum of levofloxacin solved in the artificial urine vs. purified water (Figure **1** [IH3]) presents different relative band intensities and decreased “absolute” intensity. Artificial urine has a pH value of 5, thus, this might cause the slight reorientation of the molecule on the silver surface and consequently, the different relative band intensities. The overall intensity of the SERS spectrum of levofloxacin solved in artificial urine may be affected by (1) “over aggregation” of nanoparticles and (2) competition between analyte and the molecules of the complex matrix for the free binding sites on the silver surface. To test the two factors, experiments were carried out to find out which of the components of the complex matrix has the highest influence on the SERS spectrum of levofloxacin. According to the results summarized in Figure **2** (A) [IH3], the presence of various salts causes the strongest signal decrease, while the addition of urea and creatinine leads to further intensity losses. Therefore, it is expected that the LOD and the dynamic range of LoC-

SERS for levofloxacin detection will strongly vary among individuals due to the various osmotic concentration of the urine samples.

Generally, before chromatographic separations, the biological fluids are diluted with the mobile phase in order to reduce the matrix effects. The same sample preparation step was also carried out for our studies. In Figure **2** (C) [IH3], the peak area of the Raman mode at 1391 cm^{-1} as well as the peak area of the band located at 990 cm^{-1} and ascribed to the urea molecule are plotted. The peak area of the later Raman band is increasing for increasing amount of artificial urine, whereas the former one is increasing with decreasing in-droplet concentration. This means, that by decreasing the concentration of the salts and other interfering molecules, the signal of the target molecule is inversely proportional with its concentration and the LOD value of the technique can be improved. However, one should be careful with the extent of dilution, as too strong dilution might lead to an analyte concentrations below the detection limit and useful information concerning the spectral signature of the complex matrix can be also lost.

SERS signals of molecules are generally aggregation time dependent. For optimal results the influence of the time lapses between colloid-analyte mixing and the measurement time point was assessed. For levofloxacin solved in artificial urine a short aggregation time yields the best results both for signal intensity and relative standard deviation (Figure **2** (B) [IH3]).

By taking into consideration all parameters affecting the SERS signal, concentration dependent LoC-SERS measurements were performed for levofloxacin amounts between 0.05 mM and 1 mM. Furthermore, the reproducibility of the measurements was also tested by repeated spectra acquisition on different days and with different chips. The analytical performance of the method can be summarized as follows: (1) for a not diluted matrix the LOD was ~0.1 mM and the dynamic range between 0.1 mM - 1 mM, while (2) for the diluted matrix (57% artificial urine) the detection limit was improved to 0.055 mM and the dynamic range was extended accordingly towards lower concentrations (Figure **3** (A) [IH3]). The signal reproducibility was good even when the SERS spectra were recorded on different days with two different chips.

In the case of SERS measurements done for levofloxacin dissolved in purified water, the Raman mode ascribed to the Ag-O stretching vibration was implemented as an internal standard, yielding great linear range and lower relative standard deviations. In the presence of artificial urine the position of this band is redshifted by 10 cm^{-1}, which indicates the adsorption of additional chemical species on the metallic surface. Despite this, when employing this band as an internal standard, once again improved linear dynamic range is achieved with an increased

goodness of fit from 0.96 to 0.99 over the whole measured concentration range. A possible explanation for this might be that while the concentration of the molecules of the complex matrix is constant during the measurements, the concentration of the target molecule is increasing. Thus, the intensity of the Raman band at low wavenumbers is also increasing.

In conclusion, as compared with the acquired data for levofloxacin dissolved in purified water, the LOD dropped from 0.8 μM to 0.055 mM. This is almost two orders of magnitude higher and it can be associated once, with the competition between the molecules at the silver surface, and second, with the high salt content in the matrix. Therefore, for human urine samples the SERS signals of antibiotics will strongly vary between patients, and even in between samples collected from the same patient at different time points, and traditional quantitative measurements will lead to unreliable results.

1.4.4 Human urine as matrix for antibiotic detection

Human urine samples used as complex matrix for the present thesis were either randomly collected from a healthy volunteer or received from the Institute of Medical Microbiology, University Hospital Jena. In the second case, the samples are left over volumes of routine analysis and were anonymized. In total, five samples originating from the healthy volunteer, six individual samples and three pooled samples from patients were included in the study. Neither the healthy volunteer nor the patients have undergone medical treatment with levofloxacin or NTX. As sample clean-up step, a simple filtration was carried out with a polyvinylidene difluoride syringe filter having a pore size of 0.22 μm in order to remove cells and debris. After filtration, the samples were diluted with water or spiked with the appropriate amount of drug solved in water. The degree of the dilution was decided based on observed experimental parameters. More exactly, the affinity of NTX toward the silver nanoparticles is considerably higher as compared with the case of levofloxacin. Therefore, the extent of the effect of the matrix on the SERS spectrum of the two molecules will differ. As a consequence, the matrix was diluted to 21 % for levofloxacin and 70 % in the case of NTX. However, because of the received low volume of urine samples originating from patients, for LoC-SERS-SAM measurements carried out with NTX, the samples had to be diluted to 50% in order to have enough sample volume for performing measurements.

The pH values and the osmotic concentration of human urine samples vary strongly among individuals. Thus, it is expected that the SERS signals will vary accordingly. By comparing the mean SERS spectra of the blank urine samples diluted with water, shown in Figure **4** [IH3] and in Figure **S6** [IH4], the first observation made was that the overall intensity

of the signal is significantly influenced by the pH of the urine. Namely, the samples having an acidic pH show a considerably weaker SERS signal when compared with the neutral ones. According to the previously reported publications and due to the high abundance of urea in urine samples, a strong Raman mode around 990 cm^{-1} is expected. However, the samples included in the thesis show only a very weak signal in this spectral region. Instead, all spectra contain Raman modes at 485 cm^{-1}, 637 cm^{-1} and 1123 cm^{-1} ascribed to the vibrational modes of the uric acid molecule. Furthermore, the spectral feature in the 1350-1380 cm^{-1} spectral range was assigned to the pyrrole half-ring symmetrical stretching within the hem molecule.

In the case of levofloxacin, spiked urine samples, three individual and three pools, with urinary concentration between 0.45 mM and 1.8 mM were measured. This concentration range was chosen according to the expected levofloxacin amounts in human urine after 4h from administration. Despite the rich Raman signature of the urine, the Raman characteristic bands of levofloxacin located at 1395 cm^{-1} and 1616 cm^{-1} are clearly distinguishable (Figure **S7** [IH3]) for all samples. However, as earlier predicted, because levofloxacin is inducing the aggregation of the silver nanoparticles, the intensity of the Raman bands ascribed to the molecules of the complex matrix are influenced by the presence of the molecule. In order to rule out the influence of the different aggregation degree, the Raman mode located at 637 cm^{-1} and assigned to uric acid was employed as an internal standard.

The Raman marker bands of levofloxacin are located in the same spectral range as the ones originating from the vibrational modes of the molecules of the complex matrix. Therefore, the analytical performance of LoC-SERS for levofloxacin detection in human urine samples was assessed by multivariate analysis instead of the univariate approach. For this, principal component analysis was combined with partial least square (PLS) regression. The normalized data was divided into two datasets. The first set was used for training the PLS model; model further applied for the prediction of the concentration values of the second dataset. According to Figure **5** ([IH3]), the dynamic linear range covers the whole measured concentration range and the lowest measured concentration, 0.45 mM, is above the LOD of the technique. Based on the mean SERS spectra and on the root mean square error of prediction of the PLS method, concentrations comparable to that obtained for levofloxacin solved in artificial urine are detectable. Therefore, the chemical composition of the chosen artificial urine successfully simulates the human urine samples.

In the case of NTX, urinary concentrations below 8 mg/l (42.1 µM) are considered as susceptible concentrations, whereas for NTX amounts above 16 mg/l (84.2 µM) bacteria will develop resistance. In a first run of the experiments, urinary concentration dependent LoC-SERS

measurements were performed with three randomly collected urine samples of a healthy volunteer. The measured concentrations were between 4.28 μM and 42.8 μM. As it was foreseen by the results obtained when NTX was detected in purified water, the chemical affinity of the molecule toward silver facilitates its detection at concentrations as low as 4.28 μM. The characteristic Raman modes in the 1000-2000 cm^{-1} spectral range are strongly convoluted with the Raman bands of the blank urine samples. Nevertheless, the signal at 840 cm^{-1} is situated in a background free region and the LOD was calculated based on the integrated peak area of this Raman mode. According to Figure **3** [IH4], the achieved LOD was ~3 μM. This value is comparable with the one calculated for the case when NTX was solved in purified water (LOD ~2.5 μM). Therefore, the molecules of the complex matrix do not inhibit the efficient adsorption of NTX on the surface of the silver nanoparticles. Beside good sensitivity, the LoC-SERS method also offers sufficient linear analytical response. For all three measured samples, a linear range over the whole measured concentration range was achieved.

Up to now, it was shown that LoC-SERS can detect drugs in human urine samples, and depending on the characteristics of the molecules the sensitivities differ. However, the question how to determine the concentration of a drug in clinical samples has not been addressed. As discussed before, the traditional quantitative analysis with *a priori* established calibration curves is not feasible for SERS applications. The first impediment is the batch-to-batch reproducibility of the nanoparticles. Although we have shown that the Leopold-Lendl nanoparticles are providing reproducible SERS signals (Figure **S9** [IH3]) the aging of the colloidal solution can influence the results. The second factor is represented by the high inter-individual variability of the chemical composition of clinical samples. Therefore, the combination of LoC-SERS with SAM is the most feasible approach for quantitative measurements. To demonstrate this, NTX was chosen as model analyte.

None of the individuals consumed NTX before urine sample collection. Thus, "real" clinical samples had to be simulated by first spiking human urine (250 μl) with a small volume (76 μl) of highly concentrated (~70 μM) NTX aqueous solution. Therefore, the "unknown" NTX urinary concentration to be determined with LoC-SERS-SAM was ~ 21 μM (~4 mg/l). For each sample (two from a healthy volunteer and five patients), four SAS were prepared by adding purified water or/and NTX standard solution in different volumes. Additionally, the urine sample diluted only with water, without NTX, was also measured. These spectra were used as negative control to assess the correctness of the model. The "unknown" concentration was predicted with uni- and multivariate statistical analysis. In the first case, the estimation was made based on the calculated peak area of the NTX characteristic band located ~840 cm^{-1}

(Figure **4** [IH4]). In the second case, multivariate curve resolution (MCR) combined with alternating least square regression (ALS) was applied. The predicted values were between 11.6 and 26.4 μM in the case of the univariate analysis (Table **S3** [IH4]), whereas for the MCR-ALS approach the concentration varied between 11.3 and 27.9 μM (Table **S5** [IH4]). The mean absolute percentage error was ~21 % for both statistical methods. However, in the case of MCR-ALS the "unknown" concentration of four out of seven samples was predicted with a relative error below 10 % as compared with only one in the case of the univariate analysis, whereby the results for the negative control are comparable. Regardless of the applied statistical method, predictions with significant relative errors were obtained for samples HV**4**, PS**4** and PS**5**. The source of error might come from the measurements themselves, as the linear dependency of the detected signal satisfies the requirements of SAM. If these three samples are not considered for the mean absolute percentage error calculations, than MCR-ALS delivers predictions with an error of 6.2 %, whereas the univariate approach has an error of 12.5 %. Furthermore, the univariate statistical approach cannot be applied for the quantification of molecules presenting Raman bands convoluted with the Raman signal of the molecules present in the complex matrix. Consequently, MCR-ALS is the preferred approach for the determination of the antibiotic concentration in clinical samples.

The total time needed for the determination of the "unknown" concentration for one sample was around 1 h. This time can be significantly reduced by (1) reducing the number of acquired spectra per SAS, (2) reducing the acquisition time and (3) optimizing the chip design. Currently, 600 SERS with 1 s integration time/spectrum were recorded for each SAS. In future measurements, this number can be reduced to at least half. The acquisition time can de reduced without compromising the signal-to-noise ratio by increasing the laser power. Because of the dynamic flow, local heating resulting in sample degradation is avoided. By changing these two parameters, a total run-time of 15 min/sample can be achieved. A new chip design with a single droplet generator with one inlet for the nanoparticles and five inlets for the unknown sample and the four SAS, longer meander channel as compared with the actual design, would reduce significantly the required time for measurement preparation. Furthermore, during the thesis it was also proved that the LoC-SERS setup can be easily combined with a portable Raman setup [IH3], without compromising the quality of the results (Figure 6).

In conclusion, LoC-SERS-SAM has a high potential to find its place in clinical laboratories because of its low cost, time efficiency and good sensitivity. However, before this, further studies have to be carried out for different other molecules and for clinical samples.

1.4.5 Environmental Samples – ciprofloxacin determination

Monitoring the successful removal of antibiotics in waste and surface water is of high interest to overcome the occurrence of antibacterial resistance in the ecosystem. MICs for ciprofloxacin range between 0.024 μM for *E. Coli* to 12 μM for *S. aureus*. Surface water samples were collected from the shore of the local river (Saale). Prior to the measurements, the samples were filtered with the same filter used for the clinical samples. As a result, a clear solution was obtained. The water samples were spiked with ciprofloxacin and the measurements were performed at pH 11 with the LoC-SERS platform. In Figure **3** [IH5] the mean SERS spectra of selected samples is depicted. The SERS spectrum of the blank sample shows broad bands in the 1000-1700 cm^{-1} spectral region. They have been associated with the presence of amorphous carbon as a result of the decomposition of organic materials. Although the background signal is significant in the spectral region where ciprofloxacin characteristic Raman bands are located (1389 cm^{-1} and 1616 cm^{-1}), at the lowest measured concentration, 0.74 μM, the signature of the target molecule is clearly distinguishable. For ciprofloxacin concentrations above 10μM the poisoning effect, previously discussed, appears. For data evaluation, the multivariate statistical analysis approach was successfully applied. Two independent data sets were recorded on two consecutive days with two different chips. The data of the first day was used to train the PLS model, whereas the second set was employed to assess the reproducibility of the measurements by treating it as "unknown" sample. The PLS training model was evaluated via a ten-fold cross validation. The RMSEP for cross validation was 0.375 μM, while that for the prediction on all data was 0.374 μM. The RMSEP value of prediction for the second, independent dataset, was 0.355 μM. The RMSEP value is the lowest concentration detectable and it can be used to estimate the LOD of the method. Furthermore, in the 0.74-10 μM concentration range great linearity is shown in Figure 4 (B) [IH5].

In conclusion, the LoC-SERS technique is suitable for detecting ciprofloxacin in environmental samples in the concentration range that corresponds to its MIC values. A "yes-no" answer can be obtained, namely, if a SERS signal is detected, one might conclude that the ciprofloxacin concentration in the sample is above the MIC value.

1.5. Final Remarks

Immunoassays are commercially available only for MTX detection in clinical samples, while chromatography successfully quantifies MTX, levofloxacin, and ciprofloxacin, but the method is sophisticated and it is associated with high initial cost investment. Furthermore, no reliable detection of NTX was carried out up to date.

Compared with the reference analytical methods, SERS is in its childhood when it comes to its real life application. One of the most often encountered challenges are related with the SERS active substrate. For analytical applications, the plasmonic structures used to enhance the inherently weak Raman scattering have to provide homogenous SERS signal and at the same time, they have to be easy-to-prepare and cost effective. Furthermore, it is highly desired that the target molecules have a high chemical affinity for the employed SERS substrate. Only under these conditions, its successful detection in complex matrices can be carried out. Thus, SERS is not a universal detector. Last, but not least, most of the reported measurement procedures offer no or very low automation, and hence, the measurement conditions are hard to control. Beside all this, the detection of specific molecules in complex matrices will bring additional challenges. Questions, such as: which is the best sample clean-up procedure, how to perform quantification of the molecules in chemically very divers samples or which is the optimal statistical data analysis approach, have to be answered. The aim of the current thesis was to address all the above mentioned challenges and to assess the potential of the LoC-SERS technique to be considered as an alternative analytical tool for the detection and quantification of drugs in complex matrices.

For all the studies presented in the frame of the thesis, silver metallic nanoparticles in colloidal solution have been employed. Beside the MTX study, all experiments were carried out with nanoparticles synthesized at room temperature by the fast reduction of silver nitrate by hydroxylamine hydrochloride in the presence of sodium hydroxide. The prepared batches presented similar extinction spectra and they offered stable signal enhancement up to almost one year. Commonly encountered drawbacks of traditional cuvette based SERS measurements, such as aggregation time dependent signals and the precipitation of nanoparticles, were easily overcome by combining the measurement technique with a droplet based microfluidic platform. Simultaneously, also automation is achieved. Because of the reproducible measurement conditions, the relative standard deviation of the SERS signal, when no internal standard was applied, was generally below ~12 %.

As above mentioned, SERS is not an universal detector. Molecules have to efficiently adsorbed to the surface of the metallic nanoparticles. Additionally, because of the employed LoC-SERS platform, where aqueous droplets are formed in the continuous phase of mineral oil, a high water solubility of the molecules is a pre-requisite. This is the case for MTX, levofloxacin and ciprofloxacin. Nevertheless, because of the quinolone backbone, NTX is also partially soluble in the mineral oil. As a consequence, the molecules diffuse from the aqueous droplet toward the oil phase and the recorded SERS signal is significantly reduced. However, during the thesis it was shown, that the molecule has a strong chemical affinity for the employed nanoparticles and this inhibits their diffusion toward the mineral oil.

Concerning the challenges brought by the presence of the molecules of the complex matrices for the SERS detection of the three antibiotics the following solutions were proposed: (1) filtration followed by dilution with water as sample clean-up procedure, (2) standard addition method for quantification and (3) multivariate statistic for data processing.

By applying the analytical procedure above described, the achieved results presented in the frame of the thesis demonstrate that all three antibiotics can be successfully detected in their complex matrices. Namely, due to the low metabolism rate of levofloxacin, LoC-SERS can be applied for monitoring its clearance rate short (up to 4-6 h) after the administration of a single oral dose of 500 mg. Furthermore, thanks to the high chemical affinity of NTX toward the silver surface, its successful quantification was carried out at MIC values when spiked in urine. The same was achieved for ciprofloxacin in surface water samples.

In conclusion, LoC-SERS offers manifold advantages such as: straightforward sample clean-up, specificity and sensitivity, quantification power, reproducibility and automation, small foot-print and on-site application. Future investigations should be directed toward clinical samples originating from patients under antibiotic treatment, the integration of nanoparticle synthesis in the same chip as the detection is carried out, extending the method for other drugs of interest and the investigation of other body fluids, such as blood.

References

1. Davies, S.C., et al., *Annual Report of the Chief Medical Officer: infection and the rise of antimicrobial resistance.* Lancet, 2013. **381**(9878): p. 1606-9.
2. Blair, J.M.A., et al., *Molecular mechanisms of antibiotic resistance.* Nat Rev Micro, 2015. **13**(1): p. 42-51.
3. Dasgupta, A., *Monitoring Free Drug Concentration*, in *Handbook of Drug Monitoring Methods: Therapeutics and Drugs of Abuse*, A. Dasgupta, Editor. 2008, Humana Press: Totowa, NJ. p. 41-65.
4. Meibohm, B. and H. Derendorf, *Basic concepts of pharmacokinetic/pharmacodynamic (PK/PD) modelling.* Int J Clin Pharmacol Ther, 1997. **35**(10): p. 401-13.
5. Watson, I., et al., *Editorial.* Therapeutic Drug Monitoring, 1997. **19**(2).
6. Alarcon, G.S., *Methotrexate use in rheumatoid arthritis. A clinician's perspective.* Immunopharmacology, 2000. **47**(2-3): p. 259-271.
7. Bouquie, R., et al., *A fast LC-MS/MS assay for methotrexate monitoring in plasma: validation, comparison to FPIA and application in the setting of carboxypeptidase therapy.* Analytical Methods, 2014. **6**(1): p. 178-186.
8. Chen, Y.Q., et al., *Affinity capture elution bridging assay: A novel immunoassay format for detection of anti-therapeutic protein antibodies.* Journal of immunological methods, 2016. **431**: p. 45-51.
9. Darwish, I.A., *Immunoassay Methods and their Applications in Pharmaceutical Analysis: Basic Methodology and Recent Advances.* International Journal of Biomedical Science : IJBS, 2006. **2**(3): p. 217-235.
10. den Boer, E., et al., *A U-HPLC-ESI-MS/MS-Based Stable Isotope Dilution Method for the Detection and Quantitation of Methotrexate in Plasma.* Therapeutic Drug Monitoring, 2012. **34**(4): p. 432-439.
11. Doctor, E.L. and B. McCord, *The application of supported liquid extraction in the analysis of benzodiazepines using surface enhanced Raman spectroscopy.* Talanta, 2015. **144**: p. 938-943.
12. Kaneko, T., et al., *Performance characteristics between TDxFLx and TBA-25FR for the therapeutic drug monitoring of methotrexate.* Journal of pharmaceutical health care and sciences, 2016. **2**: p. 7.
13. Krieg, A.K. and G. Gauglitz, *Ultrasensitive Label-Free Immunoassay for Optical Determination of Amitriptyline and Related Tricyclic Antidepressants in Human Serum.* Analytical Chemistry, 2015. **87**(17): p. 8845-8850.
14. Saint-Marcoux, F., F.L. Sauvagge, and P. Marquet, *Current role of LC-MS in therapeutic drug monitoring.* Analytical and Bioanalytical Chemistry, 2007. **388**(7): p. 1327-1349.
15. Song, Z.R., et al., *A validated chemiluminescence immunoassay for methotrexate (MTX) and its application in a pharmacokinetic study.* Analytical Methods, 2016. **8**(1): p. 162-170.
16. Zehnacker, L., et al., *Development of sensitive direct chemiluminescent enzyme immunoassay for the determination of dihydroartemisinin in plasma.* Analytical and Bioanalytical Chemistry, 2015. **407**(25): p. 7823-7830.
17. Bluett, J., et al., *A HPLC-SRM-MS based method for the detection and quantification of methotrexate in urine at doses used in clinical practice for patients with rheumatological disease: a potential measure of adherence.* Analyst, 2015. **140**(6): p. 1981-1987.

18. Churchwell, M.I., et al., *Improving LC–MS sensitivity through increases in chromatographic performance: Comparisons of UPLC–ES/MS/MS to HPLC–ES/MS/MS.* Journal of Chromatography B, 2005. **825**(2): p. 134-143.
19. Guillarme, D., et al., *Coupling ultra-high-pressure liquid chromatography with mass spectrometry.* TrAC Trends in Analytical Chemistry, 2010. **29**(1): p. 15-27.
20. Lucotti, A., et al., *TLC-surface enhanced Raman scattering of apomorphine in human plasma.* Vibrational Spectroscopy, 2012. **62**: p. 286-291.
21. Trachta, G., et al., *Combination of high-performance liquid chromatography and SERS detection applied to the analysis of drugs in human blood and urine.* Journal of Molecular Structure, 2004. **693**(1-3): p. 175-185.
22. Yang, Z. and S.H. Wang, *Recent development in application of high performance liquid chromatography-tandem mass spectrometry in therapeutic drug monitoring of immunosuppressants.* Journal of Immunological Methods, 2008. **336**(2): p. 98-103.
23. Zheng, L., et al., *Hydrophilic Interaction Liquid Chromatography Tandem Mass Spectrometry: An Attractive and Prospective Method for Quantitative Bioanalysis in Drug Metabolism.* Current Drug Metabolism, 2016. **17**(4): p. 386-400.
24. Bell, S.E.J. and N.M.S. Sirimuthu, *Quantitative surface-enhanced Raman spectroscopy.* Chemical Society Reviews, 2008. **37**(5): p. 1012-1024.
25. Bonifacio, A., et al., *Surface-enhanced Raman spectroscopy of blood plasma and serum using Ag and Au nanoparticles: a systematic study.* Analytical and Bioanalytical Chemistry, 2014. **406**(9-10): p. 2355-2365.
26. Huang, R.F., S.Y. Han, and X. Li, *Detection of tobacco-related biomarkers in urine samples by surface-enhanced Raman spectroscopy coupled with thin-layer chromatography.* Analytical and Bioanalytical Chemistry, 2013. **405**(21): p. 6815-6822.
27. Joshi, P., et al., *Quantitative SERS-based detection using Ag-Fe3O4 nanocomposites with an internal reference.* Journal of Materials Chemistry C, 2014. **2**(46): p. 9964-9968.
28. Villa, J.E.L. and R.J. Poppi, *A portable SERS method for the determination of uric acid using a paper-based substrate and multivariate curve resolution.* Analyst, 2016. **141**(6): p. 1966-1972.
29. Wang, C. and C.X. Yu, *Analytical characterization using surface-enhanced Raman scattering (SERS) and microfluidic sampling.* Nanotechnology, 2015. **26**(9): p. 26.
30. Wang, H., et al., *Quantitative analysis of creatinine in urine by metalized nanostructured parylene.* Journal of Biomedical Optics, 2010. **15**(2): p. 5.
31. Wang, T.L., et al., *Semi-quantitative surface enhanced Raman scattering spectroscopic creatinine measurement in human urine samples.* Optical and Quantum Electronics, 2005. **37**(13-15): p. 1415-1422.
32. Zhao, L.L., J. Blackburn, and C.L. Brosseau, *Quantitative Detection of Uric Acid by Electrochemical-Surface Enhanced Raman Spectroscopy Using a Multi layered Au/Ag Substrate.* Analytical Chemistry, 2015. **87**(1): p. 441-447.
33. Nie, S. and S.R. Emory, *Probing Single Molecules and Single Nanoparticles by Surface-Enhanced Raman Scattering.* Science, 1997. **275**(5303): p. 1102-1106.
34. Campion, A. and P. Kambhampati, *Surface-enhanced Raman scattering.* Chemical Society Reviews, 1998. **27**(4): p. 241-250.
35. Yamamoto, Y.S., Y. Ozaki, and T. Itoh, *Recent progress and frontiers in the electromagnetic mechanism of surface-enhanced Raman scattering.* Journal of Photochemistry and Photobiology C: Photochemistry Reviews, 2014. **21**: p. 81-104.
36. Cialla, D., et al., *Surface-enhanced Raman spectroscopy (SERS): progress and trends.* Analytical and Bioanalytical Chemistry, 2012. **403**(1): p. 27-54.
37. Fan, M., G.F.S. Andrade, and A.G. Brolo, *A review on the fabrication of substrates for surface enhanced Raman spectroscopy and their applications in analytical chemistry.* Analytica Chimica Acta, 2011. **693**(1–2): p. 7-25.

38. Gao, R., et al., *Real-time analysis of diaquat dibromide monohydrate in water with a SERS-based integrated microdroplet sensor.* Nanoscale, 2014. **6**(15): p. 8781-8786.
39. Guo, Z.A., et al., *Magnetic imprinted surface enhanced Raman scattering (MI- SERS) based ultrasensitive detection of ciprofloxacin from a mixed sample.* Analytical Methods, 2014. **6**(6): p. 1627-1632.
40. Wei, X. and S. Sebastian, *Rationally designed multifunctional plasmonic nanostructures for surface-enhanced Raman spectroscopy: a review.* Reports on Progress in Physics, 2014. **77**(11): p. 116502.
41. Xie, Y.L., et al., *In Situ Fabrication of 3D Ag@ZnO Nanostructures for Microfluidic Surface-Enhanced Raman Scattering Systems.* Acs Nano, 2014. **8**(12): p. 12175-12184.
42. Jahn, M., et al., *Plasmonic nanostructures for surface enhanced spectroscopic methods.* Analyst, 2016. **141**(3): p. 756-793.
43. Le Ru, E.C. and P.G. Etchegoin, *Chapter 7 - Metallic colloids and other SERS substrates*, in *Principles of Surface-Enhanced Raman Spectroscopy*. 2009, Elsevier: Amsterdam. p. 367-413.
44. Zhang, Y., et al., *Gold and silver nanoparticle monomers are non-SERS-active: a negative experimental study with silica-encapsulated Raman-reporter-coated metal colloids.* Physical Chemistry Chemical Physics, 2015. **17**(33): p. 21120-21126.
45. Shen, W., et al., *Reliable Quantitative SERS Analysis Facilitated by Core–Shell Nanoparticles with Embedded Internal Standards.* Angewandte Chemie International Edition, 2015. **54**(25): p. 7308-7312.
46. Ackermann, K.R., T. Henkel, and J. Popp, *Quantitative online detection of low-concentrated drugs via a SERS microfluidic system.* Chemphyschem, 2007. **8**(18): p. 2665-2670.
47. Chen, L.X. and J.B. Choo, *Recent advances in surface-enhanced Raman scattering detection technology for microfluidic chips.* Electrophoresis, 2008. **29**(9): p. 1815-1828.
48. Gao, R., et al., *Highly sensitive trace analysis of paraquat using a surface-enhanced Raman scattering microdroplet sensor.* Analytica Chimica Acta, 2010. **681**(1-2): p. 87-91.
49. Kaminska, A., et al., *Detection of Hepatitis B virus antigen from human blood: SERS immunoassay in a microfluidic system.* Biosensors & Bioelectronics, 2015. **66**: p. 461-467.
50. Lee, H., et al., *Various On-Chip Sensors with Microfluidics for Biological Applications.* Sensors, 2014. **14**(9): p. 17008-17036.
51. Li, Q.L., B.W. Li, and Y.Q. Wang, *Surface-enhanced Raman scattering microfluidic sensor.* Rsc Advances, 2013. **3**(32): p. 13015-13026.
52. Marz, A., et al., *Towards a quantitative SERS approach - online monitoring of analytes in a microfluidic system with isotope-edited internal standards.* Journal of Biophotonics, 2009. **2**(4): p. 232-242.
53. Quang, L.X., et al., *A portable surface-enhanced Raman scattering sensor integrated with a lab-on-a-chip for field analysis.* Lab on a Chip, 2008. **8**(12): p. 2214-2219.
54. Wu, L., et al., *Rapid and reproducible analysis of thiocyanate in real human serum and saliva using a droplet SERS-microfluidic chip.* Biosensors & Bioelectronics, 2014. **62**: p. 13-18.
55. Xia, T.H., et al., *Improving the quantitative accuracy of surface-enhanced Raman spectroscopy by the combination of microfluidics with a multiplicative effects model.* Analytical Methods, 2014. **6**(7): p. 2363-2370.
56. Hidi, I.J., et al., *Droplet based microfluidics: spectroscopic characterization of levofloxacin and its SERS detection.* Physical Chemistry Chemical Physics, 2015. **17**(33): p. 21236-21242.

57. Huang, J.A., et al., *SERS-Enabled Lab-on-a-Chip Systems.* Advanced Optical Materials, 2015. **3**(5): p. 618-633.
58. Ralf, S., et al., *Droplet based microfluidics.* Reports on Progress in Physics, 2012. **75**(1): p. 016601.
59. Cronstein, B.N., *Low-Dose Methotrexate: A Mainstay in the Treatment of Rheumatoid Arthritis.* Pharmacological Reviews, 2005. **57**(2): p. 163-172.
60. Kinder, A.J., et al., *The treatment of inflammatory arthritis with methotrexate in clinical practice: treatment duration and incidence of adverse drug reactions.* Rheumatology, 2005. **44**(1): p. 61-66.
61. Madhyastha, S., et al., *A COMPARISON OF VITAMIN A AND LEUCOVORIN FOR THE PREVENTION OF METHOTREXATE-INDUCED MICRONUCLEI PRODUCTION IN RAT BONE MARROW.* Clinics, 2008. **63**(6): p. 821-826.
62. Begas, E., et al., *Simple and Reliable HPLC Method for the Monitoring of Methotrexate in Osteosarcoma Patients.* Journal of Chromatographic Science, 2014. **52**(7): p. 590-595.
63. Guerriero, E., et al., *Unexpected Overestimation of Methotrexate Plasma Concentrations: Analysis of a Single Center Pediatric Population.* Therapeutic drug monitoring, 2014. **36**(4): p. 499-504.
64. Widemann, B.C. and P.C. Adamson, *Understanding and Managing Methotrexate Nephrotoxicity.* The Oncologist, 2006. **11**(6): p. 694-703.
65. Crews, K.R., et al., *High-dose methotrexate pharmacokinetics and outcome of children and young adults with osteosarcoma.* Cancer, 2004. **100**(8): p. 1724-1733.
66. Wagenlehner, F.M., et al., *Urinary bactericidal activity of extended-release ciprofloxacin (1,000 milligrams) versus levofloxacin (500 milligrams) in healthy volunteers receiving a single oral dose.* Antimicrob Agents Chemother, 2006. **50**(11): p. 3947-9.
67. Sun, H., H. Wang, and X. Ge, *Simultaneous Determination of the Combined Drugs of Ceftriaxone Sodium, Metronidazole, and Levofloxacin in Human Urine by High-Performance Liquid Chromatography.* Journal of Clinical Laboratory Analysis, 2012. **26**(6): p. 486-492.
68. Wang, Y., K. Yu, and S. Wang, *Vibrational spectra study on quinolones antibiotics.* Spectrochimica Acta Part A: Molecular and Biomolecular Spectroscopy, 2006. **65**(1): p. 159-163.
69. Wagenlehner, F.M., et al., *Concentrations in plasma, urinary excretion and bactericidal activity of levofloxacin (500 mg) versus ciprofloxacin (500 mg) in healthy volunteers receiving a single oral dose.* Int J Antimicrob Agents, 2006. **28**(6): p. 551-9.
70. Wagenlehner, F.M.E., et al., *Pharmacokinetics of ciprofloxacin XR (1000 mg) versus levofloxacin (500 mg) in plasma and urine of male and female healthy volunteers receiving a single oral dose.* International Journal of Antimicrobial Agents, 2006. **27**(1): p. 7-14.
71. Pletz, M. and J. Lipman, *Clinical measures for increased creatinine clearances and suboptimal antibiotic dosing.* Intensive Care Medicine, 2013. **39**(7): p. 1322-1324.
72. Torre-Cisneros, J., et al., *Tuberculosis prophylaxis with levofloxacin in liver transplant patients is associated with a high incidence of tenosynovitis: safety analysis of a multicenter randomized trial.* Clinical infectious diseases : an official publication of the Infectious Diseases Society of America, 2015. **60**(11): p. 1642-9.
73. Liu, Y.M., Q. He, and M. Wu, *LEVOFLOXACIN-INDUCED CRYSTAL NEPHROPATHY.* Nephrology, 2015. **20**(6): p. 437-438.
74. Gulen, M., et al., *Levofloxacin-Induced Hepatotoxicity and Death.* American Journal of Therapeutics, 2015. **22**(3): p. E93-E96.

75. Czyrski, A., et al., *The pharmacokinetic interaction between levofloxacin and sunitinib.* Pharmacological reports : PR, 2015. **67**(3): p. 542-4.
76. Fayyaz, M., et al., *Quality evaluation and in vitro interaction studies between levofloxacin 250mg and diclofenac sodium 50mg tablets.* Pakistan Journal of Pharmaceutical Sciences, 2015. **28**(1): p. 119-128.
77. Budny, A.M. and A.N. Ley, *Fluoroquinolone-Mediated Achilles Rupture: A Case Report and Review of the Literature.* Journal of Foot & Ankle Surgery, 2015. **54**(3): p. 494-496.
78. Bansal, N., D. Manocha, and B. Madhira, *Life-Threatening Metabolic Coma Caused by Levofloxacin.* American Journal of Therapeutics, 2015. **22**(2): p. E48-E51.
79. Gao, C.H., et al., *Personalized therapeutics for levofloxacin: a focus on pharmacokinetic concerns.* Therapeutics and Clinical Risk Management, 2014. **10**: p. 217-227.
80. Gupta, K., et al., *International Clinical Practice Guidelines for the Treatment of Acute Uncomplicated Cystitis and Pyelonephritis in Women: A 2010 Update by the Infectious Diseases Society of America and the European Society for Microbiology and Infectious Diseases.* Clinical Infectious Diseases, 2011. **52**(5 %U http://cid.oxfordjournals.org/content/52/5/e103.abstract): p. e103-e120.
81. Leopold, N. and B. Lendl, *A New Method for Fast Preparation of Highly Surface-Enhanced Raman Scattering (SERS) Active Silver Colloids at Room Temperature by Reduction of Silver Nitrate with Hydroxylamine Hydrochloride.* The Journal of Physical Chemistry B, 2003. **107**(24): p. 5723-5727.
82. Fraser, R.S. and J. Creanor, *Rapid and selective inhibition of RNA synthesis in yeast by 8-hydroxyquinoline.* European Journal of Biochemistry, 1974. **46**(0014-2956 (Print)): p. 67-73.
83. Wagenlehner, F.M.E., et al., *Urinary Concentrations and Antibacterial Activities of Nitroxoline at 250 Milligrams versus Trimethoprim at 200 Milligrams against Uropathogens in Healthy Volunteers.* Antimicrobial Agents and Chemotherapy, 2014. **58**(2): p. 713-721.
84. Hochhaus, G., J.S. Barrett, and H. Derendorf, *Evolution of Pharmacokinetics and Pharmacokinetic/Dynamic Correlations during the 20th Century.* The Journal of Clinical Pharmacology, 2000. **40**(9): p. 908-917.
85. Widmark, E. and J. Tandberg, *Über die Bedingungen für die Akkumulation indifferenter Narkotika.* Biochemische Zeitschrift, 1924. **147**: p. 358-369.
86. Brandhorst, G., et al., *Liquid chromatography-tandem mass spectrometry or automated immunoassays: what are the future trends in therapeutic drug monitoring?* Clinical Chemistry and Laboratory Medicine, 2012. **58**(1530-8561 (Electronic)).
87. Yalow, R.S. and S.A. Berson, *Assay of Plasma Insulin in Human Subjects by Immunological Methods.* Nature, 1959. **184**(4699): p. 1648-1649.
88. Dasgupta, A. and P. Datta, *Analytical Techniques for Measuring Concentrations of Therapeutic Drugs in Biological Fluids*, in *Handbook of Drug Monitoring Methods: Therapeutics and Drugs of Abuse*, A. Dasgupta, Editor. 2008, Humana Press: Totowa, NJ. p. 67-86.
89. Wild, D., *Chapter 1.2 - Immunoassay for Beginners*, in *The Immunoassay Handbook (Fourth Edition)*. 2013, Elsevier: Oxford. p. 7-10.
90. Siemens. *ARK Methotrexate Assay*. Available from: http://www.healthcare.siemens.com/drug-testing-diagnostics/emit-assays/methotrexate-assay.
91. Godefroid, M.J.G., et al., *Multicenter method evaluation of the ARK (TM) Methotrexate Immunoassay.* Clinical Chemistry and Laboratory Medicine, 2014. **52**(2): p. E13-E16.

92. Abbott. *TDx/TDxFLx Methotrexate II assay* Available from: http://www.ilexmedical.com/files/PDF/TDX_Methotrexate.pdf.
93. Florin, L., C. Lemahieu, and V. Stove, *Evaluation of the new Methotrexate CMIA assay on the Architect i2000SR.* Clinical Chemistry and Laboratory Medicine, 2016. **54**(1): p. E15-E17.
94. Shanin, I.A., et al., *Determination of fluoroquinolone antibiotic levofloxacin in urine by fluorescence polarization immunoassay.* Journal of Analytical Chemistry, 2015. **70**(6): p. 712-717.
95. Dunnivant, F.M. and J.W. Ginsbach. *GAS CHROMATOGRAPHY, LIQUID CHROMATOGRAPHY, CAPILLARY ELECTROPHORESIS - MASS SPECTROMETRY A BASIC INTRODUCTION*. 2011; Available from: http://people.whitman.edu/~dunnivfm/C_MS_Ebook/Prelim/index.html.
96. Kole, P.L., et al., *Recent advances in sample preparation techniques for effective bioanalytical methods.* Biomedical Chromatography, 2011. **25**(1-2): p. 199-217.
97. Biddlecombe, R.A. and S. Pleasance, *Automated protein precipitation by filtration in the 96-well format.* Journal of Chromatography B: Biomedical Sciences and Applications, 1999. **734**(2): p. 257-265.
98. Williams, M.G., J. Palandra, and E.M. Shobe, *Rapid determination of rat plasma uridine levels by HPLC-ESI-MS utilizing the Captiva™ filter plates for sample preparation.* Biomedical Chromatography, 2003. **17**(4): p. 215-218.
99. Mullett, W.M., *Determination of drugs in biological fluids by direct injection of samples for liquid-chromatographic analysis.* Journal of Biochemical and Biophysical Methods, 2007. **70**(2): p. 263-273.
100. Papp, R., W.M. Mullett, and E. Kwong, *A method for the direct analysis of drug compounds in plasma using a single restricted access material (RAM) column.* Journal of Pharmaceutical and Biomedical Analysis, 2004. **36**(3): p. 457-464.
101. Verdirame, M., et al., *Turbulent Flow Chromatography TFC-tandem mass spectrometry supporting in vitro/vivo studies of NCEs in high throughput fashion.* Journal of Pharmaceutical and Biomedical Analysis, 2010. **51**(4): p. 834-841.
102. Wong, S.H.Y., *ADVANCES IN LIQUID-CHROMATOGRAPHY AND RELATED METHODOLOGIES FOR THERAPEUTIC DRUG-MONITORING.* Journal of Pharmaceutical and Biomedical Analysis, 1989. **7**(9): p. 1011-1032.
103. Wong, S.H.Y., *NOVEL STRATEGIES FOR CLINICAL DRUG ANALYSIS WITH NEW COLUMN TECHNOLOGY IN LIQUID-CHROMATOGRAPHY.* Journal of Pharmaceutical and Biomedical Analysis, 1990. **8**(2): p. 185-193.
104. Eap, C.B. and P. Baumann, *Analytical methods for the quantitative determination of selective serotonin reuptake inhibitors for therapeutic drug monitoring purposes in patients.* Journal of Chromatography B-Analytical Technologies in the Biomedical and Life Sciences, 1996. **686**(1): p. 51-63.
105. Marquet, P., *Progress of liquid chromatography-mass spectrometry in clinical and forensic toxicology.* Therapeutic drug monitoring, 2002. **24**(2): p. 255-276.
106. Baranowska, I., S. Magiera, and J. Baranowski, *Clinical applications of fast liquid chromatography: A review on the analysis of cardiovascular drugs and their metabolites.* Journal of Chromatography B-Analytical Technologies in the Biomedical and Life Sciences, 2013. **927**: p. 54-79.
107. El Deeb, S., *Monolithic Silica for Fast HPLC: Current Success and Promising Future.* Chromatographia, 2011. **74**(9): p. 681-691.
108. Bunch, D.R. and S. Wang, *Applications of monolithic columns in liquid chromatography-based clinical chemistry assays.* Journal of Separation Science, 2011. **34**(16-17): p. 2003-2012.

109. Guillarme, D., et al., *New trends in fast and high-resolution liquid chromatography: a critical comparison of existing approaches.* Analytical and Bioanalytical Chemistry, 2009. **397**(3): p. 1069-1082.
110. Görgens, C., et al., *Mildronate (Meldonium) in professional sports – monitoring doping control urine samples using hydrophilic interaction liquid chromatography – high resolution/high accuracy mass spectrometry.* Drug Testing and Analysis, 2015. **7**(11-12): p. 973-979.
111. Meimaroglou, S., et al., *Direct injection human plasma analysis for the quantification of antihypertensive drugs for therapeutic drug monitoring using hydrophilic interaction liquid chromatography/electrospray ionization mass spectrometry.* Journal of Chromatography B, 2015. **1004**: p. 1-9.
112. De Abreu, C.C., et al., *Development and validation of HPLC method to determination of Methotrexate in children oncologic patients.* European Review for Medical and Pharmacological Sciences, 2015. **19**(8): p. 1373-1380.
113. Li, Y.D., et al., *A reversed-phase high performance liquid chromatography method for quantification of methotrexate in cancer patients serum.* Journal of Chromatography B-Analytical Technologies in the Biomedical and Life Sciences, 2015. **1002**: p. 107-112.
114. Schofield, R.C., et al., *Development and validation of a turbulent flow chromatography and tandem mass spectrometry method for the quantitation of methotrexate and its metabolites 7-hydroxy methotrexate and DAMPA in serum.* Journal of Chromatography B-Analytical Technologies in the Biomedical and Life Sciences, 2015. **1002**: p. 169-175.
115. Wu, D., et al., *A simple, rapid and reliable liquid chromatography-mass spectrometry method for determination of methotrexate in human plasma and its application to therapeutic drug monitoring.* Biomedical Chromatography, 2015. **29**(8): p. 1197-1202.
116. Sonemoto, E., et al., *Practical determination of methotrexate in serum of rheumatic patients by LC-MS/MS.* Biomedical Chromatography, 2012. **26**(11): p. 1297-1300.
117. Uchiyama, M., et al., *Simple and sensitive HPLC method for the fluorometric determination of methotrexate and its major metabolites in human plasma by post-column photochemical reaction.* Biomedical Chromatography, 2012. **26**(1): p. 76-80.
118. Sorel, R.H.A., C. Snelleman, and A. Hulshoff, *HIGH-PERFORMANCE LIQUID-CHROMATOGRAPHIC ANALYSIS OF NITROXOLINE IN PLASMA AND URINE.* Journal of Chromatography, 1981. **222**(2): p. 241-248.
119. Baietto, L., et al., *Simultaneous quantification of linezolid, rifampicin, levofloxacin, and moxifloxacin in human plasma using high-performance liquid chromatography with UV.* Therapeutic drug monitoring, 2009. **31**(1536-3694 (Electronic)).
120. Liang, H., M.B. Kays, and K.M. Sowinski, *Separation of levofloxacin, ciprofloxacin, gatifloxacin, moxifloxacin, trovafloxacin and cinoxacin by high-performance liquid chromatography: application to levofloxacin determination in human plasma.* Journal of Chromatography B, 2002. **772**(1): p. 53-63.
121. Djabarouti, S., et al., *Determination of levofloxacin in plasma, bronchoalveolar lavage and bone tissues by high-performance liquid chromatography with ultraviolet detection using a fully automated extraction method.* Journal of Chromatography B, 2004. **799**(1): p. 165-172.
122. Nguyen, H.A., et al., *Simultaneous determination of levofloxacin, gatifloxacin and moxifloxacin in serum by liquid chromatography with column switching.* Journal of Chromatography B, 2004. **810**(1): p. 77-83.
123. Zhou, Z.-L., et al., *A rapid and simple high-performance liquid chromatography method for the determination of human plasma levofloxacin concentration and its application to bioequivalence studies.* Biomedical Chromatography, 2007. **21**(10): p. 1045-1051.

124. Helmy, S.A., *Simultaneous Quantification of Linezolid, Tinidazole, Norfloxacin, Moxifloxacin, Levofloxacin, and Gatifloxacin in Human Plasma for Therapeutic Drug Monitoring and Pharmacokinetic Studies in Human Volunteers.* Therapeutic drug monitoring, 2013. **35**(6): p. 770-777.
125. Sousa, J., et al., *First liquid chromatography method for the simultaneous determination of levofloxacin, pazufloxacin, gatifloxacin, moxifloxacin and trovafloxacin in human plasma.* Journal of Chromatography B-Analytical Technologies in the Biomedical and Life Sciences, 2013. **930**: p. 104-111.
126. Cazorla-Reyes, R., et al., *Simultaneous analysis of antibiotics in biological samples by ultra high performance liquid chromatography-tandem mass spectrometry.* Journal of Pharmaceutical and Biomedical Analysis, 2014. **89**: p. 203-212.
127. Aguilar-Carrasco, J.C., et al., *Rapid and sensitive determination of levofloxacin in microsamples of human plasma by high-performance liquid chromatography and its application in a pharmacokinetic study.* Biomedical Chromatography, 2015. **29**(3): p. 341-345.
128. Kang, X.J. and Z.Y. Wan, *Quantitative high-performance liquid chromatographic analysis of nitroxoline and structurally related compounds.* Chromatographia, 2003. **57**(5-6): p. 405-408.
129. Hernández, F., et al., *Strategies for quantification and confirmation of multi-class polar pesticides and transformation products in water by LC–MS2 using triple quadrupole and hybrid quadrupole time-of-flight analyzers.* TrAC Trends in Analytical Chemistry, 2005. **24**(7): p. 596-612.
130. Müller, A., et al., *A new approach to data evaluation in the non-target screening of organic trace substances in water analysis.* Chemosphere, 2011. **85**(8): p. 1211-1219.
131. Loos, R., et al., *Analysis of polar organic contaminants in surface water of the northern Adriatic Sea by solid-phase extraction followed by ultrahigh-pressure liquid chromatography–QTRAP® MS using a hybrid triple-quadrupole linear ion trap instrument.* Analytical and Bioanalytical Chemistry, 2013. **405**(18): p. 5875-5885.
132. Loos, R., et al., *EU-wide monitoring survey on emerging polar organic contaminants in wastewater treatment plant effluents.* Water Research, 2013. **47**(17): p. 6475-6487.
133. Grimalt, S., et al., *Quantification, confirmation and screening capability of UHPLC coupled to triple quadrupole and hybrid quadrupole time-of-flightmass spectrometry in pesticide residue analysis.* Journal of Mass Spectrometry, 2010. **45**(4): p. 421-436.
134. Hurtado-Sánchez, M.C., et al., *Rapid and sensitive on-line solid phase extraction-ultra high performance liquid chromatography–electrospray-tandem mass spectrometry analysis of pesticides in surface waters.* Journal of Chromatography A, 2013. **1305**: p. 193-202.
135. Golet, E.M., et al., *Trace determination of fluoroquinolone antibacterial agents in solid-phase extraction urban wastewater by and liquid chromatography with fluorescence detection.* Analytical Chemistry, 2001. **73**(15): p. 3632-3638.
136. Mitani, K. and H. Kataoka, *Determination of fluoroquinolones in environmental waters by in-tube solid-phase microextraction coupled with liquid chromatography-tandem mass spectrometry.* Analytica Chimica Acta, 2006. **562**(1): p. 16-22.
137. Lee, H.B., T.E. Peart, and M.L. Svoboda, *Determination of ofloxacin, norfloxacin, and ciprofloxacin in sewage by selective solid-phase extraction, liquid chromatography with fluorescence detection, and liquid chromatography-tandem mass spectrometry.* Journal of Chromatography A, 2007. **1139**(1): p. 45-52.
138. Pena, A., et al., *Determination of fluoroquino one antibiotics in surface waters from Mondego River by high performance liquid chromatography using a monolithic column.* Journal of Separation Science, 2007. **30**(17): p. 2924-2928.

139. Esponda, S.M., et al., *Solid-phase microextraction with micellar desorption and HPLC-fluorescence detection for the analysis of fluoroquinolones residues in water samples.* Analytical and Bioanalytical Chemistry, 2009. **394**(4): p. 927-935.
140. Chen, L.G., et al., *Determination of fluoroquinolone antibiotics in environmental water samples based on magnetic molecularly imprinted polymer extraction followed by liquid chromatography-tandem mass spectrometry.* Analytica Chimica Acta, 2010. **662**(1): p. 31-38.
141. Yiruhan, et al., *Determination of four fluoroquinolone antibiotics in tap water in Guangzhou and Macao.* Environmental Pollution, 2010. **158**(7): p. 2350-2358.
142. Garcia, M.D.G., et al., *Determination of (fluoro)quinolones in environmental water using online preconcentration with column switching linked to large sample volumes and fluorescence detection.* Journal of Separation Science, 2012. **35**(7): p. 823-831.
143. Raman, C.V. and K.S. Krishnan, *A New Type of Secondary Radiation.* Nature, 1928. **121**: p. 501-502.
144. Long, D.A., *Survey of Light-scattering Phenomena*, in *The Raman Effect*. 2002, John Wiley & Sons, Ltd. p. 3-18.
145. Popp, J. and W. Kiefer, *Raman Scattering, Fundamentals*, in *Encyclopedia of Analytical Chemistry*. 2006, John Wiley & Sons, Ltd.
146. Schmitt, M. and J. Popp, *Raman spectroscopy at the beginning of the twenty-first century.* Journal of Raman Spectroscopy, 2006. **37**(1-3): p. 20-28.
147. Kim, H., et al., *Resonance Raman and surface- and tip-enhanced Raman spectroscopy methods to study solid catalysts and heterogeneous catalytic reactions.* Chemical Society Reviews, 2010. **39**(12): p. 4820-4844.
148. Fleischmann, M., P.J. Hendra, and A.J. McQuillan, *Raman spectra of pyridine adsorbed at a silver electrode.* Chemical Physics Letters, 1974. **26**(2): p. 163-166.
149. Moskovits, M., *Surface-enhanced Raman spectroscopy: a brief retrospective.* Journal of Raman Spectroscopy, 2005. **36**(6-7): p. 485-496.
150. Schlücker, S., *Surface-Enhanced Raman Spectroscopy: Concepts and Chemical Applications.* Angewandte Chemie International Edition, 2014. **53**(19): p. 4756-4795.
151. Le Ru, E.C. and P.G. Etchegoin, *Chapter 3 - Introduction to plasmons and plasmonics*, in *Principles of Surface-Enhanced Raman Spectroscopy*. 2009, Elsevier: Amsterdam. p. 121-183.
152. Stiles, P.L., et al., *Surface-Enhanced Raman Spectroscopy*, in *Annual Review of Analytical Chemistry*. 2008, Annual Reviews: Palo Alto. p. 601-626.
153. Xu, H., et al., *Electromagnetic contributions to single-molecule sensitivity in surface-enhanced Raman scattering.* Physical Review E, 2000. **62**(3): p. 4318-4324.
154. Kneipp, K., et al., *Detection and identification of a single DNA base molecule using surface-enhanced Raman scattering (SERS).* Physical Review E, 1998. **57**(6): p. R6281-R6284.
155. Krug, J.T., et al., *Efficient Raman Enhancement and Intermittent Light Emission Observed in Single Gold Nanocrystals.* Journal of the American Chemical Society, 1999. **121**(39): p. 9208-9214.
156. Lombardi, J.R. and R.L. Birke, *A Unified View of Surface-Enhanced Raman Scattering.* Accounts of Chemical Research, 2009. **42**(6): p. 734-742.
157. Lombardi, J.R. and R.L. Birke, *A Unified Approach to Surface-Enhanced Raman Spectroscopy.* The Journal of Physical Chemistry C, 2008. **112**(14): p. 5605-5617.
158. Takase, M., et al., *Selection-rule breakdown in plasmon-induced electronic excitation of an isolated single-walled carbon nanotube.* Nat Photon, 2013. **7**(7): p. 550-554.
159. Moskovits, M. and D.P. Dilellla, *Enhanced raman spectra of ethylene and propylene adsorbed on silver.* Chemical Physics Letters, 1980. **73**(3): p. 500-505.

160. Aikens, C.M., L.R. Madison, and G.C. Schatz, *Raman spectroscopy: The effect of field gradient on SERS.* Nat Photon, 2013. **7**(7): p. 508-510.
161. Moskovits, M. and J.S. Suh, *Surface selection rules for surface-enhanced Raman spectroscopy: calculations and application to the surface-enhanced Raman spectrum of phthalazine on silver.* The Journal of Physical Chemistry, 1984. **88**(23): p. 5526-5530.
162. Le Ru, E.C., et al., *Experimental demonstration of surface selection rules for SERS on flat metallic surfaces.* Chemical Communications, 2011. **47**(13): p. 3903-3905.
163. Etchegoin, P.G. and E.C. Le Ru, *Basic Electromagnetic Theory of SERS*, in *Surface Enhanced Raman Spectroscopy*. 2010, Wiley-VCH Verlag GmbH & Co. KGaA. p. 1-37.
164. Le Ru, E.C. and P.G. Etchegoin, *Chapter 6 - EM enhancements and plasmon resonances: examples and discussion*, in *Principles of Surface-Enhanced Raman Spectroscopy*. 2009, Elsevier: Amsterdam. p. 299-365.
165. Lee, P.C. and D. Meisel, *Adsorption and surface-enhanced Raman of dyes on silver and gold sols.* The Journal of Physical Chemistry, 1982. **86**(17): p. 3391-3395.
166. Chen, Y.J., W.P. Chen, and E. Burstein, *SURFACE-ELECTROMAGNETIC-WAVE-ENHANCED RAMAN-SCATTERING BY OVERLAYERS ON METALS.* Physical Review Letters, 1976. **36**(20): p. 1207-1210.
167. Moskovits, M., *SURFACE-ROUGHNESS AND ENHANCED INTENSITY OF RAMAN-SCATTERING BY MOLECULES ADSORBED ON METALS.* Journal of Chemical Physics, 1978. **69**(9): p. 4159-4161.
168. Si, M.Z., Y.P. Kang, and R.M. Liu, *Surface-enhanced Raman scattering (SERS) spectra of three kinds of azo-dye molecules on silver nanoparticles prepared by electrolysis.* Applied Surface Science, 2012. **258**(15): p. 5533-5537.
169. Zhang, K.B., et al., *A facile surface-enhanced Raman scattering (SERS) detection of rhodamine 6G and crystal violet using Au nanoparticle substrates.* Applied Surface Science, 2015. **347**: p. 569-573.
170. Mamian-Lopez, M.B. and R.J. Poppi, *Quantification of moxifloxacin in urine using surface-enhanced Raman spectroscopy (SERS) and multivariate curve resolution on a nanostructured gold surface.* Analytical and Bioanalytical Chemistry, 2013. **405**(24): p. 7671-7677.
171. Mamian-Lopez, M.B. and R.J. Poppi, *Standard addition method applied to the urinary quantification of nicotine in the presence of cotinine and anabasine using surface enhanced Raman spectroscopy and multivariate curve resolution.* Analytica Chimica Acta, 2013. **760**: p. 53-59.
172. Alharbi, O., Y. Xu, and R. Goodacre, *Detection and quantification of the opioid tramadol in urine using surface enhanced Raman scattering.* Analyst, 2015. **140**(17): p. 5965-5970.
173. Dong, R.L., et al., *Detection and Direct Readout of Drugs in Human Urine Using Dynamic Surface-Enhanced Raman Spectroscopy and Support Vector Machines.* Analytical Chemistry, 2015. **87**(5): p. 2937-2944.
174. Chen, Y.P., et al., *Discrimination of gastric cancer from normal by serum RNA based on surface-enhanced Raman spectroscopy (SERS) and multivariate analysis.* Medical Physics, 2012. **39**(9): p. 5664-5668.
175. Feng, S.Y., et al., *Nasopharyngeal cancer detection based on blood plasma surface-enhanced Raman spectroscopy and multivariate analysis.* Biosensors & Bioelectronics, 2010. **25**(11): p. 2414-2419.
176. Premasiri, W.R., J.C. Lee, and L.D. Ziegler, *Surface-Enhanced Raman Scattering of Whole Human Blood, Blood Plasma, and Red Blood Cells: Cellular Processes and Bioanalytical Sensing.* Journal of Physical Chemistry B, 2012. **116**(31): p. 9376-9386.

177. Feng, S.Y., et al., *Blood plasma surface-enhanced Raman spectroscopy for non-invasive optical detection of cervical cancer.* Analyst, 2013. **138**(14): p. 3967-3974.
178. Li, D., et al., *Label-free detection of blood plasma using silver nanoparticle based surface-enhanced Raman spectroscopy for esophageal cancer screening.* Journal of biomedical nanotechnology, 2014. **10**(3): p. 478-84.
179. Lin, D., et al., *Colorectal cancer detection by gold nanoparticle based surface-enhanced Raman spectroscopy of blood serum and statistical analysis.* Optics Express, 2011. **19**(14): p. 13565-13577.
180. Lin, J.Q., et al., *A novel blood plasma analysis technique combining membrane electrophoresis with silver nanoparticle-based SERS spectroscopy for potential applications in noninvasive cancer detection.* Nanomedicine-Nanotechnology Biology and Medicine, 2011. **7**(5): p. 655-663.
181. Ren, W., Y.X. Fang, and E.K. Wang, *A Binary Functional Substrate for Enrichment and Ultrasensitive SERS Spectroscopic Detection of Folic Acid Using Graphene Oxide/Ag Nanoparticle Hybrids.* Acs Nano, 2011. **5**(8): p. 6425-6433.
182. Stokes, R.J., et al., *Surface-enhanced Raman scattering spectroscopy as a sensitive and selective technique for the detection of folic acid in water and human serum.* Applied Spectroscopy, 2008. **62**(4): p. 371-376.
183. Yuen, C., W. Zheng, and Z.W. Huang, *Low-level detection of anti-cancer drug in blood plasma using microwave-treated gold-polystyrene beads as surface-enhanced Raman scattering substrates.* Biosensors & Bioelectronics, 2010. **26**(2): p. 580-584.
184. Fornasaro, S., et al., *Toward SERS-based point-of-care approaches for therapeutic drug monitoring: the case of methotrexate.* Faraday Discussions, 2016.
185. Liu, S.P., et al., *Raman spectroscopy measurement of levofloxacin lactate in blood using an optical fiber nano-probe.* Journal of Raman Spectroscopy, 2015. **46**(2): p. 197-201.
186. Alula, M.T. and J. Yang, *Photochemical decoration of magnetic composites with silver nanostructures for determination of creatinine in urine by surface-enhanced Raman spectroscopy.* Talanta, 2014. **130**: p. 55-62.
187. Li, M., et al., *Reagent- and separation-free measurements of urine creatinine concentration using stamping surface enhanced Raman scattering (S-SERS).* Biomedical Optics Express, 2015. **6**(3): p. 849-858.
188. Goodall, B.L., A.M. Robinson, and C.L. Brosseau, *Electrochemical-surface enhanced Raman spectroscopy (E-SERS) of uric acid: a potential rapid diagnostic method for early preeclampsia detection.* Physical Chemistry Chemical Physics, 2013. **15**(5): p. 1382-1388.
189. Han, Z.Z., et al., *Portable Kit for Identification and Detection of Drugs in Human Urine Using Surface-Enhanced Raman Spectroscopy.* Analytical Chemistry, 2015. **87**(18): p. 9500-9506.
190. Han, Z.Z., et al., *Three-Dimensional Surface-Enhanced Raman Scattering Hotspots in Spherical Colloidal Superstructure for Identification and Detection of Drugs in Human Urine.* Analytical Chemistry, 2015. **87**(9): p. 4821-4828.
191. Li, D.W., et al., *Recent progress in surface enhanced Raman spectroscopy for the detection of environmental pollutants.* Microchimica Acta, 2014. **181**(1-2): p. 23-43.
192. Alvarez-Puebla, R.A. and L.M. Liz-Marzan, *Environmental applications of plasmon assisted Raman scattering.* Energy & Environmental Science, 2010. **3**(8): p. 1011-1017.
193. Halvorson, R.A. and P.J. Vikesland, *Surface-Enhanced Raman Spectroscopy (SERS) for Environmental Analyses.* Environmental Science & Technology, 2010. **44**(20): p. 7749-7755.
194. Ayora-Canada, M.J., et al., *Novel preparation procedure for NIR-SERS measurements by using ion exchangers to provide highly improved signal enhancement and stability.* Applied Spectroscopy, 2001. **55**(2): p. 227-232.

195. He, L.L., et al., *Surface-enhanced Raman spectroscopy coupled with dendritic silver nanosubstrate for detection of restricted antibiotics.* Journal of Raman Spectroscopy, 2010. **41**(7): p. 739-744.
196. Ma, J., et al., *Detection of Antibiotics in Water Using Silver Colloid Films as Substrate of Surface-Enhanced Raman Scattering.* Spectroscopy and Spectral Analysis, 2013. **33**(10): p. 2688-2693.
197. Darby, B.L. and E.C. Le Ru, *Competition between Molecular Adsorption and Diffusion: Dramatic Consequences for SERS in Colloidal Solutions.* Journal of the American Chemical Society, 2014. **136**(31): p. 10965-10973.
198. Caro, C., et al., *Thiol-immobilized silver nanoparticle aggregate films for surface enhanced Raman scattering.* Journal of Raman Spectroscopy, 2008. **39**(9): p. 1162-1169.
199. Fales, A.M. and V.D. Tuan, *Silver embedded nanostars for SERS with internal reference (SENSIR).* Journal of Materials Chemistry C, 2015. **3**(28): p. 7319-7324.
200. Perera, P.N., et al., *Multiplexed concentration quantification using isotopic surface-enhanced resonance Raman scattering.* Journal of Raman Spectroscopy, 2010. **41**(7): p. 752-757.
201. Stosch, R., et al., *Surface enhanced Raman scattering based approach for quantitative determination of creatinine in human serum.* Analytical Chemistry, 2005. **77**(22): p. 7386-7392.
202. Zhang, D.M., et al., *Isotope edited internal standard method for quantitative surface-enhanced Raman spectroscopy.* Analytical Chemistry, 2005. **77**(11): p. 3563-3569.
203. Marz, A., et al., *Droplet formation via flow-through microdevices in Raman and surface enhanced Raman spectroscopy-concepts and applications.* Lab on a Chip, 2011. **11**(21): p. 3584-3592.
204. Wilson, R., et al., *Signal Enhancement of Surface Enhanced Raman Scattering and Surface Enhanced Resonance Raman Scattering Using in Situ Colloidal Synthesis in Microfluidics.* Analytical Chemistry, 2010. **82**(5): p. 2119-2123.
205. Wang, W., et al., *Droplet microfluidic preparation of au nanoparticles-coated chitosan microbeads for flow-through surface-enhanced Raman scattering detection.* Microfluidics and Nanofluidics, 2010. **9**(6): p. 1175-1183.
206. Harris, D.C., *Quantitative Chemical Analysis*. 2010: W. H. Freeman.
207. Miller, J.N. and J.C. Miller, *Statistics and Chemometrics for Analytical Chemistry*. 2005: Pearson/Prentice Hall.
208. Ranc, V., et al., *Preparative isotachophoresis with surface enhanced Raman scattering as a promising tool for clinical samples analysis.* Journal of Chromatography A, 2011. **1218**(2): p. 205-210.
209. De Bleye, C., et al., *Determination of 4-aminophenol in a pharmaceutical formulation using surface enhanced Raman scattering: From development to method validation.* Talanta, 2013. **116**: p. 899-905.
210. Ma, P.Y., et al., *Rapid determination of melamine in milk and milk powder by surface-enhanced Raman spectroscopy and using cyclodextrin-decorated silver nanoparticles.* Microchimica Acta, 2013. **180**(11-12): p. 1173-1180.
211. Kammer, E., et al., *Quantitative SERS studies by combining LOC-SERS with the standard addition method.* Analytical and Bioanalytical Chemistry, 2015. **407**(29): p. 8925-8929.

Chapter 2

Publications

In the present section the reprints of the publications included in the frame of the thesis are shown. Details regarding the copyright are stated on each title page.

2.1 LOC-SERS: Towards point-of-care diagnostics of methotrexate [IH1]

Izabella J. Hidi, Anna Mühlig, Martin Jahn, Falk Liebold, Dana Cialla,

Karina Weber, Jürgen Popp

Analytical Methods, 6, **2014**, 3943-3947.

Volume 6 | Number 12 | 21 June 2014 | Pages 3867–4470

Analytical Methods

www.rsc.org/methods

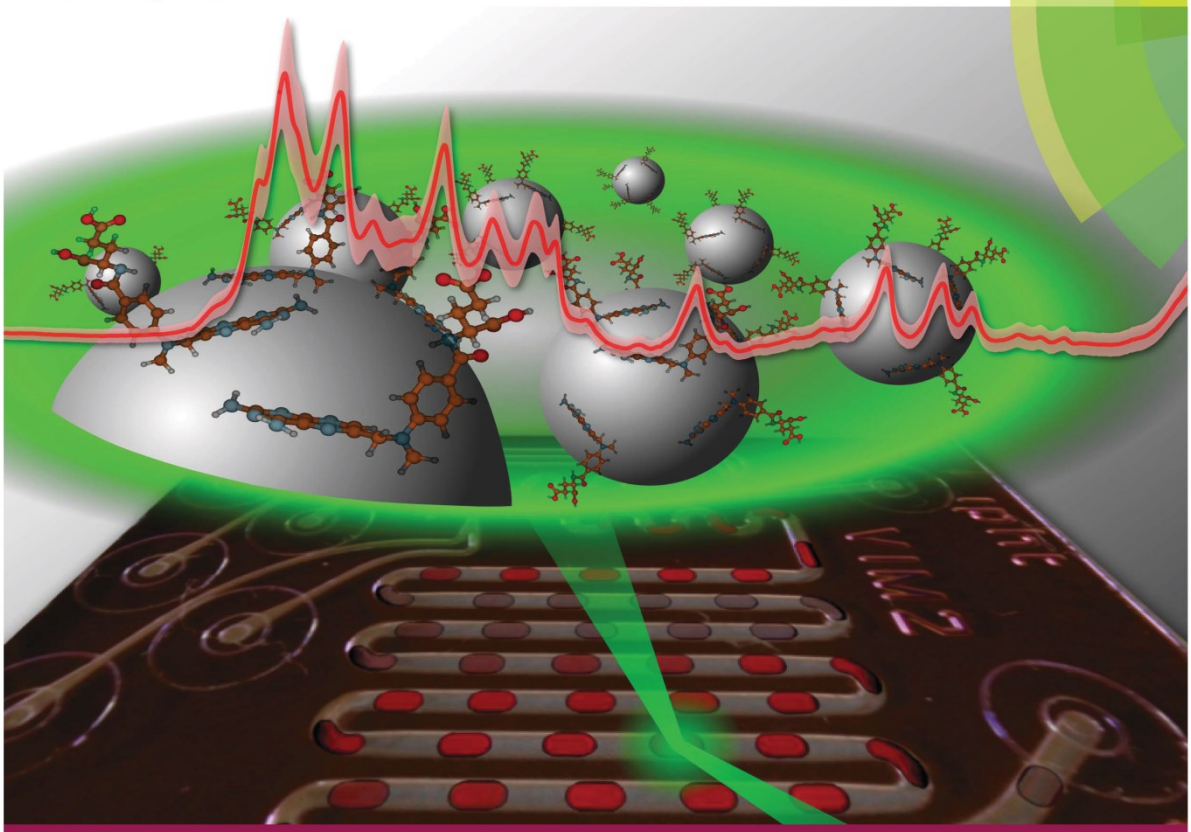

Themed issue: Clinical Diagnostics

ISSN 1759-9660

ROYAL SOCIETY OF CHEMISTRY

PAPER
J. Popp *et al.*
LOC-SERS: towards point-of-care diagnostic of methotrexate

Analytical Methods

PAPER

View Article Online
View Journal | View Issue

LOC-SERS: towards point-of-care diagnostic of methotrexate

Cite this: *Anal. Methods*, 2014, **6**, 3943

I. J. Hidi,†[a] A. Mühlig,†[a] M. Jahn,[a] F. Liebold,[b] D. Cialla,[ac] K. Weber[ac] and J. Popp*[ac]

Received 14th December 2013
Accepted 6th March 2014

DOI: 10.1039/c3ay42240b

www.rsc.org/methods

Therapeutic drug monitoring is of major importance in the case of medication with a narrow therapeutic range as well as when pharmacokinetic/pharmacodynamic variability is suspected. Methotrexate (MTX), an antifolate antibiotic, proved to be toxic regardless of the chosen treatment schedule. In this contribution, a new analytical method was used for the detection of MTX. A linear response was achieved in the 0.2–2 μM concentration range, with a limit of detection ≈ 0.17 μM. The lab-on-a-chip surface enhanced Raman spectroscopy (LOC-SERS) approach combines the fingerprint specificity and high sensitivity of SERS with the high sample throughput of a microfluidic platform. Additionally, it is shown that due to the chemical affinity of the MTX molecules towards Ag nanostructures, the pH value of the solving medium highly affects the obtained SERS signal. More specifically, SERS signals with well resolved bands can be obtained from deprotonated MTX molecules due to their binding to the metallic surface *via* the amine groups of the aromatic ring.

Introduction

Today's cancer therapy makes it essential to monitor and optimize the concentration of the administered medication in blood or other biological fluids.[1–4] A narrow therapeutic range, variability of the patient's characteristics due to age, physiology and/or disease are only a few parameters which may strongly influence the pharmacokinetic/pharmacodynamic outcome of a given drug. For example, the antifolate methotrexate (MTX) (see the chemical structure in Fig. 1), administered in both low-[5] and high-dosage[6–8] (LD-MTX and HD-MTX) treatment schemes, can exhibit high toxicity, overdosage leading to mortality.[9] Furthermore, the therapeutic range of MTX is in the concentration range of micromolar, the exact value being strongly dependent on whether it is administered as a single agent or in combination with other drugs.[10] The plasma MTX concentration at 42 hours after the start of HD-MTX infusion should be ≤1.0 μM, high risk toxic adverse effects being associated with concentrations ≥ 10 μM.[6,11,12] Therefore, from the clinical point of view concerning HD-MTX, it is essential to detect the plasma MTX concentration between 10 μM and 0.1 μM.

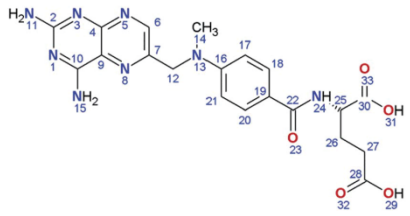

Fig. 1 Chemical structure of MTX.

In order to prevent an unwanted clinical outcome, therapeutic drug monitoring (TDM) is employed in clinical settings. Due to TDM the determination of the effective and, at the same time, safe dosage is possible. The concentration in biological fluids is commonly screened with various techniques, such as immunoassays,[13,14] gas or high pressure distribution chromatographic devices[15–18] and the dosage of the medication is regulated to the optimal therapeutic region by taking into account the patient characteristics.

However, even if chromatographic methods show high specificity and sensitivity, they are time consuming and expensive, require highly specialized personnel and more than one device in order to assess the drug concentrations. Therefore, the development of a new method with less technical complexity and faster analysing times is needed.

An innovative approach for the point-of-care (POC) diagnostic is the LOC-SERS (lab-on-a-chip surface enhanced Raman spectroscopy) technique.[19–22] Raman spectroscopy offers high specificity providing information concerning the molecular vibrations of the target molecule. As a result, labelling is not required as compared, *e.g.*, with fluorescence spectroscopy.

[a]*Friedrich Schiller University Jena, Institute of Physical Chemistry and Abbe Center of Photonics, Helmholtzweg 4, 07745 Jena, Germany. E-mail: juergen.popp@ipht-jena.de*
[b]*Analytik Jena AG, Konrad-Zuse-Straße 1, 07745 Jena, Germany*
[c]*Leibniz-Institute of Photonic Technology Jena, Albert-Einstein-Str. 9, 07745 Jena, Germany*
† These authors contributed equally.

However, the intensity of the inelastically scattered light is several orders of magnitude smaller than the excitation and therefore the efficiency is extremely poor. As a consequence, SERS is more appealing for medical diagnostics.[23–25] It gains its advantage due to a signal amplification effect of up to 8 orders of magnitude.[26] This is a result of the interaction of the analyte molecules with the intense local electromagnetic fields generated at the surface of metallic nanostructures.[26–28] Furthermore, SERS measurements carried out using a microfluidic device with a liquid/liquid segmented flow, where analyte-containing droplets are formed in a carrier fluid like oil, show great potential for bioanalytics.[19–22] To be more precise, minimal sample amounts are required and only short analysis times are needed, leading to significant cost reduction.

In this contribution, results of MTX determination using an aqueous solution by means of LOC-SERS will be presented. To the best of our knowledge, this is the first study to prove that SERS offers the possibility of detecting MTX in the target therapeutic concentration range (2 μM to 0.2 μM).

Materials and methods

Chemicals and reagents

The methotrexate hydrate powder used during measurements was purchased from Sigma Aldrich and meets the U.S. Pharmacopeial Convention testing specifications. Other reagents, such as mineral oil used for the realization of a segmented flow profile, KOH and KCl, HCl, as well as silver nitrate and sodium citrate were of analytical grade and were also purchased from the same provider.

Sample preparation

Due to the low water solubility of MTX, solutions with different pH values were prepared for preliminary tests. A first solution of pH 10 was prepared by dissolving the MTX powder in a KOH solution of 1 mM concentration. For achieving pH 12 a 150 mM KOH solution was used. Finally, by adding HCl (1 M) to the last solution, pH 2 was achieved.

For LOC-SERS measurements the 150 mM KOH solution was chosen. A stock solution of 1 mM MTX was prepared and further diluted in order to obtain the desired concentrations (10^{-4}, 10^{-5} and 10^{-6} M).

The Ag colloid was prepared by reducing silver nitrate with sodium citrate according to the Lee–Meisel protocol.[29] Transmission and scanning electron micrographs of this type of nanoparticle can be found elsewhere.[27,30,31]

Instrumentation

Extinction spectra of the as-prepared colloidal suspension, of MTX, as well as of different mixtures (*i.e.* colloid–buffer with pH 2, 10 and 12, colloid–MTX) were recorded with a Jasco V650 diode-array spectrophotometer in the wavelength range of 850–230 nm.

The reference Raman spectrum of the target analyte was recorded using as excitation a 785 nm laser line of a commercially available WITec Raman microscope (WITec GmbH, Ulm, Germany). The average power at the sample surface was 80 mW and 10 accumulated spectra of 5 s integration time were acquired.

Before the actual LOC-SERS measurements, preliminary tests were performed in order to assess the optimal measurement conditions. Therefore, for every measurement equal amounts of colloid and buffer/analyte solutions were mixed and, finally, 1 M KCl was added for inducing the aggregation of nanoparticles (mixing ratio: 1 : 1 : 0.1). The mixtures were pipetted in quartz cuvettes. For spectra acquisition, a commercially available WITec Raman microscope (WITec GmbH, Ulm, Germany) with an Ar^+ laser (514 nm) and 2 mW incident laser power at the sample surface was used. The same objective (Nikon 20×, N.A. 0.4) was employed for focusing the laser as well as for collecting the backscattered light. For acquisition, 10 accumulated spectra of 5 s integration time were recorded.

For LOC-SERS measurements, a 16 × 25 mm^2 sized all-glass microfluidic chip with six inlet ports to add the reagents was employed (Scheme 1). A more detailed description can be found elsewhere.[32,33] The aqueous droplet segments were generated with MTX and the 150 mM KOH solution at the first dosing unit. The citrate reduced Ag colloid and its activation agent, 1 M potassium chloride, was injected into these segments *via* a second dosing unit. The reproducible addition of analytes is provided by a computer controlled neMESYS Cetoni high performance syringe pump system. During measurements, the applied flow rates were fixed for the carrier medium mineral oil (0.01 μl s^{-1}), colloidal solution (0.009 μl s^{-1}) and potassium chloride (0.001 μl s^{-1}). In order to obtain different concentrations of the analyte, the flow rates of the analyte solution (0, 0.002351, 0.004703, 0.0093, and 0.014 μl s^{-1}) and mixing 150 mM KOH (0.014, 0.01165, 0.0093, 0.0047, and 0 μl s^{-1}) were changed. Therefore, dilutions occurred within the droplet created at the first dosing unit by mixing MTX solution with the 150 mM KOH medium. This resulted in the following in-droplet concentrations of the analyte before mixing in the colloid and KCl: 1.68 × 10^{-x} M, 3.36 × 10^{-x} M, 6.65 × 10^{-x} M and 1,00 × $10^{-(x-1)}$ M, where $x = 5$, 6, and 7.

In order to get optimal results, the microfluidic chip was mounted on the microscope table of a HR 800 LabRam spectrometer (Horiba Jobin-Yvon). The frequency doubled Nd:YAG laser (excitation wavelength: 532 nm) was focused into the

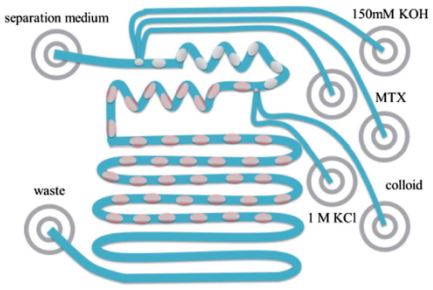

Scheme 1 LOC-SERS device.

microchannel of the microfluidic chip through an inverse microscope (Olympus IX 71 with an Olympus 20× UPlan FLN objective). The backscattered SERS signal was collected through the same objective. During measurements, a 300 lines per mm grating (resolution *ca.* 10 cm^{-1}) and a back-illuminated CCD camera (1024 × 512 pixels) were employed. Spectra were recorded continuously with integration times of 1 s during continuous flow. The power at the sample surface was 10 mW; higher laser power being necessary, as compared with the cuvette measurements, due to the dynamic flow. The time needed in order for an aqueous and an oil phase to pass through the laser spot is around 8 s. Therefore, alternating SERS spectra of analyte containing droplets, spectra of the oil phase or spectra with contribution from both phases are recorded.[34] The oil spectra are further used for wavelength calibration of the subsequent SERS spectra.

Results and discussion

UV-Vis absorption characteristics

According to the absorption profile (see Fig. 2) of the as prepared silver colloids, the plasmon resonances are located at ~425 nm. As a result of the addition of 150 mM KOH solution (pH 12) as well as 1 M HCl (pH 2) the absorption band is broadened. This is a consequence of the aggregation of the Ag nanoparticles.

Concerning MTX, its extinction profile shows three absorption peaks. This is due to the strong $\pi \rightarrow \pi^*$ and $\sigma \rightarrow \sigma^*$ electronic transitions.[35] The bands located at 257 and 372 nm are due to the pteridine group, the first one is ascribed to the $1L_a$ while the second one to the $1L_b$ transition. The 308 nm absorption is due to the *p*-amino benzoyglutamic moiety.[36,37] When the colloidal solution and the analyte are mixed, broadening of the 372 nm band occurs due to the contribution of the plasmon resonances.

Cuvette based SERS measurements

The reference spectrum of the MTX powder (Fig. 3) presents multiple bands, the vibrational analysis being previously presented by Ayyappan *et al.*[35] Compared to this, the SERS signal of the MTX solution with pH 12 is slightly different. This may be caused by the deprotonation induced by the addition of KOH molecules. The deprotonation may occur at the O29 and/or at the O31 site (see Fig. 1) due to the acidic activity of the carboxyl (COOH) group.

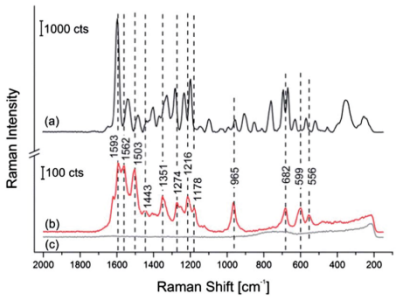

Fig. 3 Reference Raman spectrum measured on MTX powder @ 785 nm (a); SERS spectra of MTX 0.4 mM pH 12 (b) and the background signal (c) of the colloid mixed with 150 mM KOH and 1 M KCl (1 : 1 : 0.1) @ 514 nm.

An additional explanation could be given by considering that the orientation of the molecule at the metallic nanoparticle's surface also plays an important role. It is well known that vibrational modes perpendicular to the surface are significantly enhanced when compared to the ones parallel to it.[38–40] Furthermore, generally, the bonding of molecules to the silver surface can happen either through the lone pair electrons of the nitrogen or oxygen atoms.[41]

In the case of the deprotonated MTX, the attachment to the Ag nanoparticles could be *via* the amino groups. This is confirmed by the shift of the 1327 cm^{-1} band, ascribed to the NH_2 deformation, by 19 cm^{-1}. Additionally, the pteridine ring is oriented parallel to the metallic surface suggested by the disappearance of the 1403 cm^{-1} band assigned to C=N vibration (see the inset of Fig. 4). Thus, when compared with the Raman spectrum, the ring breathing mode of the aromatic ring at 965 cm^{-1} is strongly enhanced.

Concerning the similarities between the two spectra under discussion, one could argue that several bands of the SERS signal are in good accordance with the ones of the reference. More exactly, in the 1600–1300 cm^{-1} wavenumber region the 1593 cm^{-1} band can be ascribed to the scissoring of the NH_2 group while the one located at 1351 cm^{-1} to the CH_2 scissoring vibrations. Furthermore, in the 1300–900 cm^{-1} spectral region, the CH_2 wagging and C–NH_2 vibrations give rise to bands located at 1178 and 1216 cm^{-1}, respectively.

As already mentioned, SERS spectra were acquired for MTX solutions with different pH values. In Fig. 4 the SERS spectra of the MTX solutions with different pH values are presented. In an acidic environment the spectra have a small number of poorly resolved bands. As a result of HCl addition, protonation of the amine groups at the $N15H_2$ as well as $N11H_2$ affects the

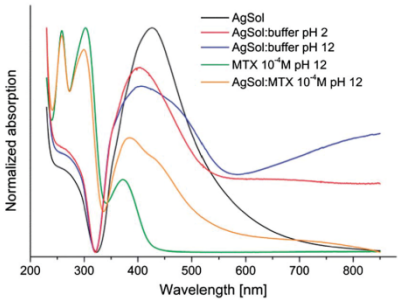

Fig. 2 UV-Vis absorption spectra of the Ag colloid (black); Ag colloid–buffer with pH 2 (red); Ag colloid–buffer with pH 12 (blue); (MTX/pH 12) 10^{-4} M (green) and Ag colloid–(MTX/pH 12) 10^{-4} M (orange) solutions.

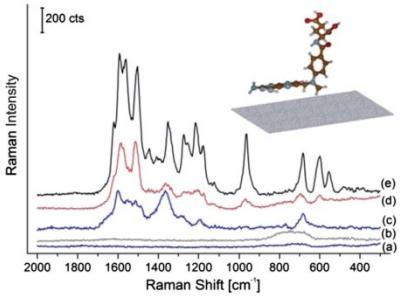

Fig. 4 SERS spectra of the pH adjusted MTX solutions (0.4 mM): colloid–buffer with pH 2–KCl (a); colloid–buffer with pH 12–KCl (b); colloid–(MTX/pH 2)–KCl (c), colloid–(MTX/pH 10)–KCl (d) and colloid–(MTX/pH 12)–KCl (e). Inset: orientation of the MTX molecule on the metal surface.

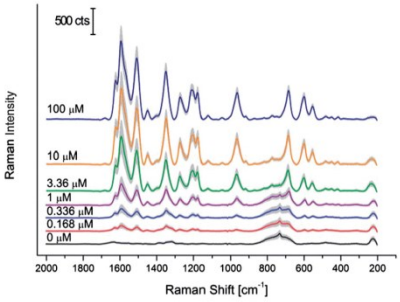

Fig. 5 Concentration dependency of the SERS signal of MTX measured by LOC-SERS.

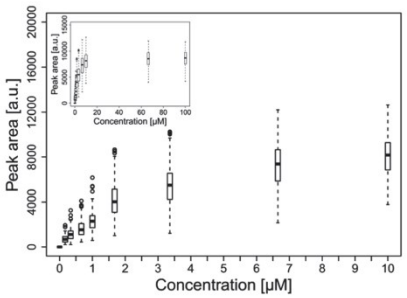

Fig. 6 Lorentz fitted peak area of the 965 cm^{-1} band against the in-droplet concentration of the MTX.

chemical affinity of the target molecule towards the metallic surface. Therefore, the number of MTX molecules at the metallic surface is low, leading to a poor SERS signal.

For alkaline conditions, by increasing the pH from 10 to 12 the Raman signal is significantly improved. This may be due to the better steric orientation of the nitrogen atoms N11 and/or N15 to the metallic surface. As the number of deprotonated MTX molecules increases the number of Ag–N binding sites increases, leading to the increment of the SERS signal.

Concerning the future experiments for detecting the target analyte out of biological fluids, pH adjustment will be possible by adding a buffer *via* one of the ports of the microfluidic chip. More exactly, in the case of blood plasma the starting pH value is slightly basic (~7.4). Based on pre-experiments, a buffer will be defined in order to reach an in-droplet pH value of 12.

LOC-SERS measurements

In order to obtain different droplet concentrations of the target analyte a flow profile was employed in the microfluidic channel. Three stem solutions of 10^{-4}, 10^{-5} and 10^{-6} M concentrations were injected in order to assess the limit of detection (LOD). As mentioned before, due to the mixing of the MTX solution with the solvent within the droplet formed at the first dosing port the measured concentrations are between 0.16 µM and 100 µM. In Fig. 5 one can see the plot of the mean spectra and their double standard deviation of selected concentration steps. Intermediate concentrations are not shown for the sake of clarity. According to this, spectral features characteristic to MTX are still present at a concentration of 0.17 µM.

For better visualisation, the Lorentz fitted peak area of the 965 cm^{-1} band was plotted against the in-droplet concentration of MTX (see Fig. 6). Therefore, one may observe that a linear dependency exists in the 0.2–2 µM region, with an LOD ~ 0.17 µM. This concentration domain is useful for the clinical practice when HD-MTX treatments are aimed. For concentrations higher than 10 µM the signal reaches saturation. This may be due to the fact that the surface of the Ag colloids is limited. Therefore, the increment of the number of MTX molecules does not lead to higher signal intensities.

Conclusions

In this study it was shown that when MTX is dissolved in a 150 mM KOH solution the deprotonated molecules bind to the silver nanoparticles *via* amine groups with the pteridine ring oriented parallel to the surface. Additionally, the pH value of the MTX solution has a strong influence on the chemical affinity of the target molecules towards the silver surface. SERS spectra with well resolved bands could be recorded when the solvent had an alkaline character. Furthermore, it was proven that LOC-SERS technology is a promising technique for the detection of biologically relevant molecules in the target therapeutic range. More exactly, in the case of MTX concentrations down to 0.17 µM were detected. Additionally, the Raman signal *vs.* MTX concentration showed linearity in the 0.2–2 µM window, the concentration range relevant for HD-MTX treatment schedules.

Acknowledgements

The funding of the PhD project of I.J. Hidi within the framework "Carl-Zeiss-Strukturmaßnahme" is gratefully acknowledged. The projects "QuantiSERS" and "Jenaer Biochip Initiative 2.0" within the framework "InnoProfile Transfer – Unternehmen Region" are supported by the Federal Ministry of Education and Research, Germany (BMBF). We thank the microfluidic group of the IPHT for providing the lab-on-a-chip devices for the measurements. Additionally, the help of Konstanze Olschewskithe with data processing is gratefully acknowledged.

Notes and references

1 V. Escudero-Ortiz, J. J. Pérez-Ruixo and B. Valenzuela, *Ther. Drug Monit.*, 2013, **35**, 796–802.
2 D. J. Cline, H. Zhang, G. D. Lundell, R. L. Harney, H. K. Riaz, J. Jarrah, Y. Li, M. Miyazaki, J. B. Courtney, I. Baburina and S. J. Salamone, *Ther. Drug Monit.*, 2013, **35**, 809–815.
3 R. E. Aarnoutse, J. M. Schapiro, C. A. Boucher, Y. A. Hekster and D. M. Burger, *Drugs*, 2003, **63**, 741–753.
4 G. L. Owens, K. Gajjar, J. Trevisan, S. W. Fogarty, S. E. Taylor, B. Da Gama-Rose, P. L. Martin-Hirsch and F. L. Martin, *J. Biophotonics*, 2013, DOI: 10.1002/jbio.201300157.
5 B. N. Cronstein, *Pharmacol. Rev.*, 2005, **57**, 163–172.
6 B. C. Widemann and P. C. Adamson, *Oncologist*, 2006, **11**, 694–703.
7 B. L. Asselin, M. Devidas, C. Wang, J. Pullen, M. J. Borowitz, R. Hutchison, S. E. Lipshultz and B. M. Camitta, *Blood*, 2011, **118**, 874–883.
8 H. Inaba, R. B. Khan, F. H. Laningham, K. R. Crews, C. H. Pui and N. C. Daw, *Ann. Oncology*, 2008, **19**, 178–184.
9 I. Sinicina, B. Mayr, G. Mall and W. Keil, *J. Rheumatol.*, 2005, **32**, 2009–2011.
10 L. Lennard, *Br. J. Clin. Pharmacol.*, 1999, **47**, 131–143.
11 K. R. Crews, T. Liu, C. Rodriguez-Galindo, M. Tan, W. H. Meyer, J. C. Panetta, M. P. Link and N. C. Daw, *Cancer*, 2004, **100**, 1724–1733.
12 K. R. Crews, Y. Zhou, J. L. Pauley, S. C. Howard, S. Jeha, M. V. Relling and C.-H. Pui, *Cancer*, 2010, **116**, 227–232.
13 C. Ritzmo, F. Albertioni, K. Cosic, S. Söderhäll and S. Eksborg, *Ther. Drug Monit.*, 2007, **29**, 447–451.
14 S. Marubashi, H. Nagano, S. Kobayashi, H. Eguchi, Y. Takeda, M. Tanemura, K. Umeshita, M. Monden, Y. Doki and M. Mori, *J. Clin. Pharmacol.*, 2010, **50**, 705–709.
15 E. den Boer, S. G. Heil, B. D. van Zelst, R. J. W. Meesters, B. C. P. Koch, M. L. te Winkel, M. M. van den Heuvel-Eibrink, T. M. Luider and R. de Jonge, *Ther. Drug Monit.*, 2012, **34**, 432–439.
16 C. Sottani, G. Poggi, F. Melchiorre, B. Montagna and C. Minoia, *J. Chromatogr. B: Anal. Technol. Biomed. Life Sci.*, 2013, **915–916**, 71–78.
17 S. Belz, C. Frickel, C. Wolfrom, H. Nau and G. Henze, *J. Chromatogr. B: Biomed. Sci. Appl.*, 1994, **661**, 109–118.
18 R. J. W. Meesters, E. den Boer, R. A. A. Mathot, R. de Jonge, R. J. van Klaveren, J. Lindemans and T. M. Luider, *Bioanalysis*, 2011, **3**, 1369–1378.
19 A. Walter, A. Marz, W. Schumacher, P. Rosch and J. Popp, *Lab Chip*, 2011, **11**, 1013–1021.
20 A. Marz, B. Monch, P. Rosch, M. Kiehntopf, T. Henkel and J. Popp, *Anal. Bioanal. Chem.*, 2011, **400**, 2755–2761.
21 A. Pallaoro, M. R. Hoonejani, G. B. Braun, C. Meinhart and M. Moskovits, *J. Nanophotonics*, 2013, **7**, 073092.
22 X. Lu, D. R. Samuelson, Y. Xu, H. Zhang, S. Wang, B. A. Rasco, J. Xu and M. E. Konkel, *Anal. Chem.*, 2013, **85**, 2320–2327.
23 M. Salehi, D. Steinigeweg, P. Ströbel, A. Marx, J. Packeisen and S. Schlücker, *J. Biophotonics*, 2013, **6**, 785–792.
24 U. S. Dinish, G. Balasundaram, Y. T. Chang and M. Olivo, *J. Biophotonics*, 2013, DOI: 10.1002/jbio.201300084.
25 P. Negri and R. A. Dluhy, *J. Biophotonics*, 2013, **6**, 20–35.
26 E. C. Le Ru and P. G. Etchegoin, in *Principles of Surface-enhanced Raman Spectroscopy*, eds. E. C. L. Ru and P. G. Etchegoin, Elsevier, Amsterdam, 2009, DOI: 10.1016/B978-0-444-52779-0.00010-6, pp. 185–264.
27 D. Cialla, A. März, R. Böhme, F. Theil, K. Weber, M. Schmitt and J. Popp, *Anal. Bioanal. Chem.*, 2012, **403**, 27–54.
28 E. C. Le Ru, S. A. Meyer, C. Artur, P. G. Etchegoin, J. Grand, P. Lang and F. Maurel, *Chem. Commun.*, 2011, **47**, 3903–3905.
29 P. C. Lee and D. Meisel, *J. Phys. Chem.*, 1982, **86**, 3391–3395.
30 D. Steinigeweg and S. Schlucker, *Chem. Commun.*, 2012, **48**, 8682–8684.
31 C. De Bleye, E. Dumont, E. Rozet, P. Y. Sacré, P. F. Chavez, L. Netchacovitch, G. Piel, P. Hubert and E. Ziemons, *Talanta*, 2013, **116**, 899–905.
32 T. Henkel, T. Bermig, M. Kielpinski, A. Grodrian, J. Metze and J. M. Köhler, *Chem. Eng. J.*, 2004, **101**, 439–445.
33 A. Marz, K. R. Ackermann, D. Malsch, T. Bocklitz, T. Henkel and J. Popp, *J. Biophotonics*, 2009, **2**, 232–242.
34 A. März, T. Bocklitz and J. Popp, *Anal. Chem.*, 2011, **83**, 8337–8340.
35 S. Ayyappan, N. Sundaraganesan, V. Aroulmoji, E. Murano and S. Sebastian, *Spectrochim. Acta, Part A*, 2010, **77**, 264–275.
36 G. Seng, J. Bolard, L. Chinsky and P. Y. Turpin, *J. Raman Spectrosc.*, 1982, **13**, 100–102.
37 Y. Ozaki, R. W. King and P. R. Carey, *Biochemistry*, 1981, **20**, 3219–3225.
38 J. E. Pemberton, M. A. Bryant, R. L. Sobocinski and S. L. Joa, *J. Phys. Chem.*, 1992, **96**, 3776–3782.
39 X. Gao, J. P. Davies and M. J. Weaver, *J. Phys. Chem.*, 1990, **94**, 6858–6864.
40 H. Grabhorn and A. Otto, *Vacuum*, 1990, **41**, 473–475.
41 M. Baia, L. Baia, W. Kiefer and J. Popp, *J. Phys. Chem. B*, 2004, **108**, 17491–17496.

2.2 Droplet based microfluidics: spectroscopic characterization of levofloxacin and its SERS detection [IH2]

Izabella J. Hidi, Martin Jahn, Dana Cialla, Karina Weber, Jürgen Popp

Physical Chemistry Chemical Physics, 17, **2015**, 21236-21242

PCCP

PAPER

View Article Online
View Journal | View Issue

Cite this: *Phys. Chem. Chem. Phys.*, 2015, **17**, 21236

Droplet based microfluidics: spectroscopic characterization of levofloxacin and its SERS detection

I. J. Hidi,[a] M. Jahn,[a] K. Weber,[ab] D. Cialla-May*[ab] and J. Popp[ab]

Received 29th October 2014,
Accepted 16th January 2015

DOI: 10.1039/c4cp04970e

www.rsc.org/pccp

Levofloxacin (Levo), a second generation fluoroquinolone, has both clinical and environmental relevance. Therefore, the implementation of fast, robust and cost effective techniques for its monitoring is required. Here, its spectroscopic characterization and its detection in aqueous environment were carried out using surface enhanced Raman spectroscopy combined with droplet based microfluidics. The Levo molecule interacts with the silver nanoparticles *via* the carboxylate group and it adopts an upright or slightly tilted orientation. Furthermore, it is shown that the presence of Cl^- ions has a strong influence on the enhancement efficiency of the Raman signal of the target molecule. Thus, for the determination of the limit of detection (LOD) the measurements were carried out in the absence of any electrolytes. The estimated LOD is ~0.8 μM and the linear dynamic window ranges between 1–15 μM. These results were achieved after the normalization of the SERS signal to the Raman mode at 230 cm^{-1}. This band was attributed to the ν(Ag–O) stretching and it accounts for the Levo molecules in the first layer on the Ag nanoparticles.

Introduction

Levofloxacin (Levo), also known as Levaquin or Tavanic, is a second generation fluoroquinolone widely used against infections caused by both gram negative and gram positive bacteria.[1–4] Similar to most antibiotics, the drug has concentration dependent bacteria killing properties. Thus, discussions are on-going concerning whether it should be administered as single high dosage or multiple low dosages.[5] Furthermore, the drug undergoes limited metabolism in the human body. More than 85% of the administered dose is eliminated in human urine as unchanged drug. The normal Levo concentrations measured in urine are around 1 mM after 6 hours from the administration of a 500 mg dose and drop to 1 μM after 72 hours.[6–9] This results in the undesired presence of the antibiotic in surface waters, wastewaters, sediments and ground water worldwide.[10–12] Therefore, the monitoring of Levo is of high importance for both clinical and environmental purposes.

The gold standard to detect Levo is chromatography coupled with different detection methods, such as fluorescence or mass spectrometry.[9,13,14] In spite of the great technological advance, chromatographic methods are available only in large medical and academic centres and reference laboratories due to the complexity of these methods. Therefore, a less complex and more readily available detection method is required.

The combination of microfluidic platforms with surface enhanced Raman spectroscopy (SERS) gained interest in the scientific community during the last years.[15–19] The method combines the fingerprint specificity of Raman spectroscopy[20–22] with the high sensitivity resulting from the excitation of plasmon resonances of the metallic nanoparticles.[22–24] Furthermore, high sample throughputs are achieved when instead of the conventional flow-through devices droplet based platforms are employed. Additionally, it was shown that quantitative detection with high reliability can be carried out either by using an isotope edited internal standard[25] or by employing the target analyte itself as a standard.[26] Therefore, the technique presents a high potential for online drug monitoring.

Before detecting biologically relevant molecules in complex matrices, an understanding of the fundamental spectroscopic characteristics of the pure analytes is necessary. Several studies have been published concerning the vibrational characterization of different quinolones.[27–30] Among these, Neugebauer *et al.*[27] focused on the vibrational spectroscopic characterization of norfloxacin, whereas Gunesekaran *et al.*[29] performed the vibrational analysis as well as the description of the electronic structure and nonlinear properties of Levo. Both works provide valuable details, however, none is going beyond the conventional Raman or Fourier transform infrared spectroscopy.

[a] *Friedrich Schiller University Jena, Institute of Physical Chemistry and Abbe Center of Photonics, Helmholtzweg 4, 07745 Jena, Germany*
[b] *Leibniz Institute of Photonic Technology Jena, Albert-Einstein-Str. 9, 07745 Jena, Germany. E-mail: dana.cialla-may@uni-jena.de*

Concerning the detection of quinolones by means of SERS, the adsorption behaviour of pefloxacin (a 3rd generation quinolone never approved for clinical practice) on silver colloids prepared by the Creighton method was presented by Lecomte *et al.*[30] However, the preparation of the employed silver nanoparticles has to be carried out in the presence of an ice bath and the resulted colloids are known to be weakly stable.[30] Hence, this would present a high limitation for the online monitoring of any drug.

To the best of our knowledge, this is the first time when Levo is detected by means of SERS and insights concerning its adsorption behaviour and orientation on the surface of Ag metallic nanoparticles are provided. Here, silver nanoparticles were produced at room temperature according to the Leopold–Lendl protocol.[31] Furthermore, the detection in purified water by means of lab-on-a-chip SERS (LOC-SERS) is also carried out. The linearity of the SERS signal *vs.* the in droplet concentration of the target molecule is improved by using the Raman mode due to the Ag–O vibration located at 230 cm^{-1} as a standard.

Materials and methods

Chemicals and reagents

Levo (HPLC, 98%), silver nitrate (ACS reagent, ≥99%), hydroxylamine hydrochloride (ReagentPlus, 99%) and sodium hydroxide have been purchased from Sigma Aldrich and used as received.

Sample preparation

Stock solutions of 1 mM concentration of Levo were prepared by solving the appropriate quantity of powder in purified water. The solutions were stored in the fridge at 4 °C and used within one week. Working solutions of 10^{-5} and 10^{-4} M were obtained by diluting the stock solutions with purified water and used on the day of preparation.

The silver colloids were prepared according to the Leopold–Lendl protocol.[31] Briefly, 0.1 mmol silver nitrate was added to a mixture of hydroxylamine hydrochloride (0.15 mmol) and sodium hydroxide (0.3 mmol) under vigorous stirring. The solution turned instantaneously to grey-yellow colour. Stirring was continued for 10 s.

Instrumentation

UV-Vis absorption spectra were recorded in the 200–800 nm spectral range with a Jasco V650 diode array spectrophotometer. The acquisition speed was set to 200 nm min^{-1} with a spectral resolution of 1 nm.

For Raman, SERS and LOC-SERS measurements a WITec Raman microscope (WITec GmbH, Ulm, Germany) was used. As excitation a continuous wave diode-pumped solid-state laser with a wavelength of 514 nm and a maximum output power of 100 mW measured before the objective has been employed (Cobolt™). The same objective (Zeiss EC "Epiplan" DIC, 20×, N.A. 0.4) was used for focusing the laser beam and collecting the backscattered light. During measurements a 600 lines per mm grating was employed with a spectral resolution of ~5 cm^{-1}. The detection was carried out with a thermo-electric cooled (down to −70 °C) CCD detector with 1024 × 127 active pixels and a pixel size of 26 μm × 26 μm.

In the case of the reference Raman spectra of Levo powder and saturated aqueous solution the laser power at the sample surface was set to 2 and 95 mW, respectively. The plotted spectra are the average of five acquisitions with an integration time of 5 s each. Concerning the SERS spectra acquired in cuvettes a laser power of 35 mW and 1 s integration time with ten acquisitions was chosen.

In order to determine the limit of detection of Levo in aqueous solution a microfluidic platform (see Fig. 1) was employed. A detailed description of the platform has been published elsewhere.[25] Briefly, the glass chip has six different inlets and one outlet. All reagents are pumped into the chip through a computer controlled pump system (neMESYS Cetoni). At the first unit Levo/H_2O droplets are generated in the continuous phase of the mineral oil. At the second unit the Ag nanoparticles and the 1 M KCl solution or H_2O are dosed into the already existing droplets. The mixing of the analytes is assured by the two meandering channels. Furthermore, the microchannels were functionalized with octadecyltrichlorosilane in order to obtain a hydrophobic surface. As a result, a minimum wettability of the aqueous droplets is achieved leading to the exclusion of memory effects usually characteristic for flow through microfluidic platforms. The flow rates of mineral oil (10 nl s^{-1}), Ag nanoparticles (9 nl s^{-1}) and 1 M KCl–H_2O (2 nl s^{-1}) were kept constant during the measurement.

In order to have different in-droplet concentrations, the flow rates at the two ports of the droplet generator unit have been varied as follows: 0, 1, 2, 4, 6, 8, 10, 12, 14 nl s^{-1} for Levo and 14, 13, 12, 10, 8, 6, 4, 2, 0 nl s^{-1} for H_2O. For LOC-SERS measurements the chip was mounted on the microscope table. The SERS spectra were acquired continuously with 1 s integration time in the third channel. For every concentration step 1200 spectra were recorded containing pure droplet, pure mineral oil and also mixed spectra.

The theoretical Raman spectrum was calculated by employing the density functional theory (DFT) method. The theoretical frequencies were determined by using the B3LYP functional, 6-31G(d,p) basis set and a scaling factor of 0.97. The vibrational modes were assigned with the help of the Gauss-View molecular visualization program package.[32]

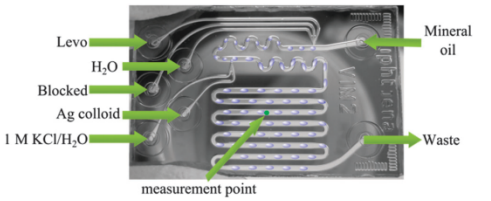

Fig. 1 Picture of the droplet based microfluidic chip used for LOC-SERS measurements together with the depiction of the droplets and the inlets.

Results and discussions

Spectroscopic characterization of Levo

The chemical structure of Levo (full name: (*S*)-9-fluoro-2,3-dihydro-3-methyl-10-(4-methylpiperazin-1-yl)-7-oxo-7*H*-pyrido[1,2,3-*de*]-1,4-benzoxazine-6-carboxylic acid) is depicted in Scheme 1. Its main backbone is formed by the quinolone ring system having attached a fluorine atom and a piperazine moiety. The first one provides increased potency against organisms while the second one is responsible for pseudomonal activity.[28] The molecule exists as a zwitterion in the aqueous phase at the neutral pH range (pK_{a1} = 6.02 and pK_{a2} = 8.15)[33,34] due to the presence of both anionic (carboxylic group) and cationic (piperazine ring) groups.

In Fig. 2 the reference Raman spectra measured on Levo powder and in the saturated aqueous solution is shown together with its calculated spectrum. In the case of the powder, the signal shows a high number of well-defined Raman modes. Most of the Raman bands involve the vibration of several atoms, their assignment to particular vibrational modes is difficult.[29] Nevertheless, the calculated Raman spectrum is in good accordance with the one presented by Gunesekaran *et al.*[29] Hence, the detailed vibrational assignment is not the subject of this publication.

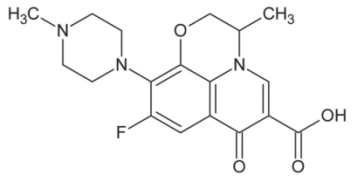

Scheme 1 Chemical structure of the Levo molecule ($C_{18}H_{20}FN_3O_4$).

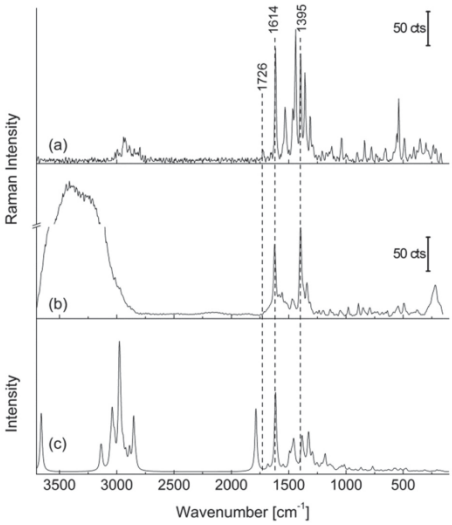

Fig. 2 Recorded Raman spectrum of (a) Levo powder and (b) saturated aqueous solution. (c) Calculated Raman spectrum obtained using B3LYP/6-31 G(d,p) method.

By comparing Fig. 2(a) with (b) one may see that the signal of the molecules in an aqueous environment strongly differs from the one of the powder. This can be explained by considering that in the case of the solid state molecules form crystals. Singh *et al.*[35] performed the conformational analysis of the Levo molecule and they also predicted the crystal structure of the hydrated and anhydrous forms. According to their results, the molecular packing is obtained through strong $\pi\cdots\pi$ interactions and bridges formed *via* the O–H$\cdots$N (*N*-methylpiperazine ring) and O–H$\cdots$O (carboxylate group) hydrogen bonds.

Once Levo is solved in water the close packing might be destroyed inducing a change in the polarization and, hence, in the Raman spectrum. The Raman modes with the highest intensities present in the case of the saturated aqueous solution are centred at 1614 cm^{-1} and 1395 cm^{-1}. The first one is ascribed to the C=C vibration of the quinolone ring system while the second one is due to the combined contribution of the vibration of the same aromatic moieties with the COO^- symmetric stretching. The presence of the carboxylate group is due to the zwitterion characteristic of the molecules. Thus, upon protonation, the carboxylic unit converts into a carboxylate group. Here, the two C–O bonds have the same length with the negative charge centred equally on the two oxygen atoms rather than on the single bonded O. Hence, one may speak about the delocalization of electrons. This is also further supported by the very weak Raman mode at 1726 cm^{-1} assigned to the ν(C=O) vibration of the carboxylic group measured on powder. Nevertheless, the same band is completely absent in the aqueous solution as zwitterions are more stable as the uncharged Levo molecules.[34]

Generally, regardless of the preparation protocol, different salts are added to the Ag colloids in order to overcome the electrostatic repulsion between the particles.[31,36,37] As a result, a considerable enhancement of the SERS signal of the target molecules is achieved. However, in the case of the Levo molecules the addition of potassium chloride induces the reverse effect. SERS spectra of different mixtures have been recorded and are presented in Fig. 3. As reference, the blank spectra of Ag colloids with and without salt addition are also plotted. The presence of KCl in a final concentration of 0.9 mM results in the increase in the intensity of the band located around 238 cm^{-1} due to the absorption of Cl^- ions on the surface of the nanoparticles. Apart from this, only bands assigned to the vibrations of the water molecules are present. Hence, no interferences of the background are expected when the SERS spectrum of the analyte is acquired.

The influence of the salt addition on the SERS spectrum of the analyte is significant as it can be observed by comparing the spectra in Fig. 3(c–e). The highest intensities were recorded when no electrolyte is added to the mixture. This may indicate that a so called ''analyte induced aggregation'' of the silver nanoparticles takes place. Nevertheless, the intensity strongly

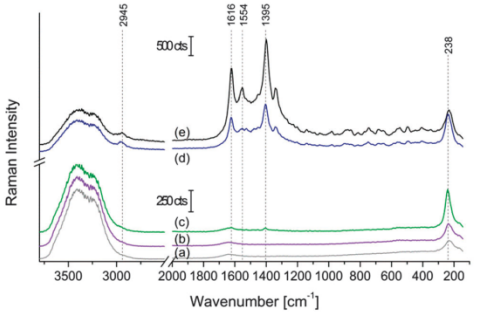

Fig. 3 SERS spectra of (a) Ag + H_2O, (b) Ag + H_2O + 1 M KCl, (c) Ag + 1 M KCl + Levo, (d) Ag + Levo + 1 M KCl, (e) Ag + Levo + H_2O mixtures. The ratio of Ag colloids to Levo or H_2O was 1 : 1. The final concentrations of Levo and KCl in the mixture was 4.5 × 10^{-5} M and 0.9 mM, respectively.

dropped when KCl was present in the solution. In both cases, the Levo molecules are allowed to interact with the Ag colloids, the 1 M KCl being pipetted in the cuvette as last. Furthermore, when the salt is added first and only afterwards the analyte, the signal is almost completely disappearing. This phenomenon may be attributed to the strong affinity of the negatively charged chloride ions for the silver nanoparticles.[30,38,39] Consequently, a competition at the metallic surface takes place between the Levo molecules and the Cl^-. This is particularly proved by the importance of the order in which the target analyte and potassium chloride is added to the Ag nanoparticles.

The presented hypothesis is further supported by the recorded UV-Vis spectra. For reference, in Fig. 4 the extinction spectrum of the Ag colloid mixed with purified water in a ratio of 1 : 1 is presented. The absorption band centred at 407 nm is in good accordance with the already published results[31] proving that the synthesis was carried out with success. When Levo with a concentration of 0.5 mM is added to the Ag nanoparticles the colour of the colloid turns from yellow to grey. This is a clear indication for the induction of silver nanoparticle aggregates. Furthermore, in the recorded UV-Vis

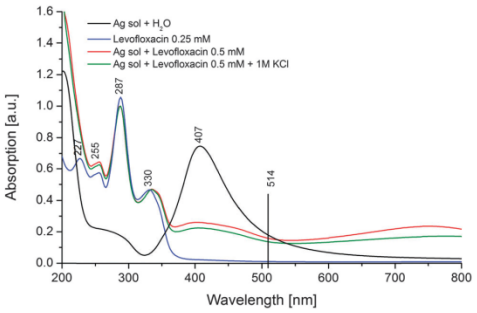

Fig. 4 UV-Vis spectra of different solutions.

spectrum of the mixture one may see that the absorption band at 407 nm considerably decreases in intensity. Additionally, a second broad band centred at 750 nm appears in the high wavelength region due to the presence of silver clusters. Beside these, strong absorption bands located in the 200–350 nm region and assigned to the strong π–π* molecular transitions of the Levo molecule[29] were detected. The absorption spectrum of the pure analyte is plotted for reference with blue line in Fig. 4. By further adding 1 M KCl solution to the Ag colloid : Levo mixture the intensity of the 407 nm absorption band and the one at 750 nm decreases further. This may indicate the creation of larger polydispersed Ag clusters which are no longer able to support plasmonic resonances, leading to the decrease of the SERS signal.

Furthermore, it is well known, that in order to obtain SERS spectra of the target analyte the molecules have to adsorb efficiently to the SERS substrate.[40] This occurs either *via* van der Waals forces or forces which involve valence bindings. In the first case no relevant differences are expected between the normal Raman and the SERS spectra. In the second case, the band intensities and positions can be affected due to the formation of metal–molecule complex. By closely comparing the normal Raman and SERS spectra (see Fig. 2 and 3) no significant band shifts are noticed. However, the ratio of the two most intense Raman modes at 1395 and 1614 cm^{-1} is changing in the following way: for powder $I_{1395/1614}$ = 0.98, for aqueous solution the ratio is 1.31, in the presence of silver nanoparticles it amounts to 1.33 while after KCl addition it increases to 1.47. The difference in the band ratio for the Raman spectra of powder and saturated aqueous solution arises due to the fact that the zwitterion is slightly more stable in aqueous environment than the uncharged form of the Levo.[34] As a result, the number of molecules with deprotonated carboxylic group increased. This leads to the disappearance of the 1726 cm^{-1} band ascribed to the C=O stretching and an increase in intensity of the 1395 cm^{-1} Raman mode. In the case of the SERS spectra, the change in band ratios was generally attributed to a change in the orientation of the target molecule. The two particular Raman modes have been ascribed to the stretching of the quinolone ring system with the difference that in the case of the 1395 cm^{-1} band the $\nu_s(COO^-)$ also has a contribution. This might suggest that the Levo interacts with the surface of the Ag nanoparticles through the COO^- group. Furthermore, the adsorption should happen *via* the lone pair electrons of the oxygen atom rather than through the delocalized electrons of the carboxylate group. The latter possibility is ruled out considering that the position of the band doesn't change as compared to the normal Raman spectrum.[41] In the literature shifts as high as 13–19 cm^{-1} have been observed when molecules containing carboxylate groups interact with the metallic surface *via* the delocalized electrons.[42,43] Beside these considerations, the downshift by 10 cm^{-1} of the Raman mode at 238 cm^{-1} due to the ν(Ag–Cl) present in the SERS spectra when KCl is added might indicate the formation of Ag–O bonds instead of Ag–Cl.

Moreover, by taking into consideration the surface selection rules[44] one may deduce the orientation of a molecule containing

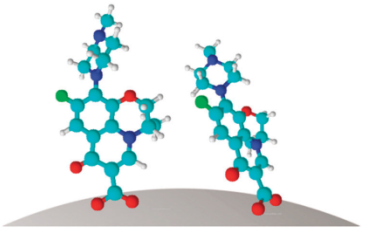

Scheme 2 Sketch of the orientation of the Levo molecule on the surface of the Ag nanoparticles.

aromatic moieties based on whether the in-plane or out-of-plane ring vibrations are predominantly enhanced. More exactly, when the Raman modes assigned to the in-plane ring vibrations are enhanced an upright orientation is assumed, while in the case of the enhanced out-of plane vibrations the molecule adopts a parallel orientation on the surface of the metallic nanoparticles. In the case of the SERS spectrum measured in the absence of KCl one may notice the presence of the Raman band centred at 1554 cm^{-1}. This was assigned to the in-plane mode of the of the quinolone ring system.[34] Furthermore, no out-of plane vibrations are detected in the 900–600 cm^{-1} region. As a result, it is assumed that the Levo molecules adopt an upright orientation with the aromatic ring system being perpendicular or slightly tilted on the Ag surface (see Scheme 2). When Cl^- ions are added to the solution, the 1554 cm^{-1} Raman mode loses intensity while no other new bands appear in the SERS spectrum as compared with the "no KCl" case. This might indicate that the target analyte is slightly tilted on the SERS substrate. This orientation is further supported by considering the Raman mode ascribed to the C–H stretching vibrations in the high wavenumber region (2945 cm^{-1}). It is well known, that these vibrations are more enhanced when the bond is perpendicular than when it lies parallel to the surface of the metallic nanoparticle.

LOC-SERS measurements

Due to the clinical and environmental relevance of Levo its detection in concentrations ranging between 1 mM to 1 μM or below is of major importance. Here, the first determination by means of LOC-SERS in the 1–100 μM range is presented. In order to provide reproducible measurement conditions and a high precision for serial dilutions a droplet based microfluidic setup has been used. According to the picture presented in Fig. 1, aqueous solutions of Levo with a starting concentration of 10^{-5} and 10^{-4} M were mixed in the chip with purified water in order to obtain 15 different concentration steps. The time elapsed between the addition of the Ag colloids to the analyte containing droplet and measurement was 3 minutes. In Fig. 5 the mean SERS spectra of all concentration steps were plotted together with the blank spectrum. For the later one only purified water was pumped at the first dosing unit. When compared with this, the two Raman modes characteristic to Levo at 1395 and 1614 cm^{-1} are visible starting with a concentration of 1.42 μM. For a better visualization the band due to the quinolone ring

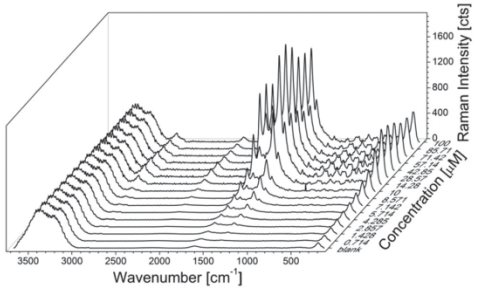

Fig. 5 Mean SERS spectra of Levo with concentrations between 0.714 and 100 μM measured in the microfluidic platform. The mean spectrum of the blank (when only H_2O is pumped through at the first dosing unit) is also shown.

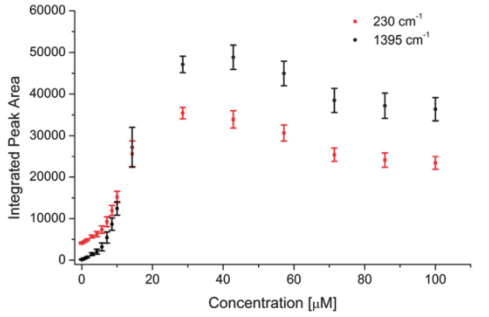

Fig. 6 Concentration dependency of the integrated peak area for the Raman mode @ 1395 cm^{-1} due to the ring vibration of the quinolone system and $\nu(COO^-)$ and the @ 230 cm^{-1} due to the Ag–O stretching.

stretching combined with $\nu_s(COO^-)$ mode was chosen. The peak area was calculated according to Simpson's rule and the mean value and its standard deviation were plotted against the in-droplet concentration of the target analyte (see Fig. 6, black scatter plot). The calculation was performed for every single spectrum of a given concentration step.

For the low concentrations an exponential increase is observed, while for concentrations higher than 20 μM a plateau region was obtained. The latter phenomenon may be explained by considering the limited free binding sites at the Ag nanoparticles' surface. Once the amount of the Levo molecules reaches a critical threshold a further addition will not lead to the increase of the signal. Furthermore, the SERS effect has a short range, the high electromagnetic field resulting from the excitation of plasmon resonances decays strongly with the distance. Therefore, only the molecules located in the first several layers on the metallic nanoparticles provide enhanced Raman signals.

Based on the fundamental characterization of the Levo molecule it was concluded that a so called analyte induced aggregation of the Ag nanoparticles takes place. Considering that no other molecules were present in the microdroplets,

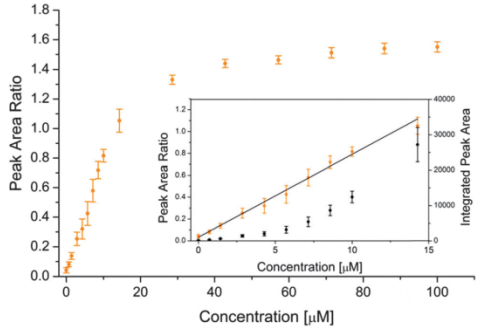

Fig. 7 The peak area ratio of the 1395 cm^{-1} and 230 cm^{-1} Raman modes against the in-droplet concentration of Levo. In the inset, the comparison of the integrated peak area of the Raman mode at 1395 cm^{-1} *vs.* the normalized peak area is shown for the 0–15 μM concentration range.

the intensity increase of the Raman mode centred at 230 cm^{-1} and assigned to the ν(Ag–O) is due to the increase of the number of adsorbed Levo molecules. Concerning the response of the peak area at the increase of the concentration a slightly different behaviour, as compared with the 1395 cm^{-1} band, is observed (Fig. 6, red scatter plot). More exactly, for concentrations below 14 μM the increment for the ν(C=C) + ν_s(COO^-) band is more pronounced. At 14 μM the two values are similar, while above this point both reach saturation. However, the peak area of the 230 cm^{-1} is smaller as compared with the other Raman mode. Therefore, the underlying mechanism behind the increment of the signal has to be different for the two Raman bands. On one hand, the Raman mode at 230 cm^{-1} band is due to the Levo molecules in the first layer on the surface of the metallic nanoparticles. On the second hand, the intensity of the 1395 cm^{-1} is increasing also due to the molecules present in the upper layers but still found in the hot-spot between the nanoparticles. Thus, for concentrations lower than 14 μM by calculating the peak area ratio of the two Raman modes a normalization of the SERS signal making use of the analyte induced aggregation can be carried out. In Fig. 7 it is shown that after the normalization a linear response with a correlation factor of 0.99 is achieved over the 0–15 μM concentration range (inset Fig. 7). Furthermore, in order to calculate the limit of detection (LOD) the so called "three times standard deviation of the blank" IUPAC criterion was used. The same integration boarders applied for the calculation of the peak area of the Raman mode centred at 1395 cm^{-1} were used for calculating the area underneath the curve of the blank spectra.

Afterwards, the value of the three times the standard deviation of the blank was used as threshold for estimating the LOD. According to this, concentrations down to 0.8 μM can be detected by employing the LOC-SERS technique.

Conclusions

In the present study, the spectroscopic characterization of the Levo molecule and its detection in the 1–100 μM concentration range in aqueous solution was carried out. It was shown that the aggregation of the silver nanoparticles is induced in the presence of the analyte and no additional salts are necessary in order to achieve high intensity SERS spectra. Furthermore, due to the competition at the surface of the Ag colloids between the Cl^- and the Levo molecules, the order in which these two chemicals are added to the silver sols has a high importance. Based on the surface selection rules, the change in the intensity ratio of selected Raman modes and the presence of the 230 cm^{-1} band ascribed to the ν(Ag–O) vibration the orientation of the molecule at the silver surface was determined. Thus, in the absence of chloride ions Levo adopts a perpendicular or slightly titled orientation, while in the presence of KCl it is titled. In both cases, the interaction of the analyte happens *via* the lone pair electrons of the oxygen atoms of the carboxylate group. In the second part of the paper it was shown that Levo can be detected in a concentration as low as 0.8 μM. Moreover, the linearity of the SERS signal *vs.* the in-droplet concentration of the analyte can be significantly improved by normalizing the signal to the Raman mode due to the Ag–O stretching vibration.

Acknowledgements

The funding of the PhD project of I. J. Hidi within the framework "Carl-Zeiss-Strukturmaßnahme" is gratefully acknowledged. The projects "QuantiSERS" (03IPT513A) and "Jenaer Biochip Initiative 2.0" (03IPT513Y) within the framework "InnoProfile Transfer – Unternehmen Region" are supported by the Federal Ministry of Education and Research, Germany (BMBF). We thank the microfluidic group of the IPHT for providing the lab-on-a-chip devices for the measurements. Additionally, the help of Dr Dirk Bender with the theoretical calculations is gratefully acknowledged.

Notes and references

1 D. S. North, D. N. Fish and J. J. Redington, *Pharmacotherapy*, 1998, **18**, 915–935.
2 A. P. Cardile, H. Briggs, S. R. Burguete, M. Herrera, B. L. Wickes and J. H. Jorgensen, *Diagn. Microbiol. Infect. Dis.*, 2014, **78**, 199–200.
3 R. F. Grossman, P.-R. Hsueh, S. H. Gillespie and F. Blasi, *Int. J. Infect. Dis.*, 2014, **18**, 14–21.
4 F. C. Adler-Shohet, J. Low, M. Carson, H. Girma and J. Singh, *Pediatr. Infect. Dis.*, 2014, **33**, 664–666.
5 G. Cao, J. Zhang, X. Wu, J. Yu, Y. Chen, X. Ye, D. Zhu, Y. Zhang, B. Guo and Y. Shi, *J. Clin. Pharm. Ther.*, 2013, **38**, 394–400.
6 F. M. E. Wagenlehner, M. Kinzig-Schippers, F. Sörgel, W. Weidner and K. G. Naber, *Int. J. Antimicrob. Agents*, 2006, **28**, 551–559.
7 A. A. Salem, H. A. Mossa and B. N. Barsoum, *Spectrochim. Acta, Part A*, 2005, **62**, 466–472.
8 M. Rambla-Alegre, J. Esteve-Romero and S. Carda-Broch, *J. Chromatogr. B: Anal. Technol. Biomed. Life Sci.*, 2009, **877**, 3975–3981.

9 H. Sun, H. Wang and X. Ge, *J. Clin. Lab. Anal.*, 2012, **26**, 486–492.
10 E. M. Golet, I. Xifra, H. Siegrist, A. C. Alder and W. Giger, *Environ. Sci. Technol.*, 2003, **37**, 3243–3249.
11 D. Fatta-Kassinos, S. Meric and A. Nikolaou, *Anal. Bioanal. Chem.*, 2011, **399**, 251–275.
12 I. Senta, S. Terzic and M. Ahel, *Water Res.*, 2013, **47**, 705–714.
13 R. Cazorla-Reyes, R. Romero-González, A. G. Frenich, M. A. Rodríguez Maresca and J. L. Martínez Vidal, *J. Pharm. Biomed. Anal.*, 2014, **89**, 203–212.
14 S. Siewert, *J. Pharm. Biomed. Anal.*, 2006, **41**, 1360–1362.
15 R. Gao, N. Choi, S. I. Chang, S. H. Kang, J. M. Song, S. I. Cho, D. W. Lim and J. Choo, *Anal. Chim. Acta*, 2010, **681**, 87–91.
16 M. Lee, K. Lee, K. H. Kim, K. W. Oh and J. Choo, *Lab Chip*, 2012, **12**, 3720–3727.
17 M. Wang, M. Benford, N. Jing, G. Coté and J. Kameoka, *Microfluid. Nanofluid.*, 2009, **6**, 411–417.
18 C. Rivet, H. Lee, A. Hirsch, S. Hamilton and H. Lu, *Chem. Eng. Sci.*, 2011, **66**, 1490–1507.
19 L. Wu, Z. Wang, S. Zong and Y. Cui, *Biosens. Bioelectron.*, 2014, **62**, 13–18.
20 P. C. Ashok, M. E. Giardini, K. Dholakia and W. Sibbett, *J. Biophotonics*, 2014, **7**, 103–109.
21 K. M. Marzec, T. P. Wrobel, A. Rygula, E. Maslak, A. Jasztal, A. Fedorowicz, S. Chlopicki and M. Baranska, *J. Biophotonics*, 2014, **7**, 744–756.
22 J. Yang, L. Zhen, F. Ren, J. Campbell, G. L. Rorrer and A. X. Wang, *J. Biophotonics*, 2014, **9999**, DOI: 10.1002/jbio.201400070.
23 D. Cialla, A. Marz, R. Bohme, F. Theil, K. Weber, M. Schmitt and J. Popp, *Anal. Bioanal. Chem.*, 2012, **403**, 27–54.
24 P. Negri and R. A. Dluhy, *J. Biophotonics*, 2013, **6**, 20–35.
25 A. März, K. R. Ackermann, D. Malsch, T. Bocklitz, T. Henkel and J. Popp, *J. Biophotonics*, 2009, **2**, 232–242.
26 E. Kammer, K. Olschewski, T. Bocklitz, P. Rosch, K. Weber, D. Cialla and J. Popp, *Phys. Chem. Chem. Phys.*, 2014, **16**, 9056–9063.
27 U. Neugebauer, A. Szeghalmi, M. Schmitt, W. Kiefer, J. Popp and U. Holzgrabe, *Spectrochim. Acta, Part A*, 2005, **61**, 1505–1517.
28 Y. Wang, K. Yu and S. Wang, *Spectrochim. Acta, Part A*, 2006, **65**, 159–163.
29 S. Gunasekaran, K. Rajalakshmi and S. Kumaresan, *Spectrochim. Acta, Part A*, 2013, **112**, 351–363.
30 S. Lecomte, N. J. Moreau, M. Manfait, J. Aubard and M. H. Baron, *Biospectroscopy*, 1995, **1**, 423–436.
31 N. Leopold and B. Lendl, *J. Phys. Chem. B*, 2003, **107**, 5723–5727.
32 A. Frisch, A. Nielsen and A. Holder, *Gaussian Inc.*, Pittsburgh, PA, 2000.
33 I. Sousa, V. Claro, J. L. Pereira, A. L. Amaral, L. Cunha-Silva, B. de Castro, M. J. Feio, E. Pereira and P. Gameiro, *J. Inorg. Biochem.*, 2012, **110**, 64–71.
34 A. Lambert, J.-B. Regnouf-de-Vains and M. F. Ruiz-López, *Chem. Phys. Lett.*, 2007, **442**, 281–284.
35 S. S. Singh and T. S. Thakur, *CrystEngComm*, 2014, **16**, 4215–4230.
36 A. M. El Badawy, K. G. Scheckel, M. Suidan and T. Tolaymat, *Sci. Total Environ.*, 2012, **429**, 325–331.
37 I. J. Hidi, A. Muhlig, M. Jahn, F. Liebold, D. Cialla, K. Weber and J. Popp, *Anal. Methods*, 2014, **6**, 3943–3947.
38 J. Aubard, E. Bagnasco, J. Pantigny, M. F. Ruasse, G. Levi and E. Wentrup-Byrne, *J. Phys. Chem.*, 1995, **99**, 7075–7081.
39 G. Lévi, J. Pantigny, J. P. Marsault and J. Aubard, *J. Raman Spectrosc.*, 1993, **24**, 745–752.
40 E. C. Le Ru and P. G. Etchegoin, in *Principles of Surface-Enhanced Raman Spectroscopy*, ed. E. C. L. Ru and P. G. Etchegoin, Elsevier, Amsterdam, 2009, pp. 367–413, DOI: 10.1016/B978-0-444-52779-0.00013-1.
41 Y. J. Kwon, D. H. Son, S. J. Ahn, M. S. Kim and K. Kim, *J. Phys. Chem.*, 1994, **98**, 8481–8487.
42 H. Park, S. B. Lee, K. Kim and M. S. Kim, *J. Phys. Chem.*, 1990, **94**, 7576–7580.
43 Y. J. Kwon, S. B. Lee, K. Kim and M. S. Kim, *J. Mol. Struct.*, 1994, **318**, 25–35.
44 M. Moskovits and J. S. Suh, *J. Phys. Chem.*, 1984, **88**, 5526–5530.

2.3 Toward levofloxacin monitoring in human urine samples by employing the LoC-SERS technique [IH3]

Izabella J. Hidi, Martin Jahn, Mathias W. Pletz, Karina Weber,

Dana Cialla-May, Jürgen Popp

Journal of Physical Chemistry C, 120 (37), **2016**, 20613–20623

http://pubs.acs.org/doi/abs/10.1021/acs.jpcc.6b01005

THE JOURNAL OF PHYSICAL CHEMISTRY C

Article

pubs.acs.org/JPCC

Toward Levofloxacin Monitoring in Human Urine Samples by Employing the LoC-SERS Technique

Izabella J. Hidi,[†,‡] Martin Jahn,[†,‡] Mathias W. Pletz,[§,∥] Karina Weber,[†,‡] Dana Cialla-May,[*,†,‡] and Jürgen Popp[*,†,‡]

[†]Friedrich Schiller University Jena, Institute of Physical Chemistry and Abbe Center of Photonics, Helmholtzweg 4, 07745 Jena, Germany

[‡]Leibniz Institute of Photonic Technology Jena, Albert-Einstein-Strasse 9, 07745 Jena, Germany

[§]Center for Infectious Diseases and Infection Control, Jena University Hospital, Erlanger Allee 101 07740 Jena, Germany

[∥]InfectoGnostics Research Campus Jena, Center for Applied Research, Philosophenweg 7, Jena, 07743, Germany

Supporting Information

ABSTRACT: The pharmacokinetics of antibiotics such as levofloxacin exhibits large interindividual differences, questioning the value of fixed dose regimens and warranting individual dosing based on therapeutic drug monitoring. Here, in a proof of principal study, it is shown that levofloxacin can be detected in human urine samples by employing lab-on-a-chip surface enhanced Raman spectroscopy (LoC-SERS). First, artificial urine is used as a matrix in order to get insights into the influence of different parameters such as matrix complexity, aggregation time, and matrix dilution on the overall SERS signal. Second, three anonymized individual and three pooled urine samples originating from patients undergoing either no or unknown medical treatments have been spiked with the target analyte. Measurements were performed with a benchtop and a portable Raman setup. In all six samples urinary levofloxacin concentrations between 0.45 mM (162.6 μg/mL) and 1.8 mM (650.5 μg/mL) have been successfully detected. According to the literature, the normal levofloxacin concentration in urine is 1.38 mM ± 0.68 mM with a minimum measured concentration of 0.45 mM after 4 h from the administration of a 500 mg dose. The presented results therefore show that LoC-SERS is a promising bioanalytical tool for urine analysis.

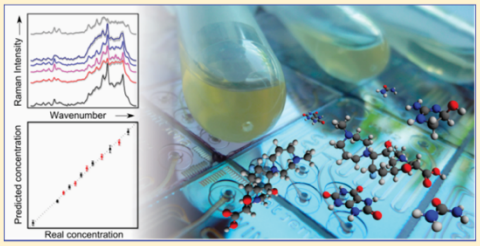

INTRODUCTION

The effective treatment of bacterial infections is a major issue due to the occurrence of antibiotic resistances. Depending on the risks associated with a given medical treatment, clinical trials may include healthy and/or patient volunteers in order to establish the pharmacokinetic and pharmacodynamic (PK-PD) parameters of drugs. In the case of antibiotics used for treating infections, most often healthy volunteers are recruited for dose finding studies. There is a growing body of literature demonstrating that fixed dose regimens derived from such studies fail in the critically ill intensive care unit (ICU) patient. Due to the high variability of PK parameters—within the same patient on different days—experts demand therapeutic drug monitoring for antibiotics in ICU patients.[1] Therapeutic drug monitoring (TDM) was introduced at the beginning of the´70s, initially to avoid overdosing and toxicity of antibiotics with a small therapeutic window, such as aminoglycosides and vancomycin.

Levofloxacin is a second generation fluoroquinolone widely used for the treatment of bacterial infections, particularly respiratory and urinary tract infections.[2,3] It is generally well tolerated by patients; however, several reports have been published concerning its adverse effects, such as, for example, tenosynovitis,[4] crystal nephropathy,[5] hepatotoxicity,[6] pharmacokinetic interaction,[7,8] Achilles rupture,[9] and metabolic coma.[10] Additionally, in the case of obese patients[11] even if the maximum concentration of the drug appeared to be similar to the case of normal-weight individuals, a significantly faster clearance rate was observed. As a consequence, the total drug exposure over time was altered and the efficiency of the treatment was decreased. Levofloxacin undergoes limited metabolism in the human body, more than 85% of the administered dose being excreted in urine as unchanged drug. Therefore, its clearance rate can be easily monitored by determining its concentration in urine. Based on the pharmacokinetic studies carried out with healthy volunteers and published by Wagenlehner et al.,[2,12,13] urinary concentrations of levofloxacin after 4 h from the administration of a

Special Issue: Richard P. Van Duyne Festschrift

Received: January 29, 2016
Revised: March 14, 2016

DOI: 10.1021/acs.jpcc.6b01005
J. Phys. Chem. C XXXX, XXX, XXX−XXX

single oral dose of 500 mg are 1.38 mM ± 0.68 mM with a minimum measured concentration of 0.45 mM.

Chromatographic methods, based on the physical separation of mixtures due to the differences in the components' partition coefficient, are the gold standard for TDM.[3,14−17] While chromatography is characterized by a high sensitivity and specificity, it is still limited by complex sample preparation steps needed in order to get a final extract fully compatible with chromatographic determination. During the last three years, the number of publications focusing on the detection of biological relevant molecules in artificial and human urine by surface enhanced Raman spectroscopy (SERS) has significantly increased. Results include the detection of free heme as biomarker for acute kidney dysfunction,[18] and of hypoxanthine as biomarker for prostate cancer,[19,20] acetyl amantadine,[21] methamphetamine,[22,23] creatinine,[24−26] 3-amino-5-methylmorpholino-2-oxazolidinone,[27] adenosine,[28,29] uric acid,[25] urea and promethazine,[30] glucose,[31,32] fructose,[33] and nicotine.[34] A significant part of these studies employs functionalized planar SERS substrates known for low spot-to-spot and substrate-to-substrate reproducibility. A small fraction uses cuvette based SERS measurements with colloidal Ag or Au nanoparticles (NPs). Nevertheless, both approaches are limited by the lack of reproducible and automatic measurement conditions. One of the solutions for these shortcomings is the so-called lab-on-a-chip SERS (LoC-SERS) technique. Here, the high specificity offered by Raman spectroscopy[35,36] is combined with the sensitivity of SERS[37,38] and high sample throughput of droplet based microfluidic platforms while the measurements are automated and fast.[39,40] Furthermore, easy to prepare colloidal solutions, such as the ones synthesized according to the Leopold-Lendl protocol,[41] can be employed.

In a previous publication of ours,[39] we could show that SERS combined with droplet based microfluidics is suitable for the detection of levofloxacin in purified aqueous solution. A linear response was achieved for a concentration range of 0.8−15 μM by using the Raman mode assigned to the Ag−O stretching vibration as an internal standard. Additionally, it was found that the analyte is inducing the aggregation of the Ag nanoparticles (Ag NPs) used as SERS substrates. Thus, no further addition of chemicals is necessary to achieve an optimal SERS enhancement. Finally, insights regarding the adsorption mechanism of the molecule on the surface of the metallic nanoparticles were also presented. As a continuation, the work presented here focuses on the determination of levofloxacin in artificial and human urine. First, an artificial urine matrix was used in order to have an easy to access and easy to handle solution mimicking human urine samples. The results obtained for artificial urine are the basis for the detection of levofloxacin in human urine samples. The final aim was to prove that LoC-SERS can be applied for levofloxacin clearance monitoring and for assessing patient compliance. Therefore, the investigated urinary concentration range was chosen to be between 0.45 and 1.8 mM (see above). To the best of our knowledge, this is the first report proving the high potential of SERS for the determination of levofloxacin in human urine samples. Furthermore, in order to demonstrate the potential of LoC-SERS as a fast bed-side analysis approach, a miniaturized Raman setup has been also applied.

■ MATERIALS AND METHODS

Chemicals and reagents. Levofloxacin (HPLC, 98%), silver nitrate (ACS reagent, 99%), hydroxylamine hydrochloride (ReagentPlus, 99%), sodium hydroxide, and creatinine (anhydrous, ≥ 98%) have been purchased from Sigma-Aldrich. $CaCl_2$ (≥94%), Na_2SO_4 (≥99%), $MgSO_4{\cdot}7H_2O$ (≥99%, p.a., ACS), KCl (≥99.5% p.a. ACS, ISO), urea (≥99,5%, p.a.), $NaH_2PO_4{\cdot}2H_2O$ (≥98%, Ph.Eur., USP), Na_2HPO_4 (≥99%, p.a., ACS), sodium citrate (≥99%, extra pure), and NaCl (≥99.5% p.a. ACS, ISO) were bought from Carl Roth while NH_4Cl (EMSURE ACS, ISO, Reag. Ph Eur) was received from Merck. All chemicals have been used as received without further purification.

Sample preparation. The silver colloidal solution was prepared according to the protocol published by Leopold and Lendl.[41] Silver nitrate was added to a mixture of hydroxylamine hydrochloride and sodium hydroxide under vigorous stirring. The final concentrations of the chemicals in the solution are 10^{-3} M for silver nitrate, 1.5×10^{-3} M for hydroxylamine hydrochloride, and 0.3×10^{-3} M for sodium hydroxide. The color of the solution turned instantaneously into gray-yellow. Stirring was continued for 10 s. The as-prepared solution was stored at 4 °C until the measurements were performed. The same batch was used for both artificial and human urine measurements. Figure S1 (in SI) presents the UV−vis spectra of the pure colloids and of the aggregated Ag NPs due to the addition of KCl. Computer simulations have shown that strong signal enhancements cannot be obtained using a pure colloidal suspension where mainly only monomer metallic nanoparticles are present.[23] Therefore, choosing a laser line for excitation at 407 nm will not provide the highest SERS enhancement. Instead, 532 nm was employed in order excite the coupled plasmonic resonances located in the "hot spots" between aggregated nanoparticles. Finally, for comparison, a second fresh batch was also prepared.

Artificial urine was synthesized according to a modified protocol published by Yang et al.[42] Briefly, the aqueous solution contains 13.72 mM $CaCl_2$, 34.21 mM Na_2SO_4, 5.92 mM $MgSO_4{\cdot}7H_2O$, 85.99 mM NH_4Cl, 162.71 mM KCl, 832.5 mM urea, 19.44 mM creatinine, 17.05 mM $NaH_2PO_4{\cdot}2H_2O$, 7.25 mM Na_2HPO_4, 5.46 mM sodium citrate and 23.69 mM NaCl with a pH value of 5. Two stock solutions having a concentration of 1 mM levofloxacin were prepared by solving the appropriate amounts of powder in high purity water or in artificial urine. For the LoC-SERS studies the stock solutions were diluted with the corresponding solvents in order to reach the desired levofloxacin concentrations.

Nine anonymized human urine samples were received from the Institute of Medical Microbiology, University Hospital Jena. Analysis of human samples was approved by the local Ethical Committee (3701-02/13). Informed consent form was waived because these samples were left over volumes of routine analysis and were anonymized. The samples were kept at 4 °C until filtration was carried out for sterilization and for removing cells and debris using a sterile syringe filter (Rotilabo-syringe filter, PVDF, sterile, pore size 0.22 μm). After filtration the samples were stored for one month at −21 °C. On the evening prior the measurement day the vials were moved to 4 °C and left to thaw overnight. A second filtration step was carried out in order to remove precipitated crystallized salts.[43] In the case of the measurements carried out with the portable Raman setup the urine sample was frozen again and kept at −21 °C for two additional months.

For all samples, a test for the presence of antibiotics ("inhibitory test"), part of the microbiological routine analysis, was performed by the Institute of Medical Microbiology. Here

DOI: 10.1021/acs.jpcc.6b01005
J. Phys. Chem. C XXXX, XXX, XXX−XXX

Bacillus subtilis was used on an agar diffusion assay. For six samples there was no visible inhibition of the bacteria growth, while for the other three the test was positive. For the latter case, patients have undergone medical treatments which caused the antibacterial activity. However, no information concerning the received medication is known, due to the anonymized nature of the samples.

LoC-SERS measurements were carried out on three individual (**S1**, **S2**, and **S3**) and three pooled samples (**P0**, **P1**, **P2**). **S1**, **S2**, and **S3** had a negative inhibitory test result and they were further used for preparing pool **P0**. The three urine samples showing antibacterial activity were used for the second pool, **P1**. Last, further three negative samples build pool **P2**. The ratio of the amount of urine to water or/and aqueous levofloxacin solution used for spiking was chosen to be 3 to 11. Therefore, the urine samples were diluted to 21.4% prior to the measurements (Scheme 1). In total 12 solutions with different levofloxacin concentrations have been prepared for each sample/pool (see Supporting Information (*SI*), Table S1).

Scheme 1. Urine Sample Handling Steps

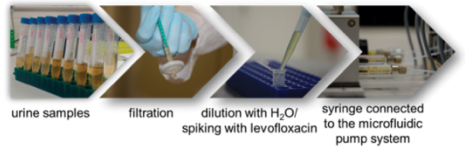

Instrumentation. The pH value of the samples was measured with a pH meter from Hanna Instruments (HI 9321) equipped with a combination microelectrode (HI 1083B).

For the LoC-SERS experiments two Raman setups have been employed. First, six measurement sets (SI, Table S2) have been performed with an XploRA INV inverted Raman microscope from Horiba Scientific. This Raman setup was equipped with a laser emitting at 532 nm with 5 mW power at the sample surface and a thermoelectrically cooled CCD camera (−69 °C). During the measurements, the same objective (Nikon 20x 0.4 N.A.) was used for focusing the laser beam on the sample's surface and for collecting the backscattered photons. The Raman spectra were recorded with a spectral resolution of 8 cm^{-1} by employing a 600 l/mm grating, a pinhole of 100 μm and slit of 200 μm. Second, in order to prove that LoC-SERS can be performed with a compact and cost-efficient Raman approach, a portable Raman setup (high resolution i-Raman© from B&WTek equipped with a laser emitting at 532 nm, 12 mW power at the sample surface and a thermoelectrically cooled CCD (+10 °C)) has been also employed. The same objective (Polytec, 20x, N.A. 0.4) was employed for focusing the laser beam and for collecting the backscattered light. The spectral resolution was ∼4 cm^{-1}. For both Raman setups, an integration time of 1s was chosen while the position of the focus on the microfluidic chip was constant during measurements. Each mean SERS spectrum is a result of 600 individual acquisitions. Automatic and reproducible measurement conditions were achieved by mounting the glass chip (Scheme 2) directly on the microscope stage. A segmented flow is created by using mineral oil as a carrier fluid and aqueous solutions for all other reagents. Six different ports allow the injection of solutions via a computer controlled pump system (neMESYS

Scheme 2. Droplet Based Microfluidic Chip[a]

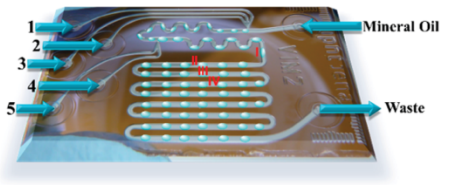

[a]Ports 1−5 are used for pumping various aqueous solutions. The numbers I−IV indicate the four different focus positions used during measurements.

Cetoni GmbH). A comprehensive description of the microfluidic platform can be found elsewhere.[39,44]

Data processing. The raw data obtained by the LoC-SERS measurements were preprocessed and analyzed by the help of the statistical programming language R.[45] During spectra acquisition, alternating SERS/Raman spectra of analyte containing droplets, spectra of the oil phase or spectra with contribution from both phases are recorded. Therefore, the first data processing step consisted in removing the oil and mixed spectra. This was done by manually setting a threshold value for the intensity of the prominent oil marker band at around 2880 cm^{-1}. Afterward, stacks of three spectra recorded within one droplet were averaged, background corrected and cut to the wavenumber region of interest. For background correction the selective nonlinear iterative peak clipping (SNIP) algorithm was applied.[46] For the artificial urine samples the iteration number was set to 16 when the peak area of a characteristic Raman mode is calculated and 60 for the plots presenting the mean SERS spectra and their double standard deviation. For data visualization, a numerical integration of a Raman marker mode was performed and its value was plotted as a function of different parameters. As integration method Simpson's rule was chosen. For evaluating the robustness of the LoC-SERS technique three different data sets have been recorded and a multivariate statistical analysis was performed. For this, principal component analysis (PCA) combined with partial least-squares regression (PLSR)[47] was chosen. A more detailed discussion of this method can be found elsewhere.[48] Briefly, a PCA is performed in order to reduce the dimensionality of the data set and, therewith, to reduce the computational costs significantly. For training the PLS model only the first four PCA scores were applied, whereby four PLS latent variables were constructed. To evaluate the quality of the created PLS model a ten times averaged 10-fold cross validation was performed. Therefore, the training data set was split into ten parts, the so-called folds, of which in every of the ten cross-validation steps one was excluded from the training process and used for prediction. Afterward, the root-mean-square error of prediction for cross validation (RMSEPCV) was calculated as the averaged RMSEP of the ten validation steps. For the prediction, either on the training data set or onto unknown data, all four PLS latent variables were used.

In the case of the human urine samples 60 iterations were used for the SNIP algorithm, while the spectra were cut to the wavenumber range 300−1800 cm^{-1}. The Raman mode centered at 637 cm^{-1} originating from uric acid is visible in all spectra and was used as an internal standard. Hence, prior to further evaluation, the SERS signals were normalized to the

DOI: 10.1021/acs.jpcc.6b01005
J. Phys. Chem. C XXXX, XXX, XXX−XXX

sum of the intensity values in the spectral range between 592 and 682 cm^{-1}. Due to the strong convolution of the levofloxacin marker bands with the background signal of the matrix, the above-described PCA−PLSR multivariate statistical model was chosen for data evaluation instead of peak integration. The data were split into training and "unknown" data set. Furthermore, a ten times averaged 10-fold cross-validation was carried out for the training data set. Therefore, the training data set is split into ten parts of which in every cross-validation step one is excluded in the training process and used for the prediction. For every step the RMSEP is calculated and the average value of all ten steps is used as the final RMSEP of the cross-validation.

■ RESULTS AND DISCUSSIONS

The chemical composition of human urine is very complex as the kidneys extract all soluble wastes from the bloodstream including excess water, sugars, proteins and many other components.[49] The resulting liquid has high concentrations of urea, uric acid, creatinine, inorganic ions i.e. chloride, sodium and potassium and pigmented products such as urobilin. Artificial urine was chosen as a matrix for levofloxacin detection in order to obtain an easy to access and easy to handle solution mimicking patient samples. The results obtained with the artificial urine as matrix were further applied to the detection of the target molecule in human urine samples.

Artificial urine. Figure 1 compares the mean SERS spectra of pure water, of the artificial urine, and of a 1 mM solution of

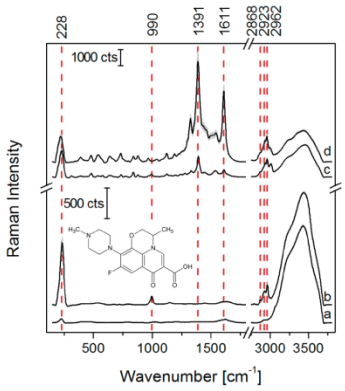

Figure 1. Mean SERS spectra and their double standard deviation for solutions containing Ag NPs and (a) H_2O, (b) artificial urine, (c) levofloxacin 1 mM in artificial urine, and (d) levofloxacin 1 mM in H_2O. Inlet: chemical structure of levofloxacin.

levofloxacin in water and in artificial urine. In comparison to pure water, the Raman signal of artificial urine shows bands centered at 990 cm^{-1}, 2868 cm^{-1}, 2923 cm^{-1}, and 2962 cm^{-1} (Figure 1(a) and (b)). The mode at 990 cm^{-1} is due to the C−N stretching vibration of urea[29,50] (SI, Figure S2), while the ones in the high wavenumber region are known to be due to C−H vibrations.[51] Furthermore, by comparing the SERS signal of levofloxacin solved in purified water and in artificial urine, one may notice that the presence of the complex matrix does not induce any shifts in the wavenumber positions of the Raman marker modes characteristic for the investigated antibiotic drug and located at 1391 and 1611 cm^{-1}. However, the matrix has an influence on the intensity of the Raman bands as well as on the band ratios.

The selective gain in intensity of the 1391 cm^{-1} Raman marker band of levofloxacin was previously attributed to a change in the orientation of the molecule on the surface of the Ag NPs.[39] The overall intensity of the SERS spectrum of levofloxacin solved in artificial urine might be affected by (1) competition between analyte and the complex matrix molecules at the surface of the Ag NPs and (2) creation of large Ag NP aggregates. In the first case, chloride ions or molecules like urea and creatinine can also adsorb on the surface of the NPs. As a consequence, the number of available free binding sites on the metallic surface for the target molecule to adsorb is reduced. In the second case, the presence of different salts can lead to Ag NP aggregates too large in order to still support optimal electromagnetic enhancement.[39]

In order to prove the effect of the matrix components on the SERS signal of levofloxacin, the target molecule was solved in four aqueous solutions having different chemical compositions. The first solution 1, contained NH_4Cl, $CaCl_2$, Na_2SO_4, $MgSO_4 \cdot 7H_2O$, $NaH_2PO_4 \cdot 2H_2O$, Na_2HPO_4 and $NaC_6H_7O_7$. Solution 2 contained additionally to the aforementioned salts also KCl and NaCl. For solution 3, urea was further added, while with the addition of creatinine, solution 4 is equal to the artificial urine itself. As reference, purified water was used as solvent (solution 0). The influence of the presence of the different molecules of the artificial urine on the integrated peak area of the levofloxacin Raman band at 1391 cm^{-1} is shown in Figure 2(A) (the recorded mean SERS spectra are presented in Figure S3(A)). Here, it is clearly shown that the presence of the various salts cause the strongest signal decrease, while the addition of urea and creatinine leads to further intensity losses. Even though the matrix has an increased complexity as compared to pure water, the Raman marker bands of levofloxacin can be clearly detected. For an improved signal-to-noise ratio for levofloxacin concentrations bellow 1 mM two parameters expected to alter the SERS enhancement have been further optimized, namely, the aggregation time of the Ag NPs and the dilution of the complex matrix were investigated.

First, the influence of the aggregation time was assessed by changing the focus position of the laser beam (see Scheme 2, positions I−IV). The first measurement position (I) is located after the second meander channel, and it is equivalent to 40 s elapsed, since the Ag NPs have been injected in the analyte containing droplets. The next ones were chosen in the middle of the first (II), second (III), and third (IV) channels corresponding to 60 s, 96 s, and 136 s, respectively. According to the results shown in Figure 2(B), with increasing aggregation time, the SERS intensity loss accompanied by the increase of the value of the relative standard deviation (RSD) of the peak area of the Raman mode at 1391 cm^{-1} is observed. Hence, aggregation time plays an important role and the ability of the LoC-SERS setup to keep it constant offers a great advantage over cuvette based SERS measurements.

As a second parameter, the influence of the dilution of the artificial urine with purified water was determined. Here, 0.5 mM levofloxacin/artificial urine was pumped through one of the ports while purified water through a second one. By varying the flow rates of the two syringes, seven different dilutions were achieved (Figure 2(C), mean SERS spectra in Figure S3(B)). In order to illustrate the changes induced in the SERS spectra, the Raman mode at 1391 cm^{-1} characteristic for levofloxacin (black

DOI: 10.1021/acs.jpcc.6b01005
J. Phys. Chem. C XXXX, XXX, XXX−XXX

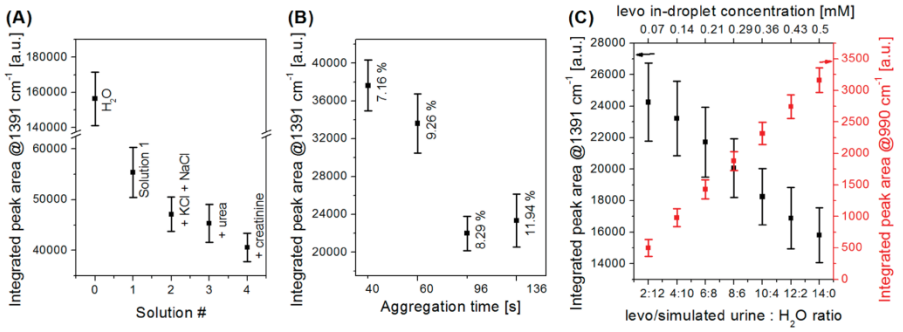

Figure 2. Influence of the (A) matrix components, (B) aggregation time, and (C) dilution with H_2O on the peak area of selected marker Raman modes of levofloxacin and urea, respectively. For (B) the labels represent the relative standard deviation of the peak area.

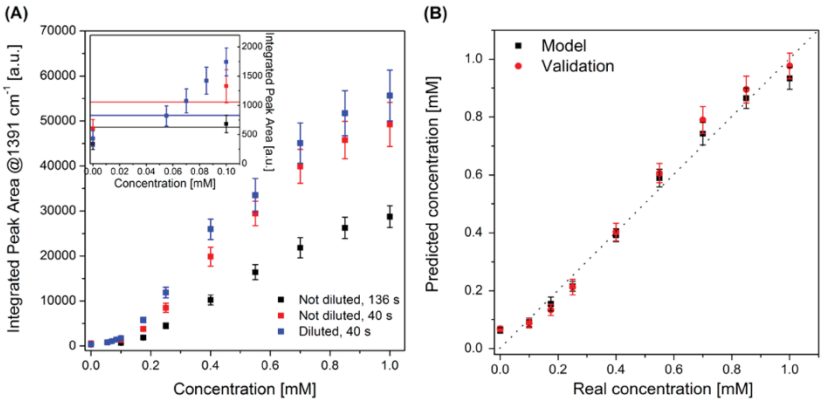

Figure 3. (A) Integrated peak area of the levofloxacin Raman mode at 1391 cm^{-1} with measurements performed under three different conditions. In the inset, threshold lines representing the LOD values are represented. (B) PLSR prediction plot for three independent data sets measured under the condition: "not diluted, 40 s".

scatter) as well as the peak area of the band located at 990 cm^{-1} and ascribed to the C−N vibration of the urea molecule (red scatter) is plotted. The upper x axis denotes the in-droplet concentration of levofloxacin while the lower x axis represents the ratio of artificial urine to H_2O. Here, the peak area of the two aforementioned Raman modes evolves dissimilar. In the case of urea, the intensity of its characteristic Raman band is increasing for increasing amounts of artificial urine. For levofloxacin, even though its in-droplet concentration, 0.07 mM, is almost 1 order of magnitude lower in the case of the 2:12 dilution ratio as compared to the nondiluted matrix, 0.5 mM, the signal is the most intense. Hence, one might use the dilution of the complex matrix with H_2O in order to reduce the matrix effects and optimize the SERS signal. However, one should be careful with the extent of dilution, as too strong dilution might lead to analyte concentrations below the detection limit and useful information concerning the spectral signature of the complex matrix can be also lost. Thus, for the following experiments a dilution ratio of 8:6 has been chosen.

In a next step, the influence of the aggregation time variation and dilution on the limit of detection (LOD) has been assessed. LOD values were defined according to the IUPAC norms and are equal to the signal of the blank plus three times the standard deviation of the blank. Three different measurements were performed: (1) nondiluted matrix, 40 s aggregation time, (2) nondiluted matrix, 136 s aggregation time and (3) diluted matrix (ratio 8:6), 40 s aggregation time. In the first two cases 0.5 mM and 1 mM levofloxacin stem solutions were filled up in the syringes, while for the third one an additional syringe contained a solution with 0.1 mM levofloxacin. The peak area of the marker band at 1391 cm^{-1} against the concentration of the analyte in artificial urine is plotted in Figure 3(A) (for the mean SERS spectra see Figure S4). Upon dilution, the LOD value was improved from 0.1 mM to 0.055 mM, while the aggregation time variation did not affect this parameter significantly. Even though the LOD value dropped from 0.8 μM[39] to 0.055 mM, when the target analyte was solved in artificial urine instead of purified water, in all three cases a good linearity was achieved for concentrations between 0.1 to 0.07 mM. This would suffice for the monitoring of levofloxacin clearance after 12 h from the administration of a single oral dose of 500 mg.[2]

DOI: 10.1021/acs.jpcc.6b01005
J. Phys. Chem. C XXXX, XXX, XXX−XXX

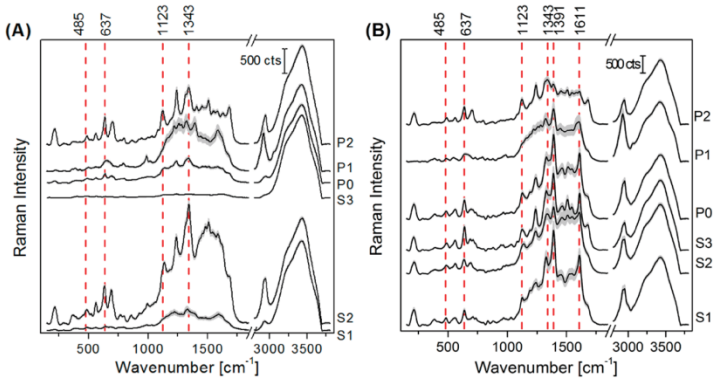

Figure 4. Mean SERS spectra and their double standard deviation of (A) the pure and (B) spiked (c_{urine} = 1.8 mM) human urine samples.

Furthermore, the robustness of the LoC-SERS technique was tested using three independent data sets where the concentration dependent SERS signal of levofloxacin solved in nondiluted artificial urine (focus position I) has been recorded. Two sets were used for the construction of the PLS model (black scatter) while the third one was applied for validation (red scatter) (Figure 3(B)). The diagonal dotted line is shown just as a ledger line, and it does not represent an actual fit. The root-mean-square error of prediction for cross validation (RMSEPCV) for the model is 0.048 mM, while the RMSEP for validation is 0.058 mM. Both values are below the limit of detection (LOD). This proves that the LoC-SERS technique provides reproducible measurements, as data from different measurement days can be used for successfully predicting the concentration of a third sample.

In our previous study[39] it was shown that by using the Raman mode assigned to the Ag−O vibration as an internal standard the linear response of the SERS signal vs concentration can be significantly improved. The measurements have been carried out with purified water as a solvent. Hence, at the surface of the metallic NPs only levofloxacin molecules were absorbed and the same molecules were inducing the aggregation of the NPs. In the case of artificial urine, various molecules are present which compete with the target analyte at the surface of the Ag NPs. The redshift of the Raman mode ascribed to the vibration of Ag (adsorbed ions) in artificial urine by 10 cm^{-1} as compared to a pure aqueous solution (see Figure 1(c) vs (d)) indicates the adsorption of other additional chemical species. Despite this competition, using the Raman mode at 228 cm^{-1} as an internal standard, once again as for the aqueous solutions, an improved linear response was obtained. Figure S5 highlights the concentration dependent peak area for the raw and normalized data. Upon normalization, the dynamic range is extended up to 1 mM while the goodness of fit is increased from 0.96 to 0.99. A possible explanation might be that while the concentration of the molecules of the complex matrix is constant during the measurements, the concentration of the target molecule is increasing. Thus, the intensity of the Raman mode at 228 cm^{-1} is also increasing.

Overall, based on the results presented so far, it is expected that clinically relevant concentrations of levofloxacin can be detected in complex matrixes. However, as compared with an "ideal" matrix where only water molecules might interfere with the Raman signal of the target molecules, the complexity of the artificial urine brings new challenges for the SERS technique. Namely, the presence of different ions, such as chloride, sulfate and phosphate reduce the available free binding sites on the metallic surface and can also induce aggregation. Therefore, when recording SERS spectra of human urine the different osmotic concentrations of the samples are expected to influence the detection of the target molecule. Furthermore, it was also shown that a short time elapsed since the mixing of the Ag NPs with the solution containing the target molecule is preferred. Thus, the RSD of the signal can be improved. Furthermore, by diluting the sample the LOD can be improved. By taking these into consideration, for the measurements carried out with human urine samples, which will be presented in the following section, the laser focus was fixed at position II and a dilution ratio of 3 parts human urine to 11 parts of pure water was used.

Human urine samples. The literature available regarding the SERS signal of human urine is continuously growing due to the availability of cost-effective portable Raman devices and due to no or minimal sample preparation requirements. However, urine spectra reported by different groups show high diversity,[52] being strongly affected by the type of the SERS substrate employed and the applied Raman excitation wavelength. In order to bring SERS to the clinical routine one should take into account two parameters: (1) cost-effective and easy to prepare SERS active substrates, and (2) a low cost, compact and easy to handle Raman setup. For the work presented here, the protocol for the Ag NP synthesis was chosen by taking into account that they can be also prepared by nontrained personal and that no special equipment is required. Furthermore, for excitation 532 nm was selected due to the cost effectiveness of available diode lasers.

The LoC-SERS measurements with the chip presented in this study are performed by using the first three ports for the injection of the analyte containing solutions and the two last ports for pumping the colloids and their aggregation agent. For obtaining a stable signal it is very important that the dosing of the NPs into the analyte containing droplets takes place uniformly. However, due to the superficial tension between the Ag NPs containing solution and the urine sample this was not achieved and the SERS signals proved to be highly inhomogeneous leading to low reproducibility (results not

DOI: 10.1021/acs.jpcc.6b01005
J. Phys. Chem. C XXXX, XXX, XXX−XXX

shown). Nevertheless, thanks to the flexibility offered by the various ports available on the microfluidic platform a new measurement layout could be used without compromising the automatic and reproducible measurement conditions. Here, the Ag NP solution and the one containing the urine sample to be measured are pumped into the main channel at the same time through port 1 and 3 and the mixing is achieved by the two meandering channels. Moreover, based on the results obtained with artificial urine as matrix, the laser was focused in the middle of the first channel (position II).

The recorded mean SERS spectra of the pure urine samples diluted with water are presented in Figure 4(A). The first observation is that the overall intensity of the signal is strongly varying in between the samples. This can be caused by the different pH values of the samples (Table 1) as well as by their different osmotic concentrations. The samples having an acidic pH (**S1**, **S3**, and **P0**) show a considerably weaker SERS signal when compared with the neutral ones (**S2** and **P2**). The pool **P1** with a pH of 5.35 originating from patients with positive inhibitory test results and with a pH of 5.35 has a background comparable in intensity with the neutral samples. Here, the higher concentration of the aggregation inducing chemical species could play a more important role than the pH value.

Table 1. pH Value of the Human Urine Sample

Sample	S1	S2	S3	P0	P1	P2
pH	5.76	7.19	5.80	6.16	5.35	7.00

According to the previously reported publications and due to the high abundance of urea in urine samples, a strong urea Raman mode located around 990 cm^{-1} is expected. Surprisingly, the samples investigated here show only a very weak urea Raman signals. Besides urea, purine derivatives can be also expected to show characteristic SERS signals. These molecules are aromatic, thus, the delocalized electrons are easily polarizable leading to high Raman signals. One of these compounds present in urine is uric acid. Raman bands ascribed to the vibrations of this molecule are located at 485 cm^{-1}, 637 and 1123 cm^{-1}[19,50] (reference Raman and SERS spectrum in SI, Figure S6). Furthermore, the spectral feature in the 1350−1380 cm^{-1} was assigned to the pyrrole half-ring symmetrical stretch within the heme molecule.[18] The clear assignment of each single Raman band is cumbersome due to the high complexity of urine and it is beyond the aim of the current study.

After measuring the blank samples levofloxacin was added to the matrix in order to assess the potential of the technique to detect the target analyte in human urine. The prepared concentrations were chosen according to the expected values of levofloxacin in human urine after 4 h from administration. In Figure 4(B) the mean SERS spectra together with their double standard deviation for the spiked samples having a urinary concentration of 1.8 mM are shown. In spite of the rich Raman signature of the urine, the characteristic Raman modes of levofloxacin can be clearly distinguished at 1391 and 1611 cm^{-1}. This is due to the high scattering cross section of the aromatic moieties of the quinolone ring system and due to the efficient adsorption of the molecule on the surface of the Ag NPs.[39] The mean SERS spectra for all 12 differently concentrated spiked urine samples are shown in Figure S7. Levofloxacin was previously proved to induce the aggregation of Ag NPs[39] when solved in water. The same is observed for some of the investigated urine samples. Namely, in the case of **S1**, **S3**, and **P0**, where the SERS signal of the blank urine

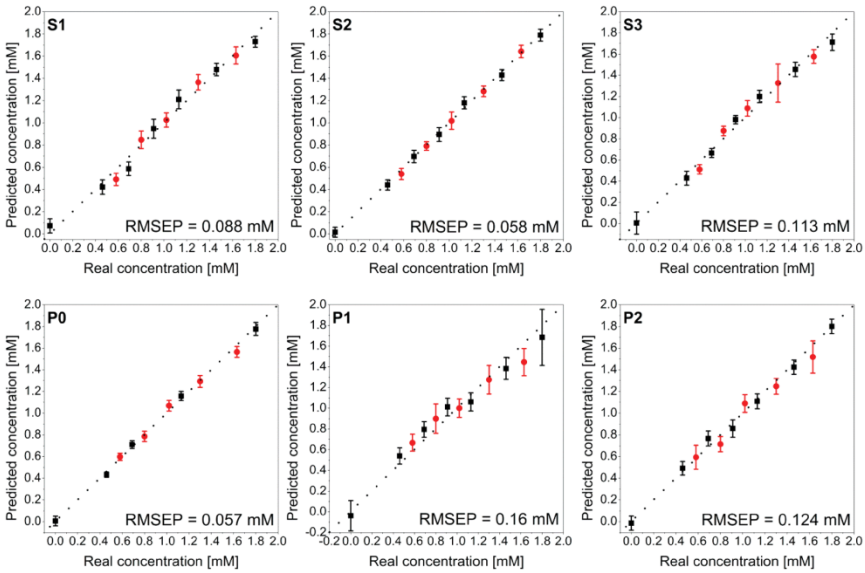

Figure 5. PLS prediction plots for spiked human urine samples using seven concentrations for training (black scatter) and five (red scatter) for predicting.

DOI: 10.1021/acs.jpcc.6b01005
J. Phys. Chem. C XXXX, XXX, XXX−XXX

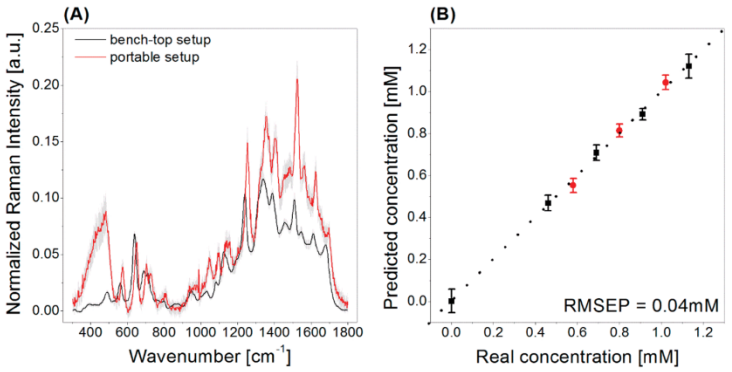

Figure 6. (A) Comparison of the mean SERS spectra of sample **S3** spiked with levofloxacin, 0.46 mM urinary concentration; (B) PLS plot where the black scatter points are the training data set and the red scatter represent the predicted values.

showed weak Raman bands. Here, with the addition of the target analyte also the Raman modes characteristic for the urine components are gaining intensity. In order to rule out the influence of the different aggregation degree on the intensity of the SERS spectra the Raman mode at 637 cm^{-1} ascribed to uric acid was used as an internal standard (normalized SERS spectra in SI, Figure S8). The main reason for choosing this Raman mode rather than the one due to the vibration of Ag − (absorbed ion) is that uric acid is an intrinsic component of urine. Further details are presented in the SI section (Figure S9).

In order to test the feasibility of the LoC-SERS technique for quantitative measurements, the recorded data were divided in two sets. The first data set was used for training the PLS model; model applied for the prediction of the concentration values of the second data set. The results obtained by using seven concentrations for training (black scatter) and five concentrations for predicting (red scatter) are depicted in Figure 5. The best prediction was obtained for the samples **S2** and **P0** with an RMSEP value of 0.058 mM while for the others the value of the parameter ranged between 0.088 and 0.16 mM (for complete results see Table S3). Nevertheless, levofloxacin was detected for all samples in a 0.45−1.8 mM concentration range, regardless the treatment received by the patient. The determination of the exact LOD value was beyond the scope of the present paper. However, based on the mean SERS spectra and on the RMSEP values, one may expect that a concentration comparable to that obtained for the artificial urine should be detectable.

One of the main challenges of the SERS technique is represented by the reproducibility of the results when using different colloid batches. Therefore, the batch-to-batch colloid reproducibility was also tested. The first batch was seven months old, while the second one was freshly prepared. The experiment was carried out for sample **S1**. The obtained RMSEP value was 0.16 mM, and the plot is shown in Figure S10. Therefore, Ag NPs prepared according to the Leopold-Lendl protocol have a long shelf life and are easy to handle.

As already mentioned previously, a low-cost measurement setup is desirable. Therefore, besides the benchtop Raman setup a portable module has been also employed for detecting levofloxacin in human urine. The whole equipment has a small footprint (SI, Figure S11(A)), being suitable for on-site and low cost applications. The same experimental design and data analysis was applied as for the results presented above. However, the measured sample, **S3**, was frozen again and kept at −21 °C for two additional months. By comparing the mean SERS spectra for the same urinary concentration measured with the two devices (Figure 6(A)), one may see that the relative intensities of some bands changed. This could be caused by the multiple freeze−thaw cycles applied during the study. Furthermore, it was also noticed that the SERS signal gets saturated once the concentration of the target molecule exceeds 1.3 mM (Figure S11(C)). Thus, only data points below this concentration have been used for the PLS analysis. With this, very good RMSEP values have been obtained (Figure 6(B)).

By comparing the data available in the literature concerning the expected urinary concentrations of levofloxacin with the ones detected by the LoC-SERS technique employed in this work, it can be concluded that the method has a high potential as a bioanalytical tool used for determining levofloxacin urine concentration in order to monitor the clearance rate or to assess patient compliance. First, a minimal sample preparation step consisting of filtration and dilution is required, followed by a fast measurement carried out under automated and reproducible measurement conditions. Second, the employed metallic nanoparticles are synthesized at room temperature, offering a good batch-to-batch reproducibility. And finally, the whole concentration window, including the minimum value of 0.45 mM, expected after 4 h from the administration of a single oral dose of 500 mg, is detected with good accuracy by a benchtop and a portable Raman setup.

■ CONCLUSIONS

The detection of levofloxacin was carried out in artificial and human urine using LoC-SERS. Artificial urine was chosen as a matrix in order to easily mimic patient samples and to get insights into the influence of various parameters on the SERS signal of the target analyte. More exactly, the signal decrease of levofloxacin solved in artificial urine as compared to the case where purified water was used as solvent was associated with (1) competition at the surface of the Ag NPs and (2) induction of large Ag NP aggregates. Furthermore, it was proven that the

DOI: 10.1021/acs.jpcc.6b01005
J. Phys. Chem. C XXXX, XXX, XXX−XXX

time elapsed from the addition of the colloids to the analyte containing droplets plays a major role in order to get optimal enhancement with improved RSD values. In a last step, artificial urine was diluted with purified water. Here, even though the in-droplet levofloxacin concentration is 1 order of magnitude lower when the highest amount of water is added, the signal is the most intense. Hence, this is another parameter which one may change in order to optimize the results. Concerning the achieved lower LODs, in the case of the nondiluted matrix, a value of 0.1 mM was achieved, while with dilution it was improved to 0.07 mM. The linear dynamic range is between 0.1−0.7 mM and 0.07−0.7 mM, respectively. This would suffice for monitoring the levofloxacin clearance after 12 h from the administration of a single oral dose of 500 mg. Similar with our previous publication, the use of the Raman band ascribed to the stretching vibrations of the Ag (absorbed ion) as an internal standard improved the linear dynamic range.

Concerning the human urine samples, the pH value and the osmotic concentration play an important role on the SERS signal intensity of the pure urine samples diluted with water. An acidic pH leads to a weaker signature as compared to the samples having a neutral or slightly basic pH. Besides urea, Raman characteristic bands for uric acid and heme molecules were identified. Here, the Raman band assigned to uric acid located at 637 cm^{-1} was used as an internal standard in order to rule out the influence of the different aggregation degree of the Ag NPs on the SERS spectra. Urinary concentrations of levofloxacin were detected in the range between 0.45 and 1.8 mM with an RMSEP value ranging from 0.057 to 0.16 mM in all three individual and three pooled samples. According to the literature, in the case of healthy volunteers after 4 h from the administration of a single oral dose of 500 mg levofloxacin, amounts were determined to be 1.38 mM ± 0.68 mM with a minimum measured concentration of 0.45 mM. Therefore, with the LoC-SERS technique, it is possible to monitor the clearance of the target analyte or to assess patient compliance. Concerning the clinical application, it was shown that the chosen Ag NPs have a long shelf life and that the LoC-SERS technique can be combined with a portable setup.

In order to answer the question concerning the determination of levofloxacin concentrations of unknown urine samples, further studies will be conducted by employing the standard addition method. It was recently shown that the combination of LoC-SERS with standard addition results in quantitative measurements.[53] Furthermore, also the influence of multiple freeze−thaw cycles on the SERS signal will be investigated.

■ ASSOCIATED CONTENT

Supporting Information

The Supporting Information is available free of charge on the ACS Publications website at DOI: 10.1021/acs.jpcc.6b01005.

Table S1: description of the sample preparation, Table S2: detailed measurement layout, Figure S1: UV−vis spectra of pure and aggregated Ag NPs, Figure S2: SERS spectra of urea at different concentrations, Figure S3: mean SERS spectra and their double standard deviation recorded in order to get insight regarding the influence of the matrix complexity and its dilution with water on the SERS signal of levofloxacin, Figure S4: concentration dependent SERS signal of levofloxacin in artificial urine (without and with dilution), Figure S5: Normalized and integrated peak area of the Raman mode at 1391 cm^{-1} ascribed to levofloxacin, Figure S6: Raman and SERS spectrum of uric acid, Figure S7: mean SERS spectra of the spiked human urine samples, Figure S8: normalized mean SERS spectra of the spiked human urine samples, Figure S9: PLS prediction plots for samples S3 without and with normalization, Table S3: summary of the PLS plots, Figure S10: PLS plots for batch-to-batch reproducibility of the SERS signal of the Ag NPs, Figure S11: portable Raman setup. (PDF)

■ AUTHOR INFORMATION

Corresponding Authors

*Phone: +49 (0)3641-206309, Fax: +49 (0)3641-206399, e-mail: dana.cialla-may@uni-jena.de.

*Phone: +49 (0)3641-206300, Fax: +49 (0)3641-206399, e-mail: juergen.popp@leibniz-ipht.de.

Notes

The authors declare no competing financial interest.

■ ACKNOWLEDGMENTS

The funding of the Ph.D. project of I. J. Hidi within the framework "Carl-Zeiss-Strukturmaßnahme" is gratefully acknowledged. The projects "QuantiSERS" (03IPT513A) and "Jenaer Biochip Initiative 2.0" (03IPT513Y) within the framework "InnoProfile Transfer − Unternehmen Region" as well as the grant 01KI1204 (M. W. Pletz) are supported by the Federal Ministry of Education and Research, Germany (BMBF). BioInter (13022-715) and InfectoGnostics (13GW0096F) are funded by the Development Bank of Thuringia and the European Union (EFRE) .We thank the microfluidic group of the IPHT for preparing the lab-on-a-chip devices for the measurements and Johanna Kirchhoff and Dr. Ute Neugebauer from the Institute of Medical Microbiology for providing the human urine samples.

■ REFERENCES

(1) Pletz, M.; Lipman, J. Clinical Measures for Increased Creatinine Clearances and Suboptimal Antibiotic Dosing. *Intensive Care Med.* **2013**, *39*, 1322−1324.

(2) Wagenlehner, F. M. E.; Kinzig-Schippers, M.; Tischmeyer, U.; Wagenlehner, C.; Sorgel, F.; Dalhoff, A.; Naber, K. G. Pharmacokinetics of Ciprofloxacin Xr (1000 Mg) Versus Levofloxacin (500 Mg) in Plasma and Urine of Male and Female Healthy Volunteers Receiving a Single Oral Dose. *Int. J. Antimicrob. Agents* **2006**, *27*, 7−14.

(3) Sun, H.; Wang, H.; Ge, X. Simultaneous Determination of the Combined Drugs of Ceftriaxone Sodium, Metronidazole, and Levofloxacin in Human Urine by High-Performance Liquid Chromatography. *Journal of Clinical Laboratory Analysis* **2012**, *26*, 486−492.

(4) Torre-Cisneros, J.; San-Juan, R.; Rosso-Fernandez, C. M.; Silva, J. T.; Munoz-Sanz, A.; Munoz, P.; Miguez, E.; Martin-Davila, P.; Lopez-Ruz, M. A.; Vidal, E.; et al. Tuberculosis Prophylaxis with Levofloxacin in Liver Transplant Patients Is Associated with a High Incidence of Tenosynovitis: Safety Analysis of a Multicenter Randomized Trial. *Clin. Infect. Dis.* **2015**, *60*, 1642−9.

(5) Liu, Y. M.; He, Q.; Wu, M. Levofloxacin-Induced Crystal Nephropathy. *Nephrology* **2015**, *20*, 437−438.

(6) Gulen, M.; Ay, M. O.; Avci, A.; Acikalin, A.; Icme, F. Levofloxacin-Induced Hepatotoxicity and Death. *Am. J. Ther.* **2015**, *22*, E93−E96.

(7) Czyrski, A.; Kondys, K.; Szalek, E.; Karbownik, A.; Grzeskowiak, E. The Pharmacokinetic Interaction between Levofloxacin and Sunitinib. *Pharmacol. Rep.* **2015**, *67*, 542−4.

DOI: 10.1021/acs.jpcc.6b01005
J. Phys. Chem. C XXXX, XXX, XXX−XXX

(8) Fayyaz, M.; Yousuf, R. I.; Shoaib, M. H.; Ali, T.; Nasiri, I.; Ashraf, N. Quality Evaluation and in Vitro Interaction Studies Between Levofloxacin 250mg and Diclofenac Sodium 50mg Tablets. *Pak. J. Pharm. Sci.* **2015**, *28*, 119−128.
(9) Budny, A. M.; Ley, A. N. Fluoroquinolone-Mediated Achilles Rupture: A Case Report and Review of the Literature. *J. Foot Ankle Surg.* **2015**, *54*, 494−496.
(10) Bansal, N.; Manocha, D.; Madhira, B. Life-Threatening Metabolic Coma Caused by Levofloxacin. *Am. J. Ther.* **2015**, *22*, E48−E51.
(11) Gao, C. H.; Yu, L. S.; Zeng, S.; Huang, Y. W.; Zhou, Q. Personalized Therapeutics for Levofloxacin: A Focus on Pharmacokinetic Concerns. *Ther. Clin. Risk Manage.* **2014**, *10*, 217−227.
(12) Wagenlehner, F. M.; Kinzig-Schippers, M.; Sorgel, F.; Weidner, W.; Naber, K. G. Concentrations in Plasma, Urinary Excretion and Bactericidal Activity of Levofloxacin (500 Mg) Versus Ciprofloxacin (500 Mg) in Healthy Volunteers Receiving a Single Oral Dose. *Int. J. Antimicrob. Agents* **2006**, *28*, 551−9.
(13) Wagenlehner, F. M.; Kinzig-Schippers, M.; Tischmeyer, U.; Wagenlehner, C.; Sorgel, F.; Naber, K. G. Urinary Bactericidal Activity of Extended-Release Ciprofloxacin (1,000 mg) Versus Levofloxacin (500 mg) in Healthy Volunteers Receiving a Single Oral Dose. *Antimicrob. Agents Chemother.* **2006**, *50*, 3947−9.
(14) Zhou, M. Q.; Peng, J. D.; He, R. X.; He, Y. T.; Zhang, J.; Li, A. P. High Performance Liquid Chromatography Coupled with Resonance Rayleigh Scattering for the Detection of Three Fluoroquinolones and Mechanism Study. *Spectrochim. Acta, Part A* **2015**, *136*, 1181−1187.
(15) Cazorla-Reyes, R.; Romero-González, R.; Frenich, A. G.; Rodríguez Maresca, M. A.; Martínez Vidal, J. L. Simultaneous Analysis of Antibiotics in Biological Samples by Ultra High Performance Liquid Chromatography−Tandem Mass Spectrometry. *J. Pharm. Biomed. Anal.* **2014**, *89*, 203−212.
(16) Siewert, S. Validation of a Levofloxacin Hplc Assay in Plasma and Dialysate for Pharmacokinetic Studies. *J. Pharm. Biomed. Anal.* **2006**, *41*, 1360−1362.
(17) Rambla-Alegre, M.; Esteve-Romero, J.; Carda-Broch, S. Validation of a Mlc Method with Fluorescence Detection for the Determination of Quinolones in Urine Samples by Direct Injection. *J. Chromatogr. B: Anal. Technol. Biomed. Life Sci.* **2009**, *877*, 3975−3981.
(18) Chi, J. M.; Zaw, T.; Cardona, I.; Hosnain, M.; Garg, N.; Lefkowitz, H. R.; Tolias, P.; Du, H. Use of Surface-Enhanced Raman Scattering as a Prognostic Indicator of Acute Kidney Transplant Rejection. *Biomed. Opt. Express* **2015**, *6*, 761−769.
(19) Del Mistro, G.; Cervo, S.; Mansutti, E.; Spizzo, R.; Colombatti, A.; Belmonte, P.; Zucconelli, R.; Steffan, A.; Sergo, V.; Bonifacio, A. Surface-Enhanced Raman Spectroscopy of Urine for Prostate Cancer Detection: A Preliminary Study. *Anal. Bioanal. Chem.* **2015**, *407*, 3271−3275.
(20) Liang, J.; Liu, H.; Huang, C.; Yao, C.; Fu, Q.; Li, X.; Cao, D.; Luo, Z.; Tang, Y. Aggregated Silver Nanoparticles Based Surface-Enhanced Raman Scattering Enzyme-Linked Immunosorbent Assay for Ultrasensitive Detection of Protein Biomarkers and Small Molecules. *Anal. Chem.* **2015**, *87*, 5790−6.
(21) Cao, G. Y.; Hajisalem, G.; Li, W.; Hof, F.; Gordon, R. Quantification of an Exogenous Cancer Biomarker in Urinalysis by Raman Spectroscopy. *Analyst* **2014**, *139*, 5375−5378.
(22) Dong, R. L.; Weng, S. Z.; Yang, L. B.; Liu, J. H. Detection and Direct Readout of Drugs in Human Urine Using Dynamic Surface-Enhanced Raman Spectroscopy and Support Vector Machines. *Anal. Chem.* **2015**, *87*, 2937−2944.
(23) Zhang, Y.; Walkenfort, B.; Yoon, J. H.; Schlucker, S.; Xie, W. Gold and Silver Nanoparticle Monomers Are Non-Sers-Active: A Negative Experimental Study with Silica-Encapsulated Raman-Reporter-Coated Metal Colloids. *Phys. Chem. Chem. Phys.* **2015**, *17*, 21120−21126.
(24) Li, M.; Du, Y.; Zhao, F. S.; Zeng, J. B.; Mohan, C.; Shih, W. C. Reagent- and Separation-Free Measurements of Urine Creatinine Concentration Using Stamping Surface Enhanced Raman Scattering (S-Sers). *Biomed. Opt. Express* **2015**, *6*, 849−858.
(25) Zhao, L. L.; Blackburn, J.; Brosseau, C. L. Quantitative Detection of Uric Acid by Electrochemical-Surface Enhanced Raman Spectroscopy Using a Multi Layered Au/Ag Substrate. *Anal. Chem.* **2015**, *87*, 441−447.
(26) Tadele Alula, M. T.; Yang, J. Photochemical Decoration of Magnetic Composites with Silver Nanostructures for Determination of Creatinine in Urine by Surface-Enhanced Raman Spectroscopy. *Talanta* **2014**, *130*, 55−62.
(27) Li, M. X.; Yang, H.; Li, S. Q.; Liu, C. W.; Zhao, K.; Li, J. G.; Jiang, D. N.; Sun, L. L.; Wang, H.; Deng, A. P. An Ultrasensitive Competitive Immunochromatographic Assay (Ica) Based on Surface-Enhanced Raman Scattering (Sers) for Direct Detection of 3-Amino-5-Methylmorpholino-2-Oxazolidinone (Amoz) in Tissue and Urine Samples. *Sens. Actuators, B* **2015**, *211*, 551−558.
(28) Xu, S. C.; Man, B. Y.; Jiang, S. Z.; Wang, J. H.; Wei, J.; Xu, S. D.; Liu, H. P.; Gao, S. B.; Liu, H. L.; Li, Z. H.; et al. Graphene/Cu Nanoparticle Hybrids Fabricated by Chemical Vapor Deposition as Surface-Enhanced Raman Scattering Substrate for Label-Free Detection of Adenosine. *ACS Appl. Mater. Interfaces* **2015**, *7*, 10977−10987.
(29) Yang, T.; Guo, X.; Wu, Y.; Wang, H.; Fu, S.; Wen, Y.; Yang, H. Facile and Label-Free Detection of Lung Cancer Biomarker in Urine by Magnetically Assisted Surface-Enhanced Raman Scattering. *ACS Appl. Mater. Interfaces* **2014**, *6*, 20985−93.
(30) Choi, C. J.; Wu, H. Y.; George, S.; Weyhenmeyer, J.; Cunningham, B. T. Biochemical Sensor Tubing for Point-of-Care Monitoring of Intravenous Drugs and Metabolites. *Lab Chip* **2012**, *12*, 574−581.
(31) Kong, K. V.; Ho, C. J.; Gong, T.; Lau, W. K.; Olivo, M. Sensitive Sers Glucose Sensing in Biological Media Using Alkyne Functionalized Boronic Acid on Planar Substrates. *Biosens. Bioelectron.* **2014**, *56*, 186−91.
(32) Yuen, C.; Liu, Q. Towards in Vivo Intradermal Surface Enhanced Raman Scattering (Sers) Measurements: Silver Coated Microneedle Based Sers Probe. *Journal of Biophotonics* **2014**, *7*, 683−689.
(33) Sun, F.; Bai, T.; Zhang, L.; Ella-Menye, J. R.; Liu, S. J.; Nowinski, A. K.; Jiang, S. Y.; Yu, Q. M. Sensitive and Fast Detection of Fructose in Complex Media Via Symmetry Breaking and Signal Amplification Using Surface-Enhanced Raman Spectroscopy. *Anal. Chem.* **2014**, *86*, 2387−2394.
(34) Mamian-Lopez, M. B.; Poppi, R. J. Standard Addition Method Applied to the Urinary Quantification of Nicotine in the Presence of Cotinine and Anabasine Using Surface Enhanced Raman Spectroscopy and Multivariate Curve Resolution. *Anal. Chim. Acta* **2013**, *760*, 53−59.
(35) Eberhardt, K.; Stiebing, C.; Matthäus, C.; Schmitt, M.; Popp, J. Advantages and Limitations of Raman Spectroscopy for Molecular Diagnostics: An Update. *Expert Rev. Mol. Diagn.* **2015**, *15*, 773−787.
(36) Ryzhikova, E.; Kazakov, O.; Halamkova, L.; Celmins, D.; Malone, P.; Molho, E.; Zimmerman, E. A.; Lednev, I. K. Raman Spectroscopy of Blood Serum for Alzheimer's Disease Diagnostics: Specificity Relative to Other Types of Dementia. *Journal of Biophotonics* **2015**, *8*, 584−596.
(37) Cialla, D.; Marz, A.; Bohme, R.; Theil, F.; Weber, K.; Schmitt, M.; Popp, J. Surface-Enhanced Raman Spectroscopy (Sers): Progress and Trends. *Anal. Bioanal. Chem.* **2012**, *403*, 27−54.
(38) Buividas, R.; Dzingelevičius, N.; Kubiliūtė, R.; Stoddart, P. R.; Khanh Truong, V.; Ivanova, E. P.; Juodkazis, S. Statistically Quantified Measurement of an Alzheimer's Marker by Surface-Enhanced Raman Scattering. *Journal of Biophotonics* **2015**, *8*, 567−574.
(39) Hidi, I. J.; Jahn, M.; Weber, K.; Cialla-May, D.; Popp, J. Droplet Based Microfluidics: Spectroscopic Characterization of Levofloxacin and Its Sers Detection. *Phys. Chem. Chem. Phys.* **2015**, *17*, 21236−21242.
(40) Walter, A.; Marz, A.; Schumacher, W.; Rosch, P.; Popp, J. Towards a Fast, High Specific and Reliable Discrimination of Bacteria

DOI: 10.1021/acs.jpcc.6b01005
J. Phys. Chem. C XXXX, XXX, XXX−XXX

on Strain Level by Means of Sers in a Microfluidic Device. *Lab Chip* **2011**, *11*, 1013−1021.
(41) Leopold, N.; Lendl, B. A New Method for Fast Preparation of Highly Surface-Enhanced Raman Scattering (Sers) Active Silver Colloids at Room Temperature by Reduction of Silver Nitrate with Hydroxylamine Hydrochloride. *J. Phys. Chem. B* **2003**, *107*, 5723−5727.
(42) Yang, Y.; Kim, S.; Chae, J. Separating and Detecting Escherichia Coli in a Microfluidic Channel for Urinary Tract Infection Applications. *J. Microelectromech. Syst.* **2011**, *20*, 819−827.
(43) Saetun, P.; Semangoen, T.; Thongboonkerd, V. Characterizations of Urinary Sediments Precipitated after Freezing and Their Effects on Urinary Protein and Chemical Analyses. *American Journal of Physiology - Renal Physiology* **2009**, *296*, F1346−F1354.
(44) März, A.; Ackermann, K. R.; Malsch, D.; Bocklitz, T.; Henkel, T.; Popp, J. Towards a Quantitative Sers Approach − Online Monitoring of Analytes in a Microfluidic System with Isotope-Edited Internal Standards. *J. Biophotonics* **2009**, *2*, 232−242.
(45) Team, R. D. C. *R: A Language and Environment for Statistical Computing*; The R Foundation for Statistical Computing: Vienna, Austria, 2011; ISBN: 3-900051-07-0.
(46) Ryan, C. G.; Clayton, E.; Griffin, W. L.; Sie, S. H.; Cousens, D. R. Snip, a Statistics-Sensitive Background Treatment for the Quantitative-Analysis of Pixe Spectra in Geoscience Applications. *Nucl. Instrum. Methods Phys. Res., Sect. B* **1988**, *34*, 396−402.
(47) Mevik, B.-H.; Wehrens, R.; Liland, K. H. *Pls: Partial Least Squares and Principal Component Regression* **2011**.
(48) Bocklitz, T.; Walter, A.; Hartmann, K.; Rösch, P.; Popp, J. How to Pre-Process Raman Spectra for Reliable and Stable Models? *Anal. Chim. Acta* **2011**, *704*, 47−56.
(49) Bouatra, S.; Aziat, F.; Mandal, R.; Guo, A. C.; Wilson, M. R.; Knox, C.; Bjorndahl, T. C.; Krishnamurthy, R.; Saleem, F.; Liu, P.; et al. The Human Urine Metabolome. *PLoS One* **2013**, *8*, e73076.
(50) Huang, S. H.; Wang, L.; Chen, W. S.; Feng, S. Y.; Lin, J. Q.; Huang, Z. F.; Chen, G. N.; Li, B. H.; Chen, R. Potential of Non-Invasive Esophagus Cancer Detection Based on Urine Surface-Enhanced Raman Spectroscopy. *Laser Phys. Lett.* **2014**, *11*, 1−6.
(51) Gunasekaran, S.; Rajalakshmi, K.; Kumaresan, S. Vibrational Analysis, Electronic Structure and Nonlinear Optical Properties of Levofloxacin by Density Functional Theory. *Spectrochim. Acta, Part A* **2013**, *112*, 351−63.
(52) Bonifacio, A.; Cervo, S.; Sergo, V. Label-Free Surface-Enhanced Raman Spectroscopy of Biofluids: Fundamental Aspects and Diagnostic Applications. *Anal. Bioanal. Chem.* **2015**, *407*, 8265−8277.
(53) Kämmer, E.; Olschewski, K.; Stöckel, S.; Rösch, P.; Weber, K.; Cialla-May, D.; Bocklitz, T.; Popp, J. Quantitative Sers Studies by Combining Loc-Sers with the Standard Addition Method. *Anal. Bioanal. Chem.* **2015**, *407*, 8925−8929.

DOI: 10.1021/acs.jpcc.6b01005
J. Phys. Chem. C XXXX, XXX, XXX−XXX

Supporting Information

Towards Levofloxacin Monitoring in Human Urine Samples by Employing the LoC-SERS Technique

Izabella J. Hidi,[1,2] *Martin Jahn,*[1,2] *Mathias W. Pletz,*[3] *Karina Weber,*[1, 2] *Dana Cialla-May,*[1, 2] *Jürgen Popp*[1, 2]

[1]Friedrich Schiller University Jena, Institute of Physical Chemistry and Abbe Center of Photonics, Helmholtzweg 4, 07745 Jena, Germany

[2]Leibniz Institute of Photonic Technology Jena, Albert-Einstein-Str. 9, 07745 Jena, Germany

[3] Center for Infectious Diseases and Infection Control, Jena University Hospital, Erlanger Allee 101 07740 Jena, and Research Campus Infectognostic, Philosophenweg 7, 07743 Jena, Germany, Germany

Spiking human urine samples with levofloxacin

LoC-SERS measurements were done on mixtures containing three parts (75 µl) of human urine and eleven parts (275 µl) of water and/or levofloxacin aqueous solutions. Table **S1** contains the number of levofloxacin moles present in each solution and two different concentrations. The first one, c_{urine}, is a "virtual" concentration and it is equivalent to the total number of levofloxacin moles which would be present in the 75 µl urine sample. The second one, $c_{in\text{-}droplet}$, corresponds to the total number of levofloxacin moles in the final volume (350 µl).

Table S1. Spiked human urine solutions used for measurements.

Nr.	0	1	2	3	4	5	6	7	8	9	10	11
n_{total} [nmol]	0	35.0	43.5	52.0	60.0	68.5	77.0	85.0	97.5	110.0	122.5	135.0
c_{urine} [mM]	0	0.467	0.58	0.694	0.8	0.913	1.027	1.133	1.3	1.467	1.63	1.8
$c_{in\text{-}droplet}$ [mM]	0	0.1	0.124	0.149	0.171	0.196	0.220	0.243	0.279	0.314	0.350	0.386

$c_{urine}=n_{total}/V_{urine}$, where $V_{urine}=75$ µl; $c_{in\text{-}droplet}=n_{total}/V_{total}$, where $V_{total}=350$ µl;

Table S2. Measurement design.

	Measurement #					
Port #	**M1**	**M2**	**M3**	**M4**	**M5**	**M6**
1	solution 0, 3	blocked	levo/SU 0.5 mM	levo/SU 0.5 mM	levo/SU/H_2O 0.1 mM, 1 mM	spiked urine
2	solution 1, 4	levo/SU 0.5 mM	blocked	SU	SU/H_2O	blocked
3	solution 2	blocked	H_2O	levo/SU 1 mM	levo/SU/H_2O 0.5 mM	Ag colloid
4	Ag colloid					blocked
5	blocked					
focus position	I	I-IV	I	I and IV	I	II

*The five different ports and the focus positions are depicted in Scheme **1**.*

M1: the influence of matrix components on the SERS signal of levofloxacin. The first solution 1, contained NH4Cl, CaCl2, Na2SO4, MgSO4·7H2O, NaH2PO4·2H2O, Na2HPO4 and NaC6H7O7. Solution 2 contained additionally to the aforementioned salts also KCl and NaCl. For solution 3, urea was further added, while with the addition of creatinine, solution 4 is equal to the artificial urine itself. As reference, purified water was used as solvent (solution 0).

M2: aggregation time dependent SERS measurements (I = 40s, II= 60s, III = 96 s, IV= 136 s);

M3: the influence of dilution with H_2O of the simulated urine matrix on the SERS signal of levofloxacin;

M4: concentration dependent SERS signal of levofloxacin in simulated urine;

M5: concentration dependent SERS signal of levofloxacin in simulated urine diluted with H_2O in 8:6 ratio;

M6: concentration rows of spiked human urine samples.

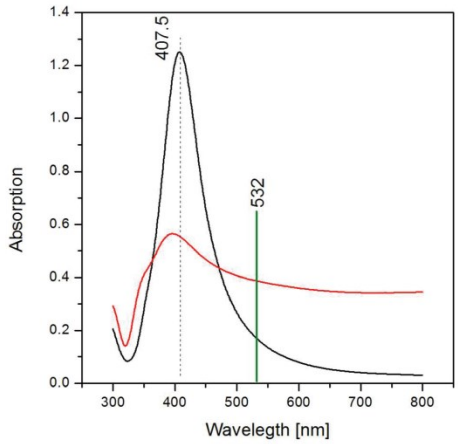

Figure **S1**. UV-Vis spectra of Ag NPs diluted with water (black) (AgNPs:H_2O = 1:1.2) and of the aggregated Ag NPs (AgNPs:H_2O:1 M KCl=1:1:0.2).

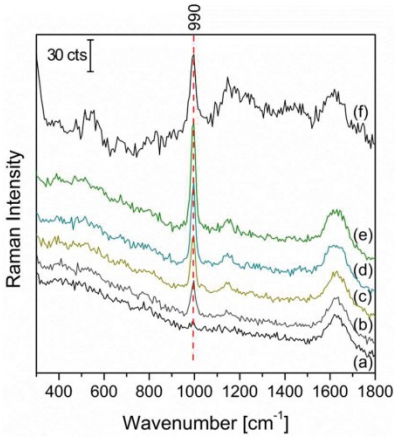

Figure **S2**. SERS spectrum of urea having a concentration of (a) 32.5 mM, (b) 232.5 mM, (c) 432.5 mM, (d) 632.5 mM, (e) 832.5 mM and (f) simulated urine.

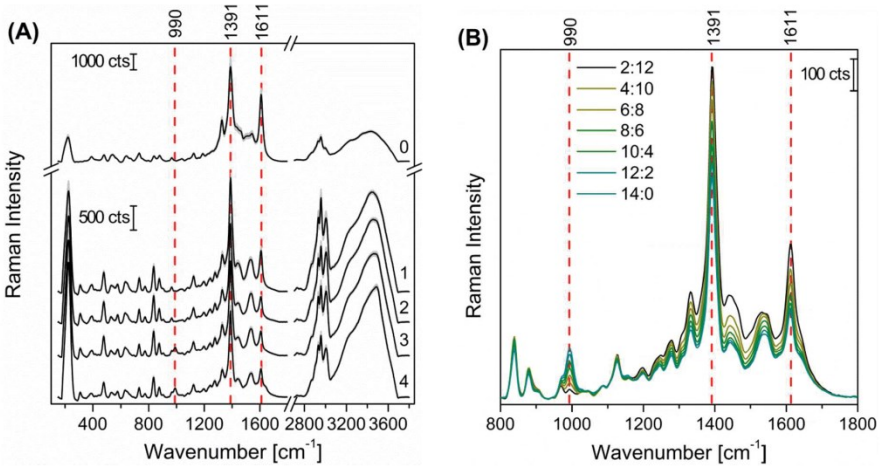

Figure **S3.** (A) Mean SERS signal and its double standard deviation recoded on Solution 0-4 in the experiment **M1**. (B) Mean SERS signal for seven simulated urine:water ratio, experiment **M3**. In both cases the Raman characteristic mode for urea (990 cm^{-1}) and two Raman marker bands for levofloxacin (1391 and 1611 cm^{-1}) are also indicated.

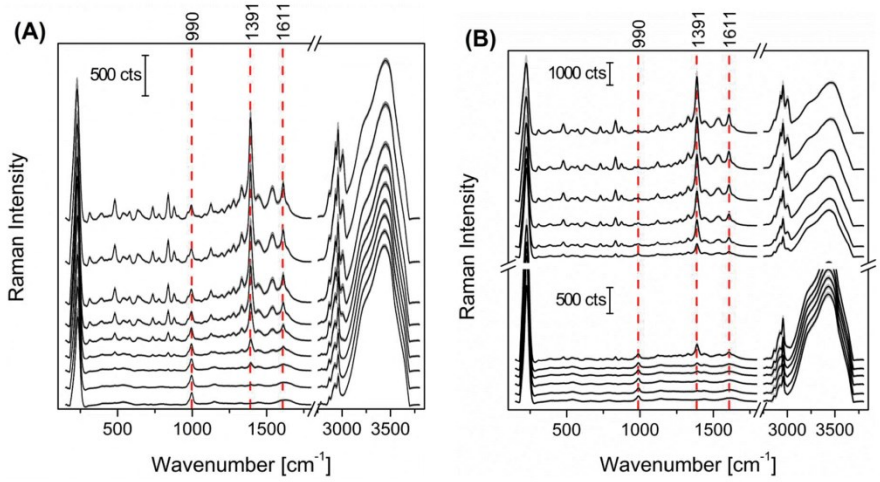

Figure **S4.** Concentration dependent SERS signal for (A) levofloxacin in simulated urine, 40 s aggregation time and (B) levofloxacin/simulated urine:H_2O= 8:6, 40 s aggregation time. For (A) the measured concentrations are (bottom to top): 0, 0.1, 0.175, 0.25, 0.4, 0.55, 0.7, 0.85 and 1 mM, while for (B) 0, 0.055, 0.07, 0.085, 0.1, 0.175, 0.25, 0.4, 0.55, 0.7, 0.85 and 1 mM.

S5

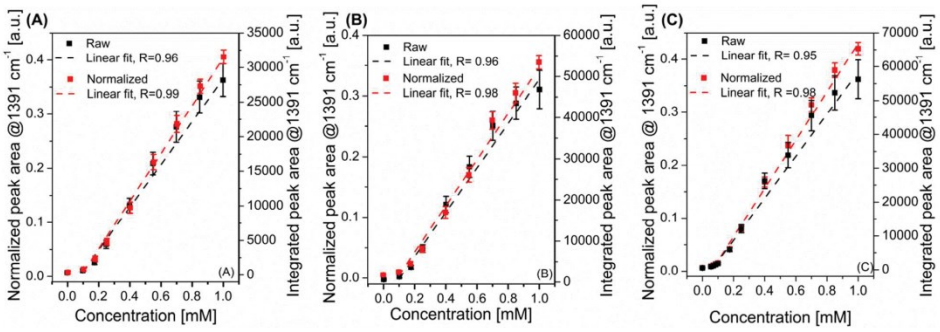

Figure **S5.** Normalized and integrated peak area of the Raman mode at 1391 cm^{-1} for (A) not diluted simulated urine and aggregation time 136 s, (B) not diluted 40 s, (C) diluted 40 s. The data points were fitted with a linear regression. For comparison the adjusted r-square values are shown for every fit.

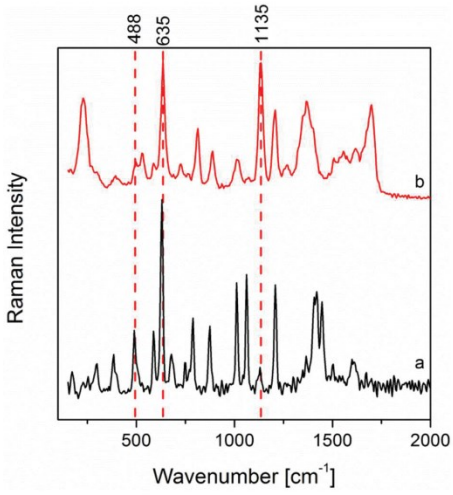

Figure **S6**. (a) Raman spectrum of uric acid sodium salt powder, (b) cuvette based SERS spectrum of 1mM uric acid sodium salt.

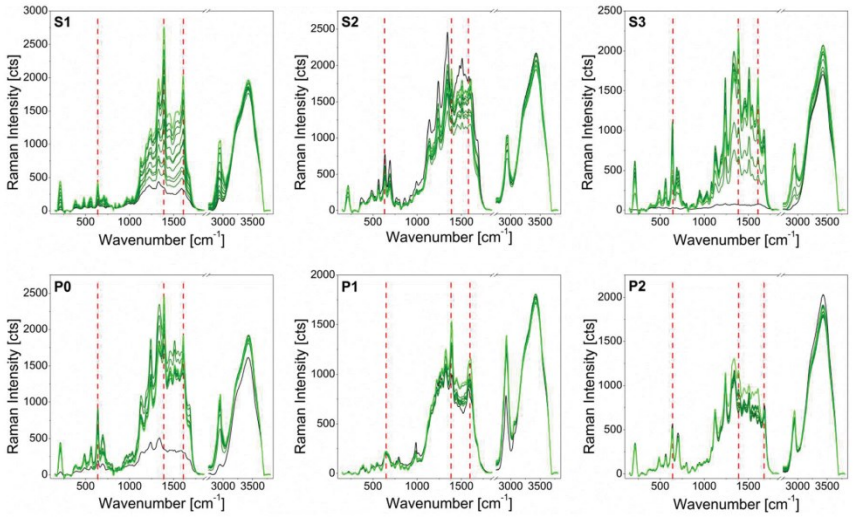

Figure **S7.** Mean SERS spectra of the spiked human urine samples: (black) pure urine, (olive) from bottom to top: 0.45 mM, 0.58 mM, 0.69 mM, 0.8 mM, 0.91 mM, 1.02 mM, 1.13 mM, 1.3 mM, 1.46 mM and 1.63 mM, (green) 1.8 mM.

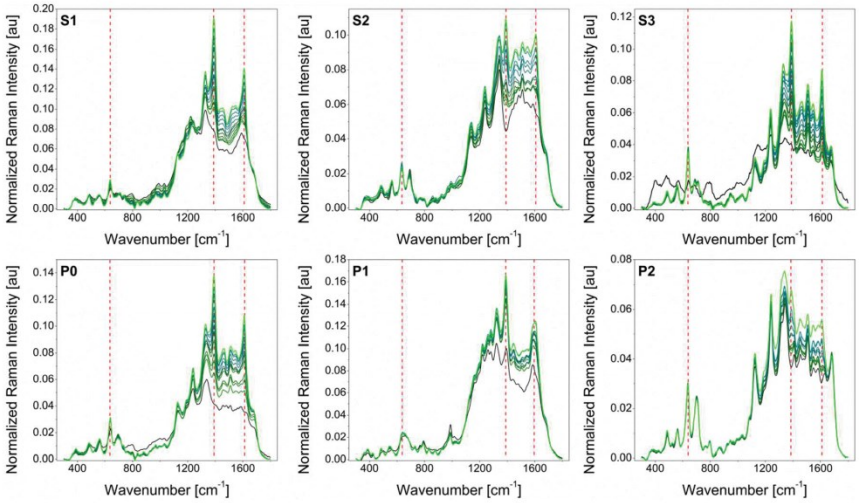

Figure **S8.** Normalized mean SERS spectra of the spiked human urine samples. (black) pure urine, (olive) from bottom to top: 0.45 mM, 0.58 mM, 0.69 mM, 0.8 mM, 0.91 mM, 1.02 mM, 1.13 mM, 1.3 mM, 1.46 mM and 1.63 mM, (green) 1.8 mM.

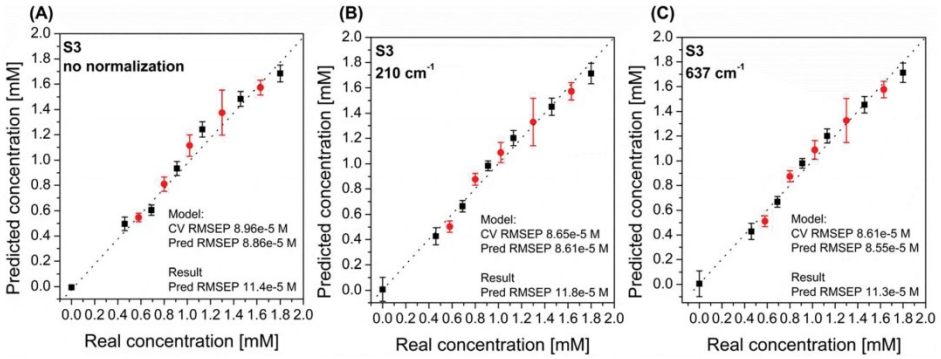

Figure **S9.** PLS prediction plots for samples **S3** using: (A) raw data, (B) normalized data using the Raman mode at 210 cm^{-1} and (C) normalized data using the Raman mode at 637 cm^{-1}. Black scatter plot: concentrations used for training the PLS model; red scatter plot: predicted concentrations. For the model cross validation (CV) and prediction on the same data set RMSEP values are given while for the result the prediction RMSEP using the previously created model is shown.

Table **S3**. Summary of the PLS results.

	S1		S2		S3		P0		P1		P2	
	CV [mM]	RMSEP [mM]	CV [mM]	RMSEP [mM]	CV [mM]	RMSEP [mM]	CV [mM]	RMSEP [mM]	CV [mM]	RMSEP [mM]	CV [mM]	RMSEP [mM]
Model	0.095	0.094	0.059	0.055	0.086	0.086	0.053	0.052	0.16	0.16	0.081	0.080
Result		0.088		0.058		0.113		0.057		0.16		0.124

CV: cross validation. RMSEP: root mean square error of prediction.

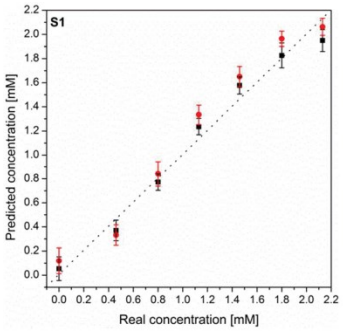

Figure **S10**. PLS results for **S1** urine sample measured using with two different colloid batches.

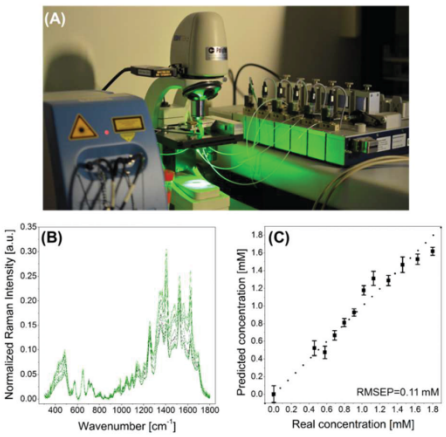

Figure **S11** (A) Picture of the LoC-SERS setup combined with a portable Raman setup; (B) mean SERS spectra of spiked S3 sample measured with the portable setup; (C) PLS plot where the same data set is used for training and predicting.

2.4 LoC-SERS combined with the standard addition method: toward the quantification of nitroxoline in spiked human urine samples [IH4]

Izabella J. Hidi, Martin Jahn, Thomas Bocklitz, Karina Weber,

Mathias W. Pletz, Dana Cialla-May, Jürgen Popp

Analytical Chemistry, 88 (18), **2016**, 9173–9180

analytical chemistry

Article

pubs.acs.org/ac

Lab-on-a-Chip-Surface Enhanced Raman Scattering Combined with the Standard Addition Method: Toward the Quantification of Nitroxoline in Spiked Human Urine Samples

Izabella J. Hidi,[†,‡,⊥] Martin Jahn,[†,‡,⊥] Karina Weber,[†,‡,∥] Thomas Bocklitz,[†] Mathias W. Pletz,[§,∥] Dana Cialla-May,[*,†,‡,∥] and Juergen Popp[†,‡,∥]

[†]Friedrich Schiller University Jena, Institute of Physical Chemistry and Abbe Center of Photonics, Helmholtzweg 4, 07745 Jena, Germany

[‡]Leibniz Institute of Photonic Technology Jena, Albert-Einstein-Strasse 9, 07745 Jena, Germany

[§]Center for Infectious Diseases and Infection Control, Jena University Hospital, Erlanger Allee 101 07740 Jena, Germany

[∥]Research Campus Infectognostic, Philosophenweg 7, 07743 Jena, Germany

Supporting Information

ABSTRACT: The emergence of antibacterial resistance and the development of new drugs lead to a continuous change of guidelines for medical treatments. Hence, new analytical tools are required for the detection of drugs in biological fluids. In this study, the first surface enhanced Raman scattering (SERS) detection of nitroxoline (NTX) in purified water and in spiked human urine samples is reported. Insights concerning the nature of the molecule−metal interaction and its influence on the overall SERS signal are provided. Furthermore, three randomly collected urine samples originating from a healthy volunteer were spiked to assess the limit of detection (LOD), the limit of quantification (LOQ), and the linear dynamic range of the lab-on-a-chip SERS (LoC-SERS) method for NTX detection in human urine. The LOD is ∼3 μM (0.57 mg/L), LOQ ∼ 6.5 μM (1.23 mg/L) while the linear range is between 4.28 and 42.8 μM (0.81−8.13 mg/L). This covers the minimum inhibitory concentration (MIC) values of the most commonly encountered uropathogens. Finally, seven clinical samples having an "unknown" NTX concentration were simulated. The LoC-SERS technique combined with the standard addition method and statistical data analysis provided a good prediction of the unknown concentrations. Additionally, it is also demonstrated that the predictions carried out by multicurve resolution alternating least-squares (MCR-ALS) algorithm provides reliable results, and it is preferred to a univariate statistical approach.

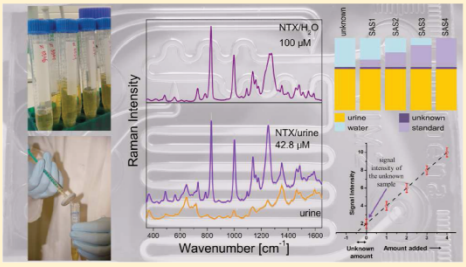

The guidelines describing the treatment of bacterial infections change throughout the years because of either the occurrence of antibacterial resistances or because of the discovery of new, more potent antibiotics. For many years, patients with urinary tract infection (UTI) were treated with trimethoprim as a single agent or in combination with sulfamethoxazole. However, if the regional resistance rate against the two antibiotics is higher than 20%,[1] this is no longer recommended. The same is true for the case of fluoroquinolones prescribed for the treatment of cystitis and acute pyelonephritis.[1] Therefore, alternative drugs are needed.

Nitroxoline (NTX), or 5-nitro-8-hydroxyquinoline, is an old but almost unknown antimicrobial agent. NTX chelates the divalent cations required for bacterial RNA polymerase.[2,3] Because of this unique mechanism of action, there is no cross resistance between NTX and other antibiotics.[4] In the 1960s it was licensed for the treatment of UTI[5] because of its favorable pharmacokinetics with short-term, low plasma levels, and almost complete renal excretion.[6] Because of the low license hurdles at that time, there are very few clinical studies on NTX and this drug was not considered in current guidelines on UTIs. However, because of rising resistance rates of urinary pathogens to most recommended treatment options, NTX is now seen as a valuable alternative and has recently been reevaluated by the German Antimicrobial Susceptibility Testing Committee.[7] The minimum inhibitory concentration (MIC) is 2−4 mg/L (10.5−21.0 μM) for various *E. coli* strains, 4 mg/L (21.0 μM) for *K. pneumoniae* and 8 mg/L (42.1 μM) for *Proteus mirabilis* and *S. saprophyticus*.[7,8] These values are in the susceptible range, while MICs ≥ 16 mg/L (84.2 μM) are regarded as resistant. Subtherapeutic urine concentration of antibiotics is a frequent cause of treatment failure and consecutive resistance development. However, literature focusing on analytical methods for

Received: June 15, 2016
Accepted: August 29, 2016
Published: August 29, 2016

DOI: 10.1021/acs.analchem.6b02316
Anal. Chem. 2016, 88, 9173−9180

NTX detection in body fluids is very scarce. The antibiotic was determined in human urine by liquid chromatography[9] combined with mass spectrometry[8] and in human blood by electroreduction.[9,10]

Surface-enhanced Raman spectroscopy (SERS) was proven to have a high potential for bioanalytical applications.[11−13] The main drawbacks of SERS represented by low reproducibility and lack of automated measurement conditions can be easily overcome by combining it with lab-on-a-chip (LoC) platforms.[14−16] We have recently shown that levofloxacin, a second-generation fluoroquinolone, can be detected with great accuracy by the LoC-SERS method in spiked urine samples of UTI patients.[14] However, the question how to determine the concentration of the antibiotic in clinical samples (originating from patients under medical treatment) has not been answered. Traditionally, quantitative measurements rely on *a priori* established calibration curves. However, if the chemical composition of the sample with the unknown analyte concentration is just slightly different as compared with the chemical composition of the standard solutions used for calibration, the obtained results might be unreliable. This is especially the case for clinical samples. The osmotic concentration of urine samples collected from different patients, or from the same patient at different time points, will strongly vary. Furthermore, the well-known poor batch-to-batch reproducibility of metallic nanoparticles in colloidal solution inhibits traditional quantitative determinations. Instead, the attention of the SERS community was directed toward the standard addition method (SAM).[16−18] Here, all analytical measurements, including the calibration curve, are performed using the clinical sample itself. Therefore, neither the matrix effect nor the quality variation between colloid batches will have a significant impact on the results. Practically, the SAM experiments are carried out by measuring the signal of several solutions containing the same volume of the clinical sample and different volumes of the standard solution of the target molecule and the solvent (i.e., water). Then, the analytical response of the solutions is plotted as a function of the added amount of the standard and the intercept of the linear regression with the x axis will give the concentration of the analyte in the unknown sample.

In the current study, the SERS detection of NTX is presented. To the best of our knowledge, no previous SERS studies of the antibiotic have been reported yet. Therefore, in the first part of the study NTX was solved in purified water to get insight concerning the nature of the molecule−metal interaction and its influence on the overall SERS signal. In the second part, three randomly collected human urine samples of a healthy volunteer are used as matrix to assess the potential of the LoC-SERS technique to detect NTX in complex matrixes. Lastly, urine samples originating from individuals, two from healthy volunteer and five from patients, with no previous NTX intake were spiked to simulate clinical samples. The as prepared "unknown" concentration was predicted by applying uni- and multivariate statistical data analysis.

MATERIALS AND METHODS

Chemicals and Reagents. NTX (96%), silver nitrate (ACS reagent, 99%), hydroxylamine hydrochloride (ReagentPlus, 99%), and sodium hydroxide have been purchased from Sigma-Aldrich, whereas potassium chloride (≥99.5% p.a. ACS, ISO) from Carl Roth.

Silver Nanoparticle (Ag NP) Synthesis. The silver colloidal solution was prepared by reducing silver nitrate by hydroxylamine hydrochloride in the presence of sodium hydroxide at room temperature.[14,19] The final concentration of the reactants in the solution is 10^{-3} M silver nitrate, 1.5×10^{-3} M hydroxylamine hydrochloride, and 0.3×10^{-3} M sodium hydroxide. The as-prepared solution was stored at 4 °C until the measurements were performed. In a previous study, the stability of the as prepared nanoparticles up to 7 months was demonstrated.[14]

NTX Solutions. A stock solution of NTX at 100 μM was prepared by adding the appropriate amount of powder to high-purity water followed by ultrasonication for 1 h at 40 °C. A second solution, at 10 μM, was obtained by diluting the previous solution with high-purity water. For the aggregation of the Ag NPs KCl at 1 M was used.

Urine Samples. In total, 10 human urine samples were included for the present study. Five samples were randomly collected from a healthy volunteer, while five other ones were received from the Institute of Medical Microbiology, University Hospital Jena, and originated from UTI patients. None of the individuals has undergone treatment with NTX. The analysis of human urine samples of both, healthy volunteer (4599-10/15) and patients (3701-02/13) was approved by the local Ethical Committee. Informed consent form was waived for the urine samples from patients because these samples were left over volumes of routine analysis and were anonymized. After sample collection, filtration was carried out for sterilization and for removing cells and debris using a sterile syringe filter (Rotilabo-syringe filter, PVDF, sterile, pore size 0.22 μm). The urine samples of the healthy volunteer were measured short after collection, whereas the ones from patients were kept in the freezer at −21 °C for 8 months before the measurements were performed. For assessing the analytical performances of LoC-SERS for detecting NTX in human urine, three urine samples collected from the healthy volunteer HV**1**, HV**2**, and HV**3** were spiked with NTX to yield urinary concentrations in the 4.28−42.8 μM range. To do so, 700 μL of urine was mixed with 300 μL of NTX aqueous solution at different concentrations (see Table S1 in the Supporting Information for details).

As none of the individuals consumed NTX before urine sample collection, for SAM measurements, the clinical samples had to be simulated. This was achieved by spiking human urine (250 μL) with a small volume (76 μL) of highly concentrated (∼70 μM) NTX aqueous solution. The "unknown" NTX urinary concentration to be determined with LoC-SERS-SAM is ∼21 μM (4 mg/L). Two samples from the healthy volunteer HV**4** and HV**5** and five from patients, PS**1**, PS**2**, PS**3**, PS**4**, and PS**5** were employed as a complex matrix. For each sample, except PS**4**, four standard addition steps (SAS) were prepared by adding purified water or/and NTX standard solution in different volumes (Scheme 1). In the case of sample PS**4**, due to low volume available, only three SAS were measured. Table S2 presents the detailed description of the prepared solutions.

Instrumentation. UV−vis absorption spectra were recorded in the 250−850 nm spectral range with a Jasco V650 diode array spectrophotometer. The acquisition speed was set to 200 nm/min and the spectral resolution to 1 nm.

The reference Raman spectrum of NTX powder was recorded with a confocal Raman microscope model alpha300 R (WITec, Ulm, Germany) and a 50× Zeiss objective. An excitation wavelength of 785 nm was provided by a cw diode laser (Toptica Photonics, Gräfelingen, Germany).

DOI: 10.1021/acs.analchem.6b02316
Anal. Chem. 2016, 88, 9173−9180

Scheme 1. Standard Addition Method

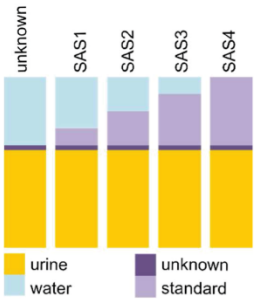

The SERS and LoC-SERS spectra were acquired with an XploRA INV inverted Raman microscope from Horiba Scientific. This Raman setup was equipped with a laser emitting at 532 nm with 13 mW power at the sample surface and a thermoelectrically cooled CCD camera (−69 °C). During the measurements, the same objective (Nikon 20× 0.4 N.A.) was used for focusing the laser beam on the sample's surface and for collecting the backscattered photons. The reference SERS spectrum of NTX was recorded with the 2400 l/mm grating (~1.8 cm^{-1} resolution), 1 s integration time and 10 accumulations. For the LoC-SERS measurements of NTX solved in purified water, the grating was changed to 1200 l/mm (~5 cm^{-1} resolution), whereas in the case of the urine samples the 600 l/mm grating (~8 cm^{-1}) was used.

For the LoC-SERS measurements, a glass droplet based microfluidic chip (Scheme 2)[14,16] was mounted on the microscope table (detailed description in the Supporting Information). Different solutions were pumped into the chip via a computer controlled pump system (neMESYS Cetoni GmbH). For this, the filled glass syringes purchased from ILS Germany GmbH were connected via Teflon capillaries with an inner diameter of 0.5 mm (WICOM GmbH) to the chip. The channel walls were silanized prior to the measurements; thus, the aqueous solutions formed droplets in the continuous phase of the mineral oil. For assessing the detection limits and dynamic range of the LoC-SERS technique when NTX is solved in purified water, the Ag NPs were pumped via port 1, NTX aqueous solutions at different concentrations (between 1 and 100 μM) via port 3, while the 1 M KCl solution was injected via port 4. For the experiments carried out with human urine samples, port 1 was used for the Ag NPs and port 3 for the samples.

Scheme 2. Droplet Based Microfluidic Platform[a]

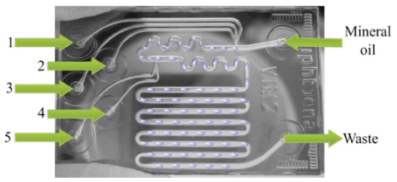

[a]Adapted from ref 14. Copyright 2016 American Chemical Society.

Data Processing. The data analysis was carried out with in-house written algorithms (GnuR).[20] The reference Raman and SERS spectra were background corrected with the selective nonlinear iterative peak clipping (SNIP) method[21] and cut to the 200−1650 cm^{-1} fingerprint region. The spectra recorded with the LoC-SERS setup were first separated in two groups by k-means cluster analysis. The first group contained the recorded mineral oil spectra, whereas the second one pure droplet and mixed droplet-oil spectra. This was followed by a wavenumber calibration, where mineral oil was used as standard.[22] The separation of the mixed and pure droplet spectra was achieved by manually setting a threshold value for the intensity of the prominent oil marker band at around 2880 cm^{-1}. Afterward, stacks of three spectra recorded within one droplet were averaged, background corrected (SNIP, 45 iterations) and cut to the wavenumber region of interest.

In order to quantify the amount of NTX in highly diverse human urine samples, two different approaches based on the SAM were applied. A straightforward, univariate analysis based on the linear dependency of the peak area of the NTX Raman marker band located at 840 cm^{-1} was first performed. The peak area was calculated according to Simpson's rule. The second approach made use of the multivariate curve resolution alternating least-squares (MCR-ALS) algorithm.

MCR is widely used for decomposing mixed spectral data of a multicomponent system into a bilinear model consisting of the pure contributions of each single component.[17,18,23,24] The decomposition is based on the following equation:

$$D = \sum_i c_i s_i^T + E = CS^T + E$$

D ($m \times n$) is the data matrix and it is composed of m spectra of mixture samples containing i substances in different concentrations. The score and loading vectors, c_i and s_i, can be interpreted as the pure profiles of the evolving parameter, e.g., concentration or elution time, and the spectra of the single components, respectively. The matrix E contains all variances that are unexplained in the framework of the assumed bilinear model. The most common method for the calculation of the pure contributions is the application of iterative algorithms, like the iterative target transformation factor analysis (ITTFA) or ALS.[25,26] In addition, chemical not meaningful results can be avoided by introducing constraints, like non-negativity, to the optimization process.

In order to combine this approach with SAM, the spectra of the unknown sample as well as the ones originating from the samples with added standard were arranged in a matrix (in rows). Assuming a two component system, the spectra of the sample matrix (pure urine) and an aqueous NTX solution were used as initial guesses for the pure spectral components. On the basis of this, the optimization process started with estimating the values of the score matrix, which are proportional to the concentration profiles. After reaching the convergence criterion, the score values of the analyte component were utilized as a pseudounivariate values. The unknown concentration and the corresponding standard deviation was calculated from the zero of the linear fit function. During the optimization by means of MCR-ALS, the score as well as the loading values were constrained to be non-negative and the threshold for the convergence criteria was chosen to be 1×10^{-3} at a maximum number of iterations of 200.

DOI: 10.1021/acs.analchem.6b02316
Anal. Chem. 2016, 88, 9173−9180

RESULTS AND DISCUSSION

SERS Detection of NTX. In Figure 1 the chemical structure of the molecule is depicted together with the Raman spectrum

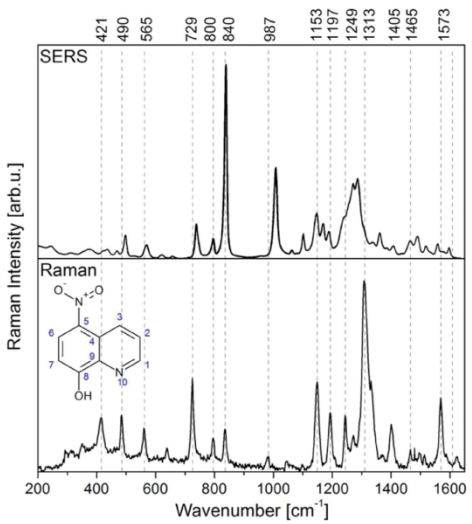

Figure 1. Reference Raman and SERS spectra of NTX powder (@785 nm) and 100 μM NTX/H_2O (@532 nm).

of NTX powder and the SERS spectrum of NTX solved in purified water at 100 μM. NTX is a quinolone derivative with an OH group bound to the carbon atom at the eighth position and a nitro ($-NO_2$) group at the fifth position. The molecule has C_s point group symmetry with 54 fundamental modes of vibrations, out of which 39 are in-plane and 15 are out-of-plane modes.[27] The Raman spectrum of the NTX powder has a very rich fingerprint in the 200−1800 cm^{-1} spectral range. The detailed vibrational analysis based on density functional theory (DFT) calculations was previously reported by Arjunan et al.,[27] and the band assignments of the marked Raman bands in Figure 1 are summarized in Table S3. Briefly, CCC bending modes give rise to Raman bands centered at 421 cm^{-1} and at 565 cm^{-1}. The Raman bands in the 800−1160 cm^{-1} spectral range are due to the aromatic C−H vibrations, whereas the ones at 729 and 1405 cm^{-1} are assigned to the vibrations of the hydroxyl group. The strongest Raman band is located at 1313 cm^{-1} and it is caused by the C−O stretching mode, while the signal at 490 cm^{-1} is assigned to the same functional group. The C−N stretching vibration is associated with the Raman band at 1197 cm^{-1}, the C−NO_2 stretching with the one at 1249 cm^{-1}, and the C═N stretching with the weak band at 1465 cm^{-1}. Finally, C═C stretching of the aromatic rings give rise to the Raman band at 1573 cm^{-1}.

For enhancing the inherently weak Raman scattering, in the present study, Ag NPs prepared according to the Leopold−Lendl protocol were used. During measurements, the ratio between the Ag NPs and the NTX solution was kept constant (1 to 1). After mixing the two solutions in a cuvette, 1 M KCl was added to induce the creation of hot-spots. The recorded UV−vis spectra of the bare Ag NPs, of NTX, and of the Ag NPs and NTX mixtures are showed in Figure S1.

The reference SERS spectrum presented in Figure 1 is significantly differing from the Raman spectrum recorded on powder. Namely, the Raman bands located at 840 cm^{-1} and at 987 cm^{-1} are strongly enhanced, whereas the ones in the 1200−1350 cm^{-1} range are strongly convoluted. For a better visualization, the two spectra presented in Figure 1 were normalized to the intensity of the Raman band centered at 800 cm^{-1} (Figure S2). This band was chosen because its intensity is not significantly influenced by the presence of the metallic nanoparticles. By comparing the normalized spectra, it was observed that the intense C−O stretching band at 1313 cm^{-1} is downshifted by ∼25 cm^{-1} and the C═N stretching mode at 1465 cm^{-1} is also enhanced. The strong influence of the presence of the Ag NPs on the overall SERS spectrum might indicate a chemisorption of the molecule on the metallic surface.

By closely analyzing the SERS spectrum, it can be noticed that even though the Raman bands at 800 and 840 cm^{-1} have been assigned to the out-of-plane bending vibration of the same functional group, the later one is significantly enhanced in the SERS spectrum as compared with the former one. The same observation is valid for the two Raman bands assigned to the C−H in-plane bending vibration at 987 and 1153 cm^{-1}. Generally, it is expected, that bands associated with the same vibrational mode will be equally influenced by the local electromagnetic field of the plasmonic structures. Because this is not the case, the two bands cannot be assigned to the same mode. Before a correct description of the molecule orientation on and interaction with the metallic surface can be given, further vibrational analysis of NTX has to be performed, which is beyond the aim of the study.

Detection in Purified Water. The MIC values of NTX against uropathogens are between 10 and 40 μM (2−8 mg/L). These are the minimum concentrations of the antibiotic at which the growth of bacteria are inhibited. Thus, after drug administration, its concentration in urine has to reach this value. In order for an analytical method to be successful in NTX detection in human urine, its sensitivity has to be higher as compared with the MIC.

To assess the limit of detection (LOD) and quantification (LOQ) of NTX solvated in high-purity water, LoC-SERS measurements were performed. For this, NTX solutions at different concentrations (see Table S4) were filled in glass syringes. The first test measurements were done by pumping the NTX containing solution at port 1, high-purity water at port 3, the Ag NPs at port 4, and the 1 M KCl solution at port 5 (see Scheme 2). The focus of the laser beam was fixed in the middle of the third channel. Contrary with the SERS signals obtained in cuvettes, the recorded SERS spectra at low NTX concentrations were identical with the Raman spectrum of purified water (Figure S3). This behavior can be explained by considering the polarity of the molecule. Generally, when SERS measurements with segmented flow platforms are performed, the target molecule must have good water solubility. Otherwise, the molecule might diffuse into the organic medium used as carrier fluid. The solubility of NTX is limited in water. Because of the quinolone backbone, the molecule is also soluble in organic solvents. Therefore, in the microfluidic chip it will diffuse from the aqueous droplet to the mineral oil used as continues phase and the recorded SERS spectra will be very weak. In order to prove this hypothesis, 500 μL of NTX at 100

DOI: 10.1021/acs.analchem.6b02316
Anal. Chem. 2016, 88, 9173−9180

μM was mixed in an eppendorf tube with 500 μL mineral oil. The eppendorf tube was rigorously shacked and after the two phases separated 100 μL of the aqueous phase was added to 100 μL of Ag NPs followed by KCl addition. The same experiment was repeated with tetradecane and with heptane. The recorded SERS spectra are shown in Figure S4. The signal intensity is decreased ~20 times after mixing the NTX with an organic solution. Thus, this is a clear indication of the NTX diffusion toward the organic phase. However, if the NTX solution is first mixed with the Ag NPs and only afterward mineral oil is added in the eppendorf tube, the signal loss is inhibited. This can be explained by a high affinity of the NTX molecule toward the metallic surface, confirming once again the chemisorption of the molecule on the Ag NPs. According to these results, the NTX solution and the colloids have to mix before the target molecule can diffuse to the mineral oil. This is easily done by pumping the two solutions though port 1 and port 3 and the KCl solution through port 4 or port 5. The as-recorded SERS spectra were background corrected and their mean signal and double standard deviation are plotted in Figure 2A.

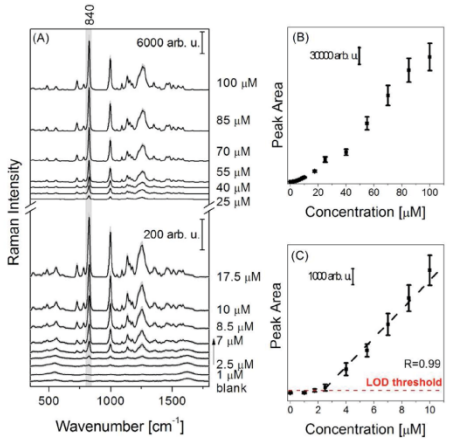

Figure 2. (A) Mean SERS spectra and their double standard deviation of NTX/H_2O. (B) Peak area of the 840 cm^{-1} Raman mode. (C) LOD of NTX ("R" is the adjusted *R* square value).

The characteristic Raman bands of NTX can be clearly identified at 2.5 μM (0.47 mg/L). According to the IUPAC definition, the LOD is equal to the signal of the blank plus 3 times its standard deviation, while LOQ is equal to the signal of the blank plus 10 times its standard deviation. The Raman band at 840 cm^{-1} was integrated with the Simpson rule. The peak area for all measured concentrations is plotted in Figure 2B, whereas Figure 2C presents the 0–10 μM range. On the basis of these plots, the LOD for NTX solved in purified water is ~2.38 μM (0.47 mg/L), while the LOQ is ~2.76 μM (0.52 mg/L). This value is 5 times lower than the lowest MIC value of uropathogens. Therefore, SERS fulfils the required sensitivity for NTX detection. The peak area has a linear dependency as a function of the concentration for the 2.5–10 μM (0.47–1.9 mg/L) range, while the dynamic range extends up to 85 μM. At this concentration the so-called poisoning effect appears, when the further addition of analyte molecules does not lead to signal increase.

Human Urine as Matrix for NTX Detection. The chemical composition of urine is very complex because the kidneys extract a high variety of molecules from the bloodstream. Additionally, Raman spectroscopy has high fingerprint specificity. These two factors will lead to a very complex SERS spectrum for the urine samples making it challenging to detect one specific molecule. In the previous section it was proved that the NTX molecule is chemisorbed with a high chemical affinity toward the silver metallic surface. As next, it will be shown that this also offers a great advantage for its detection in complex matrixes.

The three human urine samples were randomly collected from a healthy volunteer. Eight solutions with different NTX urinary concentrations (4.28 μM, 7.5 μM, 10.7 μM, 17.1 μM, 23.5 μM, 30 μM, 36.4 μM, 42.8 μM) were prepared by mixing seven parts of human urine with three parts of aqueous solution containing the target molecule. Because of the high salt content of urine samples no aggregation agent was added to induce the creation of hot-spots. The recorded mean SERS spectra of sample HV**1** at different concentrations are presented in Figure 3A.

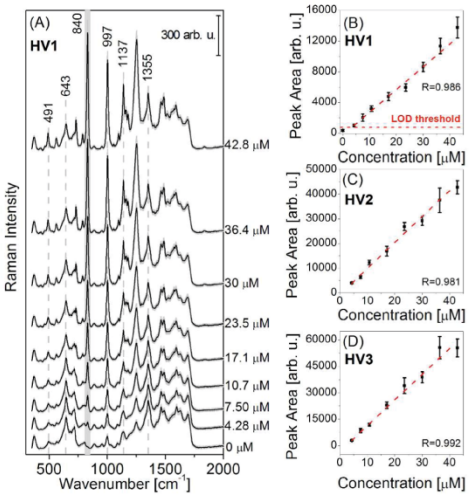

Figure 3. (A) Mean SERS spectra and their double standard deviation of sample **HV1**. Integrated peak are of the Raman band @840 cm^{-1} for sample (B) **HV1**, (C) **HV2** and (D) **HV3** ("R" is the adjusted *R* square value).

The SERS signal of the pure urine sample (0 μM) shows Raman bands located at 491 cm^{-1}, at 643 cm^{-1}, and at 1139 cm^{-1} ascribed to the vibrational modes of the uric acid molecule, at 997 cm^{-1} assigned to the C–N stretching vibration of urea, and at 1355 cm^{-1} because of the pyrrole half-ring symmetrical stretch within the heme molecule.[14,28] When NTX is added, at the lowest concentration, to the human urine sample a new band appears at 840 cm^{-1}, while the one at ~1000 cm^{-1} increases in intensity. In the 1100–2000 cm^{-1}

DOI: 10.1021/acs.analchem.6b02316
Anal. Chem. 2016, 88, 9173–9180

spectral range, the Raman modes of the molecules present in the urine sample are strongly convoluted with the ones ascribed to the vibrational modes of NTX molecule. In Figure S5 a clear comparison of the reference SERS spectrum of NTX in water with the SERS spectrum of the blank urine (sample HV**1**) and the SERS spectrum of NTX spiked in human urine at 42.8 μM urinary concentration is presented. On the basis of this, because of the high chemical affinity of the target molecule, the Raman bands characteristic for the molecules of the complex matrix are suppressed. At high NTX concentration, just two bands, 643 cm^{-1} and the one at 1355 cm^{-1}, are still distinguishable. In order to clearly visualize the response of the signal to the concentration increment, the peak area of the Raman mode at 840 cm^{-1} was determined by the Simpson algorithm and plotted in Figure 3B–D for the three measured samples. On the basis of this, the LOD for NTX spiked in human urine (sample HV**1**) is ~3.43 μM (0.57 mg/L) and the LOQ is ~6.5 μM (1.23 mg/L). The LOD value is comparable with the LOD previously obtained for NTX solved in water (2.38 μM), while the LOQ is increased due to the background signal of the molecules originating from the human urine sample. Nevertheless, the molecules of the complex matrix do not inhibit the efficient absorption of NTX on the surface of the Ag NPs. This would not be possible without a high chemical affinity of the target molecule toward the metallic surface.

Besides good sensitivity, the LoC-SERS method also offers sufficient linear analytical response. For all three measured samples a linear range between 4.28 and 42.8 μM can be seen in Figure 3, which covers the MIC values of common uropathogens. The different behavior, as compared with the case when NTX was solved in purified water, might come from the different chemical environment. Factors which might play a major role are the inorganic salts[14] present in the complex matrix and the pH of the urine samples.

LoC-SERS-SAM. The concentration determination of antibiotics in samples originating from patients cannot be done by an *a priori* established calibration curve. Instead, a new calibration has to be performed for each sample by using SAM. A good linear analytical response is a prerequisite for the successful determination of analyte concentrations by this method. In the previous section it was demonstrated, that for the three urine samples randomly collected from a healthy volunteer this requirement is fulfilled by LoC-SERS.

As none of the individuals consumed NTX before urine sample collection, for SAM measurements the clinical samples had to be simulated. In the present study the "unknown" concentration to be determined was chosen to be ~21 μM (4 mg/L). This is equivalent with an in-droplet concentration, the concentration of NTX in the final volume containing urine and water, of 10.5 μM. Two samples collected from the healthy volunteer (HV**4** and HV**5**) and five samples (PS**1**–PS**5**) received from the Institute of Medical Microbiology, University Hospital Jena were used as a matrix for assessing the feasibility of the LoC-SERS-SAM combination. Besides the solutions measured by applying SAM also, the blank urine samples diluted with only water were recoded. These spectra were employed as negative control for our study.

The mean SERS spectra of the blank urine samples, of the "unknown" solution and of the four SAS are plotted in the Supporting Information, Figure S6. According to these plots, the SERS signals of six out of seven blank urine samples diluted to 50% are similar to the one shown in Figure 3 for sample HV**1**. The SERS spectrum of the blank PS**2** sample shows a very intense Raman band at ~1355 cm^{-1}. This band was previously assigned to the pyrrole half-ring symmetrical stretch within the heme molecule. Hence, it might indicate that the sample contained traces of blood.

Regardless of the signal of the complex matrix, the NTX characteristic bands are clearly distinguishable for all seven samples at the "unknown" concentration. With the addition of the standard solution, the signal intensity of the marked Raman mode at 840 cm^{-1} is increasing. In order to predict the unknown concentration, both uni- and multivariate statistical tools have been applied. For the first case, the unknown concentration was calculated based on the peak area of the Raman at 840 cm^{-1}. In Figure 4 the integrated peak areas are shown in the form of boxplots. On the x scale, the concentration of the standard addition steps (c_{SAS}, see Table S2) are represented. The obtained predictions are expressed in in-droplet NTX concentration (true value 10.5 μM) instead of the urinary concentration (true value 21.0 μM). The linear fit was performed with the algorithm written in the statistical language R. The unknown NTX in-droplet concentration was

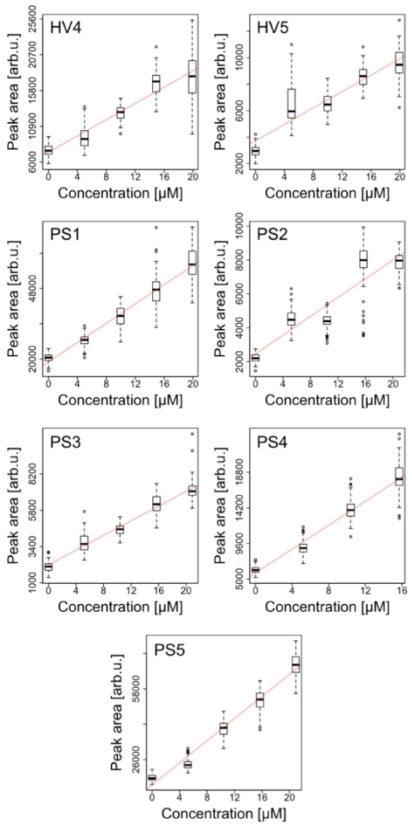

Figure 4. LoC-SERS-SAM: linear fit of the peak area @840 cm^{-1} vs the concentration of the NTX standard solution.

DOI: 10.1021/acs.analchem.6b02316
Anal. Chem. 2016, 88, 9173–9180

Table 1. LoC-SERS-SAM Results and Their Corresponding 95% Confidence Intervals[a]

	peak area			MCR-ALS		
S	c_0 [μM]	E_r [%]	c_{NC} [μM]	c_0 [μM]	E_r [%]	c_{NC} [μM]
HV**4**	13.2 ± 1.0	25.6	2.1 ± 0.5	14.0 ± 1.0	33.9	1.8 ± 0.5
HV**5**	12.1 ± 1.1	15.0	2.7 ± 0.6	10.1 ± 0.9	3.8	0.5 ± 0.5
PS**1**	9.9 ± 0.6	6.1	0.1 ± 0.3	10.1 ± 0.6	4.0	1.1 ± 0.3
PS**2**	9.1 ± 0.8	14.2	0.5 ± 0.5	9.8 ± 1.0	7.8	1.9 ± 0.3
PS**3**	9.0 ± 0.5	14.7	0.7 ± 0.4	11.5 ± 0.6	8.9	0.0 ± 0.3
PS**4**	7.5 ± 0.4	29.2	1.1 ± 0.2	6.0 ± 0.4	43.7	0.6 ± 0.6
PS**5**	5.8 ± 0.4	45.1	1.6 ± 0.2	5.6 ± 0.4	46.9	0.8 ± 0.3

[a]True value is 10.5 μM. c_0, in-droplet NTX concentration; c_{NC}, predicted NTX concentration for the blank sample (in-droplet).

predicted to be between 5.8 μM and 13.2 μM (Table 1 and Table S3). The best prediction was obtained for sample PS**1** with a relative error of 6.1%. The mean absolute percentage error (MAPE) for all predictions is 21.4%. The feasibility of the LoC-SERS-SAM technique was additionally tested by considering as the sample with an "unknown" concentration the blank urine sample. With these parameters, the predicted concentration is 1 order of magnitude lower than the true concentration.

The determination of the unknown concentration based on this univariate statistic method will fail in the case of analytes presenting Raman bands strongly convoluted with the urine background. This is the case for the Raman band located at ~1000 cm^{-1}. If the unknown NTX concentration is predicted based on the peak area of this vibrational mode, the MAPE increases to 144% (see Table S3 in the Supporting Information for details).

As an alternative analysis method, MCR-ALS was tested. For this, instead of a single Raman band, a spectral range can be selected. In the case of NTX, the 600−1100 cm^{-1} spectral window without background correction provided the best prediction. The MCR-ALS recovered spectra for the two components, urine and NTX in water, are presented in comparison with the reference spectra, applied as initial guesses, in Figure S7 in the Supporting Information. The recovered spectra show good similarity with the reference ones and a correlation of 0.89−0.99 (see Table S6) was achieved. Consequently, NTX can be determined from convoluted spectral information. The as calculated unknown concentrations are presented in Table 1 (and Table S5). Four out of seven samples were predicted with a relative error below 10% as compared with only one in the case of the univariate analysis, whereby the results for the negative control are comparable. Nevertheless, the MAPE is with 21.1% in the same range as for the univariate statistics.

Regardless of the applied data analysis, predictions with significant relative error were obtained for samples HV**4**, PS**4**, and PS**5**. The linearity of the signal for the last two samples fulfills the requirements of SAM. Thus, the source of the error might come from the actual measurements and not from the applied statistical method. Nevertheless, because of the reduced available sample volume, the measurements could not be repeated.

Overall, the univariate statistical analysis is a straightforward method; however, in the case of convoluted Raman bands the prediction will fail. MCR-ALS can be performed on selected spectral range instead of a single Raman band and without prior background correction. This will reduce the artifacts induced by algorithms for estimating the background/baseline of the recorded spectra. Furthermore, in order to compare the performance of the two applied statistical methods, one might calculate a new MAPE value by omitting samples HV**4**, PS**4**, and PS**5**. For MCR-ALS, the as calculated value is 6.2%. By comparing this with the value obtained for the univariate method, 12.5%, the superiority of MCR-ALS is clearly demonstrated. However, in order to apply MCR-ALS, the reference spectrum of the pure urine samples has to be known. This will not be available for clinical samples. One solution for this challenge is to acquire a comprehensive database containing the background signature of urine samples originating from various individuals. On the basis of this database, a series of MCR-ALS runs, with different initial guesses, can be performed. The regression parameters corresponding to the fitted curves with the highest correlation to their initial guesses will be used for the prediction of the unknown concentration.

■ CONCLUSIONS

The high chemical affinity of NTX toward the surface of the silver nanoparticles observed in the present study plays a major role in its successful detection by the SERS technique. The achieved LOD values in purified water and in human urine samples are lower than the minimum concentration of the antibiotic needed to inhibit bacterial growth. Therefore, LoC-SERS offers sufficient sensitivity for the detection of NTX at relevant clinical concentrations. Concerning the linear response of the signal at the detector vs the antibiotic concentration, it was noticed, that in the case of the complex matrix the linear range is significantly extended as compared with the case when just purified water was used as matrix. This might be due to either the different pH value of the complex matrix or due to the presence of various molecules beside NTX.

Signal linearity is one of the prerequisites for the successful quantification of molecules either by the traditional method, with *a priori* established calibration curves, or by SAM. Because of the variation of the chemical composition of clinical samples and the quality variation of colloid batches, SAM is the most feasible approach for quantification when SERS is used as a detection method. In the present study it was demonstrated that by applying various statistical methods for data analysis, the unknown concentration of NTX in human urine can be determined.

In conclusion, LoC-SERS-SAM is a very promising analytical tool for drug quantification in human urine samples. Furthermore, because of the available miniaturized Raman setups, the costs of the method can be significantly reduced, making it accessible for small clinical centers.

DOI: 10.1021/acs.analchem.6b02316
Anal. Chem. 2016, 88, 9173−9180

■ ASSOCIATED CONTENT

Supporting Information

The Supporting Information is available free of charge on the ACS Publications website at DOI: 10.1021/acs.analchem.6b02316.

Sample preparation: urinary NTX concentrations measured for samples HV1, HV2, and HV3 and LoC-SERS-SAM; band assignment of the observed Raman modes of NTX; UV−vis measurements; normalized Raman and SERS spectrum of NTX powder and 100 μM solution; LoC-SERS spectra measured with conventional configuration; chemical affinity of NTX toward Ag NPs: SERS spectra of various mixtures; reference SERS spectrum of NTX vs LoC-SERS signal of the blank urine and of NTX spiked in the urine sample HV**1**; mean SERS spectra and their double standard deviation of urine samples from healthy volunteer and UTI patients; LoC-SERS-SAM results; MCR-ALS plots; and correlation coefficients for MCR-ALS (PDF)

■ AUTHOR INFORMATION

Corresponding Author

*Phone: +49 (0)3641-206309. Fax: +49 (0)3641-206399. E-mail: dana.cialla-may@uni-jena.de.

Author Contributions

⊥I.J.H. and M.J. contributed equally.

Notes

The authors declare no competing financial interest.

■ ACKNOWLEDGMENTS

The funding of the Ph.D. project of I. J. Hidi in the framework "Carl-Zeiss-Strukturmaßnahme" is gratefully acknowledged. The projects "Jenaer Biochip Initiative 2.0" (Grant 03IPT513Y) in the framework "InnoProfile Transfer−Unternehmen Region" as well as the Grant 01KI1204 (M. W. Pletz) are supported by the Federal Ministry of Education and Research, Germany (BMBF). BioInter (Grant 13022-715) and InfectoGnostics (Grant 13GW0096F) are funded by the Development Bank of Thuringia and the European Union (EFRE). We thank the microfluidic group of the IPHT for preparing the lab-on-a-chip devices for the measurements.

■ REFERENCES

(1) Gupta, K.; Hooton, T. M.; Naber, K. G.; Wullt, B.; Colgan, R.; Miller, L. G.; Moran, G. J.; Nicolle, L. E.; Raz, R.; Schaeffer, A. J.; Soper, D. E. *Clin. Infect. Dis.* **2011**, *52*, e103−e120.

(2) Fraser, R. S.; Creanor, J. *Eur. J. Biochem.* **1974**, *46*, 67−73.

(3) Pelletier, C.; Prognon, P.; Bourlioux, P. *Antimicrob. Agents Chemother.* **1995**, *39*, 707−713.

(4) Kresken, M.; Körber-Irrgang, B. *Antimicrob. Agents Chemother.* **2014**, *58*, 7019−7020.

(5) Naber, K. G.; Niggemann, H.; Stein, G.; Stein, G. *BMC Infect. Dis.* **2014**, *14*, 1−16.

(6) Mrhar, A.; Kopitar, Z.; Kozjek, F.; Presl, V.; Karba, R. *Int. J. Clin Pharmacol Biopharm* **1979**, *17*, 476−481.

(7) NAK - Nationales Antibiotika-Sensitivitätstest -Komitee. *Nitroxoline: Rationale for the clinical breakpoints*, version 1.0; 2014.

(8) Wagenlehner, F. M. E.; Munch, F.; Pilatz, A.; Barmann, B.; Weidner, W.; Wagenlehner, C. M.; Straubinger, M.; Blenk, H.; Pfister, W.; Kresken, M.; Naberf, K. G. *Antimicrob. Agents Chemother.* **2014**, *58*, 713−721.

(9) Sorel, R. H. A.; Snelleman, C.; Hulshoff, A. *J. Chromatogr., Biomed. Appl.* **1981**, *222*, 241−248.

(10) Ghoneim, M. M.; El-Desoky, H. S.; Abdel-Galeil, M. M. *Bioelectrochemistry* **2011**, *80*, 162−168.

(11) Buividas, R.; Dzingelevičius, N.; Kubiliūtė, R.; Stoddart, P. R.; Khanh Truong, V.; Ivanova, E. P.; Juodkazis, S. *J. Biophoton.* **2015**, *8*, 567−574.

(12) Yuen, C.; Liu, Q. *J. Biophoton.* **2014**, *7*, 683−689.

(13) Strelau, K. K.; Kretschmer, R.; Moller, R.; Fritzsche, W.; Popp, J. *Anal. Bioanal. Chem.* **2010**, *396*, 1381−1384.

(14) Hidi, I. J.; Jahn, M.; Pletz, M. W.; Weber, K.; Cialla-May, D.; Popp, J. *J. Phys. Chem. C* **2016**, DOI: 10.1021/acs.jpcc.6b01005.

(15) Zhou, Q.; Kim, T. *Sens. Actuators, B* **2016**, *227*, 504−514.

(16) Kammer, E.; Olschewski, K.; Stockel, S.; Rosch, P.; Weber, K.; Cialla-May, D.; Bocklitz, T.; Popp, J. *Anal. Bioanal. Chem.* **2015**, *407*, 8925−8929.

(17) Mamian-Lopez, M. B.; Poppi, R. J. *Anal. Bioanal. Chem.* **2013**, *405*, 7671−7677.

(18) Mamian-Lopez, M. B.; Poppi, R. J. *Anal. Chim. Acta* **2013**, *760*, 53−59.

(19) Leopold, N.; Lendl, B. *J. Phys. Chem. B* **2003**, *107*, 5723−5727.

(20) R Development Core Team. *R*; R Foundation for Statistical Computing: Vienna, Austria, 2011.

(21) Ryan, C. G.; Clayton, E.; Griffin, W. L.; Sie, S. H.; Cousens, D. R. *Nucl. Instrum. Methods Phys. Res., Sect. B* **1988**, *34*, 396−402.

(22) März, A.; Bocklitz, T.; Popp, J. *Anal. Chem.* **2011**, *83*, 8337−8340.

(23) de Juan, A.; Jaumot, J.; Tauler, R. *Anal. Methods* **2014**, *6*, 4964.

(24) Villa, J. E. L.; Poppi, R. J. *Analyst* **2016**, *141*, 1966−1972.

(25) Lyndgaard, L. B.; van den Berg, F.; de Juan, A. *Chemom. Intell. Lab. Syst.* **2013**, *125*, 58−66.

(26) de Juan, A.; Rutan, S. C.; Tauler, R. In *Comprehensive Chemometrics*; Elsevier: Oxford, U.K., 2009; pp 325−344.

(27) Arjunan, V.; Balamourougane, P. S.; Kalaivani, M.; Raj, A.; Mohan, S. *Spectrochim. Acta, Part A* **2012**, *96*, 506−516.

(28) Chi, J. M.; Zaw, T.; Cardona, I.; Hosnain, M.; Garg, N.; Lefkowitz, H. R.; Tolias, P.; Du, H. *Biomed. Opt. Express* **2015**, *6*, 761−769.

DOI: 10.1021/acs.analchem.6b02316
Anal. Chem. 2016, 88, 9173−9180

LoC-SERS Combined with the Standard Addition Method: Toward the Quantification of Nitroxoline in Spiked Human Urine Samples

Izabella J. Hidi,[1, 2]‡ Martin Jahn,[1, 2]‡ Karina Weber,[1, 2,4] Thomas Bocklitz,[1] Mathias W. Pletz,[3,4] Dana Cialla-May,[1, 2,4*] Juergen Popp[1,2,4]

[1]Friedrich Schiller University Jena, Institute of Physical Chemistry and Abbe Center of Photonics, Helmholtzweg 4, 07745 Jena, Germany

[2]Leibniz Institute of Photonic Technology Jena, Albert-Einstein-Str. 9, 07745 Jena, Germany

[3]Center for Infectious Diseases and Infection Control, Jena University Hospital, Erlanger Allee 101 07740 Jena

[4]Research Campus Infectognostic, Philosophenweg 7, 07743 Jena, Germany, Germany

*corresponding author: Phone: +49 (0)3641-206309; Fax: +49 (0)3641-206399, e-mail: dana.cialla-may@uni-jena.de

Supporting Information

Table of Content:

Table S1. Sample preparation – Urinary NTX concentrations measured for sample HV**1**, HV**2** and HV**3**.

$c_{NTX/H2O}$ [µM]	$c_{NTX/in\text{-}droplet}$ [µM]	$c_{NTX/urine}$ [µM]
10	3.0	4.28
17.5	5.25	7.50
25	7.50	10.70
40	12.00	17.10
55	16.50	23.50
70	21.00	30.00
85	25.50	36.40
100	30.00	42.80

Obs.: NTX/H_2O solution at different concentrations ($c_{NTX/H2O}$) was mixed with the urine sample in 3:7 ratio. $c_{NTX/in\text{-}droplet}$ represents the concentration of NTX in the total volume ($V_{NTX/H2O}+V_{urine}$), while $c_{NTX/urine}$ is the NTX concentration in the volume of urine.

Table S2. Sample preparation – LoC-SERS-SAM

Sample	V_{urine} [µl]	V_{spike} [µl]	$V_{standard}$ [µl]	V_{H2O} [µl]
blank	250	0	0	250
unknown		76	0	174
SAS1			43.4	130.6
SAS2			87	87
SAS3			130.6	43.4
SAS4			174	0

for c_{spike}=69.4 µM and $c_{standard}$=57.4 µM (HV**4** and HV**5**)

Sample	n_{spike} [mol]	$n_{standard}$ [mol]	n_{total} [mol]	$c_{NTX/urine}$ [M]	$c_{NTX/urine}$ [mg/l]	$c_{NTX\ in\text{-}droplet}$ [M]	c_{SAS} [M]
unknown	$1.05\cdot10^{-8}$	0	$1.05\cdot10^{-8}$	$2.10\cdot10^{-5}$	4	$1.05\cdot10^{-5}$	0
SAS1		$4.99\cdot10^{-9}$	$1.55\cdot10^{-8}$	$3.10\cdot10^{-5}$	5.89	$1.55\cdot10^{-5}$	$4.99\cdot10^{-6}$
SAS2		$9.99\cdot10^{-9}$	$2.05\cdot10^{-8}$	$4.10\cdot10^{-5}$	7.79	$2.05\cdot10^{-5}$	$9.98\cdot10^{-6}$
SAS3		$1.50\cdot10^{-8}$	$2.55\cdot10^{-8}$	$5.10\cdot10^{-5}$	9.69	$2.55\cdot10^{-5}$	$1.49\cdot10^{-5}$
SAS4		$2.00\cdot10^{-8}$	$3.05\cdot10^{-8}$	$6.10\cdot10^{-5}$	11.59	$3.05\cdot10^{-5}$	$1.99\cdot10^{-5}$

for c_{spike}=70 µM and $c_{standard}$=60 µM (PS**1**-PS**5**)

Sample	n_{spike} [mol]	$n_{standard}$ [mol]	n_{total} [mol]	$c_{NTX/urine}$ [M]	$c_{NTX/urine}$ [mg/l]	$c_{NTX\ in\text{-}droplet}$ [M]	c_{SAS} [M]
unknown	$5.32\cdot10^{-9}$	0	$5.32\cdot10^{-9}$	$2.13\cdot10^{-5}$	4.04	$1.06\cdot10^{-5}$	0
SAS1		$2.60\cdot10^{-9}$	$7.92\cdot10^{-9}$	$3.17\cdot10^{-5}$	6.02	$1.58\cdot10^{-5}$	$5.21\cdot10^{-6}$
SAS2		$5.22\cdot10^{-9}$	$1.05\cdot10^{-8}$	$4.22\cdot10^{-5}$	8.01	$2.11\cdot10^{-5}$	$1.04\cdot10^{-5}$
SAS3		$7.84\cdot10^{-9}$	$1.32\cdot10^{-8}$	$5.26\cdot10^{-5}$	10.00	$2.63\cdot10^{-5}$	$1.57\cdot10^{-5}$
SAS4		$1.04\cdot10^{-8}$	$1.58\cdot10^{-8}$	$6.30\cdot10^{-5}$	11.98	$3.15\cdot10^{-5}$	$2.09\cdot10^{-5}$

Table S3. Band assignment of the observed Raman modes of NTX.[1]

Position [cm^{-1}]	Assignment
421	CCC out-of-plane bending
490	C-O in-plane bending
565	CCC in-plane bending
729	O-H out-of-plane bending
800	aromatic C-H out-of-plane bending
840	
987	aromatic C-H in-plane bending
1153	
1197	C-N stretching
1249	C-NO_2 stretching
1313	C-O stretching
1405	O-H in-plane bending
1465	C=N stretching
1573	C=C stretching

Droplet based microfluidic chip

The microfluidic platform is fabricated from glass via chemical etching and anodic binding and has a size of 16x25 mm. Glass has a low Raman scattering cross section, therefore it is an ideal material for manufacturing microfluidic chips for SERS measurements. Prior to the measurements, the surface of the micro-channels was functionalized with octadecyltrichlorosilane (ODTS) in order to obtain hydrophobic channel walls. The microfluidic platform has the following operational units: a droplet generator where the aqueous solutions are dispensed into the flow of mineral oil via a T-junction, a dosing unit where further aqueous solutions are injected into the already existing droplet, two meander channels assuring an optimal mixing of the droplet content and a long measurement loop. Generally, through port 1-3 the analyte solutions and the solvent (purified water, water or urine containing the target analyte) are pumped, while the Ag nanoparticles and KCl, as aggregation agent, are injected via port 4 and 5. The flow rate of the continuous phase was fixed at 9 nl/s, the sum of the flowrates at the droplet generator was 14 nl/s and at the dosing unit 11 nl/s. The various solutions are filled into glass syringes that are connected with the chip via Teflon capillaries. The software provided with the pump system (neMESYS Cetoni GmbH) controls the flow rates and allows the preparation of droplets containing differently concentrated samples, while maintaining the droplet volume constant.

UV-Vis measurements

The UV-Vis spectra plotted in Figure **S1** show the extinction profile of the bare Ag NPs, of the NTX molecule at 100 µM and the extinction bands of the Ag NPs and NTX mixture without and with KCl addition. The maximum of the extinction band due to the single particle resonance is centered at 408 nm proving the successful synthesis.[2, 3] The NTX molecule has several absorption bands. The detailed assignment of the bands is behind the purpose of the present study. When Ag NPs are mixed with NTX in a 1 to 1 ratio, the UV-Vis spectrum presents a broad band centered at 423 nm. This is the result of the convolution of the absorption band of the Ag NPs and

of the two bands of NTX at 363 nm and 448 nm. In order to achieve high SERS enhancements "hot-spots" are needed. Thus, the single spherical nanoparticles have to be aggregated after the analyte molecule is absorbed on the metallic surface. For this, 1 M KCl solution was added in the following ratio: Ag NPs:NTX:KCl=1:1:0.1. As a consequence, in the UV-Vis spectrum the single particle resonance is diminishing in intensity and a second broad band appears at higher wavelengths. This is associated with coupled localized surface plasmon resonances originating from two or more closely related nanoparticles. The connection between the extinction spectrum and the magnitude of the electromagnetic SERS enhancements is in general indirect. The highest enhancement is obtained from the small gaps in between nanoparticles, rather from the surface of the single ones.

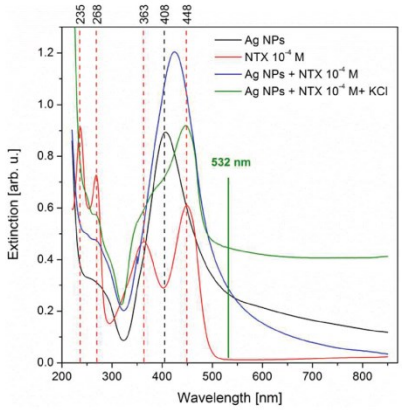

Figure S1. UV-Vis absorption spectra of Ag NPs, of NTX/H_2O at 10^{-4} M and of the non-aggregated and aggregated Ag NPs and NTX mixtures. (Ag NPs:NTX:KCl=1:1:0.1)

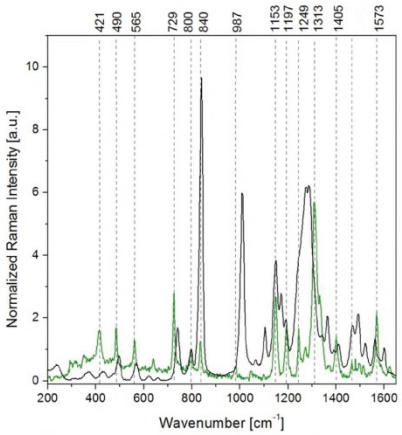

Figure S2. Normalized Raman (green) and SERS (black) spectrum of NTX powder and of an 100 μM solution.

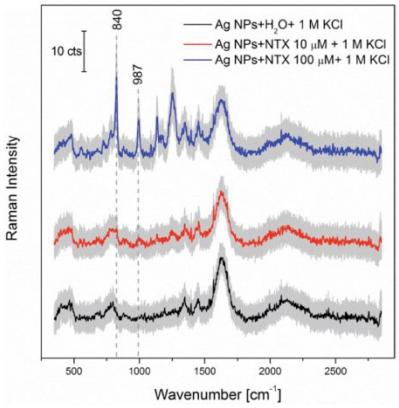

Figure S3. SERS spectra measured with the conventional configuration: port 1: NTX/H_2O, port 3: purified water, port 4: Ag NPs and port 5: 1 M KCl (chip design in Scheme **2**).

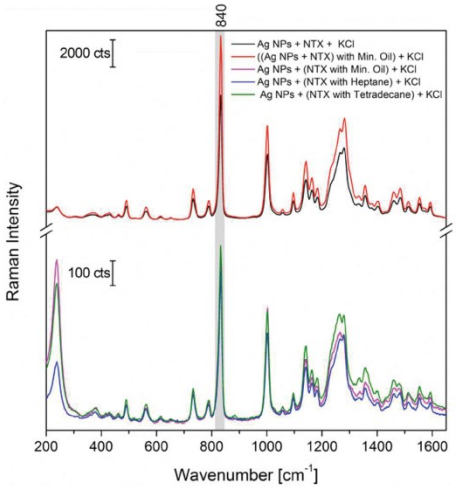

Figure S4. The chemical affinity of NTX toward Ag NPs: SERS spectra of various mixtures. NTX concentration was 100 µM.

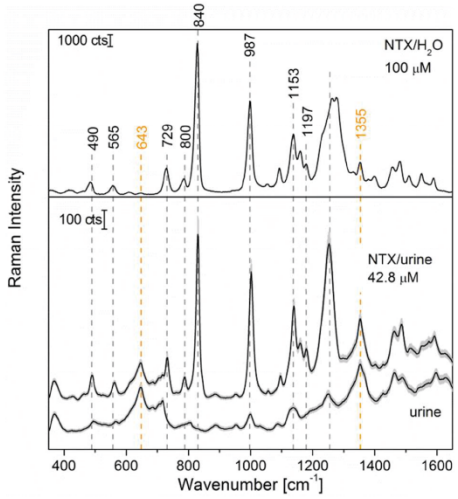

Figure S5. Reference SERS spectrum of NTX vs. LoC-SERS signal of the blank urine and of NTX spiked in the urine sample **HV1**.

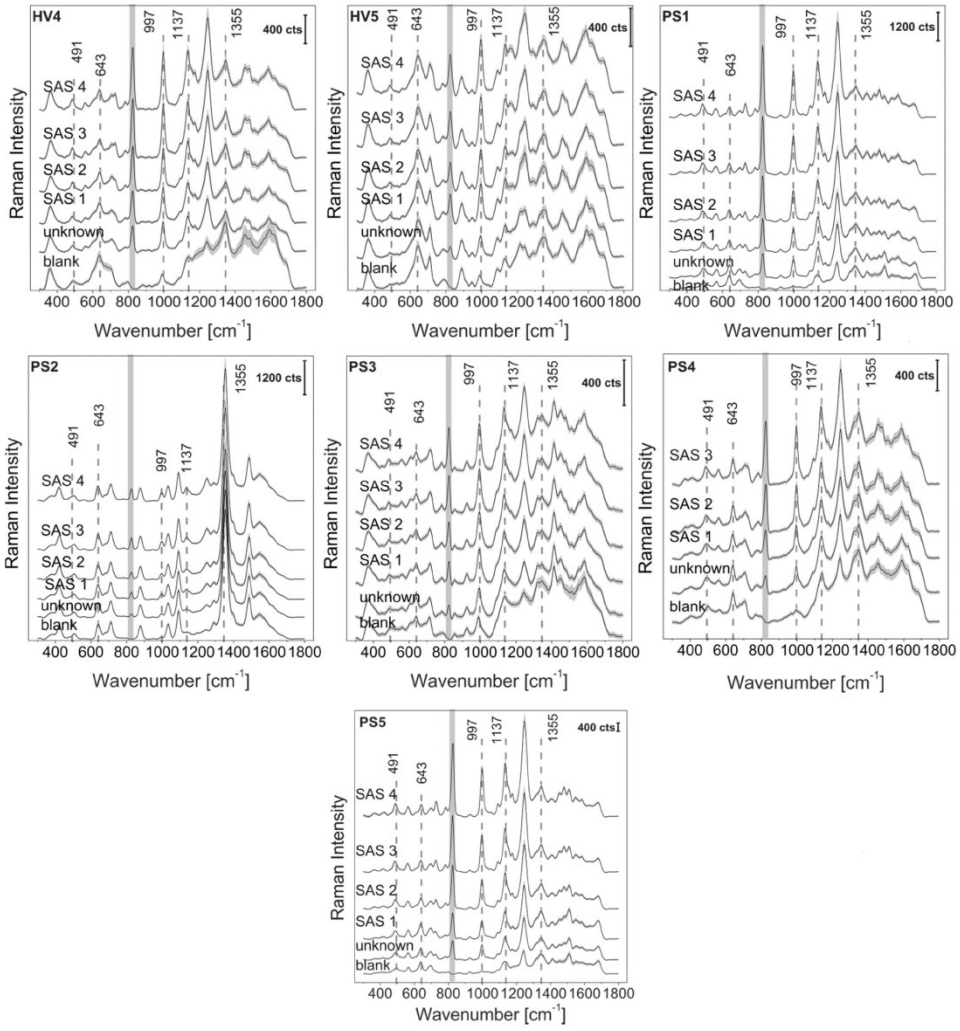

Figure S6. Mean SERS spectra and their double standard deviation of urine samples from healthy volunteer (HV) and UTI patients (PS).

S-7

Table S4. LoC-SERS-SAM results for the Raman band at ~**840** cm^{-1} based on univariate statistical analysis and their corresponding 95 % confidence intervals.

Sample	c_0 [μM]	E_r [%]	$c_{unknown}$		c_{NC} [μM]
			[μM]	[mg/l]	
HV4	13.2±1.0	25.6	26.4±2.1	5.0±0.4	2.1±0.5
HV5	12.1±1.1	15.0	24.1±2.2	4.6±0.4	2.7±0.6
PS1	9.9±0.6	6.1	19.7±1.3	3.7±0.2	0.1±0.3
PS2	9.1±0.8	14.2	18.2±1.7	3.5±0.3	0.5±0.5
PS3	9.0±0.5	14.7	18.1±1.1	3.4±0.2	0.7±0.4
PS4	7.5±0.4	29.2	15.0±0.9	2.9±0.2	1.1±0.2
PS5	5.8±0.4	45.1	11.6±0.7	2.2±0.1	1.6±0.2

c_0-in-droplet NTX concertation; $c_{unknown}$-urinary NTX concertation; c_{NC}: predicted NTX concentration for the blank sample.

Table S5. LoC-SERS-SAM results for the Raman band at ~1000 cm^{-1} based on univariate statistical analysis and their corresponding 95 % confidence intervals.

Sample	c_0 [μM]	E_r [%]	$c_{unknown}$		c_{NC} [μM]
			[μM]	[mg/l]	
HV4	25.5±1.6	142.7	51.0±3.1	9.7±0.6	18.6±1.1
HV5	20.7±1.4	97.5	41.5±2.7	7.9±0.5	14.1±0.9
PS1	14.5±0.8	37.9	29.0±1.5	5.5±0.3	4.9±0.4
PS2	26.9±1.9	153.7	53.8±3.7	10.2±0.7	20.7±1.3
PS3	58.0±2.9	447.6	116.1±5.9	22.1±1.1	48.3±1.8
PS4	23.1±1.1	117.6	46.1±2.1	8.8±0.4	19.1±0.8
PS5	9.1±0.4	14.0	18.2±0.9	3.5±0.2	2.3±0.4

c_0-in-droplet NTX concertation; $c_{unknown}$-urinary NTX concertation; c_{NC}: predicted NTX concentration for the blank sample.

Table S6. LoC-SERS-SAM results based on MCR-ALS analysis and their corresponding 95 % confidence intervals (Student's t-test).

Sample	c_0 [μM]	E_r [%]	$c_{unknown}$		c_{NC} [μM]
			[μM]	[mg/l]	
HV4	14.0±1.0	33.9	27.9±2.1	5.3±0.4	1.8±0.5
HV5	10.1±0.9	3.8	20.2±1.7	3.8±0.3	0.5±0.5
PS1	10.1±0.6	4.0	20.2±1.2	3.8±0.2	1.1±0.3
PS2	9.8±1.0	7.8	19.5±2.1	3.7±0.4	1.9±0.3
PS3	11.5±0.6	8.9	23.1±1.1	4.4±0.2	0.0±0.3
PS4	5.9±0.4	43.7	11.9±0.8	2.3±0.2	0.6±0.6
PS5	5.6±0.4	46.9	11.3±0.8	2.1±0.2	0.8±0.3

c_0-in-droplet NTX concertation; $c_{unknown}$-urinary NTX concertation; c_{NC}: predicted NTX concentration for the blank sample.

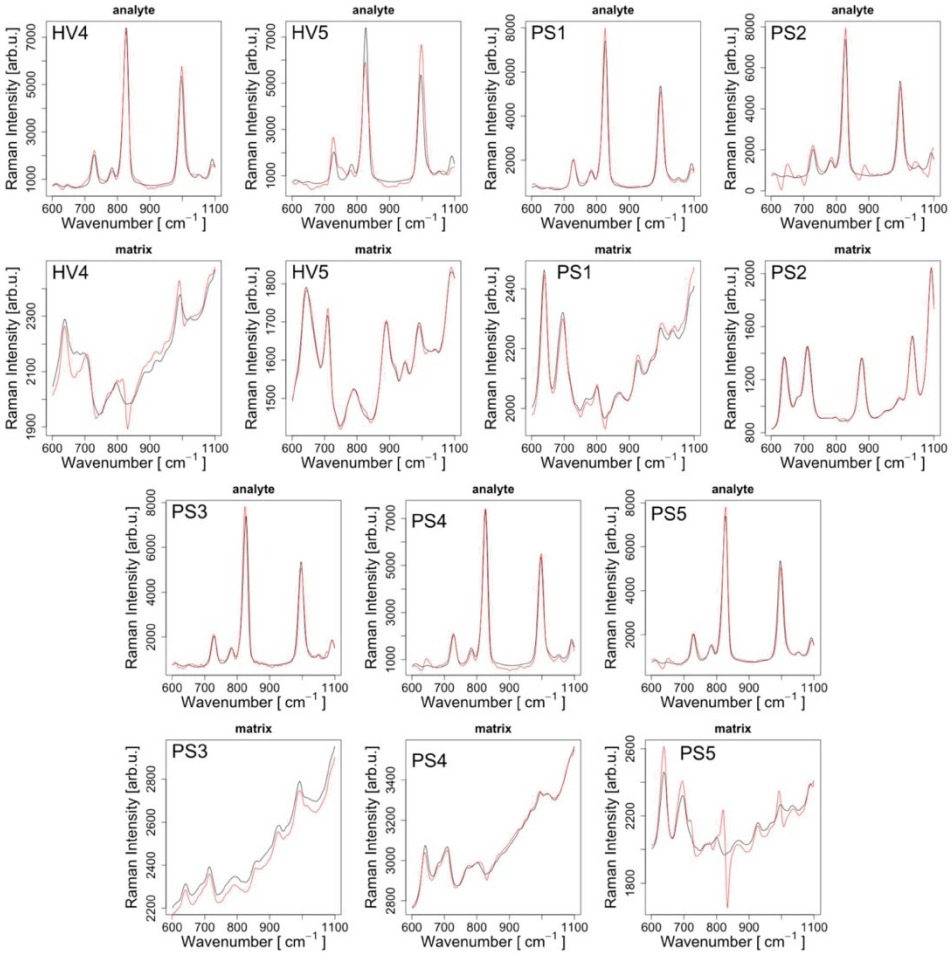

Figure S7. Reference (black) and MCR-ALS recovered (red) spectra of NTX in water (analyte) and pure urine (matrix).

Table **S7**. Pearson correlation coefficient of between reference and MCR-ALS recovered spectra.

Sample	r_{matrix}	$r_{analyte}$
HV**4**	0.965	0.988
HV**5**	0.997	0.940
PS**1**	0.989	0.991
PS**2**	0.997	0.969
PS**3**	0.999	0.979
PS**4**	0.997	0.989
PS**5**	0.899	0.987

References:

[1] Arjunan, V.; Balamourougane, P. S.; Kalaivani, M.; Raj, A.; Mohan, S. *Spectrochimica Acta Part A: Molecular and Biomolecular Spectroscopy* **2012**, *96*, 506-516.
[2] Leopold, N.; Lendl, B. *The Journal of Physical Chemistry B* **2003**, *107*, 5723-5727.
[3] Zhang, C.; Man, B. Y.; Jiang, S. Z.; Yang, C.; Liu, M.; Chen, C. S.; Xu, S. C.; Qiu, H. W.; Li, Z. *Appl. Surf. Sci.* **2015**, *347*, 668-672

2.5 Ciprofloxacin: pH dependent SERS signal and its detection in spiked river water by LoC-SERS [IH5]

Izabella J. Hidi, Jan Heidler, Karina Weber,

Dana Cialla-May, Jürgen Popp

Analytical Bioanalytical Chemistry (2016). doi:10.1007/s00216-016-9957-2

Anal Bioanal Chem
DOI 10.1007/s00216-016-9957-2

RESEARCH PAPER

Ciprofloxacin: pH-dependent SERS signal and its detection in spiked river water using LoC-SERS

Izabella J. Hidi[1,2] · **Jan Heidler**[1] · **Karina Weber**[1,2] · **Dana Cialla-May**[1,2] · **Jürgen Popp**[1,2]

Received: 7 July 2016 / Revised: 26 August 2016 / Accepted: 19 September 2016

Abstract Monitoring the successful removal of antibiotics in waste and surface waters is of high interest to overcome the occurrence of antibacterial resistance in the ecosystem. Among the newly developed analytical methods, the lab-on-a-chip surface-enhanced Raman spectroscopic (LoC-SERS) technique has gained the interest of the scientific community in the last few years. Ciprofloxacin, a second-generation fluoroquinolone, is widely used and administered to patients in dosages up to 1000 mg. In addition, more than 50 % of the antibiotic is excreted in urine as the parental drug. Thus, ciprofloxacin in environmental samples may exceed the minimum inhibitory concentration (MIC) values. The present study aims to assess the potential of the LoC-SERS technique to detect the target analyte in spiked river water samples at MIC concentrations. As sample clean-up procedure, a simple filtration is proposed, while as SERS, active substrates silver nanoparticles prepared at room temperature are employed. Ciprofloxacin was successfully quantified in the 0.7–10 μM concentration range with data that were measured on two different days. Furthermore, because of the low solubility of the antibiotic at the neutral pH range, insights into the effect of pH on the SERS signal of the target molecule are also presented.

Keywords Ciprofloxacin · SERS · Microfluidics · Surface water · LoC

Electronic supplementary material The online version of this article (doi:10.1007/s00216-016-9957-2) contains supplementary material, which is available to authorized users.

✉ Dana Cialla-May
dana.cialla-may@uni-jena.de

[1] Institute of Physical Chemistry and Abbe Center of Photonics, Friedrich Schiller University Jena, Helmholtzweg 4, 07745 Jena, Germany

[2] Leibniz Institute of Photonic Technology Jena, Albert-Einstein-Str. 9, 07745 Jena, Germany

Published online: 03 October 2016

Introduction

The discovery of antibiotics at the beginning of the twentieth century revolutionized medicine. Antibiotics act by either killing bacteria or inhibiting their growth. Many antibiotic classes have a broad antibacterial spectrum. However, because of their overuse in medical treatments and live-stock raising, the presence of antibiotics has been detected in waste and surface waters [1–3]. High antibiotic concentrations in the ecosystem can cause the development of antibacterial resistance [4–7] and consequently, the necessity of finding new drug formulations. Ciprofloxacin, a second-generation fluoroquinolone, is widely used in the treatment of infections, such as urinary tract, prostatitis, sinusitis, and bone and joint infections [8]. The drug is excreted in urine, with the parental drug representing more than 50 %. Additionally, for some prescribed treatments, dosages up to 1000 mg are administered [9]. As a result, the concentration in environmental samples can exceed the minimum inhibitory concentration (MIC) values of bacteria [2, 3]. Ciprofloxacin MICs range between 0.03 mg/l (0.024 μM) for *Escherichia coli* ATCC 25922 and 16 mg/l (48 μM) for *Enterococcus faecalis* clinical strain 55 [8]. Thus, it is important to monitor and reduce the antibiotic concentrations that enter the ecosystem. Drinking water treatment plants play an important role in removing unwanted chemicals. Nonetheless, because of strong fluctuations throughout the year, the successful removal of antibiotics must be constantly monitored.

Surface-enhanced Raman spectroscopy (SERS) was proven to be suitable for the detection of trace amounts of molecules [10–20]. The strong signal enhancements originate from

localized "hot spots" at the tip of sharp nanostructures or in the gap between spherical nanoparticles [15, 21]. Reliable and homogenous SERS active substrate development is one of the main concerns of the SERS community. Despite the high variety of available planar substrates [22–25], metallic colloidal suspensions that are obtained by chemical reduction remain the easiest-to-access and most cost-effective structures. Their main drawbacks, such as aggregation time-dependent signals, precipitation [26], proper mixing with the analyte, and automatic measurement conditions, can be easily overcome using microfluidic setups [27–30]. Here, solution dosing is achieved by computer-controlled syringe pump systems. Mixing is performed by meander or zig-zag channels [29], while the aggregation time can be controlled by fixing the focus point during measurements. Additionally, because of automatic measurement conditions, large datasets can be easily recorded [31]. Lastly, memory effects encountered when applying continues flow microfluidic platforms [32] can be easily avoided by employing droplet-based microfluidic chips. Multiple strategies are available for the fabrication of these platforms. Although polymer-based chips are preferred due to their low cost, drawbacks associated with poor chemical compatibility with many organic solvents, unstable surface modification over time, and ability to absorb small molecules into the matrix inhibit their application [33]. Recently, the attention of the scientific community was redirected from polydimethylsiloxane (PDMS) as material to thiol-ene polymer-based materials [34]. Nevertheless, polymers are well known to provide high Raman spectral features, which could interfere with the fingerprint of the targeted molecules. Therefore, glass platforms are still preferred for Raman and SERS applications.

Throughout the last years, SERS advanced from being a technique mainly used to characterize plasmonic structure-molecule interactions [16] and to detect dye molecules in distilled water to quantification of biomolecules in clinical [18, 35] and environmental samples [36]. Because of the complexity of the chemical composition of samples, both clinical and environmental, various strategies, i.e., sample clean-up procedures or functionalization of plasmonic structures, have to be applied to reduce the matrix effects and to successfully detect the target molecule. However, these procedures increase the costs and the time required for performing the analytical measurement. SERS detection of ciprofloxacin was previously carried out using TiO_2 nanoparticles [37], dendritic silver nanostructures [38], and core-shell structured magnetic molecularly imprinted polymers [39]. While in the first two cases the antibiotic was determined only in distilled water, in the latter case, diluted fetal bovine serum was also used as matrix. Here, the achieved limit of detection (LOD) was 10^{-7} M. However, no details regarding the extent of the dilution procedure is provided, while the preparation of the employed nanostructures is not straightforward.

The objective of the present study was to assess the potential of the LoC-SERS technique to detect ciprofloxacin spiked in river water samples at MIC concentrations. As sample clean-up procedure, a simple filtration is proposed, while as SERS, active substrates silver nanoparticles prepared at room temperature [40] are employed. Furthermore, due to the low solubility of the antibiotic in the neutral pH range, either acidic or basic ciprofloxacin solutions were prepared. Therefore, insights into the influence of pH on the SERS signal of the target molecule are also presented.

Materials and methods

Sample preparation

Ciprofloxacin (≥98 % HPLC), sodium hydroxide (NaOH), hydrochloric acid (HCl), silver nitrate ($AgNO_3$), and hydroxylamine hydrochloride ($H_2NOH{\cdot}HCl$) were purchased from Sigma Aldrich and used as received. To prepare aqueous solutions, high purity water was used.

For cuvette-based SERS measurements, stock solutions of ciprofloxacin with a concentration of 1 mM were prepared by solving an appropriate amount of powder in HCl or NaOH solution with a concentration of 1, 0.1, and 0.01 M. Working solutions of the target analyte with a concentration of 0.1 mM were obtained by diluting the stock solutions with purified water in a 1-to-10 ratio. The pH was checked with a pH meter and adjusted by adding additional NaOH or HCl (see Electronic Supplementary Material (ESM) Table S1).

LoC-SERS measurements were performed on spiked river water sample from the Saale River (Jena, Thuringia, Germany). The river water was collected in two 50 ml falcon tubes on the same day, from the same spot. Prior to the measurements, the sample was filtered using a syringe filter with a pore diameter of 0.22 μm (Rotilabo®-syringe filter, PVDF, sterile). Filtration was necessary in order to remove large particles, such as sediments and soil. The river water sample was spiked with ciprofloxacin by mixing 100 parts of the complex matrix with 1 part of 10 or 1 mM ciprofloxacin solution prepared in 0.1 M NaOH, respectively. As a result, working solutions with a pH value of 11 with ciprofloxacin concentrations of 0.1 and 0.01 mM were prepared. Furthermore, it is important to note that the matrix was just slightly diluted, hence, conserving the complexity of the matrix. In order to assess the robustness of the LoC-SERS technique, the measurements for the detection of ciprofloxacin spiked in river water were carried out on two different days, using two different chips but the same working solutions.

The Ag colloidal solution was synthesized according to the protocol published by Leopold and Lendl [40]. For this, silver nitrate was reduced by hydroxylamine hydrochloride in the presence of sodium hydroxide. The molar ratio of $AgNO_3$/

$H_2NOH.HCl/NaOH$ was 1:1.5:3 in the final solution. As a result, a yellow-brown solution was obtained.

Instrumentation

For the pH measurements, a pH meter from Hanna Instruments (HI 9321), which was equipped with a combination microelectrode (HI 1083B), was used.

Raman and SERS spectra were acquired using a WITec Raman microscope, which was equipped with a diode laser (Fandango, Cobolt) that emitted at 514 nm with a maximum output power of 95 mW on the sample surface. The same objective (Zeiss, ×20, 0.4 N.A.) was applied to focus the laser beam on the surface of the sample and collect the backscattered photons. For detection, a thermoelectrically cooled CCD (1024 × 127) camera and two different gratings (600 and 1800 l/mm, which had spectral resolutions of ~5 and 2 cm^{-1}, respectively) were used.

Raman measurements on the ciprofloxacin powder were performed with 1800 l/mm grating, 5 s integration time, and 1 mW power on the sample. To record the Raman spectra of saturated aqueous solutions, the laser power was increased to 95 mW and the integration time was increased to 10 s.

Cuvette-based SERS measurements were performed with the identical grating as above, a laser power of 38 mW on the sample, and a 1-s integration time. Each spectrum is the result of 10 accumulations. For the measurements, 100 μl of colloid was mixed with 100 μl of analyte and 20 μl of H_2O or KCl (0.3 and 1 M). After mixing, the cuvette was placed under the objective and the SERS spectra were recorded. For each mixture, four independent spectra acquisitions were performed using new colloid and analyte solutions.

For LoC-SERS measurements, a glass chip (Scheme 1) was used. The channel walls were functionalized with octadecyltrichlorosilane prior to the measurements to achieve hydrophobicity. As the carrier medium, mineral oil was selected. All of the analyte-containing solutions were in the aqueous phase. Hence, analyte- and colloid-containing droplets were formed in the immiscible continuous phase. A detailed description of the platform can be found elsewhere [41, 42]. To obtain differently concentrated solutions, the flow rates of the ciprofloxacin-containing syringes and of the one that contained the mixing medium were varied (Table 1). Mineral oil was pumped with 10 nl/s, whereas the colloidal solution was pumped with 9 nl/s. For each concentration step, 1200 spectra were recorded with a 1-s integration time and 38 mW power on the sample using the 600 l/mm grating.

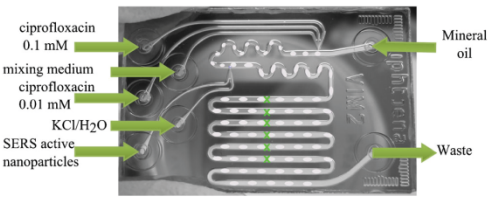

Scheme 1 Picture of the droplet-based microfluidic chip for LOC-SERS measurements with the depiction of the droplets, inlets, and laser focus point. (Adapted from Ref. [38] with permission from the PCCP Owner Societies)

Data processing

The acquired data were pre-processed and analyzed using the statistical programming language R [43]. The recorded Raman spectra and SERS spectra in the cuvette were background-corrected using the selective nonlinear iterative clipping (SNIP) [44] algorithm with 60 iterations. For better visualization, the signal was further normalized to the Raman mode at 1382 cm^{-1}.

During the LoC-SERS measurements, the spectra were continuously acquired while maintaining the fixed focus point. Therefore, alternating Raman/SERS spectra that contained the signature of the mineral oil, analyte, or analyte and mineral oil were recorded. The first preprocessing step consisted of removing the mineral oil and mixed spectra, which was performed by manually setting a threshold value for the intensity of the Raman marker band of the oil at 2888 cm^{-1}. The number of resulting spectra is listed in Table 1. After this step, the spectra were background-corrected and averaged. For the analysis, both uni- and multivariate statistics were applied. In the first case, selected Raman bands were integrated using Simpson's rule. The second method combines the principal component analysis (PCA) with partial least-squares regression (PLSR) [45, 46]. Briefly, a PCA is performed in order to reduce the dimensionality of the dataset and, therewith, to reduce the computational costs significantly. The robustness of the LoC-SERS technique was assessed by training the PLS model by using the data recorded on the detection of ciprofloxacin spiked in river water sample on the first measurement day. The PLS model was subsequently used for predicting the concentrations of a second, independent data set, measured on a second day. For training the PLS model, only the first four PCA scores were applied, whereby four PLS latent variables were constructed. To evaluate the quality of the created PLS model, a ten times averaged 10-fold cross validation was performed. Therefore, the training dataset was split into 10 parts, the so-called folds, of which in every of the 10 cross-validation steps 1 was excluded from the training process and used for prediction. Afterwards, the root mean square error of prediction for cross validation (RMSEPCV) was calculated as the averaged RMSEP of the 10 validation steps. For the prediction, either on the training dataset or onto unknown data, all four PLS latent variables were used.

Table 1 Flow rates and the corresponding measured ciprofloxacin concentrations

Flow rate [nl/s]	0.01 mM syringe	0	1	2	4	6	8	10	12	14
	Mixing medium	14	13	12	10	8	6	4	2	0
Concentration [μM]		0	0.714	1.43	2.86	4.29	5.71	7.14	8.57	10
Droplet spectra (day 1)		463	498	521	564	524	506	482	489	530
Droplet spectra (day 2)		248	424	471	438	473	506	403	461	565
Flow rate [nl/s]	0.01 mM syringe	2	4	6	8	10	12	14		
	Mixing medium	12	10	8	6	4	2	0		
Concentration [μM]		14.3	28.6	42.9	57.1	71.4	85.7	100		
Droplet spectra (day 1)		537	558	501	503	450	405	626		
Droplet spectra (day 2)		479	534	519	412	579	500	582		

Results and discussion

The effect of pH on the SERS signal of ciprofloxacin

Before assessing the potential of the LoC-SERS technique to detect ciprofloxacin in spiked river water, a series of cuvette-based measurements was performed. Contradictory to the already reported publications [37, 39], the preparation of a homogenous solution with a concentration of 0.1 mM in a pH range of 4 to 10 was not successful at room temperature, which can be explained by considering the solubility properties of the antibiotic. According to Caço et al. [47], ciprofloxacin is slightly soluble in water. At 20 °C, the measured solubility after 6 h of equilibration time was 0.067 mg/ml (0.202 mM). To assess the potential of the LoC-SERS technique to detect the target molecule in the concentration range of 0.001 to 0.1 mM, stock solutions with ciprofloxacin amounts near the solubility limit had to be prepared. For this purpose, diluted HCl or NaOH was selected as a solvent instead of pure water.

In Fig. 1, the normalized Raman spectrum of ciprofloxacin powder and saturated aqueous solutions at pH 1 and pH 13 are plotted with the normalized SERS spectra, which were measured on solutions at a concentration of 0.1 mM (at pH 1 and 13). A comprehensive band assignment of the Raman modes of the antibiotic in powder form can be found in the literature [37, 48]. Briefly, the Raman bands that are ascribed to vibrations involving the piperazinyl ring are located at 1454 cm^{-1} (CH_2 deformation), 1362 cm^{-1}, and 1263 cm^{-1} (ring stretching). The most intense signal is centered at 1382 cm^{-1} because of the aromatic ring stretching mode that is coupled with $\nu_s(COO^-)$. The band at 1616 cm^{-1} is caused by ν_{as}(C=C), that at 1541 cm^{-1} is caused by the stretching vibrations of the quinolone ring system, and that at 1591 cm^{-1} is caused by carbonyl stretching with $\nu_{as}(COO^-)$. The presence of vibrations characteristic of the carboxylate group is explained by the existence of ciprofloxacin as a zwitterion in the anhydrous form [37].

By comparing the spectrum that was measured on powder with those of saturated aqueous solutions at strongly acidic and strongly basic pH, one can observe significant spectral differences. First, the Raman mode at 1616 cm^{-1} is shifted by 13 cm^{-1} towards higher wavenumbers for the solution (see ESM Table S2 for the band positions). Furthermore, the relative intensity of the later band compared to that at 1382 cm^{-1} significantly depends on the chemical environment. At pH 1, there should only be the cationic form of the molecule, whereas at pH 13, the anionic form predominates. In the former case, the protonation occurs on the amine group of the piperazinyl ring, whereas in the latter case, the carboxylic acid moiety is deprotonated (see chemical structures in ESM Fig. S1). Therefore, at pH 13, the intensity of the Raman mode that is ascribed to the aromatic ring stretching mode coupled with $\nu_s(COO^-)$ at 1382 cm^{-1} increases because of the presence of deprotonated ciprofloxacin molecules.

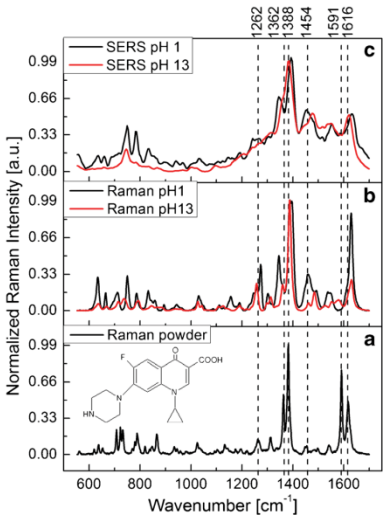

Fig. 1 Normalized Raman spectrum of **a** ciprofloxacin powder and **b** saturated aqueous solutions at pH 1 and pH 13. The spectra were recorded with a 2 cm^{-1} resolution. **c** SERS spectra of ciprofloxacin solution with a concentration of 0.1 mM, pH 1 and 13 (~5 cm^{-1} resolution)

Further differences are observed for the Raman marker bands that are ascribed to the piperazinyl ring. Upon protonation, the spectral feature at 1362 cm^{-1} is downshifted by 17 cm^{-1} and its relative intensity is higher than the case at pH 13. A higher intensity is also observed for the Raman mode that is ascribed to the CH_2 (1452 cm^{-1}) deformation of the same ring.

To record the Raman spectra of the saturated aqueous solutions, a long acquisition time and a high laser power were used. However, the MICs for the ciprofloxacin are from 0.024 μM for *E. coli* ATCC 25922 to 48 μM for *E. faecalis* clinical strain 55 [8]. Therefore, plasmonic substrates are required to enhance the weak Raman effect. Here, a silver colloidal suspension, which was obtained through the reduction of silver nitrate by hydroxylamine hydrochloride in the presence of sodium hydroxide, was used as the SERS substrate. Ciprofloxacin solutions at a 0.1 mM concentration were prepared by solving the powder in diluted HCl or NaOH solutions. As a result, three acidic (pH 1, 2, and 3) and three basic (pH 11, 12, and 13) samples have been obtained. The SERS signal for all samples is presented in Fig. 2 (for normalized data, see ESM Fig. S2).

According to Fig. 2, the most significant difference among the recorded SERS spectra is represented by their intensity. Generally, the free electron pairs of the nucleophile oxygen and particularly those of nitrogen atoms present high affinity towards the silver surface. For low pH values, the free electron pairs interact with the protons of HCl. Hence, they can no longer optimally bind to the Ag surface and the intensity is considerably lower than those of the basic solutions.

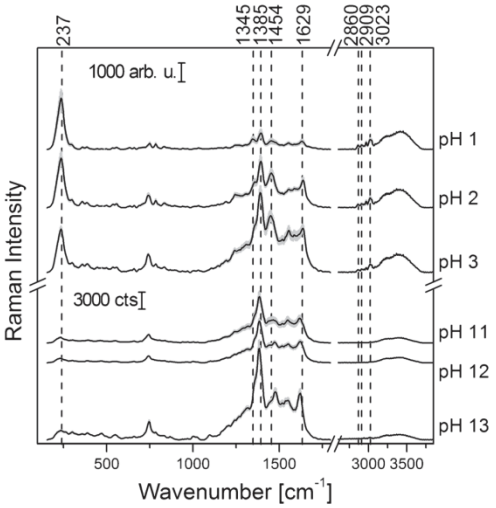

Fig. 2 Mean SERS spectra and their double standard deviation of ciprofloxacin 0.1 mM solutions at different pHs (600 l/mm grating, spectral resolution ~5 cm^{-1}). The indicated band positions belong to the protonated molecule

Additionally, Cl^- is known to have high affinity towards Ag, which is proven by the presence of the Raman mode at ~230 cm^{-1} and is ascribed to the Ag-Cl stretching vibration. Therefore, a competition between the target molecule and the ions is expected.

A further difference caused by the protonation state of ciprofloxacin can be observed by considering the intensity of the Raman mode at 1345 cm^{-1}. This band was ascribed to piperazinyl ring stretching. When the molecule is protonated, the respective Raman band is clearly visible. Upon deprotonation, it becomes convoluted with the strong Raman band centered at 1382 cm^{-1}. The identical behavior is observable in the 2800–3100 cm^{-1} spectral region. Namely, the Raman bands in this wavenumber region are significantly more intense for acidic pH than the recorded SERS spectra at basic pH values. These Raman modes are usually assigned to sp3 hybridized carbon atoms, which are localized on the piperazinyl and cyclopropane ring in the case of ciprofloxacin. Thus, one may conclude that either the two rings of ciprofloxacin cations are near the metallic surface or their polarizability tensor has such an orientation that its *zz* components are perpendicular to the surface. An additional hint concerning the orientation of ciprofloxacin on the metallic surface is given by the Raman band that is ascribed to the C=C stretching of the quinolone ring system at 1616 cm^{-1} in the Raman spectrum. This band is shifted by 8 cm^{-1} (see the high-resolution SERS spectra in Fig. 1c) when the SERS spectra are recorded under basic conditions compared to the band position in the Raman spectra of the saturated aqueous solutions. The shift may be caused by the interaction of the aromatic ring system with the Ag surface. Therefore, the deprotonated ciprofloxacin molecule probably adopts a flat orientation with interactions via the nitrogen atoms of the piperazinyl ring.

Optimization of the LoC-SERS measurements

The previous section shows that the highest signal intensities were recorded for the basic solutions. However, when experiments were conducted using the microfluidic setup, it was observed that the droplet formation was disrupted when a ciprofloxacin solution with a pH of 12 or 13 was pumped into the chip. To avoid memory effects that are characteristic to the flow through microfluidic platforms, the microchannels were functionalized with octadecyltrichlorosilane. The silane layer is not affected by the analyte-containing droplets at neutral pH levels. However, sodium hydroxide at a high concentration (0.1 and 0.01 M) can react with silane and inhibit the optimal droplet formation in the chip. Therefore, for experiments that were conducted with the LoC-SERS technique, a ciprofloxacin solution with pH 11 was selected.

Computer simulations have shown that strong signal enhancements cannot be obtained using a pure colloidal suspension in which only monomer metallic nanoparticles are

present [21]. "Hot spots," where two or more particles are separated by a small gap, must be created, which is usually achieved by adding different salts, for example, NaCl or KCl, to the colloid-analyte mixture. However, in the case of some particular molecules, the analyte itself can induce the aggregation of nanoparticles, which is also the case for the antibiotic under investigation. In order to demonstrate this, the SERS signal of ciprofloxacin solved in high purity water at pH 11 was recorded with no additional salt addition as well as in the presence of 0.3 M KCl and 1 M KCl. In Fig. S3 (see ESM), the integrated peak area of the Raman marker band located at ~1380 cm^{-1} is represented for the three measurement conditions. According to these results, an optimal SERS signal is achieved when no additional salt is present in the mixture. This proves that ciprofloxacin at pH 11 induces the aggregation of the silver nanoparticles. The same behavior was found for a structurally related antibiotic, levofloxacin, at neutral pH [41]. The decrease of the peak area when KCl is present might be explained by an "over-aggregation" of the nanoparticles resulting in large clusters unable to support high electromagnetic enhancements. Therefore, all following measurements were carried out in the absence of any additional aggregation agent.

In the same graph (ESM Fig. S3), the influence of the measurement position (channel number, focus position depicted in Scheme 1), correlated with the time elapsed since mixing the nanoparticles with the analyte solution, on the peak area is also illustrated. Although the highest signal intensity was recorded short after mixing the nanoparticles with the analyte solution, the relative standard deviation of the signal was significant (28.7 %). The lowest relative standard deviation, 12 %, was obtained for the spectra acquired after 212 s of mixing time, and thus for all subsequent measurements, the focus point of the laser beam was fixed in the middle of the 5th channel.

River water as the matrix for ciprofloxacin detection

To show the potential of the LoC-SERS technique to detect ciprofloxacin in complex matrices, samples from a local river were collected, filtered, and spiked with the target molecule. Two stem solutions of ciprofloxacin with concentrations of 0.1 and 0.01 mM and a pH of 11 were filled in glass syringes. A third syringe contained river water with the identical pH. By varying the flow rates of the three syringes, 15 differently concentrated solutions have been obtained. In Fig. 3, the mean SERS spectra and their double standard deviation for the first eight concentration steps are plotted with the blank spectrum. Figure 4a presents the integrated peak area of the Raman mode at 1382 cm^{-1} against the concentration. The first conclusion is that for ciprofloxacin amounts higher than 10 μM, no further signal increment is present, which can be caused by the limited free binding sites on the surface of the Ag

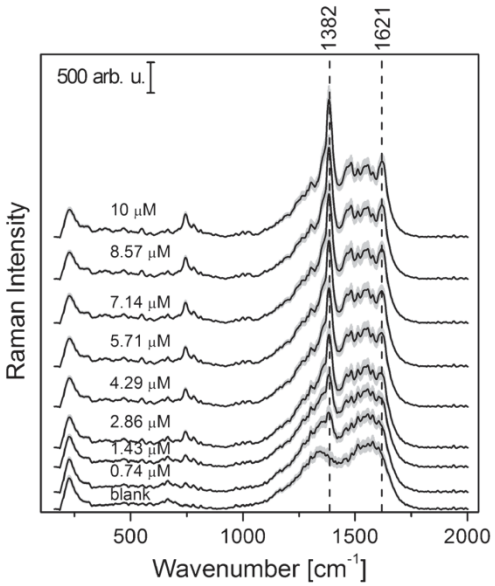

Fig. 3 Mean SERS spectra and their double standard deviation of the spiked river water samples at different concentrations

nanoparticles. Furthermore, the SERS spectrum of the blank sample shows broad bands in the 1100–1700 cm^{-1} spectral region. They have been associated with the presence of amorphous carbon as a result of the decomposition of organic materials. Although the signal of the blank is significant in the fingerprint region, one may observe by eye the characteristic Raman modes of the target molecule at the lowest concentration. According to the IUPAC definition that the limit of detection is equal to the signal of the blank plus three times its standard deviation, the limit of detection is below the lowest measured concentration (0.74 μM) (the threshold is illustrated in Fig. 4a). However, the linearity of the integrated peak area

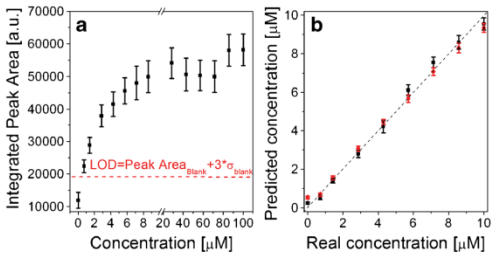

Fig. 4 **a** Univariate statistical analysis: integrated peak area of the Raman mode at 1382 cm^{-1} against ciprofloxacin concentration in spiked river water samples. **b** PLS results, where one dataset (*black scatter*) was used for training the model used to predict a second independent set (*red scatter*)

vs. concentration is weak. This might be the result of the convolution of the marker Raman band with the broad bands originating from the molecules of the complex matrix. Therefore, a univariate statistical method is not suitable to quantitatively determine ciprofloxacin in river water.

To improve the results, a multivariate statistical analysis was performed based on the combination of PCA and PLSR. Two independent datasets were recorded on two different days, with two chips and freshly prepared solutions. The first data set was used to train the PCA-PLS method, whereas the second dataset was treated as unknown. In Fig. 4b, the PLS prediction plot for the model is shown with black scattered points. The dotted diagonal line is depicted only as an eye guideline and does not represent a linear fit. To evaluate the created PLS model, a 10-fold cross validation was performed. The resulting RMSEPCV was 0.375 μM, whereas that for the prediction on all data was 0.374 μM. Both values were below the LOD, and a clear prediction for every concentration step was performed. The PLS model that was created with the first data set was used to predict the concentrations of the new one. The RMSEP value of prediction for an independent data set is 0.355 μM. Thus, the LoC-SERS technique is suitable for detecting ciprofloxacin in environmental samples in the concentration range that corresponds to its MIC values using two independent data sets. Concerning the application of the technique, a "yes-no" answer can be obtained based on the SERS results. Namely, if a SERS signal of ciprofloxacin is detected, one can conclude that the concentration in the sample is above the MIC value.

Conclusion

The effect of the pH value on the SERS signal of the ciprofloxacin solution has been assessed for the first time. To do so, three acidic (pH 1–3) and three basic (pH 11–13) solutions were prepared with a concentration of 0.1 mM. The presence of silver nanoparticles and the chemical state of the target molecule strongly affect both the absolute and relative intensities and the band positions of some marker Raman modes. First, the SERS signal is considerably stronger in the case of ciprofloxacin anions because of the higher chemical affinity and that lack of competition with chloride ions present at low pH. Second, the Raman bands that are ascribed to the C-H stretching vibrations of the piperazinyl ring have a higher intensity in the case of the protonated ciprofloxacin molecules. Third, at basic pH, the position of the band characteristic for the C=C vibration of the quinolone ring is shifted by 7 cm^{-1}. Based on these three observations, the protonated ciprofloxacin molecule can interact with the surface of metallic nanoparticles via the piperazinyl ring, whereas the deprotonated molecule interacts via the quinolone ring.

The second part of the paper shows that the LoC-SERS technology is a suitable analytical tool to detect the target analyte in environmental samples at MIC values. The multivariate statistical analysis consisting of a combined PCA-PLSR algorithm shows that quantification is possible down to 0.74 μM with RMSEP values below the LOD.

In conclusion, in the present study, it was demonstrated that SERS combined with the droplet-based microfluidic platform and appropriate data analysis procedure has high potential for detecting ciprofloxacin in environmental samples. It was shown that a simple filtration step is sufficient and easy-to-produce silver nanoparticles can be employed as SERS active substrates. Furthermore, due to the continuous development of miniaturized and portable Raman setups, LoC-SERS has high potential for on-site applications.

Acknowledgments The funding of the PhD project of I. J. Hidi in the framework "Carl-Zeiss-Strukturmaßnahme" is gratefully acknowledged. The projects "QuantiSERS" (03IPT513A) and "Jenaer Biochip Initiative 2.0" (03IPT513Y) in the framework "InnoProfile Transfer–Unternehmen Region" are supported by the Federal Ministry of Education and Research, Germany (BMBF). We thank the microfluidic group of the IPHT for preparing the lab-on-a-chip devices for the measurements.

Compliance with ethical standards

Conflict of interest There is no conflict of interest.

References

1. Xu Y, Chen T, Wang Y, Tao H, Liu S, Shi W. The occurrence and removal of selected fluoroquinolones in urban drinking water treatment plants. Environ Monit Assess. 2015;187(12):1–10. doi:10.1007/s10661-015-4963-y.
2. Ngumba E, Gachanja A, Tuhkanen T. Occurrence of selected antibiotics and antiretroviral drugs in Nairobi River Basin, Kenya. Sci Total Environ. 2016;539:206–13. doi:10.1016/j.scitotenv.2015.08.139.
3. Johnson AC, Keller V, Dumont E, Sumpter JP. Assessing the concentrations and risks of toxicity from the antibiotics ciprofloxacin, sulfamethoxazole, trimethoprim and erythromycin in European rivers. Sci Total Environ. 2015;511:747–55. doi:10.1016/j.scitotenv.2014.12.055.
4. Korb A, de Nazareno ER, Costa LD, Nogueira KDS, Dalsenter PR, Tuon FFB, et al. Molecular typing and antimicrobial resistance in isolates of Escherichia coli from poultry and farmers in the Metropolitan Region of Curitiba, Parana. Pesqui Vet Bras. 2015;35(3):258–64.
5. Zemlickova H, Jakubu V, Marejkova M, Urbaskova P. Pracovni Skupina Monitorovani R. Resistance to erythromycin, tetracycline and ciprofloxacin in human isolates of *Campylobacter* spp. the Czech Republic has been investigated using standard EUCAST. Epidemiol Mikrobiol Imunol. 2014;63(3):184–90.
6. Miller D, Flynn PM, Scott IU, Alfonso EC, Flynn HW. In vitro fluoroquinolone resistance in staphylococcal endophthalmitis isolates. Arch Ophthalmol. 2006;124(4):479–83. doi:10.1001/archopht.124.4.479.
7. Titilawo Y, Sibanda T, Obi L, Okoh A. Multiple antibiotic resistance indexing of *Escherichia coli* to identify high-risk sources of

faecal contamination of water. Environ Sci Pollut Res. 2015;22(14):10969–80. doi:10.1007/s11356-014-3887-3.
8. Wagenlehner FM, Kinzig-Schippers M, Sorgel F, Weidner W, Naber KG. Concentrations in plasma, urinary excretion and bactericidal activity of levofloxacin (500 mg) versus ciprofloxacin (500 mg) in healthy volunteers receiving a single oral dose. Int J Antimicrob Agents. 2006;28(6):551–9. doi:10.1016/j.ijantimicag.2006.07.026.
9. Wagenlehner FM, Kinzig-Schippers M, Tischmeyer U, Wagenlehner C, Sorgel F, Naber KG. Urinary bactericidal activity of extended-release ciprofloxacin (1,000 milligrams) versus levofloxacin (500 milligrams) in healthy volunteers receiving a single oral dose. Antimicrob Agents Chemother. 2006;50(11):3947–9. doi:10.1128/AAC.00477-06.
10. Sarkar S, Dutta S, Pal T. Tailored "sandwich" strategy in surface enhanced Raman scattering: case study with paraphenylenediamine and application in femtomolar detection of melamine. J Phys Chem C. 2014;118(48):28152–61. doi:10.1021/jp5111955.
11. Pradhan M, Maji S, Sinha AK, Dutta S, Pal T. Sensing trace arsenate by surface enhanced Raman scattering using a FeOOH doped dendritic Ag nanostructure. J Mater Chem A. 2015;3(19):10254–7. doi:10.1039/c5ta01427a.
12. Kim A, Barcelo SJ, Li ZY. SERS-based pesticide detection by using nanofinger sensors. Nanotechnology. 2015;26(1):015502. doi:10.1088/0957-4484/26/1/015502.
13. Kadasala NR, Wei A. Trace detection of tetrabromobisphenol A by SERS with DMAP-modified magnetic gold nanoclusters. Nanoscale. 2015;7(25):10931–5. doi:10.1039/c4nr07658c.
14. Zhang C, Man BY, Jiang SZ, Yang C, Liu M, Chen CS, et al. SERS detection of low-concentration adenosine by silver nanoparticles on silicon nanoporous pyramid arrays structure. Appl Surf Sci. 2015;347:668–72. doi:10.1016/j.apsusc.2015.04.170.
15. Dandapat A, Lee TK, Zhang YM, Kwak SK, Cho EC, Kim DH. Attomolar level detection of Raman molecules with hierarchical silver nanostructures including tiny nanoparticles between nanosized gaps generated in silver petals. ACS Appl Mater Interfaces. 2015;7(27):14793–800. doi:10.1021/acsami.5b03109.
16. Seifert S, Merk V, Kneipp J. Identification of aqueous pollen extracts using surface enhanced Raman scattering (SERS) and pattern recognition methods. J Biophotonics. 2016;9(1–2):181–9. doi:10.1002/jbio.201500176.
17. Gong T, Zhang N, Kong KV, Goh D, Ying C, Auguste J-L, et al. Rapid SERS monitoring of lipid-peroxidation-derived protein modifications in cells using photonic crystal fiber sensor. J Biophotonics. 2016;9(1–2):32–7. doi:10.1002/jbio.201500168.
18. Dinish US, Balasundaram G, Chang YT, Olivo M. Sensitive multiplex detection of serological liver cancer biomarkers using SERS-active photonic crystal fiber probe. J Biophotonics. 2014;7(11–12):956–65. doi:10.1002/jbio.201300084.
19. Yuen C, Liu Q. Towards in vivo intradermal surface enhanced Raman scattering (SERS) measurements: silver coated microneedle based SERS probe. J Biophotonics. 2014;7(9):683–9. doi:10.1002/jbio.201300006.
20. Schlücker S. Surface-enhanced Raman spectroscopy: concepts and chemical applications. Angew Chem Int Ed. 2014;53(19):4756–95. doi:10.1002/anie.201205748.
21. Zhang Y, Walkenfort B, Yoon JH, Schlucker S, Xie W. Gold and silver nanoparticle monomers are non-SERS-active: a negative experimental study with silica-encapsulated Raman-reporter-coated metal colloids. Phys Chem Chem Phys. 2015;17(33):21120–6. doi:10.1039/c4cp05073h.
22. Jahn M, Patze S, Hidi IJ, Knipper R, Radu AI, Muhlig A, et al. Plasmonic nanostructures for surface enhanced spectroscopic methods. Analyst. 2016;141(3):756–93. doi:10.1039/c5an02057c.
23. Cialla D, Hubner U, Schneidewind H, Moller R, Popp J. Probing innovative microfabricated substrates for their reproducible SERS activity. ChemPhysChem. 2008;9(5):758–62. doi:10.1002/cphc.200700705.
24. Baia M, Baia L, Astilean S, Popp J. Surface-enhanced Raman scattering efficiency of truncated tetrahedral Ag nanoparticle arrays mediated by electromagnetic couplings. Appl Phys Lett. 2006;88(14):143121–143121-3. doi:10.1063/1.2193778.
25. Lin XM, Cui Y, Xu YH, Ren B, Tian ZQ. Surface-enhanced Raman spectroscopy: substrate-related issues. Anal Bioanal Chem. 2009;394(7):1729–45. doi:10.1007/s00216-009-2761-5.
26. Shen W, Lin X, Jiang C, Li C, Lin H, Huang J, et al. Reliable quantitative SERS analysis facilitated by core–shell nanoparticles with embedded internal standards. Angew Chem Int Ed. 2015;54(25):7308–12. doi:10.1002/anie.201502171.
27. Gao R, Ko J, Cha K, Jeon JH, Rhie GE, Choi J, et al. Fast and sensitive detection of an anthrax biomarker using SERS-based solenoid microfluidic sensor. Biosens Bioelectron. 2015;72:230–6. doi:10.1016/j.bios.2015.05.005.
28. Liu HT, Liu JS, Li SP, Chen LY, Zhou HW, Zhu JS, et al. Fiber-optic SERS microfluidic chip based on light-induced gold nanoparticle aggregation. Opt Commun. 2015;352:148–54. doi:10.1016/j.optcom.2015.04.084.
29. Huang JA, Zhang YL, Ding H, Sun HB. SERS-enabled lab-on-a-chip systems. Adv Opt Mater. 2015;3(5):618–33. doi:10.1002/adom.201400534.
30. Zhao YQ, Zhang YL, Huang JA, Zhang ZY, Chen XF, Zhang WJ. Plasmonic nanopillar array embedded microfluidic chips: an in situ SERS monitoring platform. J Mater Chem A. 2015;3(12):6408–13. doi:10.1039/c4ta07076c.
31. Walter A, Marz A, Schumacher W, Rosch P, Popp J. Towards a fast, high specific and reliable discrimination of bacteria on strain level by means of SERS in a microfluidic device. Lab Chip. 2011;11(6):1013–21. doi:10.1039/c0lc00536c.
32. Kim K, Kim KL, Shin KS. Selective detection of aqueous nitrite ions by surface-enhanced Raman scattering of 4-aminobenzenethiol on Au. Analyst. 2012;137(16):3836–40. doi:10.1039/C2AN35066A.
33. Sollier E, Murray C, Maoddi P, Di Carlo D. Rapid prototyping polymers for microfluidic devices and high pressure injections. Lab Chip. 2011;11(22):3752–65. doi:10.1039/C1LC20514E.
34. Chen J, Zhou Y, Wang D, He F, Rotello VM, Carter KR, et al. UV-nanoimprint lithography as a tool to develop flexible microfluidic devices for electrochemical detection. Lab Chip. 2015;15(14):3086–94. doi:10.1039/C5LC00515A.
35. Chen YP, Chen G, Zheng XW, He C, Feng SY, Chen Y, et al. Discrimination of gastric cancer from normal by serum RNA based on surface-enhanced Raman spectroscopy (SERS) and multivariate analysis. Med Phys. 2012;39(9):5664–8. doi:10.1118/1.4747269.
36. Alvarez-Puebla RA, Liz-Marzan LM. Environmental applications of plasmon assisted Raman scattering. Energy Environ Sci. 2010;3(8):1011–7. doi:10.1039/C002437F.
37. Yang L, Qin X, Jiang X, Gong M, Yin D, Zhang Y, et al. SERS investigation of ciprofloxacin drug molecules on TiO_2 nanoparticles. Phys Chem Chem Phys. 2015;17(27):17809–15. doi:10.1039/c5cp02666k.
38. He L, Lin M, Li H, Kim N-J. Surface-enhanced Raman spectroscopy coupled with dendritic silver nanosubstrate for detection of restricted antibiotics. J Raman Spectrosc. 2010;41(7):739–44. doi:10.1002/jrs.2505.
39. Guo Z, Chen L, Lv H, Yu Z, Zhao B. Magnetic imprinted surface enhanced Raman scattering (MI-SERS) based ultrasensitive detection of ciprofloxacin from a mixed sample. Anal Methods. 2014;6(6):1627–32. doi:10.1039/c3ay40866c.
40. Leopold N, Lendl B. A new method for fast preparation of highly surface-enhanced Raman scattering (SERS) active silver colloids at

room temperature by reduction of silver nitrate with hydroxylamine hydrochloride. J Phys Chem B. 2003;107(24):5723–7. doi:10.1021/jp027460u.

41. Hidi IJ, Jahn M, Weber K, Cialla-May D, Popp J. Droplet based microfluidics: spectroscopic characterization of levofloxacin and its SERS detection. Phys Chem Chem Phys. 2015. doi:10.1039/c4cp04970e.
42. März A, Ackermann KR, Malsch D, Bocklitz T, Henkel T, Popp J. Towards a quantitative SERS approach—online monitoring of analytes in a microfluidic system with isotope-edited internal standards. J Biophotonics. 2009;2(4):232–42. doi:10.1002/jbio.200810069.
43. Team RDC. R: a language and environment for statistical computing. Vienna: R Foundation for Statistical Computing; 2011.
44. Ryan CG, Clayton E, Griffin WL, Sie SH, Cousens DR. Snip, a statistics-sensitive background treatment for the quantitative-analysis of pixe spectra in geoscience applications. Nucl Inst Methods B. 1988;34(3):396–402. doi:10.1016/0168-583x(88)90063-8.
45. Mevik B-H, Wehrens R, Liland KH. pls: partial least squares and principal component regression. 2011.
46. Bocklitz T, Walter A, Hartmann K, Rösch P, Popp J. How to preprocess Raman spectra for reliable and stable models? Anal Chim Acta. 2011;704(1–2):47–56. doi:10.1016/j.aca.2011.06.043.
47. Caço AI, Varanda F, Pratas de Melo MJ, Dias AMA, Dohrn R, Marrucho IM. Solubility of antibiotics in different solvents. Part II. Non-hydrochloride forms of tetracycline and ciprofloxacin. Ind Eng Chem Res. 2008;47(21):8083–9. doi:10.1021/ie8003495.
48. Neugebauer U, Szeghalmi A, Schmitt M, Kiefer W, Popp J, Holzgrabe U. Vibrational spectroscopic characterization of fluoroquinolones. Spectrochim Acta A Mol Biomol Spectrosc. 2005;61(7):1505–17. doi:10.1016/j.saa.2004.11.014.

Analytical and Bioanalytical Chemistry

Electronic Supplementary Material

Ciprofloxacin: pH-dependent SERS signal and its detection in spiked river water using LoC-SERS

Izabella J. Hidi, Jan Heidler, Karina Weber, Dana Cialla-May, Jürgen Popp

Table S1 Solutions to determine the effect of pH over the SERS signal

Solution	pH value	
	blank	with ciprofloxacin
HCl 0.1 M	1.1	1.1
HCl 0.01 M	1.9	1.9
HCl 0.001 M	3.1	3.1
NaOH 0.001 M	10.9	10.9
NaOH 0.01 M	12.0	12.0
NaOH 0.1 M	13.0	12.9

Table S2 Positions of the Raman bands that are ascribed to ciprofloxacin and affected by the pH and the presence of Ag nanoparticles

Measurement	pH	Band position		
Raman on powder		1362	1382	1616
Raman on saturated aqueous solution	1	1345	1388	1629
	13	1359	1397	1629
SERS	1	1345	1385	1629
	13	convoluted	1382	1621

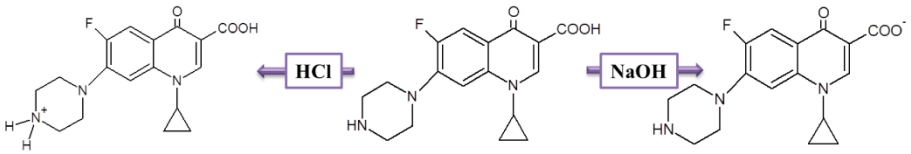

Fig. S1 Chemical structure of the protonated neutral and deprotonated ciprofloxacin molecule

3

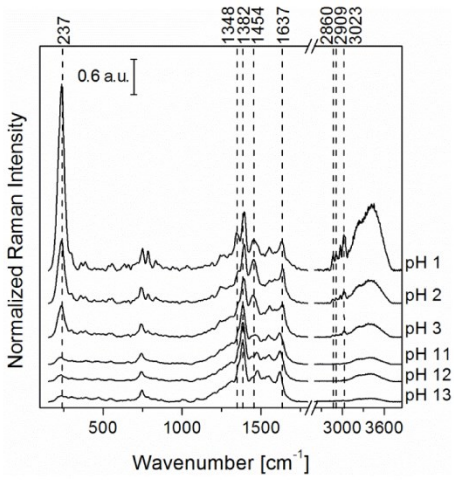

Fig. S2 Mean SERS spectra of the ciprofloxacin solution at different pH measured in cuvette

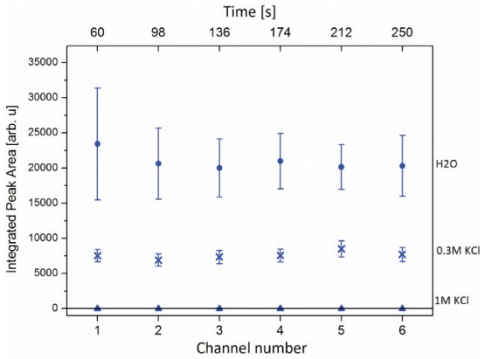

Fig. S3 The influence of KCl addition and aggregation time on the SERS signal of ciprofloxacin (Raman band at 1390 cm^{-1})

3

Author Contribution

LOC-SERS: Towards point-of-care diagnostics of methotrexate

Analytical Methods, 6, 2014, 3943-3947.

Izabella J. Hidi	concept development
	Raman measurements-concentration dependent SERS signals
	data interpretation-quantitative SERS results
	writing of manuscript
Anna Mühlig	concept development
	Raman measurements-the effect of the pH
	data interpretation-fundamental aspects of molecule-metal interaction
	writing of manuscript
Martin Jahn	data analysis
	cover page artwork
Falk Liebold	concept development
	first test measurements
Dana Cialla	discussion of experimental concept and results
	proofreading of manuscript
Karina Weber	discussion of experimental concept and results
	proofreading of manuscript
Jürgen Popp	project management
	discussion of concepts and results
	discussion and proofreading of manuscript

Droplet based microfluidics: spectroscopic characterization of levofloxacin and its SERS detection

Physical Chemistry Chemical Physics, 17, 2015, 21236-21242

Izabella J. Hidi	concept development
	Raman measurements
	data analysis and interpretation
	writing of manuscript
Martin Jahn	data analysis
	discussion of results
Dana Cialla	discussion of experimental concept and results
	proofreading of manuscript
Karina Weber	discussion of experimental concept and results
	proofreading of manuscript
Jürgen Popp	project management
	discussion of concepts and results
	discussion and proofreading of manuscript

Toward levofloxacin monitoring in human urine samples by employing the LoC-SERS technique

Journal of Physical Chemistry C, DOI: 10.1021/acs.jpcc.6b0100

Izabella J. Hidi	concept development
	Raman measurements
	Data analysis interpretation
	writing of manuscript
Martin Jahn	data analysis
	discussion of results
	writing of manuscript
Mathias W. Pletz	discussion of concepts and results
	discussion and proofreading of manuscript
Karina Weber	discussion of experimental concept and results
	proofreading of manuscript
Dana Cialla-May	discussion of experimental concept and results
	proofreading of manuscript
Jürgen Popp	project management
	discussion of concepts and results
	discussion and proofreading of manuscript

LoC-SERS combined with the standard addition method: toward the quantification of nitroxoline in spiked human urine samples

Analytical Chemistry, 88 (18), 2016, 9173–9180

Izabella J. Hidi	concept development
	Raman measurements
	data analysis and interpretation
	writing of manuscript
Martin Jahn	multivariate statistical data analysis
	discussion of results
	writing of manuscript
Thomas Bocklitz	multivariate statistical data analysis
	discussion and proofreading of manuscript
Mathias W. Pletz	sample collection
	discussion of experimental concept and results
	proofreading of manuscript
Karina Weber	discussion of experimental concept and results
	proofreading of manuscript
Dana Cialla-May	discussion of experimental concept and results
	proofreading of manuscript
Jürgen Popp	project management
	discussion of concepts and results
	discussion and proofreading of manuscript

Ciprofloxacin: pH dependent SERS signal and its detection in spiked river water by LoC-SERS

Analytical Bioanalytical Chemistry (2016). doi:10.1007/s00216-016-9957-2.

Izabella J. Hidi	concept development
	multivariate statistical analysis data analysis and interpretation
	discussion of experimental results
	writing of manuscript
Jan Heidler	Raman measurements
	univariate statistical data analysis and interpretation
Karina Weber	discussion of experimental concept and results
	proofreading of manuscript
Dana Cialla-May	discussion of experimental concept and results
	proofreading of manuscript
Jürgen Popp	project management
	discussion of concepts and results
	discussion and proofreading of manuscript

Erklärung zu den Eigenanteilen des Promovenden/der Promovendin sowie der weiteren Doktoranden/Doktorandinnen als Koautoren an den Publikationen und Zweitpublikationsrechten bei einer kumulativen Dissertation

Publikation: I.J. Hidi, A. Mühlig, M. Jahn, F. Liebold, D. Cialla, K. Weber, J. Popp, ***LOC-SERS: Towards point-of-care diagnostic of methotrexate***, Anal. Methods, 2014,6, 3943-3947			
Beteiligt an			
	Izabella J. Hidi	Anna Mühlig	Martin Jahn
Konzeption des Forschungsansatzes	**X**	**X**	
Planung der Untersuchungen	**X**	**X**	
Datenerhebung	**X**	**X**	
Datenanalyse und - interpretation	**X**	**X**	**X**
Schreiben des Manuskripts	**X**	**X**	
Vorschlag Anrechnung Publikationsäquivalente	**1,0**	**1,0**	**0,5**

Publikation: I.J. Hidi, M. Jahn, K. Weber, D. Cialla-May, J. Popp, ***Droplet based microfluidics: spectroscopic characterization of levofloxacin and its SERS detection***, Phys. Chem. Chem. Phys., 2015,17, 21236-21242		
Beteiligt an		
	Izabella J. Hidi	Martin Jahn
Konzeption des Forschungsansatzes	**X**	
Planung der Untersuchungen	**X**	
Datenerhebung	**X**	
Datenanalyse und - interpretation	**X**	**X**
Schreiben des Manuskripts	**X**	
Vorschlag Anrechnung Publikationsäquivalente	**1,0**	**0,5**

Publikation: I.J. Hidi, M. Jahn, M. W. Pletz, K. Weber, D. Cialla-May, J. Popp, ***Towards levofloxacin monitoring in human urine samples by employing the LoC-SERS technique***, J. Phys. Chem. C, 2016, 120 (37), 2016, 20613–20623.		
Beteiligt an		
	Izabella J. Hidi	Martin Jahn
Konzeption des Forschungsansatzes	**X**	
Planung der Untersuchungen	**X**	
Datenerhebung	**X**	
Datenanalyse und - interpretation	**x**	**X**
Schreiben des Manuskripts	**X**	**X**
Vorschlag Anrechnung Publikationsäquivalente	**1,0**	**0,75**

Publikation: I. J. Hidi, M. Jahn, , T. Bocklitz, K. Weber, M. W. Pletz, D. Cialla-May, J. Popp, ***LoC-SERS combined with the standard addition method: toward the quantification of nitroxoline in spiked human urine samples***, Analytical Chemistry, 88 (18), 2016, 9173–9180.		
Beteiligt an		
	Izabella J. Hidi	Martin Jahn
Konzeption des Forschungsansatzes	**X**	**X**
Planung der Untersuchungen	**X**	
Datenerhebung	**X**	
Datenanalyse und – interpretation	**X**	**X**
Schreiben des Manuskripts	**X**	**X**
Vorschlag Anrechnung Publikationsäquivalente	**1,0**	**1,0**

Publikation: I.J. Hidi, J. Heidler, K. Weber, D. Cialla-May, J. Popp, ***Ciprofloxacin: pH dependent SERS signal and its detection in spiked river water by LoC-SERS***, Analytical Bioanalytical Chemistry (2016). doi:10.1007/s00216-016-9957-2.	
Beteiligt an	
	Izabella J. Hidi
Konzeption des Forschungsansatzes	**X**
Planung der Untersuchungen	**X**
Datenerhebung	
Datenanalyse und - interpretation	**X**
Schreiben des Manuskripts	**X**
Vorschlag Anrechnung Publikationsäquivalente	**1,0**

Für alle in dieser kumulativen Dissertation verwendeten Manuskripte liegen die notwendigen Genehmigungen der Verlage („Reprint permissions“) für die Zweitpublikation vor.

Die Co-Autoren der in dieser kumulativen Dissertation verwendeten Manuskripte sind sowohl über die Nutzung, als auch über die oben angegebenen Eigenanteile der weiteren Doktoranden/Doktorandinnen als Koautoren an den Publikationen und Zweitpublikationsrechten bei einer kumulativen Dissertation informiert und stimmen dem zu.

Izabella Jolán Hidi

Name des Promovenden/der Promovendin Datum Ort Unterschrift

Ich bin mit der Abfassung der Dissertation als publikationsbasiert, d.h. kumulativ, einverstanden und bestätige die vorstehenden Angaben. Eine entsprechend begründete Befürwortung mit Angabe des wissenschaftlichen Anteils des Doktoranden/der Doktorandin an den verwendeten Publikationen werde ich parallel an den Rat der Fakultät der Chemisch-Geowissenschaftlichen Fakultät richten.

Prof. Dr. Jürgen Popp

Name Erstbetreuer(in) Datum Ort Unterschrift

Conference contributions

Oral presentations:

1. I. J. Hidi, D. Cialla, K. Weber, J. Popp, *Lab-on-a-Chip-SERS for drug detection*, Trends in Bioanalytical Imaging, 27 - 28 May 2013, Frankfurt am Main, Germany, selected poster for oral presentation.

2. I. J. Hidi, M. Jahn, K. Weber, D. Cialla, J. Popp, *Droplet Based Microfluidics Combined with Surface-Enhanced Raman Spectroscopy: towards Monitoring of Levofloxacin*, SCIX, 28 September-3 October 2014, Reno, NV, USA.

3. I. J. Hidi, K. Weber, D. Cialla-May, J. Popp, *Lab-on-a-chip SERS towards clinical application: detection of levofloxacin in simulated body fluid*, European Conference on Biomedical Optics, 21-25 June 2014, München, Germany, invited oral presentation.

4. I. J. Hidi, M. Jahn, A. Mühlig, K. Weber, D. Cialla-May, J. Popp, *Towards a new clinical tool: fast and high-throughput LOC-SERS detection of Methotrexate and Levofloxacin*, DoKDoK, 11-15 October 2015.

5. I. J. Hidi, M. Jahn, K. Weber, T. Henkel, D. Cialla-May, J. Popp, *LOC-SERS towards drug monitoring*, 8th Workshop of Chemical and Biological Micro Laboratory Technology, 23-25 February 2016, Ilmenau, Germany.

Poster presentations:

1. I. J. Hidi, D. Cialla, T. Henkel, K. Weber, J. Popp, *Drug detection using LOC-SERS technology*, DoK-DoK, 06-10 October 2013, Suhl, Germany.

2. I. J. Hidi, D. Cialla, T. Henkel, K. Weber, J. Popp, *Application of lab-on-a-chip surface enhanced Raman spectroscopy (LOC-SERS) in detection of biologically relevant molecules*, 9th FT-IR Meeting, 24-25 October 2013, Berlin, Germany.

3. I. J. Hidi, A. Muehlig, M. Jahn, F. Liebold. K. Weber, D. Cialla-May, J. Popp, *Towards therapeutic drug monitoring of the antifolate drug, methotrexate, by means of lab-on-a-chip surface enhanced Raman spectroscopy*, XXIV International Conference on Raman Spectroscopy, 10-15 August 2014, Jena, Germany.

4. I.J. Hidi, J. Heidler, K. Weber, D. Cialla-May, J. Popp, *LoC-SERS basierter Nachweis von Ciprofloxacin in Wasser*, Wasser 2015, 11.- 13. May 2015, Schwerin, Germany.

5. I. J. Hidi, K. Weber, D. Cialla-May, J. Popp, *Detection of the fluoroquinolone antibiotic, levofloxacin, in simulated urine by means of LoC-SERS: use of an external standard*, Summer school on Biophotonics `15, 6-13 June 2015, Island of Ven, Sweden.

6. I. J. Hidi, M. Jahn, K. Weber, D. Cialla-May, J. Popp, *LOC-SERS as bioanalytical tool: drug detection in spiked human urine samples*, Biosensors, 25-27 May 2016, Gothenburg, Sweden.

Acknowledgements

Foremost, I would like to express my sincere gratitude to Prof. Dr. Jürgen Popp for giving me the opportunity to be part of his research group, for his trust and support throughout my thesis. He contributed with creativity and expertise, as well as his helping hand on writing, proof reading, and publishing during my PhD time

Many thanks go to my two supervisors, Dr. Karina Weber and Dr. Dana Cialla-May, for their continuous help, support and for the multitude of advices received during the last three and a half year. My writing and presentation proficiency as well as my organizational skills were strongly shaped and influenced by their expertise.

My thesis has two key aspects: “LoC-SERS” and “complex matrix”. Therefore, I would like to thank Dr. Thomas Henkel and the Microfluidics Group of IPHT for providing me the microfluidic chips. Special thanks go to Prof. Dr. Mathias Pletz for sharing his knowledge with me, for the manuscript corrections, and for giving me access to clinical urine samples.

I would also like to thank Johanna Kirchhoff for preparing and providing urine samples, Dr. Dirk Bender for the DFT calculations for the levofloxacin molecule and Dr. Thomas Bocklitz for his support with the statistical data analysis.

Jan Heidler chose to carry out his bachelor and master thesis under my supervision. I would like to thank him for his dedicated work, the measurements and data interpretation for the ciprofloxacin study.

I am very grateful for the nice working atmosphere and the continues support of my colleagues of the SERS crew of the JBCI group, Sophie Patze, Richard Knipper, Vera Dugandzic, Andreea Radu, Martin Jahn and Sezin Yüksel. I would particularly like to single out Andreea Radu for being my colleague and friend for the last ten years, and Martin Jahn, my work colleague and future husband, for the long discussions, for being always ready to help and for the statistical data analysis without which my Ph.D. thesis would have not been the same.

I am grateful for funding by “Carl-Zeiss-Strukturmaßnahme”, “QuantiSERS” and “Jenaer Biochip Initiative 2.0”.

Last, but not the least, I would like to thank my family for supporting me throughout my whole life.

Curriculum Vitae

Personal Data

Name	Izabella Jolán Hidi
Date of Birth	27. February 1987
Place of Birth	Deva, Romania

Education

Since 11/2012	**Doctoral student** at Institute of Physical Chemistry, Friedrich-Schiller University, Jena, Germany
10/2010-07/2012	**M.Sc.** Science and Technology of Advanced Materials Faculty of Physics, Babeş-Bolyai University, Cluj-Napoca, Romania
11/2011-04/2012	**ERASMUS** training Institute of Physical Chemistry, Friedrich-Schiller University, Jena
10/2006-07/2010	**Bachelor of Engineering** Faculty of Physics, Babeş-Bolyai University, Cluj-Napoca, Romania

_____ _____

Ort, Datum Izabella Jolán Hidi

Selbstständigkeitserklärung

Ich erkläre, dass ich die vorliegende Arbeit selbstständig und unter Verwendung der angegebenen Hilfsmittel, persönlichen Mitteilungen und Quellen angefertigt habe.

Ort, Datum _____

Unterschrift _____